Università degli Studi di Napoli Federico II

Doctoral Degree in Industrial Engineering

XXXIV Cycle

PhD Thesis

TOWARDS A DECARBONIZED BUILT ENVIRONMENT: ENERGY RATINGS AND TECHNOLOGIES FOR REFURBISHING THE EXISTING BUILDING STOCK

Doctorate Program Coordinator

Prof. Michele Grassi

Tutor

Prof. Fabrizio Ascione

Candidate

Margherita MASTELLONE

Student ID: DR993537

Academic year 2020/2021

Alla mia famiglia

Index

Abstract

Climate change is one of the most discussed global issues in recent times. The main cause of global warming is anthropogenic activity, which risks irreversibly compromising the survival of our common earth and the future of next generations. Human actions affect the environment, and thus this earth, in several ways: water quality and quantity, increased pollution and greenhouse gas emissions, depletion of natural resources, urban and village overheating, global heating of both coastlines and backcountries. Although it is relatively recently that humanity is taking actions to counter global warming, this phenomenon has affected the earth for much longer. NASA's Goddard Institute has recorded an increase in the global average temperature of 1° C since 1880, with a gradual rise of 0.2° C every decade. But what does all this entail? A rapid change in the atmosphere, ocean, biosphere, and cryosphere. The rapid melting of glaciers and sea-level rise, extreme climatic events, and desertification of entire areas are increasingly frequent occurrences, and right before our eyes. We must act quickly, by introducing actions for each sector that affects global emissions, and thus transport, industry, and construction.

On a global scale, the building sector has a key role, being responsible for about the 36% of energy consumption and 39% of carbon dioxide emissions in 2018 [1], with the largest share for residential buildings. At the same time, according to the Eurostat data, the building sector has the highest potential in achieving energy savings. Indeed, even if today the building sector has a high weight on global energy consumptions, the future trends are positive, due to the international actions and regulations proposed by the countries to reach the targets of more sustainable and low emissions buildings. During the last years, CO_2 emissions have seen significant growth and the main cause is population growth and urbanization. For low-income and lower-middle income countries, urbanization is even more foreseen from now to 2050, with a consequent increase in greenhouse gas emissions. In the developed countries, besides the construction of new buildings, a big issue is the refurbishment of the existing ones, designed without considering their

environmental impact. For these reasons, international standards and legislation are focused, not only on the optimization of the design of energy-efficient new buildings but mainly on the renovation of existing buildings especially considering the low renovation rate (around 1-3 %/year before the COVID-19 pandemic) of the building stock. Presently, at the EU level, the average turnover rate is around 0.6%.

The necessity of interventions on present building stock, to improve energy efficiency and cut down energy consumption, becomes incumbent and indispensable. Until the beginning of the third millennium, because of the inefficiencies of the building envelope and the related high thermal dispersions, the most diffused way of intervention on existing buildings was simply excessive and inappropriate use of facilities, to balance the heat losses, getting an excessive increase of energy consumption and climate change emissions. By considering the European context, the very inefficient buildings of European cities, and thus the ones built quickly and without attention to thermal and energy performances (from the fifties to the seventies), already have been often interested by deep refurbishments promoted and funded starting by the Energy Performance of Building Directives. This is true mainly for cold countries. For the future, the new challenge, as it was established also by Directive 844/2018, will be focused on the improvements of thermal resilience and energy behaviors of recent buildings, the ones built around the 1990s and 2000s, often characterized by high energy demands for cooling, sometimes due to the indoor overheating related to excessive use of thermal insulation and no attention to passive mitigation strategies. This phenomenon, by also considering the pressing climate change, the condensation heat of air conditioning systems, the urban heat islands, is more and more actual. The development of new solutions and new interventions technologies in the building field is becoming necessary, with particular attention to the reduction of cooling demand.

This Thesis will lead us through a path on the energy efficiency of buildings, which starting from an overview of the current European and Italian legislative framework, will focus on traditional and innovative strategies for the improvement of the energy performance of existing buildings. With an innovative approach, the energy refurbishment of the built environment will be centered on the three levers of energy efficiency: the thermophysics of the transparent and opaque envelope, the systems for the microclimate control, and the energy conversion from renewable energy sources. To consolidated methodologies, innovative ones are coupled for the energy audit of real building case studies, public and private, with several uses, including residential or educational.

The Thesis is based on published studies developed within the research group and these are reported in the list of publications at the end of the manuscript.

The evaluation of building energy efficiency can be performed according to two different approaches, as recurrent in the available scientific literature: a) a numerical approach based on the implementation of a mathematical model, in many cases, in a simulation environment; and b) the experimental approach based on a controlled or real environment. For a complete knowledge of the building, the methods can be combined themselves to perform more detailed and accurate energy analysis. Both methodologies, widely described in CHAPTER 2, were employed in this Thesis, to characterize and analyze several case studies and the possible energy retrofit interventions.

The numerical approaches used to evaluate the building energy performances were mainly two: The Building Energy Simulation (BES) and the Computational Fluid Dynamic (CFD) analysis, that were also coupled to evaluate both the building energy consumption and its indoor environmental quality. Indeed, a BES is a time-dependent simulation, based on energy balances in a continuous thermal transient regime, performed by assuming sub-hourly time-steps and by resolving transfer functions. On the other hand, in a fixed temporary moment, a CFD simulation concurs to understand the kinetic fields of an indoor environment, the spatial trends of each parameter that define the indoor microclimate (e.g. temperature and air velocity), the thermal-hygrometric comfort, and the indoor air quality (IAQ).

Starting from real building case studies, this research work was not limited to the evaluation of the building energy performances through the cited approaches, but accurate environmental and economic analyses were performed to estimate the impact of proposed energy retrofit interventions. Cost-optimal solutions with related global costs, investment costs, payback periods of the invested capital, and economic indexes under a macro-economic analysis were calculated for a complete evaluation of the building energy retrofits.

But how do you intervene on a building for an energy refurbishment? Usually, all “levers” (i.e., building envelopes, active energy systems, renewables) for energy efficiency must be pressed, consecutively, to reduce firstly the heat gains, then the energy demands, and finally by allowing clean energy using renewable sources. This Thesis has examined, on real case studies, passive and active strategies singularly, respectively in CHAPTER 1 and CHAPTER 4, and in CHAPTER 5 interventions on all three levers of energy efficiency were accurately proposed and evaluated. Specifically, regarding the passive technologies for the building envelope, traditional and innovative cooling strategies were selected to reduce heat gains and minimize cooling loads for an educational building. Cooling strategies such as phase change materials, vented walls, cool and green roofs, are some of the technologies analyzed for the free or low-energy cooling of the building in CHAPTER 1. In the same chapter, a critical review of recent scientific investigations about green walls is reported. All parameters for the design optimization are discussed as well as the achievable social and private benefits, and all technical requirements of the green layers. The review points out “strengths”, “weaknesses”, “opportunities” and “threats” of this technology and highlights how benefits will acquire greater relevance considering the increase in global temperatures and the growing need to redevelop densely built urban centers.

However, intervening on the building envelope with passive strategies involves many benefits such as energy-saving and improvement of environmental comfort, but today, after the COVID-19 pandemic, it is almost unthinkable that an energy redevelopment does not also include intervention on the building technical systems. During the COVID-19 pandemic, the necessity of healthy and safe spaces has become prominent, and this means design effective mechanical ventilation systems to control the indoor air quality. Therefore, reduction of the building energy demand and the improvement of the livability and healthiness of spaces are equal priorities. CHAPTER 4 is entirely dedicated to the technological refurbishment of an Italian University building with the aims of improving the classrooms' quality and safety, through a comprehensive approach for the retrofit design. The scope of this investigation is to do University classrooms safe and sustainable indoor places, during the SARS-CoV-2 global pandemic. Experimental studies (monitoring and investigations of the current energy performances) are followed by the coupling of different numerical methods of investigations, and thus BES, under transient conditions of heat transfer, and CFD simulations, to evidence criticalities and potentialities to designers involved in the project of indoor spaces hosting multiple persons. Both energy impacts, in terms of increase of energy demands due to higher mechanical ventilation, and indoor distribution of microclimatic parameters were investigated, by proposing new scenarios and evidencing the usefulness of HVAC systems, equipment, and suitability of some strategies for the air distribution systems compared to traditional ones.

In CHAPTER 5 energy refurbishments of the whole building/HVAC systems are proposed. Specifically, the theoretical assessment of the performance of applied energy retrofit and seismic enhancement measures for a student dormitory of the University of Athens is presented. Different interventions were applied: the whole reorganization of the building spaces, the improvement of the thermophysical properties of the building envelope, and the replacement of the systems for the microclimatic control. In addition, a critical analysis of several passive and active energy efficiency measures for three Italian residential buildings was conducted. The buildings, representative of the most recurrent Italian residential typologies, were simulated in different Italian cities, and so in different climates, employing both semi-stationary and transient approaches. Considering the energy, environmental and economic indicators, it was shown how the new Italian funding program can boost the diffusion of energy efficiency measures characterized by the best energy performance, and not by the best cost/benefit ratio.

Finally, by considering the high complexity required by common energy simulation tools in modeling and simulation, the last chapter (CHAPTER 6) proposes a novel, accurate but user-friendly tool for building modeling and energy simulation. It is called EMAR, and couple ENergyplus and MAtlab® and address Residential buildings. Only 63 numerical inputs are necessary to perform accurate energy simulations by generating a simplified building model, all completely under MATLAB environment. To use a tool like EMAR is not required any modeling expertise, drawings, or schemes of the energy systems, but only a few input parameters. The available outputs are numerous referring to energy and economic performance as well as thermal comfort. Thus, EMAR can be a precious tool to perform user-friendly but accurate building energy modeling and simulations. Figure 1 is a graphical summary of the present Thesis work.

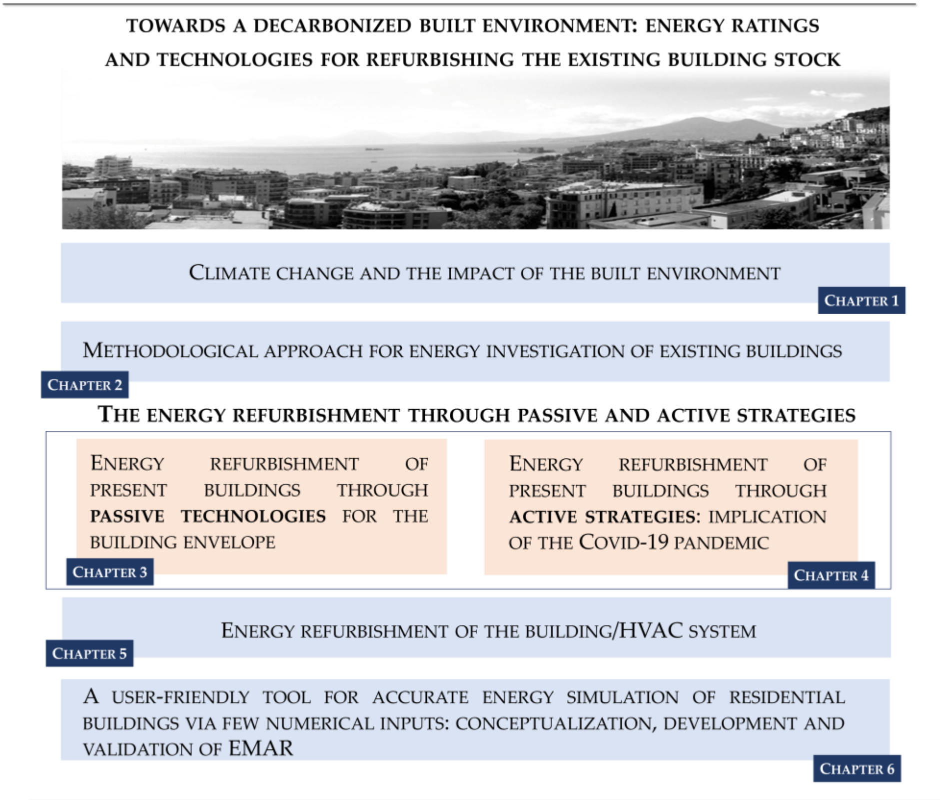

Figure 1 – Graphical abstract of the Thesis work

CHAPTER 1.

Climate change and the impact of the built environment

Global Warming and related climate change are evident from the century-scale rise of the average temperature of the earth's climate system, observed since the pre-industrial period (between 1850 and 1900). According to the Intergovernmental Panel on Climate Change (IPCC) [2], it is predominantly caused by human activities, and primarily due to the fossil fuels like coal, oil and gas. Figure 1.1 shows the increase in the global annual mean surface temperature from 1880 to 2020, which today corresponds to about 1 °C, and currently increasing by 0.2 °C per decade.

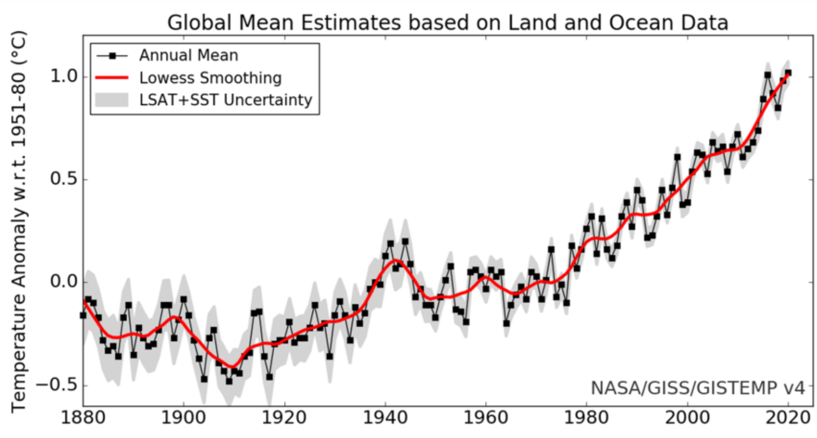

Figure 1.1 - Change in global surface temperature from 1880 average temperature to 2020 (Source: NASA's Goddard Institute for Space Studies)[3]

The current warming trend has caused a rapid change in the atmosphere, ocean, cryosphere, and biosphere. The ocean has absorbed much heat, showing a significant warming, with an average temperature increase of 0.33 °C. The mass of glaciers has decreased; Antarctica has lost about 148 billion tons of ice per year and Greenland an average of 279 billion tons of ice per year between 1993 and 2019 [4]. The future projections are not positive, indeed, if the current rate will continue to increase, the IPCC foresees a global temperature growth of 1.5 °C between 2030 and 2050. Devasting consequences are inevitable if the global temperature rises to 2°C above the pre-industrial levels, with incontrollable effects on the rising of sea levels, desertification of areas, loss of habitats, and natural species. The impact on natural and human systems occurs with extreme temperatures, heavy precipitations more frequent and intense, increase in droughts. The whole ecosystem can be completely compromised by losses and extinction of species; the biodiversity of the sea is at risk due to the increase in ocean acidity and decrease in ocean oxygen levels; entire cities could be submerged because of the rise in the sea levels. Our health and that of the planet are in danger, human security, food security, water supply, and economic growth are at risk with a temperature increase of 1.5°C [2]. Strong and immediate actions are needed.

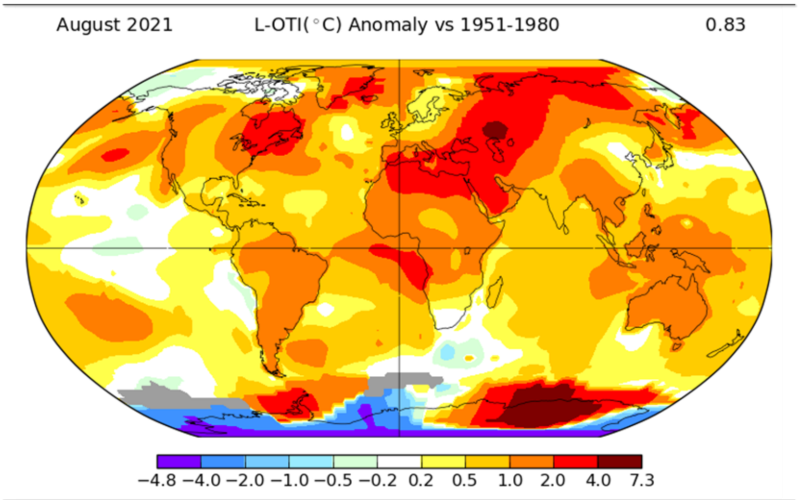

Figure 1.2 – Surface temperature anomaly in august 2021 compared to the average data of 1951-1980 [5]

As represented in Figure 1.2, South and East Europe, North Africa and part of Asia, are areas interested by a high temperature increase. In Italy, it was registered a growth of 1.58 °C from the results of 1971-2000 to 2018 and it was also observed that, between 30 warmest years from 1800, 25 years occur after 1990. The data were registered by the Italian national research council (CNR) and the Institute of Atmospheric Sciences and Climate (ISAC) coming from the historical Italian Meteorological Observatories, set up by Brunetti *et al* [6].

In Africa, Central and South America, and southeast Asia more than 30 extra seasonal heatwave days per °C of global warming are foreseen by climate modeling [7]. In Europe, heavy rainfall [8] and drought [9] will be intensified as a consequence of changes in the hydrological cycle.

The greenhouse gas emissions are directly related to global energy consumption. Primary energy consumption at global scale increased by 1.6% in 2019, less than in 2018 (2.8%), and all fuels, except nuclear, grew at below-average rates. Growth in energy consumption is mainly driven by the developing economies: China at first, India, and Indonesia following. The overall emissions from energy consumption are increased by 0.5 % in 2019 [10]. These data refer to a world condition before the diffusion of the COVID-19 virus and before the countries' lockdown, that, in a more or less restrictive way, has involved most countries and economies. 2020 was interested in a human tragedy - around four million people died due to COVID-19 – which has affected the global economy and has caused a large recession, accentuating disparities with the poorest and least developed countries. This economic recession has led to a fall in the global energy demand of 4.5% in 2020, resulting in the largest reduction since the end of World War II. Indeed, the lockdown caused a collapse in the transport-related demand and an unprecedented decimation of the oil demand. Even a positive trend in the conversion of energy from wind and solar sources was registered with an increase of more than 50% larger than any previous expansion. Consequently, the carbon emissions from energy use decreased by 6.3%, the lowest value registered from 2011. Above any prevision, the global primary energy consumption has undergone a considerable decrease (Figure 1.3).

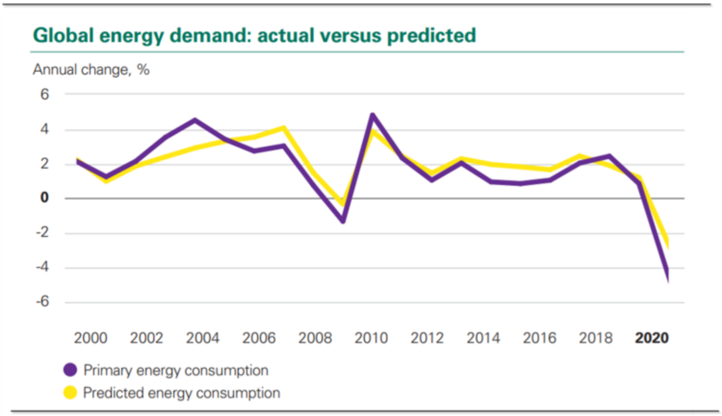

Figure 1.3 – Actual and predicted global energy demand [10]

The decline in the primary energy consumption during 2020, was largely driven by oil (Figure 1.4), whose reduction is around 9.7%. The only one increasing fuel was the one from renewables (+9.7%). The regions with the largest consumption cut were North America (-0.8%) and Europe (-7.8%) while the lowest decrease was registered in Asia-Pacific (-1.6%). The only major country where energy consumption has increased is China (+2.1%).

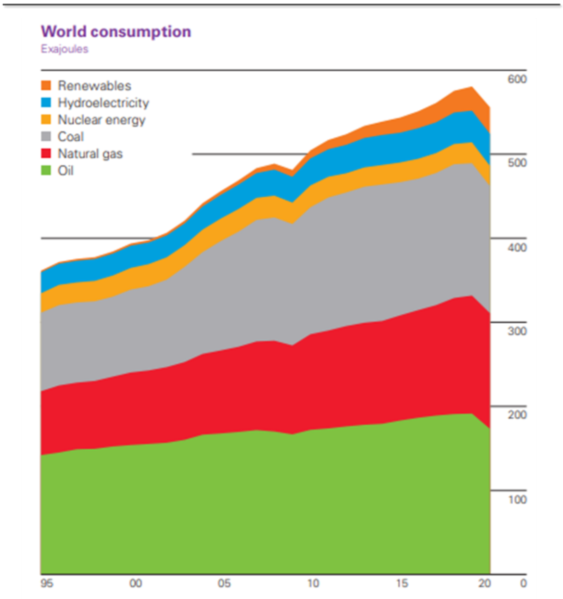

Figure 1.4 - Global primary energy consumption for fuels [10]

The growth in energy consumption over the next 30 years, is strongly related to how it is used across the main economic sectors. The industrial sector is the most energy-intensive and in 2018, it consumed around 48% of global energy. The remaining part was used by the building (29%) and transport sectors (21%). Figure 1.5 shows the annual outlook of primary energy consumption by sector based on the data available from 1990 to 2018 going until 2050. Three different provision scenarios were considered - Rapid, Net-Zero, and Business as usual - which span a wide range of possible outcomes. According to the "Rapid" scenario, the growth of the primary energy used decreases if compared to the past 20 years, with the biggest reduction in the industrial and buildings sectors. In the Net Zero scenario, the use of electricity and hydrogen is greater in the transport and industry sectors, while in BAU (Business and usual) scenario, the use of primary energy increases in all three sectors 35 [11].

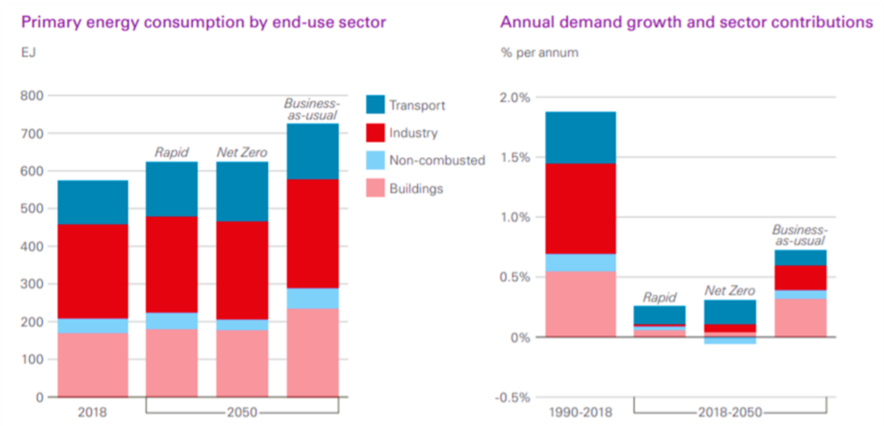

Figure 1.5 - Primary energy consumption by end-use sector and annual demand growth and sector contributions[11].

The *BP energy outlook 2020* [11], evaluate also the possible impact of the COVID-19 pandemic on the global economy and energy systems, because, today, the number of COVID-19 cases is still increasing. The future trends are highly uncertain, but it is assumed that the level of GDP (Gross Domestic Product) will be 2.5% lower in 2025 and 3.5% in 2050 due to the crisis. By considering the new habits and needs that emerged during the COVID-19, and thus behavioral changes such as work from home, less traveling, and a reduction in the use of public transports, it is assumed a reduction of primary energy demand in 2025 of 2.5% and in 2050 of 3%.

In terms of CO_2 emissions, the *BP energy outlook 2020* [11], reports for 2018, a total of greenhouse gas emissions of 33.9 Gt, dived for industry, buildings, and transport sectors (Figure 1.6). The building sector, including residential and commercial buildings, accounts for 21% of global emissions, even if the industry sector is responsible for the biggest part of global emissions (47%).

To go towards a competitive low-carbon economy and sustainable future development, the IPCC [2], has defined pressing goals for the reduction of global anthropogenic emissions over the 21st century. New pathways have been defined, on the basis of temperature trajectories, to give at least 50% probability of limiting global warming to below 1.5°C (the so-called "no overshoot"); to limit warming to below 1.6°C and returning to 1.5°C by 2100 (called "1.5°C limited-overshoot"); to exceed 1.6°C but still returning to 1.5°C by 2100 (called "higher-overshoot").

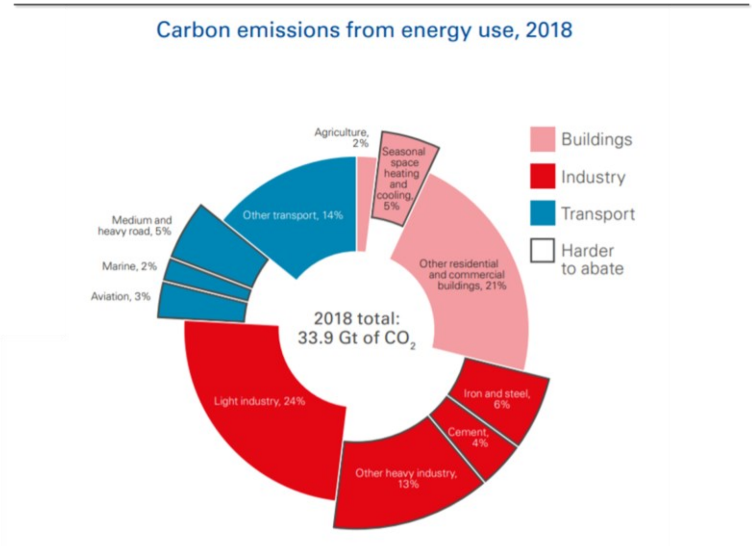

Figure 1.6 – Carbon emission divided for sectors, 2018 [11]

Having regard to the situation of environmental fragility affecting the earth, to support the development of a sustainable and low-carbon future, some national and international actions were introduced.

On an international level, during 1988, the Intergovernmental Panel on Climate Change (IPCC) was founded, as a high-level scientific committee that investigates the possible reason and impacts of climate change and the potential solutions to the issue. The first climate change convention was adopted in 1992 - the United Nations Framework Convention on Climate Change, (UNFCCC) – aiming at the stabilization of the concentration of climate change gases in the atmosphere to a lower level, enough to avoid the anthropogenic interference to the climate system. In 1977, during the third session of the Conference of the Parties (COP3) held in Kyoto in Japan, the most important protocol to operationalize the UNFCCC was adopted. Indeed, the Kyoto protocol, introduced percentage limitations in greenhouse gas emissions compared to those of 1990, for the EU and for thirty-eight industrialized countries. The protocol gave flexibility in the adoption of mechanisms for the reduction of emissions and asked countries to enact policies and measures of mitigation to be reported periodically. It entered into force in 2005 and in 2008 the EU and the thirty-seven industrialized countries were undertaken to reduce emissions by around 5% compared to 1990 levels, over a five-year period 2008/2012. In 2015 it was held the last noteworthy conference of the parties: COP21 in Paris. The conference led to the Paris agreement, a global agreement on climate change. It represents a census of the 195 parties participating in the COP21. The objective is to limit global warming to well below 2°C, preferably 1.4 °C, compared to the preindustrial levels.it was also established to hold the commitment every five years, with the aim of progressively increasing its ambitious goals.

1.1. The European framework

At the EU level, European Institutions in the climate and energy framework established, within 2030 [12], the following well-known energetic and environmental targets:

- Reduction in greenhouse gas emissions of 40% (compared to 1990 levels),
- Improvement of at least 32.5% in energy efficiency,
- Increase of 32% the use of renewable energy sources.

In the EU, the main instrument for the reduction of greenhouse gas emissions is the Emission Trading System (ETS) [13] tool which contemplates the large energy, industrial, and aviation sectors, responsible for around 45% of the EU's greenhouse gas emissions. The ETS objective is to reduce the climate change emissions from these sectors. Concerning the other sectors, and thus the building, agriculture, and trash sectors, these are involved in national emission reduction targets. Indeed, each EU country is called to implement the reduction targets set by *Effort Sharing,* each one following the national income.

To the energy EU framework for 2030, is also added the long-term strategy for 2050 [14], whose objectives are in line with those of the global climate action under the Paris Agreement. In particular, the EU attempt to become climate-neutral by 2050, with an economy based on net-zero greenhouse gas emissions.

The EU’s ambitious objectives have led to the development of several Directives, but, in the present Thesis, merely those related to the building sector are reported. In the following subsections, the weight of the building sector on global energy consumption is underlined (subsection 1.1.1), and the EU actions and Directives regarding the energy performance of buildings are reported (subsection 1.1.2).

1.1.1. The European building stock: residential, public, tertiary, and educational sector

During the last decades the European building’s performances have been steadily improved due to the EPBD Directives, but a big renovation work is already necessary because a large part of residential buildings in the EU, were built before the introduction of thermal standards. The European building stock is quite heterogeneous for what concerns the building uses, indeed, in the majority, the largest part of buildings is residential. The country with the highest number of residential buildings is Italy (89%), contrary to Slovakia (60%) and the Netherlands (61%). The energy efficiency of the building stock is largely related to the age of construction, and in most EU countries, half of the residential buildings were built before 1970, a year that signs the introduction of the first thermal regulations. Sweden, Lithuania, Germany, and United Kingdom have the oldest building stocks, while Cyprus, Spain, and Ireland have a significant share of new dwellings (built after 2000). In Italy, like in Bulgaria or Greece, the largest part of buildings was built in the period between the second post-war and 1969 (around 62%), and thus are characterized by light structures, with minimum or zero insulation levels. Figure 1.7 shows a breakdown of residential buildings by construction year in Europe [14].

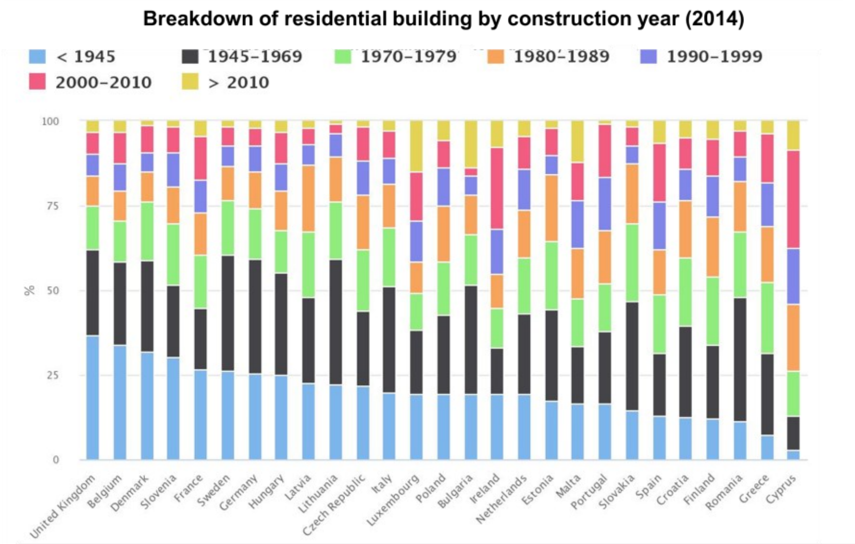

Figure 1.7 - Breakdown of residential building by construction year (2014) [14]

The typology of the residential building, i.e. single-family or multi-family houses, is significantly different across Europe. This information is important because the type of dwelling affects the space heating performances, due to the different areas of dispersing walls in contact with the outdoor. Italy and Estonia are the countries with the largest number of multifamily buildings (more than 70%), while Ireland and the United Kingdom are predominately characterized by single-family dwellings. More in general, by considering the EU average, the type of dwelling has almost the same share, with an average of 49% for multi-family dwellings.

According to the available data of the *EU Building Stock Observatory* for the residential sector, in 2013, the energy consumption by end-use has the highest share in space heating. Indeed, in most countries, the heating expense is around 60-80% of total energy consumption. A considerable share is also due to water heating (13%) and electrical appliances (12%). By considering the annual energy consumption per m^2, as an average value for all types of buildings in the EU, it was 180 kWh/m^2 in 2013. Obviously, there are big differences among countries, depending on the climatic conditions and energy performances of the building stock, evident in Figure 1.8. In the majority, the countries with the highest energy consumption for buildings are also, those with the oldest building stock, like Romania (308 kWh/m^2) or Belgium (262 kWh/m^2). On the contrary, Portugal, Cyprus, and Malta have the lowest rates for energy consumption of residential buildings, respectively 70 kWh/m^2, 69 kWh/m^2, and 47 kWh/m^2 [15].

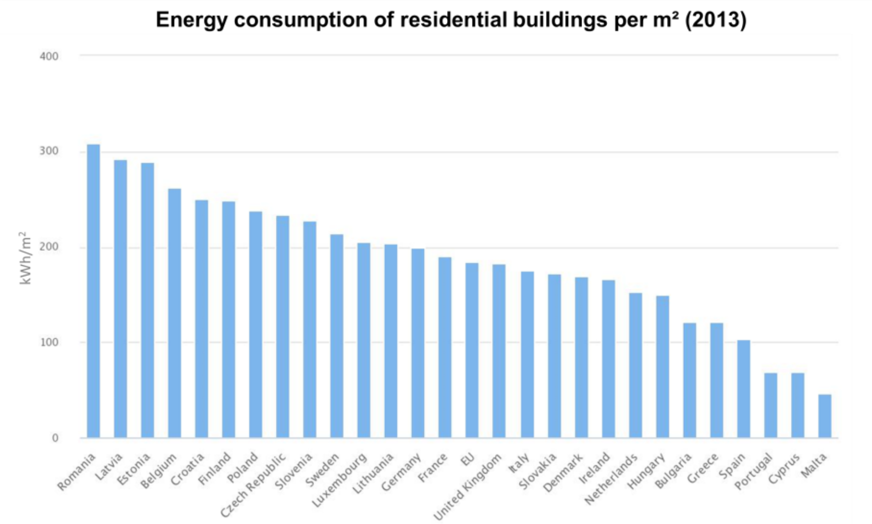

Figure 1.8 - Energy consumption of residential buildings per m² during 2013 (normal climate) [15]

As evident, the necessity of energy refurbishment of the European building stock has become prominent, and thus, starting from 2002, the EU has enacted the first Directives in energy matter. In the following sub-section (1.1.2), an overview of the European legislation about the building sector is reported.

1.1.2. European legislation in the building energy matter

By considering the high energy demand of European buildings, the EU has introduced requirements for the renovation of the existing building stock in the Energy Performance of Building Directives (EPBDs). In particular, the first EPBD was the 2002/91/EU [16] which introduced the first measures, at the EU level, in terms of energy building efficiency, regarding both existing and new buildings. This Directive sets also common methodologies for the estimation of energy consumption and the energy labels. In 2010, the EPBD 2002/91/EU [16] was replaced and integrated by EPBD recast 2010/31/EU [17] which promoted the major renovation of buildings fulfilling the cost-optimal energy performance requirements. This means: *"energy performance which leads to the lowest cost during the estimated economic life cycle".* The Directive further introduced mandatory energy labels for private buildings in case of sale or rent. The main new aspect was the definition of nearly Zero Energy Building (nZEB): *"a building that has a very high energy performance, which means that nearly zero or very low amount of energy required should be covered to a very significant extent by energy from renewable sources, including energy from renewable sources produced on-site or nearby".* New obligations were imposed for all new buildings. Indeed, all new buildings built from 31 December 2020 must be nZEB, with the exception of public buildings - occupied and owned by public authorities - which have the same obligation but starting from two years before. Article 7 of EPBD recast 2010/31/EU concerns precisely the existing building stock and incentive the MS in establishing requirements that lead to the investment in the building refurbishment and underline the importance of a global intervention for the whole sector and not as single operations. Article 2 of the same Directive, defines the major renovation, and establish that it occurs when:

- the total cost of the intervention, on the envelope or the technical systems, is higher than 25% of the building value, or,
- when surface under renovation is more than 25%.

Regarding energy efficiency of buildings, in 2012 the Energy Efficiency Directive (EED 2012/27/EU [18]) was enacted to encourage the MSs in establishing strategies for the renovation of their buildings and to annually refurbish the 3% of the central government building stock. Common measures for the promotion of Energy efficiency were established, to guarantee the achievement of the goals defined by the Climate and Energy 20-20-20 plan. In particular, the MS had to promote energy saving through national strategies and targets. This Directive was updated and included in Directive 844/2018 [19] which accelerate the building renovation by employing more energy-efficient systems and smart solutions for energy management. In particular, to promote the improvement of building energy efficiency and the renovation of the building stock by 2050, this regulation forces each Member State to establish a long-term renovation strategy and to transpose its provisions within 20 months. The use of smart technologies, electromobility infrastructure deployment in building car parks, building automation are some of the novelties introduced.

Starting from 2002, the MSs put themselves on the line to implement the EPBD into national legislation, each one in a different manner, and at different times, but with a common aim: reach the EU goals and recommendations. New requirements for new and existing buildings, cost-effective measures, financial supports for the construction of NZEB or for the major renovation of existing buildings are the key points of the European regulations.

The aforementioned EU Directives were transferred into national legislations, and even if not all the MSs transposed the last update of EPBD, each of them has promoted incentive mechanism for the building energy refurbishment during the last years. The financial incentives could be part of structural funds, other public funding, as well as EU or national funding. In any case, cost-optimal levels must be considered when the incentives are provided for new construction or major renovation. According to the group of buildings, public or private, residential or nor, the policy packages about the implementation of EPBD prescriptions on investments for energy renovations or new constructions, are different.

For what concerns residential buildings, many policies have been enacted in the EU countries to promote the renovation of buildings and the use of RES but two packages can be considered exemplary: the Danish initiative “BetterHouses” and the UK’s “Green Deal” policy. Both programs are aimed at supporting the owners to finance and plan the energy renovations of their buildings. The first one provides consultant support in all the phases of the renovation, starting from the screening of the building to the construction and follow-up. The second one, discontinued in 2015, was based on a Green Deal Advice Report that identified the possible energy refurbishment interventions with relative savings. The building owners, once decided the measures to apply, could take out a loan and have a paid back through the energy bills. In Finland, a subsidy program was set by the Ministry of Environment and is available for small houses or public and private buildings. Information campaigns and advice programs are encouraged by the Finnish program, such as “Kuluttajien energianeuvonta” (consumer energy advice program), which promote the use of RES and energy efficiency in homes and households, and the information campaign for housing companies launched by the Ministry of Environment in 2016 to help for the implementation of energy efficiency measures [20]. In France, from September 2020, France new objectives in the stimulus plan were established, giving prominence to the energy-efficient renovation of buildings: 4 billion euros has been devoted to the refurbishment of public buildings. For the period 2021-2022, a new bonus for global renovation is accessible for private housing.

Even the Italian Incentive mechanisms have undergone an important increment and update during the last year, and the following sub-section (sub-section 1.2.1) is entirely dedicated to the new Italian funding program, and some examples of application on real case studies are reported in CHAPTER 5.

1.2. The Italian framework.

Evaluating the national situation, one of the most important acts in the Italian legislative framework, is the Italian Decree n. 63 of the 4th June 2013 [21] concerning "*Urgent provisions for the implementation of Directive 2010/31/EU of the European Parliament and of the Council of 19th May 2010 on the energy performance of buildings for the definition of infringement proceedings put in practice by the European Commission, as well as other provisions in the matter of social cohesion*". During 2015, another significant decree entered into force (the Italian Ministerial Decree 26/06/2015 [22]) to define the energy performance calculation methods and establish obligations and minimum requirements for buildings. It introduces new prescriptions, both for the construction of new buildings and the renovation of the existing ones, and specifies the methodologies for calculating the energy performance of buildings. The Decree implemented Law no. 90/2013 [23] and integrates and modifies Decree no. 192/2005 [24].

According to the Italian Decree 26/06/2015 [22], during the design phase, some parameters must be verified, including those referring to single building components, such as thermal transmittances of the building envelope, and those referring to the whole building, like the EP indicator. The index identifies the energy performance of the building that can be evaluated by comparing the building under investigation and a reference one. These two buildings have the same location, shape, function, and size but the reference building has reference parameters to define the envelope and technical systems. Therefore, for each building to be evaluated, a reference building must be defined.

The Italian Decree 26/06/2015 [22], for the EP calculation method refers to the UNI/TS 11300 series, which specifies a quasi-steady state calculation method based on EN ISO 13790 and EN 15316 series. The relevant standard describes how to calculate the primary energy for space heating, cooling, and

DHW and how to consider the heat gains in the energy calculation. In any case, standard building use and climate input data are considered for the asset energy rating.

The last Italian Decree is the Decree n. 48 of the 10th June 2020 which implements Directive 2018/844 of European Parliament and of the Council of 30th May 2018, amending Directive 2010/31/EU on energy performance in buildings and Directive 2012/27/EU on energy efficiency. It promotes the improvement of the energy performance of buildings, by considering the local and external climatic conditions, as well as of the requirements related to indoor climate and effectiveness in terms of the costs of the planned actions, optimizing the relationship between charges and benefits for the community.

1.2.1. The Italian funding programs

A new impulse in the research on building energy-saving and mainly on the evaluation of economically feasible designs has been given by the COVID-19 pandemic. Indeed, according to the International Energy Agency, the COVID-19 pandemic brought an increase in energy consumption in the residential sub-sector due to restrictions to free mobility, extended lockdown, the spread of teleworking, and e-Learning. In 2020, in the United States, the energy demand increased by 6-8% compared with the previous year. On the other hand, the economic crisis due to the pandemic heavily impacted construction activities and related sectors, which employ around 10% of the global workforce [25]. To face this crisis, with high risks of loss of jobs, the EU has put in place strategies and investments for doubling the annual energy renovation rates over the next ten years, reducing the greenhouse gas emissions, and creating up to 160 000 additional jobs in the construction sector by 2030 [26].

Before the COVID-19 pandemic, in Italy, the financial support to energy efficiency measures in private buildings consisted of a tax reduction from 50 to 85% over 10 years (called “Eco-bonus"). In special cases, also 90% could be achieved. In May 2020, the so called “Recovery Decree” [27], converted in law on July 2020 and modified with the Budget Law of 30th December, concerning social policies to face the COVID-19 emergency, increased the tax deduction rate to 110% for expenses incurred from July 2020 to the end of June 2022 (for some measures also June 2023), to support the building sector renovation. It is the so-called “Super-bonus”.

The tax reduction must be divided into 5 annual rates, with an equal amount, for the costs incurred by 31st December 2021, and in 4 rates for the expenses incurred during 2022. In addition to the tax deduction, it is also possible to transfer credit to suppliers or other active parties or even to obtain (if the construction company agrees) an equal direct discount of the costs; in this case, the construction company becomes the owner of the credit.

The tax reduction is recognized for investments aimed at increasing the energy performance of multi-family buildings and individual homes, common parts of multi-family buildings, or units functionally independent and with one or more independent accesses.

The tax reduction of 110% is recognized if at least one of the main EEMs, called “driving measures” is applied:

- Driving 1: thermal insulation of building envelope with an incidence ≥ 25% of the total heat transfer surface (i.e., the building envelope area), using insulation materials complying with minimum environmental criteria [28].
- Driving 2: replacement of heating systems with (i) condensing boiler; (ii) heat pump; (iii) hybrid system; (iv) micro-cogeneration system; (v) solar collectors; (vi) biomass boiler; (vii) district heating, if specific performance criteria are met.
- Driving 3: anti-seismic interventions for the building located in seismic zones 1, 2 or 3 according to the Italian classification.

For driving 1 and driving 2 measures the maximum expense is respectively 50’000 € and 20’000 € for individual apartment units. Some requirements must be respected for achieving the incentive. For both considered driving measures, the energy labeling at the end of the work must demonstrate an improvement of at least two energy classes; when this is impossible, the best class (i.e., the A4 according to Italian standard) must be obtained. Moreover, in the case of Driving 1, the obtained values of thermal transmittance must respect the high insulation standard recommended in the Ministerial Decree [29]. For instance, according to the climatic zone, the threshold value for the vertical envelope varies from 0.22 W/m^2 K to 0.38 W/m^2 K; for the windows, it ranges from 1.00 W/m^2 K to 2.60 W/m^2 K.

Moreover, for the replacement of the heating system, the standard to be respected depends on the type of system. For instance, the air-to-air electric heat pump must be characterized by a minimum coefficient of performance (COP) of 3.9 during heating use and a minimum energy efficiency ratio (EER) of 3.4 during cooling operation. Moreover, for the replacement of heating systems with condensing boilers, the seasonal energy efficiency must be equal or greater than 90% (i.e., class A according to regulation 811/2013 of the European Commission [30]) or, for condensing boilers with a power exceeding 400 kW, the thermal efficiency should be not lower than 98.2%, measured according to UNI EN 15502 [31] standards.

Other EEMs (such as window replacement, solar shields, PV system, devices for home automation, and so on) called “driven measures”, if applied jointly with at least one of the “driving measures”, can also benefit from the tax deduction of 110%. It is possible also to carry out two “driving measures” simultaneously in the same building.

1.3. Energy refurbishment of existing buildings: the state-of-art.

Considering the premises of previous sections, the energy refurbishment of existing buildings assumes a role of central interest during this historical period. Indeed, in accordance with the high and ambitious goals of the EU Directive 844/2018 [19], within 2020 the EU countries must have a quite decarbonized building stock, so that the standard of NZEB has been extended, progressively, also to the existing built environment.

An energy refurbishment can be approached according to different intervention technologies:

1) Passive strategies for the building envelope.

2) Active strategies for the improvement of systems for the microclimatic control (Heating, Ventilation, and Air Conditioning).
3) Integration of systems powered by renewable energy sources.

As inferred by [32], usually all three “levers” (i.e., building envelopes, active energy systems, renewables) for energy efficiency must be covered, consecutively, to reduce firstly the heat gains, then the energy demands, and finally by allowing energy conversion by means of renewable sources.

In this regard, Kuusk *et al.* [33] investigated the energy criticalities and refurbishment potential of buildings of the sixties and seventies, both in Estonia and Germany, by considering all levers of energy improvements and thus renovation of the building components and envelopes, replacement of windows, new and renovated heating and ventilation systems complying with the new national requirements implementing the EU guidelines. It is very interesting to note that, according to the authors, to fulfill the goal of a decarbonized building stock by 2050 and to do this target really cost-effectively, a doubled renovation rate of 3%/years would be necessary.

The renovation of existing buildings is a very wide theme, indeed, in addition to the climatic zone in which the building is located, the age of construction of the building varies the design of energy efficiency measure according to the thermophysical properties of the building and the existing system for the microclimate control. For a historic building, for example, the refurbishment interventions are very dissimilar compared to a building from the 70s and often, some interventions must be excluded to preserve the historical value of the building. The external thermal insulation of the envelope or the installation of wall integrated PV panels cannot be carried out on a wall of artistic value. The topic of the refurbishment of protected buildings is proposed by Sugár *et al.* [34] that considered the traditional apartment houses of Budapest, usually dated between the end of the 19th and the beginning of the 20th century. The refurbishment need is very up-to-date, being Hungary characterized by a very low turn-over rate in the building sector (1.7%/yr). Their target was to achieve the nZEB standard, by improving also the structural behavior, by finding the best trade-off between preservation and energy-structural improvement and it was demonstrated the reliability of these goals, by reducing till the 69% the energy demands for the space heating and the production of DHW.

Generally, the most common energy refurbishment cases are those of reinforced concrete buildings built between 1960 and 1990 which have a poor quality envelope, dated microclimatic control systems, and lighting systems.

About that, Monzón-Chavarrías *et al.* [35] propose cases studies in two extreme Portuguese climates. These are multifamily buildings, with dwellings of 80-100 m^2, 2-3 floors, and construction periods between 1960 and 1990 (around 45% of buildings are built in these years). The buildings were in reinforced concrete (like in Italy, Spain, Greece) with double-brick walls with an inner air chamber, single glass windows (U_{value} = 5.7 W/m^{2}K), gas/GLP/butane boilers for DHW, gas or electric systems for the space heating, electric systems for cooling. The locations were Faro (the warmer city of Portugal) and Guarda (in the north, the colder one). In the original state, the primary energy demand was about 46-223 kWh/m^{2}y in Faro, 134-627 kWh/m^{2}y in Guarda. The nZEB retrofit requires interventions on both building envelope and energy systems. To achieve the nZEB target the thermal and energy demands should be lower by about 13 kWh/m^{2}y and 51 kWh/m^{2}y (heating energy annual nominal needs) in Faro and Guarda, respectively, while the total primary energy demands are variable, and it depends on the installed systems. The Portuguese regulations oblige to cover at least 50% of the primary energy needs by renewable energy sources. In both cities, to fulfill this standard, it was necessary to retrofit both the building envelopes (with U_{values} much more restrictive than those indicated for major renovations) and to replace the active energy systems.

After this brief overview of energy refurbishments of European buildings, this Thesis work will present interesting energy retrofits of predominantly reinforced concrete buildings built between 1960 and 1990, through different technologies, innovative and traditional, and different approaches.

CHAPTER 1 – References

[1] Global Status Report for Buildings and Construction 2019. https://www.iea.org/reports/global-status-report-for-buildings-and-construction-2019. Accessed in November 2021

[2] Intergovernmental Panel on Climate Change. Printed October 2018 by the IPCC, Switzerland. ISBN 978-92-9169-151-7. Summary for Policymakers are available from the IPCC website www.ipcc.ch. Accessed in November 2021

[3] National Aeronautics and Space Administration (NASA) - Goddard Institute for Space Studies. https://data.giss.nasa.gov/gistemp/ Accessed in November 2021

[4] Levitus, S.; Antonov, J.; Boyer, T.; Baranova, O.; Garcia, H.; Locarnini, R.; Mishonov, A.; Reagan, J.; Seidov, D.; Yarosh, E.; Zweng, M. (2017). NCEI ocean heat content, temperature anomalies, salinity anomalies, thermosteric sea level anomalies, halosteric sea level anomalies, and total steric sea level anomalies from 1955 to present calculated from in situ oceanographic subsurface profile data (NCEI Accession 0164586). Version 4.4. NOAA National Centers for Environmental Information. Dataset. doi: 10.7289/V53F4MVP https://www.nodc.noaa.gov/OC5/3M_HEAT_CONTENT/index3.html. Accessed in November 2021

[5] National Aeronautics and Space Administration (NASA) - Goddard Institute for Space Studies, GISS Surface Temperature Analysis. https://data.giss.nasa.gov/gistemp/maps/. Accessed in November 2021

[6] M. Brunetti, M. Maugeri, F.Monti, T. Nanni, Temperature and precipitation variability in Italy in the last two centuries from homogenised instrumental time series, International Journal of Climatology 26: 345–381 (2006) Published online 25 January 2006 in Wiley InterScience. Doi: 10.1002/joc.1251. www.interscience.wiley.com. Accessed in November 2021

[7] Perkins-Kirkpatrick, S. E., & Gibson, P. B. (2017). Changes in regional heatwave characteristics as a function of increasing global temperature. Scientific Reports, 7(1), 1-12.

[8] Fischer, E. M., & Knutti, R. (2016). Observed heavy precipitation increase confirms theory and early models. Nature Climate Change, 6(11), 986-991.

[9] Hegerl, G. C., Black, E., Allan, R. P., Ingram, W. J., Polson, D., Trenberth, K. E., ... & Zhang, X. (2015). Challenges in quantifying changes in the global water cycle. Bulletin of the American Meteorological Society, 96(7), 1097-1115.

[10] BP Statistical Review of World Energy 2021. Available online: https://www.bp.com/content/dam/bp/business-sites/en/global/corporate/pdfs/energy-economics/statistical-review/bp-stats-review-2021-full-report.pdf. Accessed in November 2021

[11] BP energy outlook 2020 edition. Available online: https://www.bp.com/content/dam/bp/business-sites/en/global/corporate/pdfs/energy-economics/energy-outlook/bp-energy-outlook-2020.pdf. Accessed in November 2021

[12] EU 2030 climate and energy framework. https://ec.europa.eu/clima/policies/strategies/2030_it#:~:text=Obiettivi%20chiave%20per%20il%202030,5%25%20dell'efficienza%20energetica. Accessed in November 2021

[13] EU Emissions Trading System (EU ETS) https://ec.europa.eu/clima/policies/ets_en. Accessed in November 2021

[14] EU 2050 long-term strategy. https://ec.europa.eu/clima/policies/strategies/2050_en. Accessed in November 2021

[15] EU Buildings Factsheets - Energy use in buildings. https://ec.europa.eu/energy/eu-buildings-factsheets_en. Accessed in November 2021

[16] EU Commission and Parliament Directive 2002/91/EU of the European Parliament and of the Council of 16 December 2002 on the energy performance of buildings. Off. J. Eur. Union 2003. Available online: https://eur-lex.europa.eu/legal-content/EN/TXT/PDF/?uri=CELEX:32002L0091&from=EN. Accessed in November 2021

[17] EU Commission and Parliament, Directive 2010/31/EU of the European Parliament and of the Council of 19 May 2010 on the energy performance of buildings (EPBD Recast). Off. J. Eur. Union 2010. https://eur-lex.europa.eu/LexUriServ/LexUriServ.do?uri=OJ:L:2010:153:0013:0035:EN:PDF. Accessed in November 2021

[18] Directive 2012/27/EU of the European Parliament and of the Council of 25 October 2012 on energy efficiency, amending Directives 2009/125/EC and 2010/30/EU. https://eur-lex.europa.eu/legal-content/EN/TXT/?uri=CELEX:32012L0027. Accessed in November 2021

[19] Directive (EU) 2018/844 of the European Parliament and of the Council of 30 May 2018. Available online: https://eur-lex.europa.eu/legal-

content/EN/TXT/PDF/?uri=CELEX:32018L0844&from=IT. Accessed in November 2021

[20] Finnish code of building regulation, Helsinki, Finland

[21] DECRETO-LEGGE 4 giugno 2013, n. 63. Availabe online: https://www.gazzettaufficiale.it/eli/id/2013/06/05/13G00107/sg. Accessed in November 2021

[22] DM, 2015. Italian Ministerial Decree DM 26/06/15. Applicazione delle metodologie di calcolo delle prestazioni energetiche e definizione delle prescrizioni e dei requisiti minimi degli edifici. Official Bulletin of the State n. 39 of July 15th 2015. (In Italian)

[23] LEGGE 3 agosto 2013, n. 90. https://www.gazzettaufficiale.it/eli/id/2013/08/03/13G00133/sg (In Italian). Accessed in November 2021

[24] DECRETO LEGISLATIVO 19 agosto 2005, n. 192. https://www.gazzettaufficiale.it/eli/id/2005/09/23/005G0219/sg (In Italian). Accessed in November 2021

[25] International Energy Agency, The Covid-19 Crisis and Clean Energy Progress, Report June 2020.

[26] EU Commission, A Renovation Wave for Europe - greening our buildings, creating jobs, improving lives, Brussels, 2020.

[27] DL n. 34, 19/05/ 2020, Italian Law Decree, “Urgent measures in the field of health, support for work and the economy, as well as social policies related to the epidemiological emergency from COVID-19”, 2020.

[28] Decree 11 October 2017, n.259, “Minimum environmental criteria for the award of design services and works for the new construction, renovation and maintenance of public buildings”, 2017.

[29] DM 6/9/2020, Italian Ministerial Decree, “Requisiti tecnici per l'accesso alle detrazioni fiscali per la riqualificazione energetica degli edifici - cd. Ecobonus”, (In Italian), 2020.

[30] Commission Delegated Regulation (EU) No 811/2013 of 18 February 2013 supplementing Directive 2010/30/EU of the European Parliament and of the Council with regard to the energy labelling of space heaters, combination heaters, packages of space heater, temperature control and solar device and packages of combination heater, temperature control and solar device.

[31] UNI EN 15502-1: Gas-fired heating boilers - Part 1: General requirements and tests. 2015.

[32] Santamouris, M.; Kolokotsa, D. Passive cooling dissipation techniques for buildings and other structures: The state of the art. Energy Build. 2013, 57, 74–94.

[33] Kalle Kuusk, Jens Naumann, Annina Gritzki, Clemens Felsmann, Michele De Carli, Massimo Tonon and Jarek Kurnitski, Nearly zero energy renovation concepts for apartment buildings, 12th Nordic Symposium on Building Physics (NSB 2020), E3S Web of Conferences 172, 18009 (2020) Volume 172, 2020, article number 18009, 7 pages, https://doi.org/10.1051/e3sconf/202017218009.

[34] Viktória Sugár, Attila Talamon, András Horkai, Michihiro Kita, Energy saving retrofit in a heritage district: The case of the Budapest, Journal of Building Engineering, Volume 27, 2020, 100982, ISSN 2352-7102, https://doi.org/10.1016/j.jobe.2019.100982.

[35] Marta Monzón-Chavarrías, Belinda López-Mesa, Jaime Resende, Helena Corvacho,The nZEB concept and its requirements for residential buildings renovation in Southern Europe: The case of multi-family buildings from 1961 to 1980 in Portugal and Spain, Journal of Building Engineering, Volume 34, 2021, 101918, ISSN 2352-7102, https://doi.org/10.1016/j.jobe.2020.101918.

CHAPTER 2.

Methodological approach for energy investigation of existing buildings

The energy efficiency of buildings has assumed the main role in the international and national legislation, and in the design and construction phases of the buildings. Traditional and innovative energy efficiency solutions, both for the passive and active systems, (e.g. phase change materials…) are analyzed and developed to reduce the building energy demand and to achieve environmentally friendly buildings. However, what is the main methodological approach to evaluate the technologies and solutions proposed for a building energy refurbishment? This chapter answers this question by describing the main methodologies for the energy investigation of buildings.

As recurrent in the scientific literature and in the current practice, two different approaches can be used to evaluate the energy efficiency measures proposed for a single building component or the whole system "building envelope/HVAC plant":

a) the numerical approach based on the implementation of a physical/mathematical model, in many cases in a simulation environment;
b) the experimental approach based on a controlled or real environment.

Obviously, the two methods can be combined to perform a more detailed and accurate energy analysis. In any case, the choice of the methodological approach depends on the available time and economic sustainability, as well as the computational and experimental available resources.

It should be also underlined that a building is a complex system from a physical point of view, and it is influenced by a wide range of boundary conditions. Indeed, an energy efficiency intervention can also affect the illuminance conditions of the building or its acoustic performance. For these reasons, a complete evaluation of the building under investigation needs a multi-domain analysis to characterize the building also in other fields of environmental comfort (acoustic, daylight, etc.) than merely the thermal and hygrometric ones.

This chapter will present an overview of the numerical methods for the building energy analysis, focusing on the Building Energy Simulations (BES) and Computational Fluid Dynamic (CFD) simulations. Moreover, the economic analysis for an energy refurbishment will be presented, as a cost-optimal evaluation of the energy efficiency interventions.

2.1. Energy analysis through a numerical approach

The evaluation of the energy performances of the HVAC-building systems can be performed through two types of numerical approaches: a) a simplified or even semi-stationary method and b) the dynamic thermo-energetic method. The first one analyzes the interaction between the building and the external environment on a macroscopic perspective, through a set of algebraic equations, while the second one is based on a dynamic simulation, numerically solved through iterations, that considers all the transitory phenomena affecting the performances of the integrated system building-HVAC plants (i.e., hourly and sub-hourly weather conditions, electric equipment, occupancy, thermal transmittance and inertia of the building envelope, transient heat transfer phenomena, scheduled use of systems and facilities, the performance of the systems for the microclimatic control at the part loads conditions, etc.). In this case, two modeling approaches are possible: the nodal network or multizone model, and the computational fluid dynamics [1].

The nodal network or multizone approach is a zero-dimensional evaluation, that considers each building zone as a node with homogeneous thermal, hygrometric and pressure distributions. It is a time-dependent simulation that treats the building and its ventilation plants as a group of nodes representing rooms, environment conditions, equipment connection points, and so on. Doors, windows, fans, ducts, and pumps are represented by internodal connections. To each component is then assigned a model that defines its mass flow rate as a function of the prevailing pressure difference.

The multizone modeling approach is employed by a lot of building energy simulation software, because the computation time is reasonable, and the implementation is easy. The limitation of a BES tool is that the stratification of airflows, spatial variation of indoor microclimate, distribution of species and contaminants, cannot be simulated, and thus the distributions of local thermal comfort and air quality of the occupied zone cannot be predicted.

In the CFD analysis - based on two different approaches, and thus FVM and FEM (Finite Volume and Finite Element Methods, respectively), the building zones are assimilated to a computational grid, and are divided into several control volumes, whose airflow is described by solving the Navier Stokes equations. This analysis carries out a space domain simulation, by means of a spatial discretization, and it can predict the airflow and temperature distribution for each control volume of the building zone. A CFD analysis requires high computational efforts, and the results depend on the boundary conditions. In the majority, the CFD simulations are performed by considering fixed boundary conditions (fixed supply airflow rate and temperatures, fixed wall temperatures, and heat flux through the envelope). Really, wide, and large application of CFD in buildings is not very common, due to the lack of codified methods, the great computational effort, difficulties in calculating dynamic boundary conditions in buildings.

In general, a CFD analysis evaluates the temperature and airflow distribution of a building in a space domain, while a BPS predicts the energy performance of a building and quantifies all the relevant aspects for the design, construction, operation, and control of the building in a time domain. In any case, to overcome the limitations of both analyses, a coupled approach CFD and BES [2] can be the right to come out with a critical and complete analysis of the building energy performance and of its indoor comfort conditions.

In the following sub-sections, the BES with nodal networks model and CFD analysis are presented, focusing also on a coupled approach of both numerical simulations.

2.1.1. Simulations in the time domain: BES for building audit

A dynamic energy simulation estimates the energy performances of an HVAC-building system, taking into account both the microclimatic control performances and the energy demand. Several energy simulation tools were developed over the last years, with different levels of complexity and response to different variables. The most diffused area: EnergyPlus, ESP-r (Energy Simulation Software tool), TRNSYS, the IDA ICE (Indoor Climate Energy), and IES-VE (Integrated Environmental Solutions - Virtual Environment). The numerical codes for BES can be based on different algorithm resolution methods and can be structured in different ways, but a common logical scheme can be defined. In general, all the BES tools provide for the building modeling, and thus the definition of geometry and thermophysical properties, and the definition of the systems for the microclimatic control. In the following chapters (CHAPTER 1 to CHAPTER 5), some case studies will be described, and various dynamic energy analyses will be proposed by using the calculation engine EnergyPlus [3] (U.S. Department of Energy). This simulation engine is well-accredited by the international scientific community and collects many program modules that work together to carry out results in energy terms (i.e., heating, cooling, ventilation) by adopting various systems, innovative or traditional, and energy sources (Figure 2.1). The energy flows in systems, the transient thermal heat transfer phenomena, and the overall behavior of the facility in terms of energy consumption for each active system, internal loads, and generation from renewable sources, are effectively evaluated by the code, as many validations papers and tests testify: https://energyplus.net/testing. Energy balances of complex systems exposed to different environmental and operating conditions can be solved by this code. The main module of the EnergyPlus is the building and HVAC simulation manager. The architecture of the code is complex and interactive, and several boundary conditions are necessary to obtain reliable results, as shown in Figure 2.1.

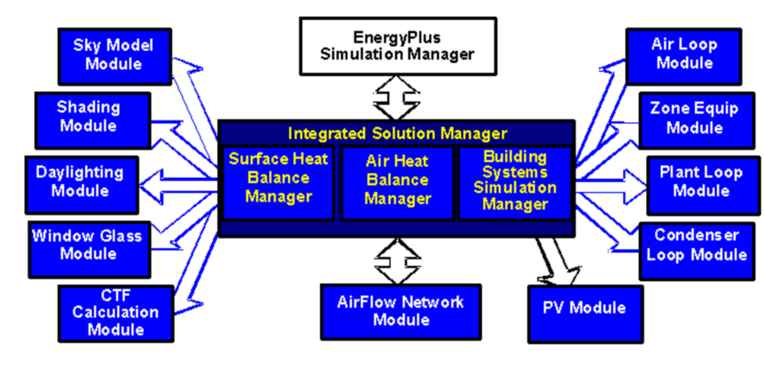

Figure 2.1 – Schematic program of EnergyPlus: architecture of the code (source: EnergyPlus Documentation)

The definition of a numerical model for the dynamic energy simulation is quite the same in all the available simulation codes because even if different, the architecture is similar. In the first stage, the thermophysical properties of the building envelope are defined, both for the opaque and transparent, as well as the component layers of the envelope and the building geometry. All the endogenous gains are defined with proper schedules (i.e. lights, occupants, and electric equipment) and the systems for the microclimatic control with relative components are implemented. At the same time, the weather conditions must be defined, by selecting a weather file. The most diffused weather files are TRY [4], IWEC [5], or TMY2 [6] or developed by the users, by using some software (e.g., https://meteonorm.com/en) or experimental measured data. The resolution method commonly employed for the evaluation of the building thermal loads, of the energy demand required by the HVAC, and the thermodynamic condition of the indoor air, is the Conduction Transfer Functions (CTF). The thermal loads, which consist of the sensible heat loads and the latent ones, are evaluated through the resolution of transfer functions, that, for each building component, describe the physical phenomena among the emerging variables and the editing ones, and thus between the causes and effects. A stated by the developers of EnergyPlus, the main strength of CFT is the elegance; indeed, in the common adoption of the state – space representation, outputs (i.e., heat flows) are calculated directly through the inputs (i.e., indoor and outdoor series of temperatures), by neglecting the thermal fields in the building component and thus by avoiding the resolution and calculation of nodal temperatures.

When thermal field and temperature distributions inside the wall have to be calculated, other sets of solution algorithm can be employed for the energy simulation, such as the conduction finite-difference algorithm (Con-FD), with a Crank Nicholson difference scheme, that is generally used for the BPS of buildings with Phase Change Materials in the building components (CHAPTER 1).

In general, by considering a building energy refurbishment, a BPS is a necessary instrument to evaluate the energy efficiency measures proposed, concerning both the building envelope and the HVAC systems, in terms of energy saving, environmental impact, and economic profitability. The limitation of a BES is that the whole environment, or thermal zone, is represented by a single node (i.e zero-dimensional evaluation) by assuming a perfect mixing ventilation condition, so it cannot give results about the thermal stratification or the airflow distribution of the selected environment.

To solve the energy balances, the simulation codes are based on a set of mathematical equations, which can be divided into two main groups: the first one contains the resolution algorithms for the delimiting surfaces of the building (walls, roof, basement, windows, and, generally, all the surfaces that compose the building envelope (Equation (2.1)), the second relates to the indoor air conditions (Equation (2.2).

$$q_{i,cond} + q_{i,s-rad} = \sum_{k=1}^{N} q_{ik,rad} + q_{i,conv} \tag{2.1}$$

$$\sum_{i=1}^{N} q_{i,conv} \cdot A_i + Q_{other} - Q_{extract} = \left(\rho \cdot V_{room} \cdot c_p \cdot \Delta T_{room}\right)/\Delta t \tag{2.2}$$

where

- $q_{i,cond}$ = conduction thermal flux interesting the surface i;
- $q_{i,s\text{-}rad}$ = radiative thermal flux interesting the surface i, between the surface and an internal or solar heat source;

- $q_{ik,rad}$ = radiative thermal flux between the surface i and a surface k;
- $q_{i,conv}$ = convection thermal flux interesting the surface i;
- $\sum_{k=1}^{N} q_{i,conv} \cdot A_i$ = convective heat exchange between the surface i (area = A_i) and the indoor air;
- Q_{other} = thermal gains due to the presence of people, installed equipments, artificial lightings, etc…;
- $Q_{extract}$ = total thermal loads that has to be balanced;
- $(\rho \cdot V_{room} \cdot c_p \cdot \Delta T_{room})/\Delta t$ = energy exchange relative to the indoor air;
- ρ = air density;
- c_p = air specific heat capacity;
- ΔT = indoor air temperature difference;
- Δt = time step reference period (usually 1 hour).

Equation 2.1 provides results for the indoor surface temperatures and quantifies the convective energy exchanges involving these surfaces. Equation (2.2) evaluates the mean indoor air temperatures and the total thermal load that should be balanced. Indeed, it can be written:

$$q_{ik,rad} = h_{ik,rad} \cdot (T_i - T_k) \tag{2.3}$$

$$q_{i,conv} = h_{i,conv} \cdot (T_i - T_{i,air}) \tag{2.4}$$

where

- $h_{i,rad}$ = linearized radiative heat exchange coefficient;
- $T_{i,}$ = temperature of the inner surface i;
- $T_{k,}$ = temperature of the inner surface k;
- $T_{i,air}$ = temperature of the indoor air near the surface k;
- $h_{i,conv}$ = convective heat exchange coefficient (usually assumed constant, or estimated through empirical equations);

The EnergyPlus code allows the simulation of cooling, heating, lighting, and ventilation, and all the energy flows and is structured into three main sections:

- the simulation manager,
- the heat balance simulation manager,
- the system simulation manager

The simulation manager is the tool that provides and controls the interaction between the other simulation tools at the same time-step (hourly or sub-hourly) and for the whole simulation period. It also manages the input and output boundary conditions.

For what concerns the heat and mass balance simulation module, it is based on evolved BLAST [7] procedures and manages the sub-modules for energy balances of the indoor air and the building surfaces, acting as a bridge between the heat balance and the simulation manager of the building system. It provides for the thermal zone calculation, assuming the indoor air and the room surfaces with uniform temperature levels. In addition, it is assumed that the building envelope is interested in the same long and short-wave irradiation and one-dimensional heat conduction. The simulation manager of heat and mass balance implements different calculation tools (Comis, Window 5, Daylight module, Ground Heat Transfer), in order to evaluate and simulate different technical solutions.

Finally, the building system simulation tool controls the calculation of HVAC and electrical systems in the same temporary range, by considering the zone conditions as regards the microclimatic indoor control. It is based on the HVAC air-side and the water (water loops) modules that represent the center of the code sections; these are user-changeable, to allow the variation and implementation of several kinds of water pipes and air ducts, such as defined in the real building.

The potentiality of a simulation engine like EnergyPlus is that new modules and features can be added, with quite extended flexibility, to implement new physical solvers and extend the tool routines. Today, it is one of the most employed codes for the evaluation of the building and HVAC performances, both as regards the microclimatic conditions and the energy request.

Among EnergyPlus, the software DesignBuilder [8] was employed in most of the studies presented in the following chapters. The software is a graphical interface of EnergyPlus that allows the geometric modeling of the building and the export of simulation results. In addition, it was used for CFD simulations, in order to evaluate the conditions of purity and healthiness of the air, as well as the distributions of temperature and air velocity in indoor environments (CHAPTER 4). Really, many other interfaces have been released in the last years, for both pre-processing and post-processing. Finally, EnergyPlus is a powerful engine, often accompanied by the use of libraries and tools developed by third parties.

2.1.2. Simulations in space domain: CFD analysis for the building indoor environment

A Computational Fluid Dynamic simulation is a valid tool to evaluate the indoor air conditions of indoor environments. This analysis can forecast the performances of a mechanical ventilation system and estimate the distribution of the conditioned and supply air in indoor spaces. In a fixed temporary moment, a CFD simulation concurs to understand the kinetic fields of an indoor environment, the spatial trend of each parameter that define the indoor microclimate (e.g. temperature and air velocity), the thermal-hygrometric comfort, and the indoor air quality (IAQ). The CFD results require significant computational effort, due to the creation of the simulation model, but mainly the resolution of complex systems of equations, necessary to obtain detailed information on the kinetic, thermal, and hygrometric fields related to the indoor air thermodynamic states. For this reason, the CFD analyses are generally limited to single rooms, in steady-state conditions. It means that, unless a very high specialization (with an enormous computational effort), time dependent CFD simulations are not common for buildings.

To give results about thermal and fluid-dynamic phenomena that characterize an indoor environment, a CFD simulation, through a conceptual model, assimilates a specific problem to a mathematical model based on conservation principles and relative boundary conditions: In all applications of airflows and heat exchange, the set of equations remains the same, but the boundary conditions vary according to the specific situation (e.g. the room envelope could have different characteristics, as well as the air velocity). The performing of a CFD simulation means solving a set of complex partial equations, simultaneously and successively. The numerical procedure, with a computer solver, is the only way to solve the complex set of equations, that do not have an analytic resolution.

A CFD analysis has high applications in the assessment of the performance of air-conditioning systems in buildings and the main potentialities are:

- The reduction in the number of experimental studies,
- the possibility of carrying out several analyses through the same numerical model, by varying the design conditions,
- the visualization of the results, that can provide informative and both quantitative and qualitative indications.

By predicting the parameters of air distribution, the efficacy of the system for the microclimatic control can be verified. In particular, the thermal-hygrometric comfort, the quality of the air, and the concentration of pollutants can be evaluated for indoor spaces, as deeply described in CHAPTER 4.

The mathematical model

The CFD studies are based on a mathematical model, which describes the behavior of airflows. In an air-conditioned environment, the airflows are usually quite turbulent and are characterized by causality, diffusivity, and energy dissipation. The turbulence is a characteristic of the airflow motion and, conversely to the viscosity or thermal conductivity, it is not a property of the fluid. The behavior of the airflow, as well as the convective hat exchanges and the distribution of contaminants, are governed by the equations of mass, energy, and momentum conservation (equations of Navier-Stokes), which can be expressed as partial differential equations, non-linear and coupled. The relative conservation law, with reference to a generic a variable φ, is reported below (Equation (2.5)[9]):

$$\frac{\partial}{\partial t}(\rho\phi)+\frac{\partial}{\partial x_j}(\rho U_j\phi)=\frac{\partial}{\partial x_j}\left(\Gamma_\phi\frac{\partial\phi}{\partial x_j}\right)+S_\phi \tag{2.5}$$

where:

- t = time
- ρ = air density;
- φ = transport property (e.g. air velocity, temperature, contaminant concentration);
- xj = distance relative to the j direction;
- Uj = speed component referred to the j direction;
- Γφ = diffusion coefficient;

For non-compressible fluids, the dependent variables can be decomposed in the sum of a temporal averaged value with a related execution. This procedure was introduced by Reynolds, and it is called the approach of Navier-Stokes, averaged according to Reynolds (i.e., Reynolds-averaged Navier–Stokes) [9]. The resolution of the procedure is possible when the values of the variables are known in the first moment, assumed as the initial one. In addition, on the calculation domain frontier, it is necessary to assign the conditions that represent the interactions between the field of motion and the surrounding environment.

The resolution of cited equations is based on a mathematical procedure that discretize the domain in many control elements. Largely employed in several other engineering fields, such as structural or aeronautical, this numerical technique is adopted because it is impossible to solve directly the differential set of equations representing the rooms flow regime; therefore, these are transposed into a finite group of algebraic relations to be solved for each point of a calculation grid (Figure 2.2). The CFD simulator solves the mathematical problem by employing the Boussinesq approximation, which does not contemplate the effects induced by the pressure on the air density. Indeed, this simplified approach considers the air as an ideal gas and treats the forces as a generation term, so that, even if it does not result effectively to solve the system of equations, it does not compromise the nature of the physical phenomenon.

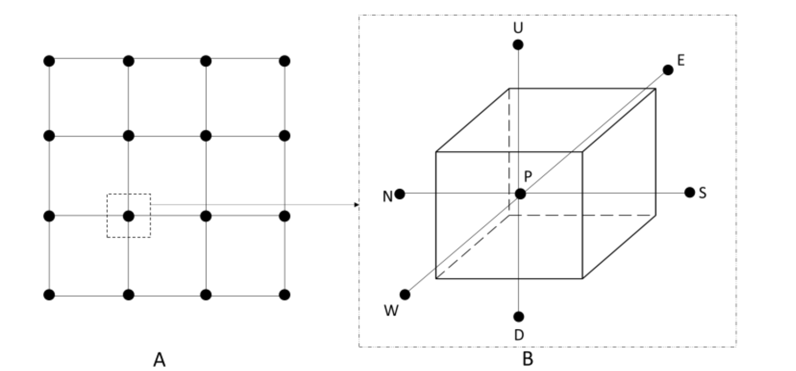

Figure 2.2 – A regular computational mesh (A) and the control volume of the point P (B)

The resolution of the airflow turbulence relies on the “two equations k-ε” standard, which is based on the equation of the turbulent kinetic energy (k) and its dissipation rate (ε). This turbulence model is valid only for completely developed turbulent flows, but as common for the airflows in a room, these are not completely developed everywhere (i.e. are characterized by high Reynolds numbers). Nevertheless, quite good results can be obtained by the resolution of airflows characterized by low levels of turbulence by adopting the k-ε turbulence model, as confirmed by experimental and numerical comparisons.

The Launder-Sharma model is apt for the calculation of the effects of a low turbulence model with low Reynolds numbers [10], as well as the more elaborated model “Reynolds stresses”. The last cited turbulence model improves the k-ε standard by evaluating the anisotropic effects of turbulence and including additional transport equations. In general, the “Reynolds stresses” model does not give significant improvements in the results of the air velocity fluctuations, but for what concerns the mean velocities and the temperature profiles, it provides better results if compared to the k-ε standard [9].

The computational mesh

The resolution of the CFD simulation starts with the definition of the computational domain, which is represented by a grid. The environment under investigation is divided into smaller control volumes, and for each of them, the equations governing the heat exchange and the flow are solved. The set of small regions that compose the environments are called mesh or grid. The accuracy in the definition of the computational mesh is a key element to obtain reliable results. Indeed, a too much approximate mesh could give inaccurate results, while a too much detailed mesh could excessively extend the computational time and sources.

The cells can have different shapes: the most common are the quadratic or triangular, adopted for bi-dimensional geometries, while the tetrahedral and hexahedral are adopted for three-dimensional geometries. In general, a well-structured mesh should have:

- equilateral cells preferably,
- high number of cells with an elevated gradient of temperature and air velocity,
- an expansion ratio for contiguous cells between 2 and 5.

The computational meshes can be orthogonal or not and, are generally adopted for squared and curved geometries respectively. In addition, the grids can be classified as structured and unstructured. The use of a structured mesh simplifies the achievement of convergence in the CFD calculation because a regular geometry for the matrix of the algebraic equations is employed. The limit in using such computational meshes is that the very complex geometries cannot be described.

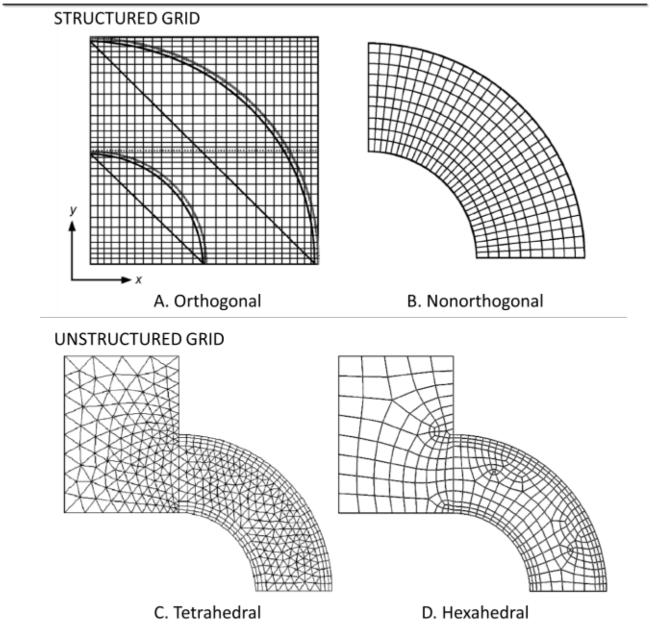

Figure 2.3 – Structured and unstructured computational grids (source: ASHRAE [9])

Conversely, unstructured grids are very flexible and can characterize spaces of any type of shape. Figure 2.3 shows structured and unstructured grids. To give more accurate CFD results, the computational grids, are denser along with the boundary, and thus along the room envelope, because the gradient of temperature and humidity could be higher in these regions. To verify the reliability of the CFD simulation, it is important to compare the results of two simulations performed with two different meshes and ensure that the results are independent from the computational grids. This kind of test is commonly known as "Mesh independence study".

<u>The boundary conditions</u>

Another important aspect related to a CFD study is the definition of the boundary conditions, indeed the accuracy in the assignment of the starting conditions affects the whole set of CFD results. The boundary conditions define the chemical and physical fluid characteristics, which can be constant or variable during the simulation period; a correct definition of these is necessary to solve properly the Navier-Stokes equations and the turbulence field. The main boundary conditions, for a CFD analysis of an air-conditioning problem, are related to the definition of:

- air diffusers in the indoor environments,
- the room envelope and indoor surfaces of the conditioned space
- symmetrical surfaces,
- fixed parameters that represent elements of generation or destruction.

The air diffusers have a significant role in the definition of the boundary conditions because, they are responsible for the fluid motion, temperature, and moisture distribution, and of the contaminant concentration. Indeed, velocity, pressure, and mass flow rate of the supplied air, are the main parameters to define and air diffusers. Generally, it is preferable to use simple air diffusers because a complex air diffuser requires the definition of detailed information that could cause inaccurate results.

By considering the air extraction grills, these can be modeled by defining the mass flow rate of the extracted air, assuming a constant working pressure. The exiting air velocity, determined from this information, requires corrections during the simulation process, to comply with the principle of mass conservation during the time. For what concerns the walls delimiting the environment under investigation, the velocities are considered equal to zero.

The definition of symmetrical surfaces can be a key element to simplify the CFD calculation, but even if a geometry results symmetric, this does not mean that airflows have the same characteristics concerning the same plane, for example, mixing regions of two different flows could cause instability of the flow.

Finally, the definition of heat, momentum, or contaminant sources and sinks is important to model thermal fluxes incoming from walls as well as those induced by people, radiators, or other sources of contaminants. The effects of these elements can vary over time and the choice of including them in the CFD calculation depends on the real effects that they could have on the CFD results. In general, the correct definition of the boundary condition consists of the best physical approximation of the real effects induced by a parameter.

The choice of the turbulence model

The resolution of the flow fields, as previously described, requires the definition of other equations that govern the fluid-dynamic phenomenon and concur to define the turbulence model. Several aspects concur in the selection of the proper turbulence model, but the two mains are the solving simplicity and the accuracy. The best compromise between the computational effort and accuracy of the model is the basic criterion in the choice of the turbulence model [11]. So that, to select the most suitable turbulence model, the following aspects must be considered:

- The possibility of implementation and the computational effort,
- the accuracy of the achievable results, based on literature and experimental studies,
- base hypotheses of the model and its limits in the application.

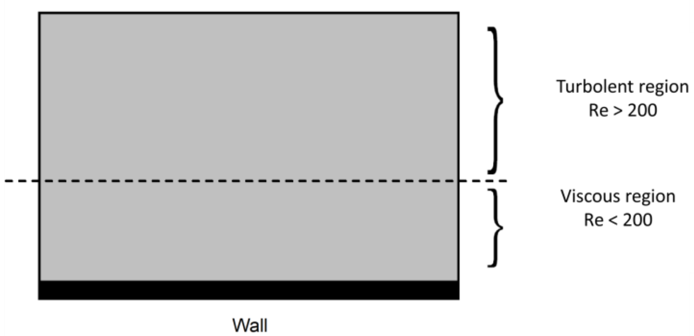

Figure 2.4 – The turbulent and viscous regions near a room wall (source: ASHRAE [9])

The most common turbulence model, currently used in CFD analysis is the standard two equations k-ε, where "k" stands for the kinetic turbulent energy and "ε" for its rate of dissipation. The advantage of using this method is the high capability of resolution of flow-fields, even if it is not the most appropriate for the resolution in the wall region and in particular in the viscous-conductive sub-layers.

Figure 2.4 shows the different computational domains near a room envelope, with reference to the region where there is the influence of the wall viscosity and the region where the airflow is completely developed.

Today, the standard two equations k-ε is implemented in all the CFD commercial codes that solve fluids in turbulent regimes and is considered the best compromise of results accuracy, simplicity in the implementation, and computational stability. It is also the most accredited instrument for CFD simulations of indoor spaces, even if it requires high computational time and effort. Other turbulence models have been developed to counter these disadvantages, among which is the zero-equation model. It does not consider the additional transport equation by reducing the computational effort and speeding up the calculation time of ten times if compared to the k-ε standard. The disadvantage of using this method is that it cannot solve correctly the aspect related to the turbulent heat exchange when a significant variability of the problem properties occurs. The last information about available commercial codes for CFD application in buildings. To representing and solving the set of PDEs – partial differential equations - describing the transport of momentum, energy, and turbulence quantities, the available numerical approaches are based on FVM, and thus Finite Volume Method, or FEM, namely the Finite Element Method. Both numerical procedures are adopted in commercial codes.

2.1.3. The coupling of BES and CFD

Building energy performance simulations and computational fluid-dynamic simulations can be coupled for detailed and more accurate results. The possible coupling strategies between CFD and BES simulations, according to the present literature, [13] - [14], are based on the same connection logics: static or dynamic. In the first case, the data exchange between the two simulations occurs in one step or two steps depending on the accuracy of the simulation, while - in the second case - the data exchange is continuous and dynamic.

The two analyses performed singularly, and particularly for the study of an air-conditioned environment, give partial results without providing a full description of the problem. At the same time, the BES and CFD coupling allow the interconnection of information between the two analyses, for example, the boundary conditions for CFD simulations, can be directly implemented by the BES, as well as the building characteristics. So, it is possible to avoid many hypotheses and to impose arbitrary conditions.

A dynamic energy simulation analyses the whole thermal zone, including heating, cooling, ventilation, and an average spatial evaluation of the microclimatic conditions of the indoor environment. For a defined period and with sub-hourly time steps, a BES calculates the energy demand of the building, its thermal loads, and microclimatic conditions. Conversely, a CFD simulation forecasts the airflow phenomena of an environment in a single moment and provides for all the data to determine the indoor microclimatic comfort, such as the temperature, humidity, air velocity, and quality. So, the predicted mean value PMV or the predicted percentage of dissatisfied PPD, as well as the mean age of air, can be predicted [15].

Coupling a zero-dimensional but dynamic simulation (i.e. BES) and a three-dimensional but temporally static simulation (i.e. CFD) can give valid results for planning a building refurbishment, analyzing both the building energy demand and the microclimatic conditions of the indoor environments. When merely an energy simulation is performed, some limitations must be taken into account: the inner air is assumed perfectly mixed and the thermal loads are defined approximately because the convective heat transfer coefficients cannot be calculated accurately. So, a BES singularly, cannot give a complete analysis with detailed results.

The integration of both BES and CFD results in a new possibility of evaluation and reduces the approximations of the singular analysis. For example, a coupled approach allows the evaluation of the different types of conditioning systems, with relative air diffusers and extractors, by evaluating both the energy-saving and the indoor environmental conditions.

The CFD and BES codes can be coupled according to different procedures of integration as shown in Figure 2.5. The set of data exchanged between BES and CFD simulation can be classified into "interface data" and "state data" [2]. The first ones are the data at the boundaries of the two different physical domains (examples are the surfaces' temperature, heat fluxes, airflow rates, supply temperatures, and so on). The state data, conversely (e.g. PPD, PMV, indoor air temperatures, relative humidity, and air velocity), belong to one of the physical domains, and thus, by having a non-uniform distribution, after the evaluation through the CFD analysis, these can be transferred to the BES. It’s important to underline that the iteration between the simulation codes is not a simple exchange of information and data, eventually retired to obtain the converge, but several difficulties are present and among all:

- The difference in the “time scale”: the BES is based on sub-hourly time steps, while the CFD simulation is performed in a single moment or few seconds [15].
- Modelling discontinuity: for the analysis of the indoor conditions, a BES analysis average data referred to a space, while a CFD simulation forecasts the entire spatial distribution of a large field of variables [15].
- Computational time discontinuity: the computational time required by a BES is very lower (few minutes or in any case less than one hour) if compared to those of the CFD simulation (at least 30 hours) [15].

To overcome these limitations, some strategies of connection between the codes are adopted. for what concerns the problem in the different time scale between a BES and CFD simulation, the coupling methodology “quasi-dynamic” [13] can be employed.

According to this coupling strategy, the CFD analysis is performed merely in a crucial and critical instant of a specific day and upgrades the boundary conditions of the BEPS simulations as regards that specific moment.

The discontinuity in the modeling is another of the crucial limitations in the coupling methodology. This is due to the difference in the computational domain of the two simulation codes that is partly solved by a numerical approximation. Finally, as regards the computational time discontinuity, as previously explained, the adoption of a simple turbulence model to ease the CFD calculation, is required for the realization of affective connection strategies.

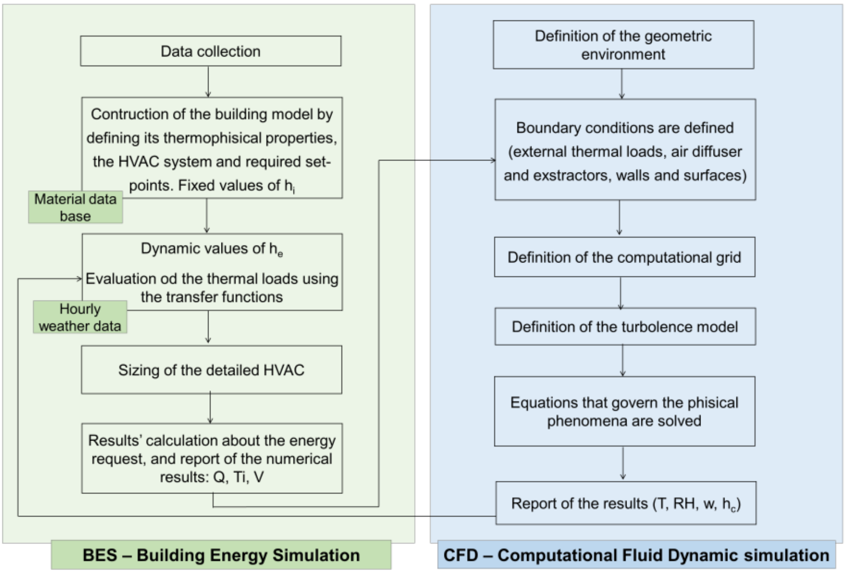

Figure 2.5 – A flow chart of the coupling logic between CFD and BES

In the following lines, some examples in the recent scientific literature, about the use of the CFD - BES coupled approach for different types of building and different building components.

The studies about the coupled approach of BES and CFD are various; some authors, for example, focused on the evaluation of double skin façade performances [16], or on advanced air-conditioning control strategies [17]. On a larger scale, the study of Gobakis & Kolokotsa [18] focused on the correlation between the external conditions and the indoor environmental quality in the Campus of the Technical University of Crete. Furthermore, Ascione *et al.* [19] investigated the energy refurbishment of a historical University building in Naples, through a coupled approach, in which BES was employed to evaluate possible retrofit scenarios and a CFD simulation was applied to verify the fan coil positioning for a better indoor thermal comfort. Fan & Ito [20] integrated CFD and BES for the evaluation of different types of ventilation systems in an office building. Moreover, Alnusairat *et al.* [21] applied this for the comparison, in terms of thermal comfort and energy demand, of configurations of sky court in high-rise office buildings.

Coupling CFD and BES analysis could be necessary for suitable energy-efficient design and the project of comfortable and healthy spaces [14].

2.2. Energy diagnosis and cost-optimal approach

In the previous subsection (2.1.1) the building energy simulation (BES) was widely described, focusing on the numerical approach for the building energy modeling and simulation of its energy performances. But from a methodological point of view, the evaluation of the building energy performances consists of two main phases: the experimental and numerical one. The experimental evaluation involves in-situ measurements to verify the energy performances of the state of fact, to evaluate and analyze the building energy uses as a starting point to identify the measures for energy saving. This phase is followed by the numerical verification and comparison of the energy efficiency measures assumed, by considering the energy, emissions, and cost-saving, in the perspective of cost optimal. The first stage of data collection can be assimilated into five categories of data:

- Historical and architectural,
- building envelope and its thermophysical properties,
- systems for the microclimatic control and equipment characterization,
- historical energy demands,
- thermal zones with relative uses.

The main steps for an energy audit, including the experimental and numerical approaches, are reported in Figure 2.6.

Firstly, a document collection is necessary, to characterize the building from a historical and architectural point of view. This step is important to evaluate possible architectural prescriptions and limitations aiming at building conservation. During the same phase, all the information about the building envelope (i.e transparent and opaque) and its structural and thermophysical properties must be collected through technical sheets and available design but also through experimental in-situ analysis such as endoscopic examinations, conductance measurements, and thermography. As regards the technical systems, for the lighting and HVAC systems characterization, both documental investigations and experimental analysis are necessary. Measurements of the flow or temperature of the heated and cooled water, or the thermography to evaluate the uniformity of air temperature near diffusers and generation systems, can be possible in-situ analysis.

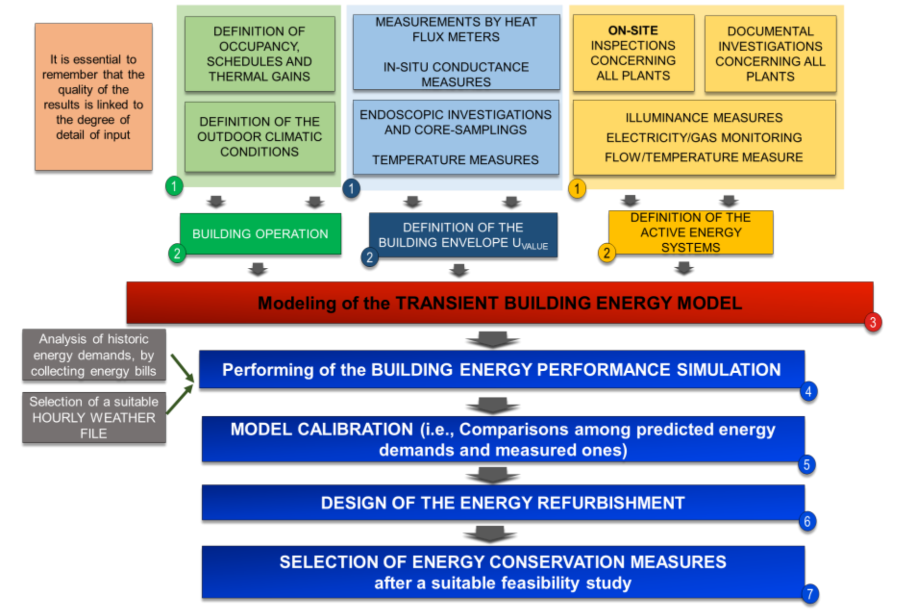

Figure 2.6 – The main steps for a building energy audit

In the many scientific studies, less importance is given to the operational conditions of the building, indeed, lighting, occupancy, and electric equipment schedules are assimilated to predefined conditions. In the reality, this aspect has a large impact on the BES results, and cannot be overlooked. The number of occupants, the power, and a number of the electric, and lighting devices must be counted for each thermal zone during the first stages of the building energy audit, as well as the occupation and utilization patterns during both weekdays and weekends. For what concern the identification of the building thermal zones, a simplification can be adopted: when the rooms have the same internal loads, external climatic solicitations (orientation and exposure), type of enclosure, type of HVAC system and lighting sources, they can be merged, to avoid excessive extension of computational times which in terms of results would add few and not relevant information.

Also, the monitoring of the energy demand has an important role in the phase of knowledge of the existing building, because it identifies the energy performances of the state of fact and is a necessary step for the calibration of the building model. Monthly bills of three or more years must be analyzed to evaluate the historical consumptions of energy and in addition, daily monitoring with punctual measurements could be necessary in some specific cases. The proposed approach, applied in the next chapters (CHAPTER 1 to CHAPTER 5) on different real case studies, to assure the reliability of the building energy model, provides the calibration of the numerical model through monthly energy consumptions, an essential requirement before the identification and evaluation of the energy efficiency interventions.

Other instruments of knowledge of the building are the occupant interviews or questionnaires about their typical habits, and thus the interaction with the HVAC systems, the judgment of thermal comfort, and their satisfaction about the building livability.

The collected data and information are used to calibrate the building energy model, to predict the energy performances of the building and its systems after the energy refurbishment in a simulation environment. Once the model is calibrated, the energy efficiency measures can be compared and evaluated following the cost-optimal approach, by considering the energy, economic and environmental aspects.

The calibration of the energy model

As previously described, according to the methodology adopted in the following chapters, to check the reliability of the numerical models, the results of the simulations are compared with the energy bills relative to the electricity demands of the last years The comparison with historical consumption and the knowledge of profiles of use of the plants and the installed systems for the calibration of the numerical model was performed by using the indicators proposed by the ASHRAE (American Society of Heating, Refrigerating and Air-conditioning Engineers) Guideline 14 [22] and the M&V Guidelines [23]. A first calibration index, for investigations based on monthly values, is the Mean Bias Error (MBE). The index compares the correspondence between energy demands required by the real building and the building's model. It identifies the average percentage error by comparing energy consumption in individual months and throughout the year. This calculation, therefore, allows us to understand how much the energy requirement of the numerical model differs from the monitored building on a monthly basis. The MBE value is obtained through Equation (2.6), where "M" means the consumption measured annually in kWh, and "S" is the same value but referred to the numerical model:

$$MBE\left[\%\right] = \frac{\sum_{period}\left(M - S\right)_{month}}{\sum_{period} M_{month}} x\,100 \tag{2.6}$$

As suggested by relevant standards [22] - [23], another important indicator, to evaluate the mean monthly error, is the CV(RMSE) calculated by Equation (2.7):

$$CV(RMSE_{month})\left[\%\right] = \frac{RMSE_{month}}{A_{month}} x\ 100 \tag{2.7}$$

For the calculation of the coefficient of variation, the RMSE (namely, the root-mean-squared monthly-error) and the A_{month} should be evaluated, respectively by means of the following Equations (2.8) and (2.9):

$$RMSE = \sqrt{\frac{\sum_{month}\left(M - S\right)^2_{month}}{N_{month}}} \tag{2.8}$$

$$A_{month} = \frac{\sum_{year} M_{month}}{N_{month}} \tag{2.9}$$

According to the M&V Protocol 2015 [23], the values of MBE and CV(RMSE), when monthly values are used for monitoring and simulations, are acceptable only within the following thresholds:

- MBE_{month} (%) ≤ ±5%
- CV(RMSE) (%) ≤ 15%

The aforementioned indicators are useful to compare the different simulations and related monthly energy consumptions, with the real energy uses of the building. Different parameters can be modified, according to present regulations, to obtain the validated model such as the hours of switching on and off of the HVAC system during the hot and cold periods, the infiltration, the power of equipment and lighting systems, the occupation schedule.

2.2.1. Energy audit of existing buildings

The energy performance of building Directives defines the energy audit as a "systematic procedure" that identifies, quantifies, and reports the energy consumption and energy saving opportunities for existing buildings, both public and private. An energy audit consists of inspection surveys and evaluations of the building energy performances to identify the greatest cost-effective opportunities for energy saving. Primary issues for occupied buildings are the preservation or improvement of human comfort, health, and safety.

In the European standard EN 16247 – 1 [24], all the general requirements, methodologies, and deliverables for energy audit are described for each form of establishments and organizations, and each type of energy and uses of energy, excluding individual private dwellings. It also contains prescriptions for special buildings, industrial processes, and transportation.

The energy audit aims at analyzing the energy performances of building systems, envelope, and electrical equipment, in order to identify possible energy saving measures to be evaluated from an economic, energy, and environmental point of view. This analysis combines experimental and numerical analysis and thus in-field inspections for data collection and calculation tools for the building energy modeling (elaboration of the numerical model of the building/systems).

The main stages necessary to perform the energy analysis are:

- In-field inspections for the preliminary knowledge of the Building HVAC systems, to define the structural characteristics and all the parts that have an influence on heat losses.
- Identification of historical energy consumption of the building.
- Identification of the envelope thermophysical properties which represent a base stage for the construction of the building numerical model.
- Identification of the primary energy demand of the building.
- Simulation of the energy model and comparison of the energy results with the real historical consumption of the building, to calibrate the numerical model. This is an important step to obtain a reliable building energy model.
- Simulation and evaluation of the energy efficiency measures identified by employing the reliable numerical model of the building.

The energy audit should also evaluate the efficiency and the programming of mechanical systems (heating, ventilation, air conditioning equipment) and thermostats. Finally, the user's behavior could affect considerably the building energy consumption, indeed, their habits, the number of hours they live in the building, or the way they manage the heating and cooling systems have a high weight on the building energy demand. This aspect will be widely discussed in CHAPTER 5, section 5.4.

2.2.2. Cost-optimal method and macro-economic analysis

The cost-optimal procedure was introduced by the energy performance of Building Directive 2010/31/EU [25] as the base methodology to reach minimum energy performance requirements for buildings, their building elements, and technical systems. The Directive specifies that each MS must *"assure that minimum energy performance requirements for buildings or building units are set with a view to achieving cost-optimal levels"*. For the first time, considering the global lifetime cost of the building, became a prerequisite in the building energy refurbishments, to achieve the energy performance requirements.

To calculate the cost-optimal levels of minimum energy performance for buildings and building elements, the Cost-Optimality Commission Delegated Regulation, has established a proper methodology, and the Commission Delegated Regulation (EU) No 244/2012 of 16 January 2012 [26], supplementing the Directive 2010/31/EU [25] has introduced a comparative methodology to calculate the cost-optimal levels of minimum energy performance for buildings and building elements. In any case, the EU regulations and guidelines give large flexibility to the Member States, in the definition of the input data for the calculation of cost-optimal, reference buildings, and energy costs. The cost-optimal evaluation considers all the possible costs included in the whole building lifecycle, such as investments, maintenance, operating costs, and energy savings.

According to the cost-optimal method, the energy retrofit measures, are selected following six steps:

- Definition and modeling of the existing building (thermophysical properties, technical systems, climatic conditions, occupancy, etc)
- Identification of possible energy efficiency measures for the whole building or building elements.
- Numerical evaluation of the building energy demand, before and after the energy refurbishment, and calculation of costs of the energy efficiency measures in the reference life cycle. The evaluation of costs includes the investment costs, maintenance, and operating costs, as well as earnings from produced energy and emissions.
- Development of a sensitivity analysis that includes the results of the macroeconomic evaluation.

In the majority, the cost-optimal evaluation results in more than one package of measures applied to the reference building, and rarely as a single cost-optimal solution. A set or a collection of cost-optimal curves there will be for each building, relying upon the building characteristics and the variables combined in the cost-optimal evaluation.

For the case studies of the following chapters (CHAPTER 1 and CHAPTER 5), cost-optimal solutions with related global costs, investment costs, payback periods of the invested capital, and economic indexes under a macro-economic analysis were calculated, as explained below.

Cost calculation

Starting from the earnings from produced energy, the reduction of primary energy demand for cooling and heating was calculated as the absolute (or percentage) difference between the base building primary energy consumption (EP^{B}) and the one of the building as refurbished (EP^{EEM}) (Equation (2.10)). In the same way, but referring to operating costs and polluting emissions, the emission and cost reductions have been calculated (Equations (2.11) and (2.12):

$$\Delta EP = EP^{B} - EP^{EEM} \tag{2.10}$$

$$\Delta C = C^{B} - C^{EEM} \tag{2.11}$$

$$\Delta EM = EM^{B} - EM^{EEM} \tag{2.12}$$

The investment costs were calculated considering common costs from price lists for public construction projects. More in-depth, regional price lists consist of specifications for finished works and/or supplies with installation, the cost of which includes all the necessary work phases for the definition of the complete work and realized to the perfect state of the art; the listed costs have been compared with metric calculations of similar construction works in the same country and the same zone. When a material or a specific typology of work was not listed in the price list, its cost was obtained by comparing the construction work with a similar one [27]. Besides, the technical-economic feasibility was evaluated through usual indicators, and thus the Discounted

Pay Back (Equation (2.13)) and Net Present Value (Equation (2.14)). For what concerns the investment Global Cost, for an overall cost assessment, it has been estimated according to European Regulation 244/2012 [26]. The Global Cost is the sum of the initial investment costs, management costs, and replacement costs (referring to the starting year), as well as disposal costs. For the Global Cost calculation, the European Regulation establishes - in the cost-optimal methodology framework in section 4.2 point 8 - that residential and public buildings shall use a period of calculation of 30 years [26], conversely, commercial and non-residential buildings should provide a calculation period of 20 years.

The additional costs of greenhouse gas emissions were added for the macroeconomic calculation (Equation (2.15)), according to instructions and methodologies of the EU Delegated Regulation 244/2012 [26].

The energy efficiency measures have been finally investigated according to optimal levels of energy efficiency depending on costs:

$$DPB = N\colon \sum_{i=1}^{N} \frac{F_i}{(i + R_d)^i} = C_i \tag{2.13}$$

$$NPV = \sum_{i=1}^{LF} \frac{F_i}{(1 + R_d)^i} - C_i \tag{2.14}$$

$$C_g(\tau) = C_I + \sum_{i=1}^{\tau} [(C_{a,i}(j) R_d(i) + C_{c,i}(j)) - V_{f,\tau}(j)] \tag{2.15}$$

With reference to the above equations, the following terms are defined:

- F_i = based on i-th year, annual cash flow;
- R_d = discount rate;
- N = number of years;
- C_i = investment cost of the intervention;
- LF = life cycle of the technology installed;
- $C_g(\tau)$ = global cost;
- $C_{c,i}(j)$ = cost of carbon emissions for the measure or set of measures j during the year i;

- $C_{a,i}(j)$ = annual cost of *j* measure (management and maintenance) in the year *i*;
- $V_{f,\tau}(j)$ = residual value of the measure or set of measures at the end of the calculation period.

The technical-economic analysis was carried out for specific case studies by considering electricity and gas costs depending on the intended use of the building, residential, educational, or industrial, and nation of location.

CHAPTER 2 - References

[1] Wang, L., & Wong, N. H. (2009). Coupled simulations for naturally ventilated rooms between building simulation (BS) and computational fluid dynamics (CFD) for better prediction of indoor thermal environment. Building and Environment, 44(1), 95-112.

[2] Tian, W., Han, X., Zuo, W., & Sohn, M. D. (2018). Building energy simulation coupled with CFD for indoor environment: A critical review and recent applications. Energy and Buildings, 165, 184-199.

[3] EnergyPlus simulation software; U.S. Department of Energy: Washington, DC, USA.

[4] Test Reference Year, Try, 1985, Data sets for computer simulations of solar Energy Systems and Energy Consumptions in Buildings. Commission of the European Communities, Directorate General XII for Science, Research and Development, 1985.

[5] International Weather for Energy Calculations (IWEC), International Weather for Energy Calculations (IWEC Weather Files) Users Manual and CD-ROM, Atlanta, ASHRAE, ASHRAE, 2001.

[6] Typical Meteorological Year 2 (TMY2), National Renewable Energy Laboratory (NREL), User's Manual for TMY2s, NREL/SP-463-7668, and TMY2s, Typical Meteorological Years Derived from the 1961-1990 National Solar Radiation Data Base, Golden, Colorado: National Renewable Energy Laboratory, 1995.

[7] BLAST (Building Loads Analysis and System Thermodynamics), program users manual. Volume 1: Supplement (version 3.0), Final Report Army Construction Engineering Research Lab., Champaign, IL, 1992.

[8] DesignBuilder v.6.0. https://designbuilder.co.uk/. Accessed in November 2021

[9] ASHRAE 2005, ASHRAE Handbook – Fundamentals, Chapter 34 Indoor Environmental Modeling, American Society of Heating, Refrigerating and Air-Conditioning Engineers, Inc., Atlanta GA, USA, 2005

[10] Z. Zhai, J. Zhang, W. Zhang, Z. Chen, Y. Qingyan, Evaluation of various turbulence models in predicting airflow and turbulence in enclosed environments by CFD: Part 1 - summary of prevalent turbulence models, Magazine article from: HVAC & R Research, 2007.

[11] C. Teodosiu, R. Hohota, G. Rusaouën, M. Woloszyn, Numerical prediction of indoor air humidity and its effect on indoor environment, Building and Environment 38 (2003), pp. 655-664.

[12] D.B. Crawley, L.K. Lawrie, F.C. Winkelmann, C.O. Pedersen. "EnergyPlus: A New-Generation Building Energy Simulation Program," in Proceedings of Forum 2001: Solar Energy: The Power to Choose, 21-25 April 2001, Washington, DC. Boulder, Colorado. ASES, 2001

[13] Z.J. Zhai, Q. Chen, 2005, Performance of coupled building energy and CFD simulations, Energy and Buildings 37 (2005), pp. 333-344.

[14] Zhai, Z., Chen, Q., Haves, P., & Klems, J. H. (2002). On approaches to couple energy simulation and computational fluid dynamics programs. Building and Environment, 37(8-9), 857-864.

[15] Z.J. Zhai, Q. Chen, J.H. Klems, P. Haves, Strategies for coupling energy simulation and computational fluid dynamics programs. Lawrence Berkeley National Laboratory: Lawrence Berkeley National Laboratory, 2002

[16] Zeng, Z., Li, X., Li, C., & Zhu, Y. (2012). Modeling ventilation in naturally ventilated double-skin façade with a venetian blind. Building and environment, 57, 1-6.

[17] Tian, W., Sevilla, T. A., Zuo, W., & Sohn, M. D. (2017). Coupling fast fluid dynamics and multizone airflow models in Modelica Buildings library to simulate the dynamics of HVAC systems. Building and Environment, 122, 269-286.

[18] Gobakis, K., & Kolokotsa, D. (2017). Coupling building energy simulation software with microclimatic simulation for the evaluation of the impact of urban outdoor conditions on the energy consumption and indoor environmental quality. Energy and Buildings, 157, 101-115.

[19] Ascione, F., De Masi, R. F., De Rossi, F., Ruggiero, S., & Vanoli, G. P. (2017). NZEB target for existing buildings: case study of historical educational building in Mediterranean climate. Energy Procedia, 140, 194-206.

[20] Fan, Y., & Ito, K. (2012). Energy consumption analysis intended for real office space with energy recovery ventilator by integrating BES and CFD approaches. Building and environment, 52, 57-67.

[21] Alnusairat, S., Hou, S., & Jones, P. (2017). Investigating spatial configurations of skycourts as buffer zones in high-rise office buildings. Presented at: The 5th eCAADe Regional International Symposium 2017, Cardiff, 26-28 April 2017.

[22] ASHRAE—American Society of Heating. Refrigerating and Air-ConditioningEngineers, Guideline 14 2002, Measurement of Energy and Demand and Savings; ASHARE: Atlanta, GA, USA, 2002.

[23] U.S. Department of Energy, Federal Energy Management Program (FEMP). M&V Guidelines: Measurement and Verification for Performance-Based Contracts; FEMP: Washington, DC, USA, 2015.

[24] UNI – Italian Unification Body. UNI CEI EN 16247-1: Diagnosi energetiche – Parte 1: Requisiti generali. 2012. (In Italian).

[25] European Parliament, Directive 2010/31/EU of The European Parliament and of the Council of 19 May 2010 on the energy performance of buildings (recast). Official Journal of the European Union. L 153/13, 18.6.2010.

[26] Commission Delegated Regulation (EU) No 244/2012 of 16 January 2012. Available online: https://eur-lex.europa.eu/legal-content/EN/TXT/PDF/?uri=CELEX:32012R0244&from=GA. Accessed in November 2021

[27] Argenziano M., Mastellone M. TIPOLOGIE EDILIZIO PREZZARIO aggiornamento 2020 - “Il prezzario per tipologie edilizie di Napoli e provincia” (2021) promosso da ACEN - Associazione Costruttori Edili di Napoli. Edizioni Graffiti, ISBN 978-88-86983-945.

CHAPTER 3.

Energy refurbishment of present buildings through passive technologies for the building envelope

This chapter is entirely focused on passive technologies for the building envelope. The first section introduces passive strategies and their scientific state of art. The second section is dedicated to green walls and reports a wide review study about vertical greening systems. Mathematical models for the Greening Systems and performance evaluation parameters for technical characterization will be described by referring to current scientific studies. In addition, a critical analysis of available research results is reported, distinguishing the behavior of green vertical systems in three main areas: urban quality, building performance and sustainability.

The second section focuses on the energy refurbishment of a real case study, through innovative and traditional passive technologies. In detail, in view of cost-optimal, green roof, cool roof, vented facades, thermal insulation and PCM, will be evaluated, in an energy, emission and economic perspective.

3.1. State of the art and Research significance

A suitably designed building envelope reduces heat gains and minimizes thermal loads. In the case of heat gains, cool colors, solar screens, new generation windows glass, and thermal mass are suitable solutions to decrease the building overheating. Heat gains can be mitigated through the thermal capacity storage or accumulation of latent heat and, moreover, useful heat dissipations can be obtained with the building envelope capacity to disperse heat to lower temperature environments, like the sky, ambient air, ground, and water [1]. Cooling strategies such as phase change materials, natural night ventilation, vented walls and roofs, green walls and roofs, water ponds, dynamic thermal insulation, earth-tubes, and solar chimney are technologies for the free or low-energy cooling of buildings. In detail, some of these exploit the conversion of solar and wind energy for reducing the building heat gains and cooling loads, by means of various physical phenomena and heat transfer mechanism, and thus convection, reflection, long-wave radiation, stack effect, evaporative cooling and evapotranspiration and so on.

Obviously, the building must perform properly, and this is achieved by means of deep studies concerning the operating boundary conditions (that affect greatly the efficiency of passive cooling strategies) and by nullifying the penalizing effects of punctual and local inefficiencies, such as common criticalities caused by thermal bridges [2]. Ascione [3] has accurately studied themes like energy conservation and renewable technologies aiming a lowered use of cooling systems. He discussed traditional and emerging technologies in the bioclimatic field, oriented to summer cooling and microclimatic internal conditions enhancement, focusing also on active equipment and the active use of renewable energy sources.

In the following lines, even if briefly, some descriptions of common and emerging technologies for the passive and low-energy cooling of buildings are reported to underline their working principle and for identifying limits and potentialities.

Green roofs and walls are bioclimatic solutions that improve thermal comfort and reduce summer and winter energy consumptions of the building, giving, therefore, a positive grant to urban heat island. These systems exploit solar radiation to activate chlorophyll photosynthesis of vegetation, and through the evaporative cooling induce a lower heat transfer toward the indoor building.

Green roofs have been studied by many researchers. Alcazar *et al*. [4] investigated the positive effects of green roofs in internal and external microclimatic conditions for the Mediterranean–continental climates and observed a temperature reduction of 1 °C of internal areas not directly irradiated by sun and a reduction of 2 °C at the street level. Yaghoobian *et al*. [5] studied the variations of roof surface temperature in combination with the variation of plant coverage and concluded that the higher is the plant coverage, the lower is the surface temperature. Obviously, this effect is due to the reduced solar absorbed by the soil and the incremented evapotranspiration by soil and vegetation. Finally, a higher leaf area index (LAI) is recommended in order to increase the green roof performance [6] - [7]. In the same way, Gagliano *et al.* [8], through a multi-criteria analysis, contrasted the performance of traditional, cool and green roofs in the Mediterranean climate, and confirmed the positive effects of cool and green roofs on summer energy consumption. In particular, green roofs with different insulation thickness were compared and, in its specific case, the extensive and moderately insulated green roof resulted more convenient in terms of energy needs and UHI (Urban Heat Islands) mitigation.

The cool coatings are another quite innovative technology based on a well-known, for many centuries, heat transfer principle, namely the reflection of solar radiation by means of suitable coatings. In more detail, a cool coating can reflect solar radiation and emit thermal energy in the infrared wavelengths. Pisello *et al.* [9] developed a new typology of roof by combining a cool and green roof, through the implementation of a particular type of plant reflecting the short-wave radiation. In this way, the reduction of summer space overheating, in terms of hours, around 98.2% was obtained. Santamouris *et al.* [10] analyzed inexpensive passive cooling techniques to improve the life conditions of low-income households. In particular, the aim was to show the efficiency of cool and reflective materials, by comparing them with traditional ones and to evaluate the potentiality of earth tubes and new ventilation systems for improving indoor thermo-hygrometric comfort conditions.

In the tradition of the building sector, a relevant role is occupied by the thermal insulation of the envelope. Several materials, from the traditional to the innovative ones, can be mentioned: organic and inorganic materials, metallic or metalized reflective membrane, aerogels, thermal insulators from waste materials and composite materials. The organic thermal insulator can be natural (flexible wood fiber) or synthetic (cork, polyurethane or polystyrene) [11]. Expanded polyurethane is formed by a chemical expansion reaction, where the pores are filled by an expansion gas. Some researchers are working on the improvement of this high-performance material. Cao *et al.* [12] studied a novel functionalized graphene (FGN) to improve fire resistance and smoke suppression. They obtained positive results with a reduction of the values of over 60%. More in general, Cabeza *et al.* [13] examined the performance of three insulation materials on a Mediterranean construction. They compared polyurethane, mineral wool (MW) and polystyrene (XPS) on a cubicle. The results showed a reduction in energy consumption for cooling and heating. Specifically, the cubicle with a polyurethane insulation material, during a typical summer week, had an energy consumption for cooling 18% and 26% smaller than the ones of the MW and the XPS cubicles.

Another strategy that gives positive effects on thermal indoor conditions and on the reduction of primary energy consumption is the vented façade. The ventilated slab of external walls, thanks to the stack effect in the vertical cavity, determines a heat exchange by convection and it cools the walls' surface. This solution was widely studied by Stazi *et al.* [14], who considered the variation of the height, the solar radiation and the effect of wind as the main factors that influence the system working. Varying the system height from 6 m to 12 m, the results have shown that increasing the height, the temperature and the air velocity in the cavity are higher during sunny days. Marinosci *et al.* [15] investigated the performances of a vented façade, focusing on the variation of open joints, ventilation grills and the thickness of the cavity. The outcomes highlight that it is important to minimize the longwave radiation and reduce the pressure losses to limit the temperature values in the cavity.

A new frontier of energy efficiency in buildings, with regard to the improvement of the summer performances, is the use of phase change technologies. Their use in buildings is already diffused and more and more increasingly.

These materials are suitable for intervention on the opaque horizontal (i.e., roofs) and vertical envelope of buildings, particularly characterized by a diurnal use, like offices, educational and university edifices. Usually, different layers are separately added to the vertical envelope, specifically, a traditional or innovative thermal insulation material and a PCM coupled with night ventilation. PCMs ensure the same advantages of thermal mass; indeed, these are suitable for storing thermal energy at a constant temperature and thus allowing no indoor overheating of a building when interested by heat gains, due to high indoor temperature, solar radiation on the facades, indoor gains due to persons, lighting and equipment.

The use of PCMs is becoming more and more diffused in the building sector. Kasaeian *et al.* [16] proposed a large review about the possible applications of PCMs and nano-PCMs in buildings. The study started from passive applications for the space cooling and heating and concluded with the investigation of active use of PCMs in the building HVAC systems. In the same way, Baetens *et al.* [17] reviewed the possible use of PCMs for buildings, focusing deeply on the typologies of PCMs. The three macro-categories of PCMs are the organic phase change compounds (paraffin and non-paraffin), inorganic phase change compounds (hydrated salts) and eutectics (organic-organic, inorganic-inorganic, inorganic-organic eutectics). Furthermore, Feldman *et al.* [18] evaluated the application of an organic bio-PCM in the specific case of a gypsum wallboard. Feldman *et al.* demonstrated the considerable increment of thermal storage (twelve times higher) of the PCM wallboard (23% impregnation) compared to the traditional coating. Theodoridou *et al.* [19] applied PCM-enhanced lime plasters in a vernacular and contemporary architecture in the southern Europe climate conditions, and analyzed the thermal, physical and mechanical performances of the innovative material. It was observed the improvement of thermal characteristic and no significant change of mechanical properties between the PCM plaster and the traditional one.

The main limit in the use of PCMs is in the fact that these are a relatively new technology so that their capabilities and achievable performances are not well-known, the costs are not always low and also the installation techniques are not usual for construction companies. In some cases, further barriers can be the difficulties in the macro or micro-encapsulation or risk of flammability. All these criticalities can be overcome. For instance, against flammability, there is the possibility of adding a fire retardant, and this is proposed, as a valid solution, in Sittisart *et al*. [20]. For what concerns problems related to the encapsulation, this constructive phase today is quite consolidated and consists of a process of coating or surrounding the material particles or droplets with a polymeric film (shell) to produce capsule in the order of micrometers or millimeters [21]. So, even if there are some criticalities in the application of PCMs, many studies confirm their advantages and consider it as an emerging technology, partly still to be studied.

Many authors focus their research on the improvement of building efficiency with a particular attention to passive solutions. Gil-Baez *et al.* [22] enhanced the sustainability of a school in the Mediterranean climate, through passive solutions for the building envelope. They analyzed technologies like internal and external insulation, external vented façade, internal cavity insulation and external prefabricated façade for the opaque envelope and solar screens and low emissivity glazing for the transparent envelope. They combined a set of measures on the building: solar window protection, external canopy, a screen of trees, external Thermal Insulation Composition System, low-emissivity glazing, external roof insulation, and a removable textile canopy. The results of this combination showed a 15.9% reduction of energy consumption for cooling, without compromising the functionality and accessibility of the building.

De Santoli *et al.* [23] in the same way, focused on the building envelope to improve the energy performance of a school building in Rome. They compared the passive intervention on walls and windows frames with the improvement of the active systems. In general, they underlined the environmental benefits of passive strategies despite the higher investment costs.

Starting from the aforementioned studies, aimed at describing, even if very synthetically, the passive technologies and some authoritative examples of their applications, this chapter will be entirely dedicated to passive strategies for improving the building energy performances. In detail, section 3.2 is focused on GWs and LWs, with a detailed review study that will bring out new and interesting outcomes. Section 3.3 focuses on the analysis of passive measures applied to an existing building owned by public Institutions that, according to the recent EU Directives in matter of energy efficiency in buildings, must have demonstrative and exemplary roles.

3.2. Green Walls: Knowledge Gaps, Design Parameters, Thermal Performances, and Multi-Criteria Design Approaches

The green wall is an engineered technology for stormwater management and climate change mitigation at the urban level. At the building scale, these energy efficiency measures are suitable for improving indoor comfort conditions and for reducing energy needs. Several guidelines are available about vertical greening systems, but these propose design parameters and performance evaluation criteria, often incomparable. In order to facilitate the implementation of proper technical standards, this section proposes a critical review of more recent scientific investigations. All parameters for the design optimization are discussed as well as the achievable social and private benefits by taking into consideration the type of study (numerical or experimental), the climate conditions, the analysis period, all technical requirements of the green layer as well as of the back wall. It comes out that a multi-criteria design approach is needed for green vertical systems. Thus, the section is concluded with a SWOT analysis, evidencing “strengths”, “weaknesses”, “opportunities” and “threats”. The analysis shows that the highlighted benefits will acquire greater relevance considering the increase in global temperatures and the growing need to redevelop densely built urban centers, while some negative aspects may be filled in the future with a deeper preparation of designers and careful choice of materials. The study of review shows, therefore, drivers and barriers occurring designing and implementing green walls

3.2.1. Introduction: motivation for a new critical literature state-of-the-art

One of the 17 objectives of the Agenda for Sustainable Development forward 2030 is to make cities and human settlements inclusive, safe, resilient and sustainable. Among the most environmentally friendly solutions, the green wall (GW) can be utilized as a key strategy for cleaning air and water, for climate change mitigation and adaptation and for promoting the local biodiversity and character [24]. *GW* is the most common term used to refer to all forms of a technological system consisting of vertical building elements covered with common classification [25] -[27] distinguishes between: a) Green Façades (GFs) and b) Living Wall (LWs).

The green façades are made of climbing plants growing on a wall without additional infrastructures (direct system), or with the use of stainless steel or wooden trellis, meshwork, or cabling as a support (indirect system). A GW can be created both with plants grown in garden beds at its base or with containers installed at different levels across the building. Some Asian examples are reported in Figure 3.1, while other European examples are shown in Figure 3.2.

LWs are characterized by vegetation that is not connected to the façade but rather it is fully integrated with the building envelope. Plants and substrate are both placed on the vertical surface of the external wall, typically on the external side of an impermeable and anti-root membrane, in order to protect the structure from moisture, with or without an air gap.

CITY OF SINGAPORE: THREE EXEMPLES

Silver leaf and Cloud forest - Gardens by the Bay NTU campus

Figure 3.1. Three examples of green walls in the City of Singapore.

Figure 3.2. Examples of green walls in Europe.

Continuous and modular systems [25] - [27] are both possible technologies. Some admirable architectures, for both public and private uses, have become iconic due to the perfect integration between the vegetation and the architectural project, for example: the “Caixa Forum” of Herzog & de Meuron in Madrid, the “Solaris” office building of Ken Yeang in Singapore, the “University Pole of Management Sciences” of Lacaton&Vassal in Bordeaux, the “Hardman Square Pavilion” of Sheppard Robson in Manchester or the “Vertical Forest” of Stefano Boeri in Milan.

These systems can reduce the energy demand of buildings both in summer and winter mainly by means of the following mechanisms:

- The shading produced by the vegetation.
- The evaporative cooling achieved by evapotranspiration from the plants and from the crop substrate.
- The insulation provided by vegetation and substrate as well as the variation of the wind effect [28].

Despite the advantages, the adoption of green systems has a penetration into the construction market still too low. The main criticalities [29] seem to consist in: a) high investment and maintenance costs, b) lack of a shared constructive standard, c) hard interpretation of not uniform experimental data and d) unavailability of certified commercial simulation models.

Some review studies on green vertical systems are already available, and these are mainly focused on:

- classification [25] of typologies,
- state of the art of technologies [30], [31],

- evaluation of the thermal performance [32], [33] or of the human health benefits [34],
- estimation of effects on thermal comfort and carbon emission reduction [35].

Reasons and motivations for a new review study are:

- ❖ the aim of a deep focus on the discussion of designing and performance evaluation methodology,
- ❖ deepening of aspects related to numerical simulations, with clear indication on data concerning the parameters for characterization,
- ❖ the research of univocal and clear data interpretation in term of benefits and problems,
- ❖ a new comparison among the same GW in different climates.
- ❖ The motivations

The research question and the objectives of a review study

This section (2.1) contains a review study which aims at proposing a critical analysis of available results with experimental or numerical approach, in terms of designing methodology and environmental benefits, with the scope to orientate the future research and to help designers. The main topics discussed are:

a) Given the correlation between vegetation characteristics and the effective performance, how many parameters are needed for describing the energy behavior of a GW? Could these parameters be considered constant over time? How they can be measured? Are they available for different type of plants? General description will be translated to concrete technical data as leaf area index (LAI), height, substrate type, irrigation type and schedule;
b) Which are the advantages and disadvantages of green vertical systems? Experimental and numerical data are compared according to the climate (location), the system composition, the considered period, the indoor conditions;

c) Can the scientific results be translated into shared building standards and methods for the optimal design?

The following sub-section will discuss these topics in detail. After the illustration of the methodology adopted for the review study, the following sub-section (3.2.2) discusses the accuracy of available experimental data and the reliability of adopted simulation models for characterizing the GWs' performance. Moreover, sub-section (3.2.3) presents a critical analysis of available results taking into account the effects on urban rehabilitation, building performance improvement, sustainability and profitability during the lifecycle. Then, a discussion is proposed (sub-section 3.2.4). Finally, the section ends with a SWOT matrix that allows visualizing the different internal strengths and weaknesses of a building solution and its external opportunities, threats and weaknesses that might be faced during project management.

Materials and method of the review study

To review the scientific literature, the publications on different topic combinations stored in the Web of Science (www.isiwebofknowledge.com) database were analyzed. A protocol for providing a revision of GWs does not exist. Papers, of the past and recent literature (latest 20 years) were collected, according to experimental and numerical criteria, by taking into account 101 studies. The selection of the reviewed studies has been organized according to a two-step methodology: in a first step, papers about the GW systems and its characteristics were reviewed, in a second step, the ones based on the environmental effects of a GW system have been summarized.

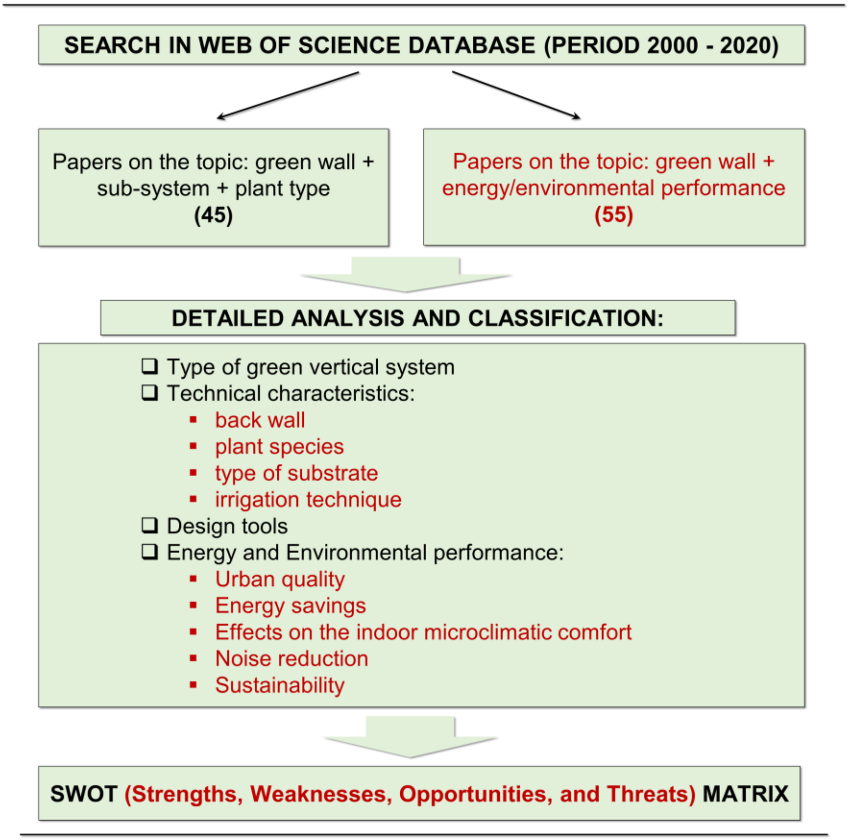

Figure 3.3 - PRISMA flow diagram: the review method.

More in detail:

- Around 45 scientific studies were reviewed on the topics of “green wall” + “sub-system” + “plant system,” in order to evaluate the availability of technical data.
- Around 55 scientific studies were review on the topics of “green wall” + “energy and /or environmental performance” with which vantages and disadvantages of this technology have been found.

Figure 3.3 shows a diagram of the literature research approach. The search strategy in the Web of Science Database was performed by defining keywords such as green walls, living walls, green facades, green systems but also the more generic ones such as bioclimatic solutions or wall systems. In some cases, the papers’ research was carried out by selecting the name of authors already known for published papers about GFs such as Perini, Prodanovic, Olivieri, Pérez, and Djedjig. Of course, some limits were applied to circumscribe the search results: only articles published after 2000, in the English language, in international journals and authoritative conference proceedings.

Please, note that the citation of each paper can be singular or twice or it can happen even more times. The data extracted, are referred to different climates, different approaches and different observation periods, so that often, some divergences occur, and not unique trends are always achieved.

3.2.2. Vertical greening systems performance evaluation

This study of review proposes to split out the problem of performance evaluation in two categories, by taking into account the availability of:

a) accurate description parameters or their measurements for experimental studies,
b) numerical model for parametric studies or predictive evaluations.

<u>Parameters for Technical Characterization</u>

Some examples of green walls are proposed in [36], in which the authors show some typologies of hanging greenery as a solution for improving the Environmental Sustainability of buildings. The parameters needed for studying the behavior of vertical green systems can be obtained by the analysis of involved heat transfer phenomena:

- ✓ long and short-wave radiative heat transfer within the vegetation canopy,
- ✓ long and short-wave radiative exchange within the wall not covered by plants or the soil not covered by the plants,
- ✓ plant-wall or plant-soil radiative heat transfer,
- ✓ plant canopy effects on convective heat transfer,
- ✓ transpiration from plants, and evaporative effect from soil,
- ✓ heat conduction from and to the back wall and soil layer,

✓ the role played by the wall and soil thermal inertia.

Some necessary definitions should be provided immediately. First of all, the Leaf Area Index (*LAI*) quantifies the fractional vegetation coverage; it is the "total one-sided projected leaf area" to "the ground surface area" ratio [37]. For instance, a *LAI* equal to 3 indicates that there are 3 m^2 of projected leaf per 1 m^2 of below (or behind) surface. *LAI* sometimes is dimensionless, sometimes is reported with the unit: i.e., m^2 (foliage)/m^2 (soil). The main measurement methods for the determination of *LAI* [38] are:

- DIRECT: harvesting the vegetation and measuring the area of all the leaves within a delimited area;
- SEMI-DIRECT: collecting leaves of deciduous plants, drying and weighing them and after converting the mass into leaf area by multiplying the collected biomass by the Specific Leaf Area (*SLA*);
- INDIRECT: measuring the transmission of radiation through the canopy, by using the radiative transfer theory.

The first one is an accurate but a destructive method; it is really suitable for vegetation of small structure. An example of application is reported by Charoenkit and Yiemwattana [39]. The second one is non-destructive, but the estimation of *SLA* is difficult due to its variation with species, site fertility, date and year, duration of remaining in the traps, weather. Conversely, non-destructive indirect methods need calibration procedure. It has been verified that the indirect methods underestimate (from 25% to 50%) the *LAI* compared with direct measurement. Several indirect methods were experimented.

Koyama *et al.* [40] have used digital pictures taken each week. It is an easily implemented method and non-invasive, but it does not give the information about the stratification of leaves and thus the real *LAI*. Pérez *et al.* [41] have compared a direct method based on delta-T image analysis system and an indirect method based on the estimation of *LAI*, using the amount of light energy transmitted by a plant canopy. In this case, the values are convergent: for the proposed case study, *LAI* is 3.1 with the direct method and 3.3 with the indirect method of measure. Conversely, for the same type of plants, Susorova *et al.* [42] have found *LAI* = 1.8, by measuring the area of a typical leaf and counting the area of ivy leaves in an image of the vegetal wall. It can be concluded that it is very difficult to obtain a representative *LAI* for the same plant species.

In order to evaluate peculiarities and performances of *GW*s, another important parameter is the radiation attenuation coefficient (k) that indicates the decrease in the absorbed radiation of the leaves; for instance, this parameter is 0 if leaves are perpendicular to the wall.

The evaluation of short wave radiative exchanges needs of absorption coefficient (α_l) and also of transmission coefficient through the plant layer. For the long wave radiation exchange, the emissivity of the leaf (ε_l) is also necessary. The same parameters are also needed for the soil (in the following α_s is absorption coefficient and ε_s is emissivity) and for the back wall not covered by the vegetation. Moreover, it should be noted that, as known, spectral parameters can vary if soil and/or wall are wet or dry.

Since it affects the wind velocity on the wall surface, the height of the plants plays an important role in convective heat transfer and evapotranspiration. The transpiration of the plants is a natural physiological process during which the water taken from the soil by roots, passes through the plant and then is evaporated from cells (called stomata) in the leaf. It is described by leaf stomatal conductance (or conversely the stomatal resistance, r_l). Transpiration is the rate of water vapor that leaves through the pores on the leaf. It depends on the number of stomatal pores per leaf surface area and the pore size [42]. In addition, evaporation from the soil depends on the maximum volumetric moisture content of the soil layer (saturation), the minimum (residual) volumetric moisture content of the soil layer and the initial volumetric moisture content of the soil layer. However, the effectiveness of evapotranspiration is strongly influenced by climatic conditions in which the plants live and are subjected and by the status and suitability of their growth. According to [43], the direct measurement of evapotranspiration could be made by using soil evaporimeters and lysimeters. These tools and techniques are categorized according to their method of operation:

a) Weight based, which use mechanical scales to account for changes in water content.
b) Hydraulic based, which use the hydrostatic principle of weighing.
c) Volumetric based, in which water content is kept constant and evapotranspiration is measured by the amount of water added or removed.

Moreover, the transpiration of the plants could be obtained as difference between measured evapotranspiration and measured evaporation. Direct methods for measuring the evaporation are evaporation pans and lysimeters; indirect methods are the water-budget, the energy-budget, the aerodynamic approach or combination of these.

For the heat conduction and heat storage in the back wall and in the soil layer, thermal conductivity (λ), density (ρ), specific heat (c_p) and thickness of each material have to be considered. Once again, for the substrate, these values could vary with the water content. Few studies present the experimentally measured values. For instance, the study [44] proposes the in-lab evaluation of thermal conductivity of each element; more in detail, they have found conductivities of 0.062 W/m K for sphagnum moss, 0.060 W/m K for outdoor planting mix, and 0.105 W/m K for clay balls and 0.051 W/m K for the substrate from a green-wall, 0.220 W/m K for Hedera and 0.274 W/m K for Virginia creeper. He *et al.* [45], with reference to an indirect *LW* system in Shanghai, have indicated measured value: in detail, Vinca major Varegata plant is adopted ($\alpha_l \approx 0.70$ and $e_l \approx 0.95$) with a substrate (6 cm, $c_p \approx 600$ kJ/K, $\alpha_s \approx 0.8$ and $e_s \approx 0.9$) made of peat soil, powdered perlite, vermiculite aggregate and organic fertilizer; for the soil conductivity, the authors indicated this as a function of temperature, and thus $\lambda = 0.374*(T)^{0.403}$ W/m K. In that paper, they have estimated a *LAI* of 4 and the height of plant equal to 15 cm.

Table 3.1 collects all information concerning the technical data for designing a *GW*, by considering all sub-systems. For each paper, it has been evidenced the type of green vertical system (*GST*), the main materials of the back wall (U_{value} is thermal transmittance) and the presence of air gap, the plant species, their height and the *LAI*, the type of substrate and the irrigation technique. The table cannot be found elsewhere, and it is useful for providing information to the decision-maker about which plant, substrate and irrigation system could be used, by considering the climate zone and the *GW* type.

Moreover, if more than one plant is analyzed in the same study, the thermal behavior of them (and so the best one) can be deduced from tables presented in the following sections. Indeed, for each one of the selected papers, energy and environmental behaviors are deeply discussed.

The analysis of Table 3.1 allows one to see that the description of all technical sub-systems of a *GW* is usually not detailed and all parameters needed for the solution of heat and moisture balances are not specified. There are not studies where the stomatal resistance is calculated, while this parameter is available for green roofs; moreover, volumetric moisture content is often not declared. Only the *LAI* and height of plant are frequently indicated. The most common value for plant height is 10 cm. When it is specified, the air gap is usually open for indirect *LW*s, but the thickness is greatly variable. There are not comparable configurations for the selection of vegetation species, the only recurring type is the *Parthenocissus tricuspidata* for the *GF*s.

Some information can be found from the European map, created starting from the Plant Hardiness Zone Map, published in 2012 by the Department of Agriculture of the United States; this is the standard used by gardeners and growers for determining which plants are most likely to thrive at given location. More in detail, the green façades need climbing plants. To assure the growth of these species, the main parameters that must be considered are temperature and humidity. Basing on tolerance to the minimum temperatures and on the length of the winter period, the climbing plants are divided into:

- hardy species: these can live also with very low temperatures and in presence of frost (*Clematis montana, Fallopia baldschuanica* and *Schizophragma hydrangeoides*);
- half-hardy species: these can resist only occasionally at frost and must be protected during cold winter (*Akebia quinata, Bouganvillea*

glabra, Plumbago auriculata, Trachelospermum jasminoides and *Doxantha unguiscati*).

Some general conclusions can be also found from a critical review. First of all, the plants adaptable in hot-dry conditions are: *Smilax aspera, Clematis flammula, Eriocereus bonplandii, Tecomaria capensis* and *Delairea odorata*. Coversely, *Hedera helix* and *Jasminum officinale* can be adapted in each climate [46]; in this case, therefore, the main aspect for the selection is the attachment mechanism [47]. Climbing plants that find a suitable support have greater performance and fitness. Plants with secretory adhesive pads (*Parthenocissus tricuspida*) can cling to a building wall, whereas ones with tendrils (*Clematis virginiana*) can cling only to narrow stems or trellises [48]. For the direct green façades, the most suitable climbing plants are the root-climbers or leaf-climbers ones, with clinging roots or adhesive pads, as *Hedera helix* (common ivy), *Parthenocissus tricuspidata* (Boston ivy) or *Wisteria* (Virginia creeper).

Moreover, for indirect green façades, climbers as tendril-bearers, hook-climbers or twining plants are necessary: for example, *Camellia, Ceanothus, Chaenomeles, Coronilla valentine, Garrya, Fuchsia, Magnolia grandiflora* and *Pyracantha* [46].

Furthermore, for continuous *LW*s, the most suitable species come from Gramineae group, which can be divided into six subfamilies for a total of about 7500 species [49]. The turf species are generally suitable for trampling, and they have an excellent ability to recovery from stress phenomenon. These are divided into two groups: micro-thermal and macro-thermal. The macro-thermal species requires an air temperature of about 27–35 °C [50]. They also slow their growth rate with temperatures below 20 °C to stop completely below 10 °C. They are native species of tropical, sub-tropical and temperate areas. The macro-thermals are characterized by a deep and extensive root system, while the leaf width and their density are variable parameters, both between the species and the cultivars (cultivated or a man-made variety of a plant species). The macro-thermal belong to two subfamilies: the Eragrostideae family that includes *Cynodon, Zoysia* and *Buchloe* [46], and the Panicoideae group that contains *Paspalum, Stenotaphrum, Pennisetum, Axonopus* and *Eremochloa*. The micro-thermal species grow in climates with temperatures ranging from 15 °C to 24 °C and these do not tolerate summer stress like high ambient temperatures and lack of water. On the other hand, they can face the coldness and they can preserve their color during the winter months. All told, these are suitable for vertical surfaces not exposed excessively to the sun. The micro-thermal species come from Asia and Europe, but nowadays these are spread almost everywhere in the world [51]. Some important genera are *Festuca, Poa, Lolium* and *Agrostis*.

For modular *LW*s, herbaceous perennials should be used, since these require less maintenance and nutrients compared to turfgrass. Some plants used for modular *LW*s in different parts of the world are:

- Sedum generis (*Ajuga, Hedera Helix, Liriope, Sedum acre, Sedum album, Sedum Reflexum, Sedum sarmentosus, Sedum Sexangulare, Sedum spurium, Sedum caeruleum, Sedum pulchellum, Sedum roseum*);
- Rosids class (*Cotoneaster salicifolius, Cotonesater dammeri, Hypericus calycinum, Aubretia Deltoides*); Magnoliophyta class (*Berberis, Crategus, Pernettya, Cistus, Rosmarinum officinalis, Alyssum saxatile*).

Whittinghill *et al.* have shown [52] that greenery systems with woody plants, including shrubs and herbaceous perennials, have higher carbon content than the turfgrass and the sedum. So the selection of these plants is more suitable. According to Charoenkit and Yiemwattana [35], in order to optimize not only the carbon storage, but also the thermal performance in hot and humid climates, plants with dense foliage, small leaf and woody branches should be chosen, like *Cuphea hyssopifola* H.B.K.

For what concerns the substrate and its correlation with plant species, scarce information can be found in the literature. Some of the main characteristics of the substrates are the well-draining behavior and the proper organic content (chemical, physical and microbial). The growing media can be made by organic materials such as coconut coir, peat, tree bark, or inorganic materials such as expanded clay pebbles, gravel, perlite, mineral soil, mineral wool, sand, vermiculite. Different materials are often combined; in this case, the organic component usually is less than 10% of the mix, providing, on the other hand, important nutrients to the plants [53]. The containers for plants and growing medium have to be breathable, or made with holes, because these have to favor the free outflow of excessive water. These have to be enough large to allow the spreading of the roots, but not too big, to prevent the phenomenon of suffocation and rotting due to high humidity. More in general, the space for the roots has to be proportional to the total transpiration surface of the plant, which depends on the quantity and type of its foliage. Another important aspect for the designers is the “amount of soil” to “the pot capacity” ratio. Indeed, if this ratio is high, it means much evapotranspiration and so much more frequent need of watering; on the other hand, a low value of this ratio determines greater water retention and so less frequent watering.

As regards the back wall, the direct green façades require systems that have not holes and cracks in order to avoid any possible infiltration of the climbing plants that can damage the structure. For the indirect system, one of the main issues concerns the non-self-standing species that require a support system. Considering the *LW*s, a critical aspect is the waterproofing of the envelope. The adoption of an air gap between the back structure and the *LW* is a possible solution to limit this problem. Chen *et al*. [54] have carried out an experimental campaign in hot and humid climates, showing that a *LW* with a sealed air layer performs better compared to a naturally ventilated air layer, in terms of cooling effect, but the back wall is subjected to higher humidity. The insulation level of back wall is usually not indicated and thus it is not possible to discuss the effect of green system on thermal resistance; it could be interesting an optimization of the back wall composition in function of *GW* type, plant species and climatic conditions. The numerical study of Kontoleon and Eumorfopoulou [55] only indicates that for a direct *GW* located in a humid subtropical climate zone, the cooling load is lower if the insulation is located in the middle or in the inner sides.

The design of the irrigation system is not discussed in the available literature. It is important for the survival of plants and it implies an additional electric consumption, due mainly to pumps. This cost has to be taken into account in the annual energy balance of the building, in order to evaluate the economic and energetic profitability of a green system. The pumps could be scheduled or, even more appropriate, these could be automatically activated by a humidity sensor placed in the root area. The historical trend of rainfall on the site has to be compared with the rate of water that the plants need in order to understand and clearly identify the contribution of the direct irrigation. This is the precaution to overcome the unsustainable use of water for irrigation [30]. There are some strategies to decrease the consumption of water. For instance, Manso and Castro-Gomes [56] have installed, on the same wall, plants that require less watering on the top (like *Sedum* species), and plants that need more water on the bottom part (like *Thymus* species). In this way, it is possible to take advantage by the vertical displacement of irrigation water by gravity. Another possibility, as explained in Mårtensson *et al*. [57], is the selection of materials for the substrate with high water holding capacity (i.e. rockwool panel) that could be irrigated with larger volumes at sparser intervals, without risk of increasing runoff.

As regards the sizing of the spaces, the information to consider are:

- the pipes' diameter (which depends on the rate, the speed and the pressure of water),
- the pumps,
- the sensors,
- the drip tray placed at the bottom for collecting the water excess runoff from the system.

It must be also emphasized that the irrigation system needs ordinary and extra-ordinary maintenance, with the aim of checking for water leaks, clearing debris from irrigation injectors, inspecting any controllers and sensors, replacing electronic devices if needed, verifying the proper water flow and pressure [53].

About the climatic conditions, the knowledge and also the evaluation of air temperature and surface temperature are not enough for studying the *GW* thermal behavior. These could be considered the most representative parameters but, in the same way, these are not exhaustive of all benefits that a *GW* can bring. Susorova *et al.* [42], by means a sensitivity analysis, have shown that the most effective weather parameters, in order of their importance, are solar radiation, wind speed, relative humidity, and outdoor air temperature.

Hunter *et al*. [33] have suggested six parameters that all experimental studies about green façade should report, to have an adequate quantification of thermal performance and microclimatic benefit:

- ✓ solar radiation in front of or away from the green façade;
- ✓ air temperature in front of or away from the green façade;
- ✓ wind speed in front of or away from the green façade;
- ✓ solar radiation between green façade and the wall;
- ✓ air temperature between green façade and the wall;
- ✓ wind speed between the green façade and the wall.

According to authors, for accurate characterization of the green façade, also the infrared radiation emitted and intercepted by the green canopy and the relative humidity in front of and away from the green façade could be interesting in order to better understand the contribution of such systems for what concerns the reduction of heat islands and the improvement of hygro-thermal conditions. Moreover, considering the *LW* systems, according to us, surface temperature and the inside temperature of the substrate can provide other important information concerning the usefulness and the thermal performances.

Table 3.1 - Data available in scientific literature for GWs (please, note that GF is Green Façade, LW is Living Wall and N stands for configuration).

Ref.	*GST*	Air Gap	Back Wall (in to out)	Plant Species	*LAI* [m^2/m^2]	Height [cm]	Substrate Type	Irrigation Type and Schedule
[39]	Indirect *LW*	0.05 cm	Fibercement	1. Cuphea hyssopifola, 2. Tibouchina urvilleana, 3. Excoecaria cochinchinensis	1. 5.06 2. 3.69 3. 3.85		Marked available mixture of plant residues, husk, coconut fiber and cow dung	Daily irrigation at 8.00 and 16.00. Fertilizer 16-16-16 twice in February and May.
[40]	*GF*	-	-	Momordica charantia, Ipomoea tricolor, Canavalia gladiate, Pueraria lobate, Apios American Medikus			Akadama soil	
[41]	Indirect *GF*	Open 20 cm	Gypsum - alveolar brick-cement mortar–U_{value} = 0.784 W/m^2K	*Parthenocissus tricuspidata*	3.5–4.0			Simple drip irrigation during summer
[42]	Direct *GF*	-	Bricks	*Parthenocissus tricuspidata*	1.8	12		
[45]	Indirect *LW*	Close, 20 cm	Foam sandwich panel	Vinca Major Varegata	4.0	15	Peat soil, powdered perlite, vermiculite and organic fertilizer	One for day.
[54]	Indirect *LW*	Open 3 to 60 cm.	U_{value} = 0.25 W/m^2K	Six plant species not specified			Mix of light growth media	Once a day with an electrically system
[56]	Direct *LW*	-	Sandwich panels with polyurethane foam covered by painted steel sheets in both sides	Sedum album, Sedum sediforme, Thymus serphyllum, Valgaris, Prostrates, Mastichina, Archillea millefolium			60% organic and 40% inorganic materials	Every two days at 17:00, between 4 and 7 min until the modules are completely wet.

Ref.	*GST*	Air Gap	Back Wall (in to out)	Plant Species	*LAI* [m^2/m^2]	Height [cm]	Substrate Type	Irrigation Type and Schedule
[57]	Direct *LW*	-	Masonry wall	Achillea millefolia, Bergenia cordifolia, Dianthus deltoides, Molinia caerulea, Nepeta faassenii, Salvia nemorosa and Sesleria heufleriana			**1.** Rockwool panelsystem **2.** Pumice-filled pocket system	**1.** Three times for day for 10 min. After twice a day for 15 min **2.** Three times a day for 10 min. After 1 h every-day.
[58]	1. Indirect *GF* 2. Indirect *LW*	1. Open, 25 cm 2. Open	gypsum - alveolar brick-cement mortar U_{value} = 0.784 W/m^2K	*1. Parthenocissus tricuspidata* 2. Rosmarinus officinalis and Helichrysum thianschanicum			Coconut fibers	
[59]	Direct *GF*	-	Bricks	Hedera helix		10		
[60]	Direct *GF*	-	Bricks	1) Stachys, 2) Fuchsia, 3) Jasminum, 4) Hedera, 5) Lonicera, 6) Prunus	1) 4.5, 2) 8.0, 3) 7.0, 4) 6.7, 5) 10.8, 6) 5.2			
[61]	Direct *GF*	-	Plaster - limestone - brick	*Parthenocissus tricuspidata*	2.0	20		

Ref.	*GST*	Air Gap	Back Wall (in to out)	Plant Species	*LAI* [m²/m²]	Height [cm]	Substrate Type	Irrigation Type and Schedule
[62]	1. Indirect LW 2. Indirect LW 3. Indirect LW	1. Open 2. Sealed **3.** Open	1. Plaster – Concrete blocks – plaster 2. Plaster – Bricks – Plaster 3. Concrete blocks	1. Sedum, Geranium, Anemone, Viva minor, *Parthenocissus tricuspidata*, Heuchera micrantha Palace Purple, Salvia nemorosa, Lonicera pileata, Pittosporum tobira, Rosmarinus officinalis, Alchemilla mollis, Bergenia cordifolia, Oenothera missouriensis, Plumbago capensis 2. Zoysia species 3. Zoysia matrella, Zoysia tenuifolia, Zoysia japonica, Cynodon dactylon, Stenotaphrum secondatum, Dicondra, Paspalum vaginatum, Cynodon transvalensis			1. Threefold felt layer 2. Threefold felt layer 3. Soil	flexible pipe providing 2.1 l/h of water by each nozzle
[63]	N1: *LW,* N2: *GF*, N3: *LW*, N4: *LW*, N5: *LW*, N6: *LW*, N7: *LW*, N7a: *LW*, N8: *LW*			N3: Hemigraphis repanda N6: Phyllanthus myrtifolius		N1: 10, N2: 10, N3: 12, N4: 12, N5: 11, N6: 5.5, N7a: 12, N8: 20	N1, N3: mixed substrate N4, N7: inorganic substrate N5: green roof substrate N6, N7a, N8: soil substrate	N4: integrated irrigation
[64]	Direct *LW*	-		Zoysia japonica			Grodan® hydroponic medium	Water-soluble fertilizer (Lawn Food with chelated iron, Schultz, Bridgeton, MO) twice a day (8:00 and 14:00)

Ref.	*GST*	Air Gap	Back Wall (in to out)	Plant Species	*LAI* [m²/m²]	Height [cm]	Substrate Type	Irrigation Type and Schedule
[65]	Direct *LW*		Concrete block coated with mortar	Helichrysum thianschanicum			Mix of compost and coconut fibers	Two pipes: a pressurized (2–5 bar) fertigation injection system.
[66]	1. Direct *GF* 2. Indirect *LW* 3. Indirect *LW*	1. - 2. Open–20 cm 3. Open–4 cm	1. clay bricks 2. clay bricks 3. plywood	1. Hedera helix 2. Hedera helix, Vitis, Clematis, Jasmine and Pyracantha 3. Different evergreen plants		1. 20 2. 10 **3.** 10	1. – 2. Soil 3. potting soil	2) and 3) computer-controlled system for water and nutrients
[67]	Direct *GF*		Plaster-insulated brick- plaster	Parthenocissus triscupidata		25		
[68]	1. Indirect LW 2. Indirect LW	1. Open–5 cm 2. Close–5 cm	1. Concrete blocks 2. Brick wall	1. Vertical garden 2. Grass	1. 3.0 2. 5.8		1. Felt 2. Felt	
[69]	Direct *LW*	-	Extruded polystyrene	Sedum			Felt	Drip irrigation system to the enclosure
[70]	Direct *LW*	-	Plaster - concrete blocks - plaster					Drip irrigation pipe

Ref.	***GST***	**Air Gap**	**Back Wall (in to out)**	**Plant Species**	***LAI* [m²/m²]**	**Height [cm]**	**Substrate Type**	**Irrigation Type and Schedule**
[71]	Direct *LW*	-	Brick	Goodenia pinnatifida, Brachyscome ciliaris, Poa labillardieri, Enneapogon nigricans, Kennedia prostrata, Atriplex semibaccata, Ixiolaena leptolepis, Ptilotus nobilis, Hardenbergia violacae			Two soil media (scoria and clay)	Drip irrigation system with pressure compensating drippers
[72]	1. Direct *GW* 2. Indirect *GW* 3. Indirect *LW* 4. Indirect *LW*	1. No 2. Open, 5 cm 3. Open, 5 cm **4.** Open, 5 cm	Bricks –air – mineral wool – limestone	1. Hedera helix 2. Hedera helix 3. Pteropsida 4. Pteropsida		1. 20 2. 10 3. 10 **4.** 10	1. Terrestrial soil 2. Terrestrial soil 3. Potting soil 4. Wool fleece	
[73]	Direct *LW*		Masonry wall	Allium schoenoprasum, Chamaecyparis persifera, Euonymus fortuneii, Ilex crenata, Luzula sylvatica, Vinca minor, Vaccinium vitis-idea.			Rockwool panels (Vertigreen^{TM}, Zinco GmbH)	• Three times a day for 10 min with a rate of 4.6 l/min. Fertilizer 20 ml/panel one week after planting and in the beginning of July. • Three times a day for 10 min with a rate of 0.8 l/min. • Evening and morning for 15 min.

Finally, it can be concluded that available studies do not present a complete replicable characterization of green vertical systems; there are only a few experimental studies that explicit the base performance parameters or that describe how these have been calculated. Surely, the actual research is not exhaustive in the matter of thermal and bio-physic characteristics.

<u>*Mathematical Models for the Greening Systems' Performance Evaluation*</u>

Another important question to answer is the shortage of validated simulation models. Indeed, this research area is today under development. A validated model of a GW could help the optimization of design parameters and the evaluation of urban and building benefits as well as it would allow reliable evaluation of the effects on sustainability; the availability of data also allows to increase the awareness of designers and citizens about this technology. Table 3.2 presents a critical analysis of available mathematical models also evidencing if they have been implemented in commercial simulation engines. In this case, for each paper, it has been deduced the type of tool used, the typology of heat flux, the parameters or index of the validation and the validation data.

The most common assumptions made by models are cited in the following bullet list:

- mono-dimensional heat flux;
- constant parameters for describing leaves behavior;
- leaf angles are not considered;
- plants and substrate are homogeneous;
- the biochemical reactions and heat conduction through plants are not considered.

Only one paper [42] specifies that the model considers plants only during the growing season, the temperature of a leaf is assumed to be the same as the air temperature, the external factors that may vary with height are assumed to be constant, the level of soil moisture at plant roots is constant.

Table 3.2 - GW models

	Type/ Tool	Heat Fluxes	Validation Parameter or Index	Data for Validation
[42]	RC model with numerical bisection method	• short-wave radiative transmission through the plant; • long-wave radiative exchange with environment; • convective heat transfer to and from vegetation; evapotranspiration.	Outdoor surface temperature: coefficients of determination between modeled and measured values are 0.97 for the bare wall and 0.96 for the *GF* on the sunny day; on the cloudy day they are 0.87 and 0.86 respectively.	Data of 4 days for validation.
[45]	Implicit finite difference scheme and predictor-corrector method	• plant shading; • transpiration effect; • substrate evaporation; • insulation effect.	Temperature of canopy layer and substrate: the Root-Mean-Square Error is respectively 0.61 and 0.50 in summer and 0.25 and 0.23 in winter.	• summer experiment: 2–7 August 2015; • winter experiment: 12 February 2014–12 July 2014.
[68]	Finite volume approach and RC network	• convection; • radiation; • conduction; • evapotranspiration.	Surface temperature and heat flux on the back wall: • the Nash–Sutcliffe efficiency index is 0.7 in summer and it varies between 0.4 and 1.0 in winter; • the Root-Mean-Square Error is between 0.5 and 8.0.	• One week of the summer and of winter for validation.
[74]	Dynamic/ TRNSYS	• short- and longwave radiation; • sensible heat fluxes; • latent heat fluxes.	Temperatures at a depth of 2 cm below the surface of the substrate: mean difference is 0.8 °C, and 80% of the computed temperatures have a precision of ±10%.	• Validation with measures on green roof; • Data of 19 days for validation.

[75]	Dynamic/ EnergyPlus	• short-wave radiation by foliage and soil; • long-wave radiation exchange within plant canopy; • evapotranspiration; • sensible heat flux exchange with air in the canopy and substrate.	The correlation coefficients are: • for indoor air temperature, 0.97 in the study A and 0.81 in the study B; • for exterior surface temperature, 0.88 in the study A and 0.80 in the study B; • for inner surface temperature, 0.90.	• study A: Wuhan, China July 25, 2012 (during the summer); • Study B: New Territories, Hong Kong, June–September (during the summer).
[76]	2R3C model/ SOLENE-Microclimate	• short and long-wave radiative exchange; • evapotranspiration; • convection.	Leaf and substrate temperature: the difference between measured and simulated values are lower than 2 °C for sample 1 and 2 and lower than 1 °C for sample 3.	Monitoring during May 2009 in Geneva on three of 1 m^2.

These limitations, by considering the proposed equations, probably affect also other models that, analogously, also consider these parameters as constant.

Susurova *et al.* [42] have proposed a model focused on plant physiological processes, including evapotranspiration and radiative and convective heat exchanges interesting the plant layer, the facade, the surrounding environment and the ground: the model takes into account individual plant characteristics inputs and weather data; it should be noted, furthermore, that this model was verified with a set of experiments that measured thermal performance of both bare and vegetated facade of an educational building in Chicago, during the summer. Scarpa *et al.* [69] have defined a mathematical model validated against in-field measurements for two different kinds of LWs, with open or closed air cavities, monitored in Central and Northern Italy. Djedjig *et al*. [74] have developed a model for the evaluation of the coupled heat and mass transfers through a green module that, in addition to a street canyon model, was integrated into TRNSYS code [77]. He *et al*. [45] have developed a model that evaluates the one-dimensional distribution of temperature and moisture. The main assumptions are: constant wind speed along the height direction; constant water content distribution under daily irrigation, ignoring gravity effect and precipitation; plant canopy is considered as a semi-transparent medium. The model has been validated with in-field experiments carried out on two test rooms in the Jiading campus. In 2017 Dahanayake *et al.* [75] proposed the integration of a mathematical model based on heat balance principle of the foliage layer and soil layer in EnergyPlus, basing on the equations of the green roof module. The model has been validated by means of two experimental studies. A hydro-thermal model of GWs has been carried out by Malys *et al.* [76] for the implementation in the urban microclimate simulation software SOLENE-Microclimate. Kontoleon and Eumorfopoulou [55] have modeled the behavior of a building zone with a GW by employing a RC-network model with transient nodal solution, which allows the adjustment of the various parameters in discrete time steps. The following mechanisms are taken into account: conduction, convection and radiation through envelope, heat storage within the thermal mass, heat transfer mechanisms through the foliage canopy. The model allows to take into account the wall orientation, the covering percentage of plant foliage, and the type of wall configuration. However, validation indexes are not proposed, and the reliability of the model cannot be discussed. Finally, basing on experimental data, Olivieri *et al.* [78] have developed an autoregressive fitted model that allows the prediction of temperature difference between a module without vegetation and a module with vegetation, by using as input values only outdoor climate conditions: temperature, relative humidity and the vertical irradiance on the surface.

The previous analysis allows concluding that some mathematical models are available, but these are not already implemented in commercial software, not validated according to standard procedures and these are not easily adoptable by designers and researchers for studying thermal and energy performances of GW systems.

Often, simulation tools, e.g. EnergyPlus, have implemented merely a module for simulating green roof, specifically validated for surfaces with low inclinations. As asserted by some studies [79], this module can predict, approximately, the behavior also of green vertical walls, although the results have not been validated by the developers. The main difference is the great amount of water held by the roof compared to the wall but also the dynamics of hydro-thermal mechanisms on a vertical (and thus not horizontal) surface.

3.2.3. A Critical Overview of Vertical Greening Systems' Performances

*GW*s and *LWs* are investigated and reviewed according to several points of view. At the building level, the most studied effects of vertical green systems are:

- reduction of heating and cooling energy demand,
- improvement of thermal comfort,
- noise reduction,

- protection of the exterior coatings from *UV* radiation or extreme weathering.

Moreover, several aspects can be underlined about the urban rehabilitation: the reduction of urban heat island (*UHI*) effect, the improvement of storm-water management and the absorption of air pollutants in the atmosphere. In addition, building greenery allows to increase the vegetation in the urban context without occupying any space at street level and to enhance the biodiversity with the indirect improvement of urban image.

This sub-section proposes a critical analysis of available research results, distinguishing the behavior of green vertical systems in three main areas: urban quality, building performance and sustainability.

3.2.3.1. Urban Quality

Considering the available studies, the most measured parameter is the reduction of surface temperature between the bare wall and the green coverage. This can be related to potentialities in terms of *UHI* mitigation due to spectral characteristics of plants that determine a selective absorption of heat wave radiation and the reduction of re-radiation, but it is also related to the cooling effect of urban space and the reduction of building energy need during the summer. This surface temperature is usually measured by means of an infrared camera or with surface temperature sensors.

Really, it has to be underlined that many studies compare the monitored temperature on the bare wall and the values at the same point when the wall is covered by a green layer and therefore the temperature measure is not on the substrate or on the leaves. This kind of measure cannot be considered useful for the evaluation of urban heat island mitigation and surface temperature reduction. Really, it can give information about the energy saving also if, often, it is not possible to distinguish the contribution of vegetation mechanism and the air gap (usually present) effect. For instance, two studies have been done in the Mediterranean climate [62]-[80]; according to these, the external surface temperature difference between the bare wall and the covered wall goes from 9 °C (*Pandorea jasminoides* variegated and

Rhyncospermum jasminoides) to 20 °C (threefold felt layer with evergreen or seasonal plants), during sunny days.

Table 3.3 summarizes only the results of reviewed papers that consider the temperature difference between the bare wall and the substrate/foliage. For each paper, the way through which results have been achieved is evidenced. In particular, the following nomenclature is adopted: Exp = experimental and *Num* = numerical. The climatic zones are named according to Köppen-Geiger classification, and other considered parameters are the observation period, the vegetation species as well as the type of green vertical system, the orientation and the average or maximum value of external surface temperature reduction. A star (*) near the value means that this has been obtained with some elaborations.

.

Table 3.3 -. Results about surface temperature reduction

Ref	Type	Climate	Period	Plant Species	*GST*	Orientation	External Surface Temperature Reduction
[39]	*Exp.*	Phitsanulok (Aw or As - Tropical wet and dry or savanna climate)	December 2015–May 2016	False Heather, Princess Flower, Chinese Croton	*LW*	South	**Average values** • Summer: Day: 1.6°C, Night: 0.73 °C • Winter: Day: 2.6 °C, Night:1.15 °C
[45]	*Exp.*	Shanghai (Cfa - Humid subtropical climate)	August 2015 December 2015	Vinca Major Varegata	*LW*		**Maximum values** • Summer: Day: 28 °C, Night: −2 °C • Winter: Day: 10 °C, Night−10 °C
[55]	*Num.*	Thessaloniki (Cfa - Humid subtropical climate)	June–August	Parthenocissus triscupidata	*GF*	North East South West	**Average values** • North: ≈ 2.73 °C * • East: ≈ 11.53 °C * • South. ≈ 7.46 °C * • West: ≈ 17.85 °C *
[56]	*Exp.*	Covilhã (Csb – Warm summer Mediterranean climate)	February−March	Sedum species and Thymus species	*LW*	South	**Maximum value**: 15 °C
[58]	*Exp.*	Puigverd de Lleida (Csa - Hot-summer Mediterranean climate)	June−July December−February	1. *GF*: Boston Ivy - *Parthenocissus tricuspidata* 2. *LW*: Rosmarinus officinalis and Helichrysum thianschanicum	*1. GF* 2. *LW*	East South West	**Average values** • Summer: East: *LW* 17.0 °C; *GF* 13.8 °C South: *LW* 21.5 °C; *GF* 10.7 °C West: *LW* 20.1 °C; *GF* 13.9 °C • Winter: East: *LW* 4.5 °C; *GF* -0.2 °C South: *LW* 16.5 °C; *GF* 0.7 °C West: *LW* 6.5 °C; *GF* -0.3 °C

Ref	Type	Climate	Period	Plant Species	*GST*	Orientation	External Surface Temperature Reduction
[59]	*Exp.*	Nottingham (Cfb - Temperate oceanic climate)	3 weeks	Hedera helix	*GF*		Maximum value 6.1 °C on sunny days and 4.0 °C on cloudy days
[60]	*Exp.*	Reading (Cfb - Temperate oceanic climate)	19 August	Prunus laurocerasus	GF	South	**Average value**: 6.3 °C
[63]	*Exp.*	Singapore (Af - Tropical rainforest climate)	24 February 2008, 28 April 2008 21 June 2008	N3: *LW* Hemigraphis repanda N6: *LW* Phyllanthus myrtifolius	N1: *LW*, N2: *GF,* N3: *LW,* N4: *LW*, N5: *LW,* N6: *LW*, N7: *LW,* N7a: *LW*, N8: *LW*		**Maximum value** • 24/02: N1:5.23 °C, N2: 2.45 °C, N3: 4.92 °C, N4: 5.30 °C, N5: 4.48 °C, N6: 3.25 °C, N7: 4.25 °C, N8: 3.72 °C • 28/04: N1: 7.93 °C, N2: 7.32 °C, N3: 9.21 °C, N4: 8.95 °C, N5: 8.48 °C, N6: 6.11 °C, N7a :6.12 °C, N8: 7.84 °C • 21/06: N1: 5.33 °C, N2: 6.35 °C, N3: 5.69 °C, N4: 6.34 °C, N5: 6.53 °C, N6: 4.04 °C, N7a: 4.97 °C, N8: 6.61 °C
[67]	*Exp.*	Thessaloniki (Cfa - Humid subtropical climate)	July−August 2006	Parthenocissus triscuspidata	*GF*	East	**Average value**: 5.7 °C **Maximum value** < 8.10 °C *

Ref	Type	Climate	Period	Plant Species	*GST*	Orientation	External Surface Temperature Reduction
[71]	*Exp.*	Mawson Lakes (Csb - Warm-summer Mediterranean climate)	December 2014– July 2015	Goodenia pinnatifida, Brachyscome ciliaris, Poa labillardie, Enneapogon nigricans, Kennedia prostrata, Atriplex semibaccata, Ixiolaena leptolepis, Ptilotus nobilis, Hardenbergia violacae	*LW*	West	**Average values** • Warm days: Day :3.4 °C *, Night: 1.9 °C* • Cold days: Day 0.22 °C *, Night−0.05 °C* **Maximum values** • Warm days: 14.90 °C • Cold days: −5.88 °C
[75]	*Num.*	Hong Kong and Wuhan (Cfa - Humid subtropical climate)	one hottest summer day one coldest winter day	1. Peperomia claviformis 2. Plant not specified	*1. LW* 2. *LW*	1. Exposure not specified 2. West	**Hong Kong maximum values** • Hottest summer day: 24.2 °C • Coldest winter day:16.9 °C **Wuhan maximum values** • Hottest summer day 26.2 °C • Coldest winter day: 18.4 °C
[76]	*Exp.*	Geneva (Cfb - Temperate oceanic climate;)	May (1 week)		*LW*	South	**Maximum value**: 13 °C*
[81]	*Exp.*	Santiago of Chile (Csb - Warm-summer Mediterranean climate)	January (12 days)	Highly dense sedum, medium dense sedum	*LW*	North	**Maximum value:** 30 °C

* please, note that GF is Green Façade, LW is Living Wall, N stands for configuration, 1. and 2. are used when two different GST are investigated.

Briefly, 13 papers published in indexed international journals during last 10 years have been found; the highest percentage (85%) refers to experimental studies. Among these, only two studies carried out a monitoring campaign for six months at least. Globally, data are incomparable because these are very different in terms of climate, exposure and monitoring/simulation periods and, therefore, it is not possible to create a unique forecast scenario. However, the data reported in the table suggest some interesting general conclusions. These are here briefly reported.

First of all, the *LW* is more studied compared with *GF* but only two papers [58], [63], for different climates, compare their behavior in the same conditions. Then, it can be observed that, during the summer, the *LW* assures, for each exposure, the highest reduction of temperature with better results on the south side. The results are not so obvious for a tropical climate because for some conditions the *GF* works better than *LW*.

The *LW*s are characterized by major temperature reduction, for chosen conditions, with highest values (≈30 °C) in warm-summer Mediterranean climate and humid subtropical climate. It can be concluded that LWs seem to be more effective in terms of surface temperature reduction due to shading and evapotranspiration effects, also favored by the substrate that increases also the surface mass of the walls. Hence, there is a potential of *LW*s to face the *UHI* phenomena.

Moreover, there is not a general conclusion about the effectiveness of some plant species for *LW*. The increment of leaf index has a positive effect on the reduction of surface temperature as well as the adoption of evergreen plants. Some general considerations about the plants for *GF* can be found. The greatest temperature reductions are observed on the points where the foliage is thicker and more intensive, and closer to the ground where the evaporative cooling is dominant [55]. Hedera and the silver-leaved, semi-herbaceous Stachys might be the best species for temperate oceanic climate; however, Cameron *et al.* [60] suggested that, if the other species increase their canopy density during the growing, they may provide better cooling potential, particularly if they are well irrigated with the aim to maintain consistent the evapotranspiration. Similarly, for humid subtropical climate, Kontoleon *et al.* [55] have shown that, when the covering percentage of the plant foliage increases, there is an improvement of their behavior.

The effect of orientation is clear for *GF*; when the same configuration is compared on different exposures, the exposures for maximizing the cooling effect are the West and the East ones. For *LW*, the best orientation seems to be the south and very often this is the selected exposure for experimental and numerical studies. However, this is not always true. Indeed, the paper [45], by means of a validated heat and moisture transfer numerical model, shows that, for the climate of Shanghai, without any shading from other surrounding buildings, the preference sequence is West → East → South → North.

More recently, to study the influence of vegetated wall on *UHI* problem, Feitosa and Wilkinson [82] have adopted the heat index (*HI*) that combines the effect of air temperature and relative humidity. They have compared two houses, one of these fully covered with vegetation, in two cities: Rio de Janeiro (Brazil) and Sydney (Australia). For Rio de Janeiro, they have not recorded *HI* higher than 15 °C and the occurrences were 1.4% and 14.9%, respectively between 10 °C and 15 °C, and 5 °C to 10 °C. For the case study in Sydney, *HI* attenuation between 15 °C and 20 °C was observed over 0.7% of the duration of the experiment; the frequency between 10 °C and 15 °C has been 1.8% and equal to 4.1% of the time for the temperature range from 5 °C to 10 °C. Another approach was presented by Herath *et al*. [83]; they have compared, by means of simulations, the outdoor air temperature at a height of 1.5 m with the measured real ground temperature values. This evaluation has been done in a tropical warm humid area (Sri Lanka). The temperature reduction has been of 2.03 °C for the scenario with *GW*s (100% of total wall area) in East–West orientation, neighboring buildings on three sides and asphalt road from one side. Moreover, the temperature reduction was of about 1.59 °C when there are neighboring buildings on two sides, asphalt road from one direction.

For tropical climate, the paper [63] considers the measurement of air temperature at intervals of 0.15 m, 0.30 m, 0.60 m and 1.00 m away from the substrate surface, during the 1st December 2008, with 8 different vertical greenery systems installed in HortPark (Singapore). The *GF* type does not influence the ambient temperature while the *LW* number 4 is felt as far as 0.60 m away with maximum reduction value of 3.33 °C at a distance of 0.15 m. According to the authors, their results demonstrate the highest potentialities of *LW*s to cool the ambient temperature in building canyons.

The study of Razzaghmanesh *et al.* [71] has pointed out that the difference between recorded temperatures cannot be considered significant in warm-summer Mediterranean climates. More in detail, during the warm scenario, at 0.50 m away from the bare and *LW*, the temperature is almost the same in most hours; the temperature in front of the bare wall is warmer from 2:30 p.m. to 6:30 p.m., with the maximum difference of 1.68 °C. In a further study, by considering summer conditions in Berlin, with measured data on *GF*s with three different climbing plants (*Parthenocissus tricuspidata, Hedera helix* and *Fallopia baldschuanica*), Hoelscher *et al*. [84] have asserted that a cooling effect for the ambient air in the street canyon is not assured although the difference between external surface temperatures of green and not covered walls were up to 15.5 °C. Analogously, for the *GW* of the Caixa Forum Museum (Madrid, Spain), summer experimental activities have demonstrated that the air temperature reduction varies between 2.5 °C and 2.9 °C [85].

Finally, Susorova *et al.* [61] have shown that, in a cold climate, during the summer days, compared to values near the bare walls, the outdoor air temperature near the vegetated facade is on average 0.8–2.1 °C lower (depending on orientation), the relative humidity is 2–4% higher and the air velocity is 18–3% lower.

Another investigated effect is air pollution control. Marchi *et al.* [86], using a dynamic simulation model, have shown that a *LW* of 98 m^2, placed in central Italy, can capture, averagely, a carbon dioxide flow of 13.4–97.0 kg CO_{2eq} per year. Considering a mixed green cover of different plant species, the authors have estimated an average carbon dioxide flow of 60.87 kg CO_{2eq} per year. Othman and Kasim [87] have pointed out that the carbon sequestrated by individual creepers and climbers ranges from 30 to 170 kg CO_{2eq} per year.

Charoenkit and Yiemwattana [39] have found that the carbon content of *LW*s decreased by 50% in six months, indicating a lack of capacity in carbon sequestration. In particular, this decrement has been found only in the substrate, due to the extraction of nutrients by plants and to the absence of decomposed plants, while the plants had a higher amount of carbon. Considering *LW* plants alone, the amount of carbon sequestrated ranges from 4.35 to 30.26 g CO_2/m^2. Among three plant species, *C. hyssopifola* H.B.K (small leaves) had the highest amount of carbon content, followed by E*. cochinchinensis* and *T. urvilleana*. More recently, Paull *et al.* [88] have presented the results of some morphological, physiological, and biochemical tests on eight common *GW* plant species, before and after exposure of 5 weeks to highly concentrated diesel fuel combustion effluent. They have concluded that the fig family is the most tolerant species.

The benefits in terms of storm-water management were not evidenced with experiments in the available scientific literature meanwhile few papers evaluate if a *GW* can work as water treatment systems [89], [91]. The aim is to reach an acceptable quality of treated wastewater so that it can be used for building uses and irrigation. Prodanovic *et al.* [89] have tested some suitable media and it has resulted that slow media have higher performances because these can remove around 90% of total suspended solids (*TSS*), 50% of total nitrogen (*TN*), 30% of total phosphorus (*TP*), 70% of chemical oxygen demand (*COD*) and 80% of Escherichia coli (*E. coli*). On the other hand, it was observed that fast media can remove averagely 80%, 30%, 15%, 30% and 20% of *TSS, TN, TP, COD* and *E. coli* respectively. Perlite was found to have the best hydraulic and treatment performance among the fast media while coco coir was the best slow media. Then, the same authors [90] have studied the effect of percentage variation of coco coir and perlite in the filter media mix on the performance of *GW*s as a passive greywater treatment system. It is clear that available studies are mainly focused on the evaluation of the impact of greywater on vegetation and these do not quantify the benefit in terms of urban and building management.

Another aspect that can be underlined is the adoption of *GW*s for reestablishing the habitats for some species; since the modern cities are dominated by the built environment, this has determined the loss of many species [92], [93]. About it, Francis and Lorimer [94] have discussed the potential of green vertical systems for the reconciliation ecology, intended as the modification of the environment to promote the preservation of biodiversity and, more in general, the non-human use, without compromising the social utilization. This could be the right approach for the restoration, in a new ecological key, of urban areas. In the same vein, Chiquet *et al*. [95] have found benefits for nesting, food and shelter resources for urban ornithology. The correct design of vertical greening system [96] is, therefore, deliberate manipulation of the habitat template, in order to maximize vegetation cover for visual relief, building energy savings, or other.

Using the city of Southampton as a case study, Collins *et al.* [97] have estimated the public's perceived value of *GW*s to urban biodiversity, in the form of their "willingness to pay" (*WTP*). More in deep, *LW* and *GF* designs have been compared against 'no green policy'. In this study, a higher level of *WTP* was associated with the *LW*. Attitudinal characteristics such as knowledge of biodiversity and aesthetic opinion were significant to determine the value of the greening policies higher than the estimated investment cost.

A quite interesting topic, non-completely investigated, is the economic effect due to vegetation on property value. Briefly, Gao and Asami [98], employing hedonic pricing of greenery, have estimated that an increase in greenery quality level would increase the land price by 1.4% in Tokyo and by 2.7% in Kitakyushu. Des Rosiers *et al*. [99] have estimated that hedges or *GW*s increase 3.9% the property value.

As it can be seen, the last part of the analysis regarding the effect on urban quality allows evidence that there are few papers about carbon sequestration potentialities of a *GW* (compared with green roof). Analogously, there are even fewer papers about the increasing of urban biodiversity or storm-water management as well as of the economic value of the building. This poor information does not allow general conclusions. Thus, scientific research should be improved in these fields for a complete characterization of the urban impact of green vertical systems.

3.2.3.2. Building Performance

1) Energy savings

Several papers are focused on the energy saving evaluation. These were classified in Table 3.4, by considering the main aspects related to performance calculation. Indeed, it is reported the green system type differentiating “direct” configuration, if the green or the substrate are in full contact with the wall, and “indirect” one if there is an air gap between green/substrate and back wall.

The climate and the calculation or monitoring periods were indicated as well as the type of application in terms of exposure. Finally, the temperature set-point value is indicated, as well as the global energy saving achieved. For a better reading, please note that a star near the value means that it has been obtained with author elaboration.

Only five papers are based on the experimental approach and the other ones calculate the energy saving by implementing models (more or less accurate) with different simulation programs.

Some comparisons can be done by considering the experimental results. The *GF*s in Mediterranean climates have limited potential in terms of electricity reduction during the summer period. Indeed, for a *GF* covering approximately 50% of the south facade of a cubicle made of alveolar brick without insulation, with maximum outside temperatures between 37 °C and 39 °C, the energy saving for one week in July (2011) is 5.5% [100]. For the same conditions [41] but considering the application on three exposures of Boston ivy species, during summer 2015, with a higher foliage development (*LAI* ≈ 3.5–4), the declared energy saving during one week of August is 36%. Starting from the data reported by the authors, the daily energy-saving varies between 29% to 52%. More in general, for *GF*s, it can be concluded that the energy-saving increases with the *LAI* (leaf area index); moreover, the configuration that seems to maximize the shadow effect - and thus the energy benefit - consists in the installation of plants on the south, east and west exposures. The comparison for *LWs* is not possible because only few experimental studies are available, and these refer to different climatic conditions.

In the city of La Rochelle (France), characterized by an Oceanic climate, the experiments of *GW*s revealed positive effects in summer while, concerning the winter season, also moderate reduction of heat losses was verified [101]. The paper [58] allows the comparison between *GF* and *LW* in the same conditions (internal and external) also by adopting different plant species. Briefly, for each cooling set-point temperature, the *LW* under investigation has the best behavior.

Very significant results, in terms of quantifications, are obtained in [102]; really, these outcomes are very optimistic and probably this is because, for this passive technology, the cooling load was estimated with a simplified steady-state method. In the same vein, also the study proposed in [55] can be only partially used as a reference, because the behavior of a *GF* is analyzed only for one day of the cooling period; thus, these data are not comparable with experiments for the same climatic conditions, nor with other numerical studies.

As can be seen from these notes, all papers about *LW*s differ for climatic conditions, type of system and plant species. This implies that comparisons cannot be done.

Finally, it can be also underlined that buildings with vegetated facades can influence (often significantly) the performance of a building without a green system, as shown by Djedjig *et al.* [77]. They have found that *GW*s, east and west oriented, installed on a building, reduces by 37% the cooling load of nearby buildings with an aspect ratio (height to width of the street canyons) equal to one, in Mediterranean summer climate.

Some papers investigate also the effect of *GW*s during the heating period. More in detail, some authors, with the simulation approach [79], [103], have shown that there is no penalty during the winter when the *LW* is placed on the north side or if it covers all façades. Conversely, the study [75] highlights an increase in heating demand (around 2–3%), by underlining that the summer performance is however sufficient for compensating this effect in the annual energy balance. Also in this case, it is not possible to give some general conclusions since climate, mathematical model, indoor conditions are really different in the available papers. Several phenomena must be taken into account also during the winter period; first of all, the greenery system protects the façade and composes a buffer that is warmer than the exterior temperature causing a higher surface temperature, moreover, it modifies the thermal resistance of the wall, affects the wind convection, but it also reduces the heat gains during the sunny hours. Tudiwer and Korjenic [106] have presented an experimental in-depth analysis about the winter behavior for an oceanic climate, bordering a humid subtropical climate (Cfb - Köppen classification). They have explored a method to calculate the resistances of the facades with measured data. More in detail, the additional heat resistance is counted in the surface external resistance. The authors have calculated an increment of the total thermal resistance between 0.31 m^2K/W and 0.68 m^2K/W. This result cannot be generalized because it depends on the greening system (plants and ventilation gap) and its location. For this reason, He *et al*. [45] have defined a formulation for the additional equivalent thermal resistance. By means of a validated model, they have found that it is about 9.16 m^2K/W in summer and 0.97 m^2K/W in winter, so it is not the same value during different seasons. Moreover, Perini *et al.* [66] have concluded that, when the foliage or the other layers reduce the wind speed outside (<0.2 m/s), the external surface resistance can be equalized to internal one; thus the thermal resistance of the wall increases of 0.09 m^2K/W. The comparison between experimental and numerical results is difficult to do, considering the available studies. In details, papers based on comparison between monitored and simulated energy savings are not available in the literature. However, only for the Mediterranean climate, looking to results reported in [58] and [79], it seems that the simulation studies underestimate the energy penalty during the winter and also the benefit during the summer.

Table 3.4 - Results about energy saving.

Ref	Type	Climate	*GST*	Plant Species	Application	Period	Indoor	Energy Saving
[41]	*Exp.*	Puigverd de Lleida (Csa - Hot-summer Mediterranean climate)	Indirect *GF*	Boston Ivy - *Parthenocissus tricuspidata*	East, south and west façades of a test room	One week of August 2015	$T_{set\text{-}poit}$: 24 °C	34%
[54]	*Exp.*	Wuhan (Cfa - Humid subtropical climate)	Indirect *LW*		One façade west oriented of a test cell	One day of cooling period	$T_{set\text{-}poit}$: 24 °C	11.8% *
[55]	*Num.*	Thessaloniki (Cfa - Humid Subtropical Climate)	Direct *GF*	Parthenocissus triscupidata	Exposures singularly valuated	One summer day	$T_{set\text{-}poit}$: 20 °C (8:00 – 20:00)	**North:** 4.18–4.98% * **East:** 16.05–19.45% * **South:** 6.69–8.30% * **West:** 17.76–21.51% *
[58]	*Exp.*	Puigverd de Lleida (Csa - Hot-summer Mediterranean climate)	Indirect *GF* Indirect *LW*	*GF*: Boston Ivy - *Parthenocissus tricuspidata* *LW*: Rosmarinus and Helichrysum thianschanicum	East, south and west façades of a test room	Cooling: 18 °C: 10 days 21 °C: 11 days 24 °C: 12 days Heating: 26 days	Cooling period: $T_{set\text{-}poit}$: 18 °C $T_{set\text{-}poit}$: 21 °C $T_{set\text{-}poit}$:24 °C Heating period: $T_{set\text{-}poit}$:22 °C	**Cooling period:** 18 °C: *LW* 31.16%; *GF* 5.01% 21 °C: *LW* 42.93%; *GF* 20.32% 24 °C: *LW* 58.94%; *GF* 33.83% **Heating period:** *LW* 4.2%; *GF* 1.9%
[70]	*Num.*	Al-Ain City (Bwh - Hot desert climates)	Direct *LW*		East-façade of a test room	One year	$T_{set\text{-}poit}$: 25 °C *Inf.:* 0.5 ACH	20.5%

Ref	Type	Climate	*GST*	Plant Species	Application	Period	Indoor	Energy Saving
[75]	*Num.*	Hong Kong Wuhan (Cfa - Humid subtropical climate)	Direct *LW*		One façade of a flat of a building	One year	Cooling period $T_{set\text{-}poit}$: 24 °C Heating period $T_{set\text{-}poit}$: 20 °C	**Cooling period:** Hong Kong 3% Wuhan 3% **Heating period** Hong Kong−2% Wuhan−2.7%
[79]	*Num.*	Siena (Csa - Hot-summer Mediterranean climate)	Indirect *LW*	Plants embedded in the felt layers, without substrate, with mass of 20 kg/m^2	One façade south orientated of a building	One year		**Cooling period:** Massive wall + *LW* (open air cavity): 15.2% Massive wall + *LW* (closed air cavity): 14.0% Insulated wall + *LW* (open air cavity): 6.7% Insulated wall + *LW* (open air cavity): 6.2% **Heating period:** No variation
[100]	*Exp.*	Puigverd de Lleida (Csa - Hot-summer Mediterranean climate)	Indirect *GF*	Ivy (Hereda helix), Honeysuckle (Lonicera japonica), Boston Ivy (Parthenocissus Tricuspidata) and Clematis	Half façade south oriented of a test room	6 days of cooling period	$T_{set\text{-}poit}$: 24 °C	1% Daily

Ref	Type	Climate	*GST*	Plant Species	Application	Period	Indoor	Energy Saving
[101]	*Exp.*	La Rochelle (Cfb - Oceanic climate)	Indirect *LW*	Six different species on Chile sphagnum of 15 cm	West façade of test room	August 2012 December 2012		August: 67% *; December: 20%
[102]	*Num.*	Hong Kong (Cwa - Humid subtropical climate)	Indirect *GF*	Divided Creeper: deciduous	Whole Building	Cooling period	$T_{set\text{-}poit}$: 24 °C	76%
[103]	*Num.*	Kelowna (Dfb - Warm-summer humid continental climate)	Direct *LW*		All façades of a building	One year		**Cooling period**: 7.3% **Heating period**: ≈ 0%
[104]	*Num.*	Genoa (Csa - Mediterranean climate)	Indirect *GF*	20 species both climbing plants and shrubs.	South façade of an office building	June-September	$T_{set\text{-}poit}$: 26 °C	26%
[105]	*Num.*	Singapore (Af - Tropical rainforest climate)	Indirect *LW*	Turfing	Whole building (Different Windows to Wall ratio)	Cooling period	$T_{set\text{-}poit}$: 24 °C	Scenarios: 1A: 74.29% 2B: 10.35% 3C:17.93%

Considering the aspect of building energy performance, the state of art seems quite incomplete; moreover, it can be underlined that all studies investigate the thermal performances in terms of the energy needs and not the primary energy saving, meanwhile the performance of the whole "building-*HVAC* system" could be interesting to investigate. This would make it possible to highlight the influence on the performance of different types of systems due to the lower internal temperature fluctuations and the reduction of peak values. Moreover, there are no studies about the incidence of energy consumptions for pumps and other irrigation equipment; these could influence, negatively, both the annual energy balance and economic profitability.

2) Effects on the indoor microclimate comfort

The great part of available studies analyzes the incidence of a *GW* on indoor comfort in terms of air and surface indoor temperature reduction. Table 3.5 summarizes the results of selected papers evidencing that only one of these adopts the numerical approach. Really, the correct evaluation of effects on thermo-hygrometric comfort would require also the evaluation of other parameters, and thus time lag, time shift, discomfort hours, relative humidity, indoor airspeed as well as the calculation of predicted mean vote and percentage of people dissatisfied. Really, only a few studies calculate some of them, and not uniquely; for this reason, they are not shown in the table. Moreover, according to authors, the effect of vegetated walls in terms of a surface temperature reduction should be evaluated by considering a free-floating regime because the passive effect of a green system is directly evaluated. Oppositely, several papers present the results of monitoring when the *HVAC* systems run.

The organization of Table 3.5 is similar to the previous ones. The type of paper is indicated as well as the climate, the type of *GW*, the reference period, the boundary conditions and the monitored data.

The Mediterranean climate is most frequently investigated and also the application of greenery on the south exposure. Direct *LW*s are most diffused and the characterization period is usually the summer. Indeed, only two papers also analyze the winter period showing a reduction of air temperature: 0–2 °C in the Mediterranean climate [107] and 2–3 °C in tropical climate [39]. Considering the *LW* in the Mediterranean climate, the reduction of surface temperature seems consistent for the analyzed set-up and comparable among these experiments. For the air temperature, west exposure shows the lowest potentiality. Data for indirect systems are not comparable because these are available for different climates. Instead, by comparing direct *LW* and indirect *GF* in Mediterranean climates, the *GF*s are characterized by the worst performance. The analysis of data for direct *GF*s suggests that, for air-conditioned buildings, the climates have not particular effect on surface temperature reduction.

A general conclusion is that the reduction of surface temperature reflects the external surface variation, thus the analysis of climatic data can be used for choosing the best orientation of a *GW*. Moreover, by limiting the diurnal fluctuation of wall surface temperatures, the lifespan of building facades is prolonged, slowing down wear and tear as well as savings in maintenance cost and the replacement of some parts. However, the quantification of these aspects in terms of life cycle cost analysis was not performed. Finally, it could be an interesting research field.

3) Noise reduction

The greenery systems also modify the acoustic performance of a traditional wall. Van Renterghem *et al.* [107] have shown that the effect of wall vegetation strongly depends on the assumptions of the material parameters. This study is performed with a numerical evaluation of impacts on road traffic noise. Their study has also indicated that the substrates usually used for *GST* have high porosity and low density and consequently these show complex acoustic behavior. Horoshenkov *et al*. [108], by means of an experiment in an impedance tube on four different plant species, have concluded that the absorption coefficient of plants is controlled predominantly by the leaf area density and angle of leaf orientation.

Table 3.5 – Results indoor thermal comfort

Ref.	Type	Climate	*GST*	Application	Period	Indoor	Indoor Temperature Reduction	
							Air Temperature	**Surface Temperature**
[39]	*Exp.*	Phitsanulok (Aw or As - Tropical wet and dry or savanna climate)	Indirect *LW*	One façade of test-box south exposed	6 months (December–May)	NS	Mean values: Summer: Day: 1.28 °C / Night:1.16 °C Winter Day: 2.63 °C/ Night:1.90 °C	Mean values: Summer: Day: 0.99 °C/ Night: 0.65 °C Winter Day: 2.16 °C/ Night:1.17 °C
[41]	*Exp.*	Puigverd de Lleida (Csa - Hot-summer Mediterranean climate)	Indirect *GF*	All facades of a test room	Summer 2013 Summer 2015	Free floating		Mean daily values: • 2013: 2.5 °C; • 2015: 2.0 °C.
[42]	*Exp.*	Chicago (Dfa - Hot-summer humid continental climate)	Direct *GF*	Part of building wall South exposed	3 days of August 1 day of September	Air-conditioned office		Mean value: 29/08: 1.5 °C 30/08: 0.6 °C 31/08: 0.7 °C 1/09: 0.8 °C
[54]	*Exp.*	Wuhan (Cfa - Humid subtropical climate)	Indirect *LW*	One façade of a test room West oriented	1 day of July	Free floating	Mean value: 4 °C Maximum value: 1.1 °C	Maximum value:7.7 °C
[55]	*Num.*	Thessaloniki (Cfa - Humid Subtropical Climate)	Direct *GF*	All façades of a test room	Cooling period	Cooling period $T_{set\text{-}poit}$: 20 °C (Schedule 8:00–20:00) Infiltrations: 1Ach		Maximum values: North: 0.65 °C East: 2.04 °C South: 1.06 °C Weast: 3.27 °C

Ref.	Type	Climate	*GST*	Application	Period	Indoor	Indoor Temperature Reduction	
							Air Temperature	**Surface Temperature**
[56]	*Exp.*	Covilhã (Csb - Warm-summer Mediterranean climate)	Direct *LW*	One façade south oriented	• 7–20 October • 26 November–9 December	$T_{set\text{-}poit}$: 20 °C		Maximum values: Oct: 4.8 °C; Nov: 5.9 °C.
[61]	*Exp.*	Chicago (Dfa - Hot-summer humid continental climate)	Direct *GF*	All facades of a building	6 days of July	Air-conditioned office		Mean values: East: 0.3 °C South: 0.5 °C West: 0 °C North: 0.3 °C
[67]	*Exp.*	Thessaloniki (Cfa - Humid Subtropical Climate)	Direct *GF*	One façade of a flat of East oriented	One month (July–August)	NS		Maximum value: 0.4–1.6 °C Mean value: 0.9 °C
[69]	*Exp.*	Colmenar Viejo (Csa - Hot-summer Mediterranean climate)	Direct *LW*	One facade South-oriented	2 months (July–august)	Free floating	Mean value: 4.1 °C	Mean value: 6.4 °C
[70]	*Exp.*	Al-Ain City (BWh - Hot desert climates)	Direct *LW*	One façade east oriented	1 month (July)	Free floating	Day: 4–6 °C Night: 1–2.5 °C	Day: 4.5–6.5 °C Night: 1.5–5 °C
[71]	*Exp.*	Mawson Lakes (Csb - Warm-summer Mediterranean climate)	Direct *LW*	Part of a building façade West oriented	8 mounts (December–July)	Free floating	Maximum daily values: • Warm days: 1.75 °C; • Cold days: 0.75 °C.	

Ref.	Type	Climate	*GST*	Application	Period	Indoor	Indoor Temperature Reduction	
							Air Temperature	**Surface Temperature**
[78]	*Exp.*	Colmenar Viejo (Csa - Hot-summer Mediterranean climate)	Direct *LW*	One facade of a test room South-oriented	3 years (2009–2011)	NS	Mean values: Winter: 0–2 °C Summer: 2–7 °C Spring: ≈ 2–7 °C Autumn ≈ 2–7 °C	Mean values: Summer: 1–11 °C Spring: 5–12 °C Autumn 5–12 °C
[100]	*Exp.*	Puigverd de Lleida (Csa - Hot-summer Mediterranean climate)	Indirect *GF*	One façade of a test room South oriented	6 days of September	Free floating	1 °C	0.5–2 °C

Hong-Seok *et al.* [109] have performed several measurements in a reverberation chamber, by showing that also a thin soil layer with a depth of 50 mm can provide a significant absorption coefficient (about 0.9 at around 1000 Hz). A significant decrease was observed with the increase in soil moisture content. Conversely, with the growth of the vegetation coverage, the absorption coefficient increases by about 0.2 at low and mid frequencies.

Jang *et al.* [110], with a scale model of a street canyon, have shown that the noise reduction is less than 2 dB, at pedestrian level. Wong *et al.* [111] have carried out an experimental campaign on eight greenery systems placed in Singapore. Some of the investigated systems have shown a good noise reduction (5–10 dB) for low to middle-frequency range, due to the absorbing effect of substrate, some others an insertion loss ranging from 2 dB to 3.9 dB. A smaller attenuation was observed at high-frequency spectrum due to scattering from greenery. Thus, the authors have concluded that also by considering the high costs of installation and maintenance, vertical greenery systems should not be chosen only for acoustics interventions. Lacasta *et al.* [65] have measured the absorption coefficients of a modular greenery wall with *Helichrysum thianschanicum* species and they have found that it is approximately 0.7. Then, by means of numerical evaluations, they have found a maximum value of 4 dBAs, a noise reduction index for realistic situations. These results do not agree with the conclusions of Azkorra *et al*. [112]. Indeed, these authors have found, with laboratory measurements, a weighted sound reduction index equals to 15 dB and a sound absorption coefficient of 0.40. This difference can be attributed to the level of development of vegetation.

Fernández-Bregón *et al.* [113] have studied the effects of vertical greenery on sound mitigation for an indoor installation on a concrete wall fully covered with a combination of 16 species of plants that have determined an average canopy height of 250 mm. They have concluded that, for noise longer than 1 s, the sound reduction mitigation varies between 6% to 8% for the selected frequency.

In conclusion, all results demonstrate the *GW* capacity of reducing noise pollution, but, as underlined by Perez *et al.* [114], some improvements must be applied in the selection of materials to increase the potentialities in the sound insulation mainly with reference to the traffic noise.

3.2.3.3. Sustainability

The sustainability of a green vertical system must be investigated more accurately; indeed, the results of the available papers lead to discordant conclusions. The studies [115] and [116] have pointed out some aspects that should be considered significant for evaluating the sustainability of *GST* in a technical standard. They have defined 40 environmental requirements to be considered for the whole building process, following the CEN/TC 350 – "Environmental sustainability of construction works". On the base of the studies analyzed in this investigation, the main environmental requirements for *GST* were identified by authors and shown in Table 3.6.

The sustainability of green systems' design was discussed by Feng and Hewage [117], which have compared the lifecycle assessment of three *LW*s in the Netherlands: trellis system, planter box system, and felt layer system. The last one resulted in the worst in terms of environmental sustainability since it needs as many as 23 years to balance the emissions, but its lifetime is about 10 years. Moreover, some general indications were given: first of all, the materials have to be provided closer to the construction site and with a large percentage of recycled or reused ones; secondly, the vegetation should require little fertilizer and low replacement. Instead, considering the main element of a greening system (bare wall, support system and vegetation), Manso *et al.* [118] have found that the support has a major impact mainly in terms of Global Warming Potential, representing 96% of the total environmental burden of this category.

To be sustainable, a product for the building sector must be also economically profitable. For evaluating the economic impact of *GST*, Perini and Rosasco [119] have carried out a "cost-benefit analysis" of different *GW*s placed in Mediterranean climates, by taking into account costs and benefits for people (real estate, savings for heating and air conditioning, cladding longevity, and tax incentives) and society (air quality improvement, carbon reduction, habitat creation, aesthetic impact, urban heat island mitigation and tax incentives). The authors have concluded that the most economically sustainable system is the direct green façade.

Table 3.6 - Main environmental requirements for GST

ENVIRONMENTAL REQUIREMENTS FOR *GST* MANUFACTURING
- Minimizing the thicknesses and weights of the materials that make up the building element • Maximizing the use of materials produced with low environmental impact techniques • Maximizing the use of recycled materials • Maximizing the use of natural materials • Maximizing the use of materials locally produced • Maximizing the use of materials with similar lifetime - Maximizing the use of products which can bring benefits in different fields - Maximizing the use of reused structures coming from partial or total building demolition
ON-SITE INSTALLATION
- Maximizing the use of modular and pre-fabricated elements - Maximizing the use of elements with an easy installation - Maximizing the use of devices characterized by interoperability for the use of sources (water, electricity, etc.) - Maximizing the use of energy conversion systems powered by renewable sources
USE AND MAINTENANCE
- Choosing plant species easily adaptable to the climatic zone (saving water and fertilizer) - Selecting fertilizers with low environmental impact (i.e. organic fertilizers over mineral ones) - Selecting innovative and performing technologies for the irrigation system (i.e automatic systems, reuse of water technology) - Choosing high-performance solutions under different point of views: energy, acoustic, indoor air quality
END OF LIFE
- Maximizing the use of elements with an easy dismantling - Maximizing the use of products that could be recycled - Maximizing the use of products that could be reused

The same authors [120], by considering eight different scenarios in terms of life span (25 and 50 years), economic incentives and disposal at the end of the life span, have found that in the Mediterranean climate, the economic sustainability is obtained only if there is a tax reduction. One of the best scenarios brings to a net present value of 202.93 €/m^2 for a lifespan of 50 years, by considering tax reduction, reduction of exercise costs due to cooling saving, the increment of building rent and biomass production. Comparable results were achieved by Ottelé *et al*. [72]; in particular, these authors have shown that *LW* with felt has a high environmental burden while the ones based on planter boxes have not a major footprint since the materials affect positively the thermal resistance of the system. The relevant impact of the felt-based *LW* systems on the life cycle assessment was also shown by Oquendo-Di Cosola *et al.* [121]. The study pointed out that in the manufacturing, construction and maintenance stage, the *LW*s with felt have a higher impact than the *LW*s plastic-based.

In the last decades, a new environmental assessment method, called 'eMergy evaluation', has been adopted; it takes into account some complementary information that allow evaluating the design sustainability, by considering both 'environmental costs' and 'benefits'. With this method, Pulselli *et al.* [79] have obtained that, for a *LW* and a *GW* installed on a massive envelope, 'benefits' do not compensate 'costs' within a reasonable lifespan since the Cost to Benefit Ratio (*CBR*) is $CBR_{47} = 1$ for *LW* and $CBR_{151} = 1$ for *GW*. These values were calculated as "the initial energy investment" (without renewables and human work) to the "the yearly energy benefit" ratio. This result is mainly due to the need for water supply. Thus, rainwater harvesting systems can be useful.

Probably, the most critical aspect for the sustainability of a *GST* is the water consumption; the results proposed by Perez Urrestarazu *et al.* [122] have only indicated that the amount of needed water depends on the type of substrate used and the emitter flow rate. Briefly, the issue of irrigation and the incidence on the economic profitability is not completely investigated. The design can become truly sustainable only if designers and industry will develop the systems not only in terms of materials but also considering the rainwater storage tanks and water content sensors [29].

Other problems could be related to the maintenance of a *GW*. Manso *et al.* [25] indeed, underlined that, in case of the necessary replacement of some plants, it is difficult to restore the continuity of the green surface and for climbing plants, it is complex to ensure the absence of gaps in the facade for the spontaneous growth of the vegetation.

The choice of plants, suitable for the climate conditions, affects the maintenance cost of the green systems. Mårtensson *et al.* [73], for a *LW* in cold climates, indeed, underline that it is essential to select evergreen plants that easily adapt to excessive or poor irrigation and to frigid temperatures.

Obviously, the water consumption, the maintenance, the design complexity, the materials involved affect the cost of a green system: a direct or indirect green system is cheaper than a *LW* system [123].

In conclusion, the available literature suggests that, considering the environmental and economical sustainability, *GW*s are better than *LW*s. Taking more into account the social benefits of vertical greening systems, the governments should incentive their installations (for new and existing buildings) and surely the economic sustainability of such systems could be significantly increased. However, professionals and researchers should give more importance to the study of water usage because it influences the optimal performance of a green system but also the economic sustainability of the system.

3.2.4. Remarks from the Review Process

Different programs, action plans, guidelines were applied to diffuse this technology and, for this reason, each researcher and designer applies different performance evaluation criteria: thus, the results are often incomparable. However, some general conclusions can be found also by evidencing the main topics that the future research should investigate.

The plant species have a significant impact on the green system behavior. The key aspects for their selection are the natural supporting mechanism, the adaptability to the type of outdoor environment not only in terms of climate conditions, but also the pest problem, the need for maintenance and irrigation. These aspects are really interrelated, because, for instance, if the species are well adapted to the environment, they require lower maintenance.

This implies a reduced amount of water for irrigation, fewer fertilizers and poisons for pest. A proper selection of the plants is really important, because some types cannot survive with a poor maintenance. In any case, periodic inspections must be done for verifying the health of the plants and their pruning. A green façade has a better behavior than a *LW* under this point of view. Moreover, the environmental adaptability includes the resistance to drought and winter injury—that can cause wilting and leaf firing—as well as the traffic tolerance. For very high buildings, wind can create significant problems for what concerns the plant attachment. Foliage may be stripped under extreme wind conditions, so foliage type and size should be matched to the level of exposure and likely wind strengths at the site.

The heat exchange is greatly influenced by the plant species selection; it must be based on climatic zone, also by considering the effects of wind and light exposure, the installation in a hardiness zone or amenity context and the consideration of realistic growth time for plants. Each plant requires an adequate choice of substrate and irrigation method that must consider the short and long term maintenances to secure the health (sufficient watering and the regular trimming); this aspect has a great incidence on the exercise costs of the system.

Considering the available literature, it is clear that experimental and numerical studies are realized, very often, without considering the presence of inner loads but these influence greatly the whole heat transfer process; for this reason, the available result can be considered only partially representative of the *GW* behavior. Moreover, it must be considered that the effect on thermo-hygrometric comfort should be evaluated by considering free-floating temperature regime, while often the *HVAC* system is turned on during the monitoring activities. In addition, the evaluation of energy saving is often proposed for very short periods, while the behavior along all seasons should be monitored for evaluating the whole, seasonal and annual, energy balance. Indeed, for some passive technologies, it happens that the benefits during the summer period are negatively compensated by highest energy requirements during the winter months. Studies could be carried out to evaluate how the annual budget changes, and therefore the energy saving according to the type of plant, whether it is deciduous or evergreen. About the influence on the building performance, the only possible conclusions are:

- the energy savings provided by *GW*s depend on the orientation,
- the *LW*s seem to have better performance than *GF*s and their design is more difficult,
- the temperature of the interior surface of the vegetal façade is significantly more stable than the temperature of the interior surface of the façade without vegetation, but the calculation of thermal lag seems to demonstrate that *GF* and *LW* systems do not provide any significant variation of the thermal inertia of the construction system.

Despite some evident benefits, there are contrasting opinions among researchers, about the sustainability of *GW*s. Nevertheless, these systems contribute directly to achieving credits in the application of green rating systems but, considering a complete life cycle analysis, the whole impact is not always suitable. Moreover, it seems necessary to perform appropriate studies about the evaluation of irrigation rate; indeed, it influences the evapotranspiration process and thus the efficiency of the whole system as well as the maintenance costs and the economic profitability of the technology.

The review analysis allows also to evidence that the scientific results are mainly focused on the monitoring of green vertical systems, without explaining the consideration about the selected plants and the influence of the kind of back wall. Indeed, there are not many numerical studies and, really, some parametric evaluations could be very useful for choosing the optimal configuration of a green system by varying climate conditions, building kind of use and type of material or technological solution coupled with green layers. For instance, it could be interesting the evaluation of the adoption of recycled materials for the substrate or the integration of phase change material on the back whole. Moreover, the technical parameters that characterize each sub-system should be detailed in appropriate guidelines both in terms of:

- performance requirements,
- proposition of suitable catalogues for designers.

It can be also remarked that some numerical tools were proposed and used for performance estimations, but a complete characterization was not proposed, e.g. the description of boundary conditions for the heat and moisture balances is quite always inadequate and incomplete, and thus the model cannot be used by other researchers. Moreover, there are no studies that accurately perform computational fluid dynamic (*CFD*) investigations and, analogously, there is a lack of monitored data, that allow the evaluation of the thermal field of each substrate as well as the incidence of vapor diffusion phenomena.

The proposed analysis allows to evidence that the design, installation and maintenance of a *GW* regard several multidisciplinary aspects (structural, energetic, economic and so on) that must be considered simultaneously by designers or decision-makers for optimizing the behavior of system and also for minimizing related costs. Indeed, *GF* and *LW* could require different evaluations that do not concern merely the thermal, energy or comfort fields. For instance, Sheweka and Magdy [124] have remarked the importance of satisfying the structural requirements; indeed, the anchorage system to the building envelope has to be studied, as well as the calculations of loads due to substrate, plants and all elements, included the non-constant ones like wind, rain or accumulated snow. It is also important to verify the competencies of installers so that the project can be successfully completed.

Considering all the discussed aspects, it seems advisable the adoption of a multi-criteria decision-making approach for vertical *GW* design. With the aim to help designers and researchers in the evaluation of impact of the main elements of a vertical green system (i.e., layout, vegetation, substrate, supporting element, irrigation and drainage), it is proposed a matrix of strengths, weaknesses, opportunities, and threats (*SWOT*) that could be intended as a starting point to select the criteria and evaluation indexes when the design is approached.

The strengths of envelope solutions might include their ability to improve the whole building performance or to impact on the environmental issues related to energy use in building. Factors that can be considered as part of an analysis of strengths include:

- the advantages that these solutions can provide,
- what the solution does better than other technologies,
- the market penetration,
- the quantity of saved not-renewable energy sources.

Figure 3.5 shows the proposed matrix for the green vertical systems, according to all aspects evidenced in the review analysis. The weaknesses include designers or installation teams that do not have specific knowledge and experiences, unreliable technical data of each sub-system (which aspects can be improved by the scientific research).

Some threats can be external, such as a slow-down in the building sector, absence or negative changes of normative approach. Other threats may be internal, such as a poor knowledge or available technical tools. Factors that can be considered as part of an analysis of threats include potential obstacles due to high costs or negative impacts of life cycle sustainability. Indeed, a green system can add a big value to the development of the building sector, with creation of accessible, secure and healthy built environments, but it should respect some constraints during the life cycle to be a sustainable solution. This means that the design must assure low impacts in terms of energy, water and raw materials.

Finally, by considering the threats, it can be underlined that, in order to improve the features of products and the design, a key role may be played by the definition of international technical standards. These can also contribute to avoid criticalities due to not appropriate designing, unsustainable or inadequate irrigation rate, structural problems, infiltrations of water, and so on.

Several strengths and opportunities must be considered by designers and researchers, in order to accelerate the process of dissemination of this technology. More in detail, benefits in terms of reduction of energy needs for building air-conditioning and improvements of the global indoor and outdoor comfort must be quantified. As previously cited, it could be difficult to compare the results of the different studies, because every researcher has adopted different evaluation criteria. In the case of the energy-saving, the orientation, the climatic zone, the typology of vegetation, the *LAI*, but also the stratigraphy of the wall, could have a key role in its determination. As reported in table 3, the typology of green system, and thus a direct or indirect *GF* and a direct or indirect *LW*, can have a different impact on the energy demand of the building. For what concerns the *UHI* mitigation, some general conclusions can be underlined:

- At the same conditions, a *LW* assures the highest reduction of temperature in the warm-summer Mediterranean climate and humid subtropical climate, with better results on the southern façade.
- Evergreen plants and the increment of *LAI* have positive effects on the reduction of the surface temperature.
- For *GF*, the temperature reduction is highest when the foliage is more intensive, thicker and closer to the ground [51].

The reduction of the internal surface temperature and thus the improvement of the summer indoor comfort is strongly related to the reduction of the external surface temperature. Moreover, the limitation of the diurnal fluctuation of wall surface temperatures could prolong the lifespan of building facades, by slowing down wear and tear. Moreover, the is also the opportunity of savings in maintenance costs and the replacement of some parts. Other strengths points of a green system are the air pollution control, depending on the plant species, and the stormwater management even if not evidenced by experimental studies. Furthermore, the reduction of traffic noise in an urban context was proved by numerical and experimental studies and it could be improved by a meticulous selection of the *GW* materials. Opportunities can arise from expanding the building market, improving other aspects at the social level, using the expertise of a particular sector to anticipate where the market will go next. A *GW* is an opportunity also for the preservation of biodiversity, without compromising the social utilization of the urban space.

Figure 3.4 shows some photo insertions made by the author, of green walls integrated in a cemented urban context or in a backcountry place.

Figure 3.4 - Examples of applications of GW, spontaneously or in façade retrofit.

With reference to the *SWOT* matrix, the main shown opportunities and the strengths are the advantages widely demonstrated by researchers and these will acquire greater importance by considering the increase in global temperature and the growing need to redevelop urban centers. It is obvious that, by increasing the number of green walls or roof integration in densely urbanized areas, the phenomena of noise reduction, improvement of indoor and outdoor comfort, the contribution to urban biodiversity, the limitation of air pollution will become more and more relevant. The negative aspects evidenced in Figure 3.5, summarized in weakness and threats, could be partially limited in the future. For example, the inexperience of designers or the lack of technical data could be filled by intensive technical preparation and in the same way, the environmental impact or the weight of material could be solved by greater attention during the design and selection of materials. Certainly, some of these aspects could be improved with future public regulations and normative standards. The cited points in the figure below should be intended as examples, and thus these are indicative and not exhaustive.

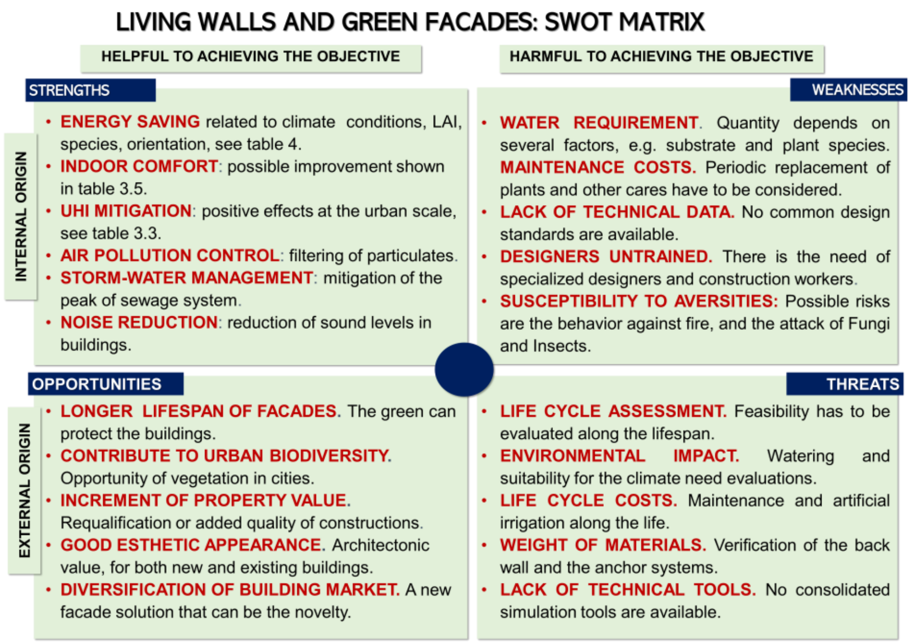

Figure 3.5 - SWOT matrix for green vertical systems

3.2.5. Conclusive remarks

GWs have a great potential for improving the building energy performance, the acoustic and the indoor microclimatic comfort. Moreover, several positive effects are achieved at the urban scale, and thus positive environmental changes in dense urban areas.

Here, a large review study was proposed, allowing to conclude that, although the research in the field of vertical greening is already fairly well advanced, this technology is not yet adequately diffused in consideration of the large potentialities.

In matter of scientific research, the available papers propose information on system functionality and achievable benefits, often without specifying designing methodology or technical data, and thus designers are not completely allowed to characterize all subsystems.

Some criticalities emerge like the incomparability of experimental and numerical results in terms of energy saving and thermal comfort. Often, results reflect only partially the behavior under real conditions (inner loads are usually not considered) and there are not parametric evaluations for the same configurations in different climatic conditions. Moreover, it is difficult to understand the sustainability level during the life cycle and also it is often impossible the quantification of the incidence of irrigation costs on economic profitability.

These studies should be done with a multidisciplinary approach. Indeed, the proposed *SWOT* Matrix has been developed to reveal the drivers and barriers in the course of implementing *GW*s. Finally, this investigation also attempts to explore the internal and external conditions, which can contribute to the customization and prioritization of policy recommendations for the adoption of international standards.

3.3. Phase Change Materials for Reducing Cooling Energy Demand and Improving Indoor Comfort: A Step-by-Step Retrofit of a Mediterranean Educational Building

After a large depending on the scientific literature about the GWs and LWs, as passive solutions for the vertical envelope, this section illustrates the implementation of other passive strategies for the building envelope, both vertical and horizontal, for the energy retrofit of an existing building. The case study is a public educational building of the University of Molise, located in Termoli, Southern Italy. It is provided a comparison of the results obtained by different dynamic simulations of passive strategies to improve thermal comfort and energy behavior of the building during the summer regime. In a first stage, the building model is calibrated against historical consumption data. Then, a subsequent step involves the technical-economic analysis, by means of building performance simulations, of energy upgrading scenarios. In particular, the following energy conservation measures are initially evaluated, with the aim to reduce mainly the cooling demands:

- Cool roof technology.
- Green roof technology.
- Thermal insulation and thus increment of envelope thermal resistance.
- Application of a wall phase change material.
- A vented façade.

Improving the indoor thermal comfort and reducing the thermal energy demand during summertime through innovative solutions will be the primary objectives. The energy efficiency measures are compared from the energy, emissions, costs, and indoor comfort points of view. The results will show the positive effects of their application, according to previous scientific studies, and the best solution in terms of reduction of cooling energy demand will result in the adoption of plaster with phase change material (PCM). During the summer regime, this innovative material, with a melting temperature of 23 °C and a freezing temperature of 21 °C, provides an energy saving of 11.7% and an increase of thermal comfort hours of 215 h. The choice of the phase change temperature of the PCM, as described in Section 3.3.2, is performed through an optimization of the results of different PCM, with different melting temperatures and by considering the summer and winter energy savings. An accurate study on the advantages and the costs of the additional hours of comfort, resulting from the application of the PCM, is reported too.

On the other hand, even if consolidated, other energy efficiency measures provide an energy-saving, but not as remarkable as the PCM, for the case study here discussed. These results depend on the typology of the building and its constructive features. The building was renovated in 2005 and, even if it doesn't have prestigious passive technologies for the building envelope, the current thermal transmittance of the components is already quite low, so that the positive effects of proposed retrofit solutions are limited. For this reason, the traditional solutions cannot give substantial effects on energy saving, with a consequent acceptable payback period. Conversely, passive technologies, which act on the decrement factor of the heat transfer and on time lag effect, by increasing inertia and thermal storage capability (sensible or latent), from the inner side, can be considered a valid solution. A phase change material is one of these.

In the next sub-section, the energy conservation measures will be compared, also with reference to the baseline building (i.e., the present one) and carefully examined according to the lower energy consumption based on costs.

3.3.1. The case study of the Italian University of Molise and the methodology of investigation

The building case study is a public educational building, refurbished in the last fifteen years which, starting from the 2006, is used by the Italian University of Molise (UNIMOL). It is developed in the north-south direction, and it is composed of four floors, one of which is partially buried, as shown in Figure 3.6. The inter-floor height is 3.2 m and the overall height aboveground is around 13.2 m. The building surface area and the overall volume are 2626

m^2 and 9456 m^3 respectively. The net conditioned building area is 2113 m^2, the net conditioned volume is 7606 m^3.

The building shape is quite regular, constituted by two different rectangular blocks, connected by the stairwell. Each floor has a different use as illustrated in Figure 3.6. The analysis of the requalification interventions will focus on the achievable energy savings in the spaces that actually are air-conditioned. Finally, technical rooms, presently not provided with heating and cooling services, also in the refurbishment here proposed will remain in conditions of free-running indoor temperatures.

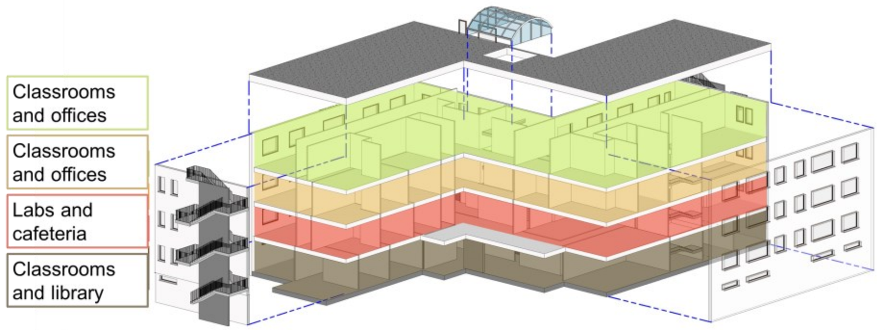

Figure 3.6 - Axonometric exploded view with the uses for each floor.

Through the technical reports, provided by the technical office of the University of Molise, all the necessary information and data about materials, systems and equipment, fruition and occupancy, required for characterizing the building systems, were transposed.

Space active heating and cooling are allowed, mainly, by a direct expansion system— a VRV Variable Refrigerant Volume) air-to-air heat pump—with a nominal heat capacity of 133 kW, at rated conditions. Indoor units are installed in the ceiling and the thermoregulation, for each area, operates through the control of the internal temperature. The remote management system provides adjustments based on the outdoor climatic conditions and the hourly operations are allowed through a programmable daily thermostat that acts on the zone valves with a proportional action.

As said, the gross volume is about 9500 m^3 but 1850 m^3 were evaluated as not conditioned. The following primary energy demands were calculated, by converting electricity into primary energy, by considering the ISPRA (higher institute for environmental protection of research) value on energy efficiency of thermo-electric plants, equal to 0.488 Wh_e/Wh_p[125]:

- space heating energy demand: 35,364 kWh_e/year, and thus 72,467 kWh_p/y → 34.3 kWh_p/m^2y;
- space cooling energy demand: 29,640 kWh_e/year, and thus 60,738 kWh_p/y → 28.7 kWh_p/m^2y;
- annual energy demand for the domestic hot water: 20,894 kWh_e/year and thus 42,815 kWh_p/y → 20.26 kWh_p/m^2y.

The energy efficiency interventions on the building, analyzed in the next sub-sections, will influence exclusively the consumption of the HVAC system, and so the energy demand for cooling and heating, (including the auxiliary energy), reported in Table 3.7.

Table 3.7 - HVAC energy consumption of the calibrated building model.

Calibrated Building HVAC Consumption	**HVAC Energy Consumption**		
	kWh_e	kWh_p	kWh_p/m^2
Energy demand for cooling	35,364	72,467	34.3
Energy demand for heating	29,640	60,738	28.7
Total/year	65,004	133,205	63.0

All told, the total end uses for the electric systems, including heating, cooling, interior equipment, interior lighting, fans and water systems is about 127,296 kWh_e/year (260,853 kWh_p/y, 123.5 kWh_p/m^2y). Obviously, the energy demand of the building depends not only on the electric systems, but also on the thermo-physical features of the thermal envelope. Specifically, two different typologies of opaque envelope characterize the building. In detail, the partially buried floor has a thermo-concrete external wall with a thermal transmittance (U_{value}) of 0.51 W/m^2K, while the walls above the ground have two hollow brick layers with an intermediate air gap, and a calculated U_{value} of 0.66 W/m^2K. Moreover, the basement slab on the aerated crawl space and the building roof have respectively U_{values} of 0.40 W/m^2K and 0.37 W/m^2K. The transparent building envelope is characterized by double glazing windows with aluminum frames (equipped with a thermal break technology) and thus an overall U_W equal to = 3.67 W/m^{2}K. Some indoor spaces have solar shadings. The energy performance investigations of the present building, and the impact analysis of the applied energy efficiency measures (EEMs, in the following lines) were realized through dynamic simulation studies, by using the well-known software EnergyPlus [126], by defining the model geometry through DesignBuilder [127] (Figure 3.7).

The numerical model, for an accurate dynamic analysis of the building, has been built through the definition of the 3D geometry and other information about the location and the building orientation, the thermo-physics of the building envelope, the definition of the activity and operation parameters. Input information for the calibration are reported in Table 3.8.

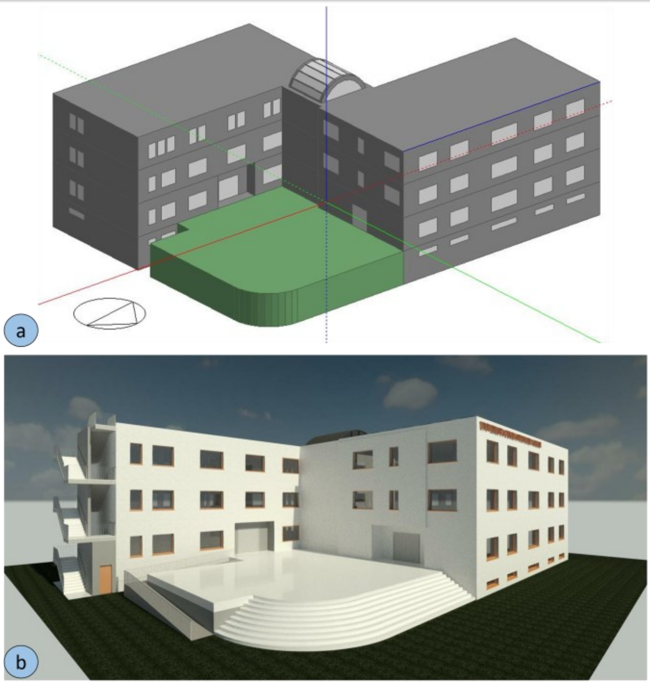

Figure 3.7 - Geometrical 3D model (DesignBuilder) and realistic view (Revit Architecture).

Table 3.8 - Information data for the building modelling.

BUILDING GEOMETRY – MAIN DATA			
Gross roof area	681 m^2	Gross wall area	2167 m^2
Total building area	2626 m^2	Window opening area	333 m^2
Net conditioned area	2113 m^2	Total building volume	9456 m^3
Gross height above ground	13.2 m	Conditioned total volume	7606 m^3
DIGITAL MODEL – MAIN BOUNDARY CONDITIONS			
Setpoint during the heating season	20 °C	Number of thermal zones	57
Setpoint during the cooling season	26 °C	Simulation Time steps per hour	6
BUILDING ENVELOPE THERMOPHYSICS			
U_{value} wall	0.67 W/m^2K	Shading System	Horizontal slats
U_{value} roof	0.37 W/m^2K	U_{value} windows	3.2 W/m^2K
U_{value} slab on the ground	0.41 W/m^2K	Infiltration and natural ventilation	4.0 ACH
INTERNAL GAINS			
People occupancy: classrooms and labs	0.7 people/m^2		
People occupancy: circulation and other thermal zones	0.3 people/m^2		
Lighting average, Watt per zone floor area	3.0 W/m^2		
Electric equipment, Watt per zone floor area	5.0 W/m^2		
HVAC SYSTEM			
Typology	VRV air-to-air heat pump, direct expansion system		
In room cooling and heating terminals	Indoor Units installed in the ceiling		
Supply fan total efficiency	0.7		
Energy efficiency of thermo-electric plants (ISPRA)	0.488 Wh_e/Wh_p		
Emission factor for electric energy (ISPRA)	0.308 tons CO_2/MWh_e		

In order to check the reliability of the numerical model, the results of the simulations were compared with the energy bills relative to the electricity demands of the last three years. The comparison with historical consumption and the knowledge of the use profiles of plants and installed systems allowed the calibration of the numerical model using the indicators proposed by the ASHRAE (American Society of Heating, Refrigerating and Air-conditioning Engineers) Guideline 14 [128] and the M&V Guidelines [129] as previously described (section 2.2 - Energy diagnosis and cost-optimal approach).

Different parameters were modified, according to present regulations, to obtain the validated model. According to the Italian Presidential Decree (D.P.R.) n. 412/'93 [130] The climatic zone C, in which Termoli is located, has operating limits of thermal plants, with reference to the cold season, from 15 November to 31 March, for a maximum of 10 h/day, with a maximum ambient temperature of 20 °C ±2 K. Conversely, the cooling period has no stringent limitations but, usually, the operation of chillers is not admitted before June and after September. Finally, with reference to the building here studied in Termoli, the values of *MBE* and *CV(RMSE*) respect the thresholds of the M&V Protocol 2015, with the following values:

- MBE_{month} (%) = + 2.0%,
- *CV(RMSE)* (%) = 10.9%.

Moreover, the energy consumption derived by building simulations, compared to the one of the existing building, follows the same monthly evolution (Figure 3.8), and the corresponding values are reported in Table 3.9. Thus, the numerical model can be considered calibrated. Of course, these significant correspondences have been achieved after several corrections, mainly concerning the definition of building use and every choice and schedule has been supported by surveys. It should be noted that, in summer, the building is not used only for few days so that the energy demands of August is comparable to the one of other warm months.

To achieve the aforementioned *MBE* and *CV(RMSE)* indicators, compared to standard and literature average data, the people occupancy, profiles, were corrected by taking into account the use of the single space. Of course, it was verified that each schedule is compatible and reasonable with the use of a single room. Besides endogenous gains, the occupant presence and behavior affect deeply also (a) the natural ventilation, (b) infiltration due to the opening of windows and doors, (c) local adjustment of set points. To avoid aleatory definitions, these three input categories weren't changed.

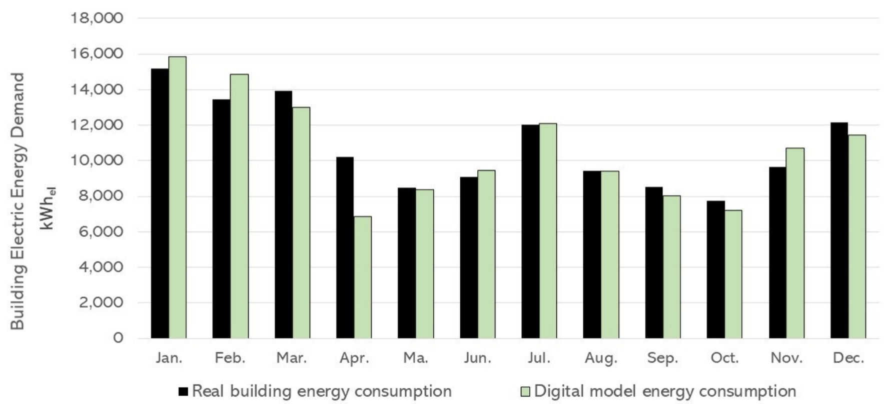

Figure 3.8 Monthly comparisons of energy demands between monitored and simulated data

Table 3.9 - Energy consumption (all energy uses) for the calibration of the numerical model.

Calibration Data	**Main Building Energy Consumption**		**Digital Model Energy Consumption**		***MBE***	***CV(RMSE)***
	kWh$_e$/year	kWh$_p$/year	kWh$_e$/year	kWh$_p$	%	%
summer energy consumption	57’724	118’287	54’206	111’079		-
winter energy consumption	72’177	147’903	73’090	149’774	-	-
tot/year	129’901	266’190	127’296	260’853	2.0	10.9

Once the model was calibrated, various solutions for the improvement of summer conditions were examined, by taking under deep consideration investment costs, profitability, reduction of polluting emissions, energy consumptions, indoor thermal comfort.

Then, the costs of investment, the payback periods of the invested capital, the evaluation of economic indexes and global costs under a macro-economic analysis were calculated, as explained in section 2.2.

The technical-economic analysis was worked out by considering the following prices and emissions factors:

- Electricity costs deduced from monthly energy bills, equal to 0.20 €/kWh$_e$,

- Emission factor for electric energy equal to 0.308 tons CO_2/MWh_e [131].

The calculation period of global cost was assumed as 30 years as established for public buildings [132]. The calculation of CO_2 equivalent emissions requires a cost of 20 € per ton of CO_2 equivalent up to 2025, 35 € up to 2030 and 50 € after 2030 [132]. This is the approach of the EU Institutions in order to penalize buildings strongly impacting on the environment.

The base building has an energy demand for all energy uses, including heating, cooling, interior equipment, interior lighting, fans, and water systems, of about 260,853 kWh_p/year, to which corresponds a cost of 25,459 €/year and 39.2 ton of CO_2 emissions/year. Specifically, the energy consumption for heating during the winter period is 72,467 kWh_p/year, and the one for cooling during the summer period is 60,737 kWh_p/year. In Figure 3.9 the monthly energy consumptions, during winter and summer seasons, respectively, are reported. These are the results of a thermo-energetic analysis, performed with a time-step of 6 (i.e., six time-steps per hour, and thus an energy balance every ten minutes), on the existing building, which corresponds to the real needs. The annual costs for heating are around 7073 €/year and for cooling 5928 €/year. The emissions during the winter period correspond to 10.9 tons of $CO_{2\text{-equiv}}$/year and, concerning the summer, the emissions are around 9.1 tons of $CO_{2\text{-equiv}}$. As said, to convert electricity into primary energy, a conversion factor of 0.488 Wh_e/Wh_p was used.

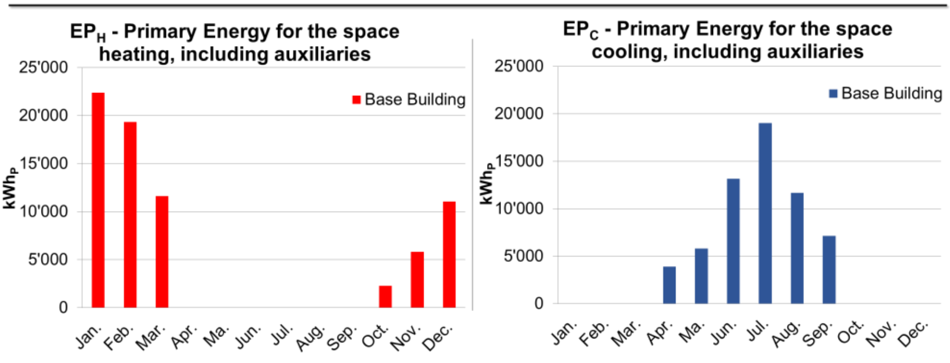

Figure 3.9 - Heating and cooling primary energy demand.

Beyond emissions, costs and energy analysis, the different energetic measures were compared in terms of thermal comfort. As it is well known, the indoor thermal comfort in buildings depends on environmental and psychophysical factors, so on objective and individual parameters. The first ones depend on dry bulb air temperature, average radiant temperature, the relative humidity of the air and relative average airspeed. The second ones are related to the thermal resistance of clothing and energy metabolism and thus are directly connected to the personal perception of the occupant. The comfort methods employed in the current study are both the traditional Fanger approach, suitable for fully-conditioned buildings, and the ASHRAE 55-2004 comfort analysis, adaptive approach useful for the summer period. Being the building case study heated and cooled, each energy efficiency measure was analyzed by considering its impact on thermal comfort along all occupied hours, during the heating and cooling seasons. Finally, comfort has been evaluated for all the occupied hours. In the specific case of the PCM intervention, a deeper detailed Fanger analysis was performed, evaluating and comparing the monthly PMV and PPD values with the ones of the base building.

Moreover, the next sub-sections describe the energy efficiency measures adopted and their positive impact on building energy performance.

3.3.2. Passive strategies for the building envelope: application and results

The evaluated energy efficiency measures for the building retrofitting concern the opaque building envelope and in particular the vertical and horizontal components. In depth, two possibilities of improvement of the horizontal envelope were examined: 1) cool roof and 2) extensive green roof.

Conversely, with reference to the vertical opaque thermal envelope, addition of 3) a traditional thermal insulation and 4) a PCM layer were evaluated. A further investigation will concern the adoption of a vented façade 5).

Further passive technologies for the improvement of the summer behavior of the buildings, specifically applicable on the vertical envelope, are green facades and infrared-reflective coatings. In this study, these two strategies are not evaluated, for the following reasons. A green façade provides for complex boundary conditions and is also quite difficult to model without significant risks of errors, as previously discussed in sub-section 3.2.2.

In a matter of energy refurbishment of existing buildings, and also for new projects, a promising technology could be the adoption of infrared reflective coatings. In this regard, Becherini *et al.* [133] characterized experimentally two coatings, performed durability tests, and carried out a large study both in the laboratory, real buildings, and employing numerical simulations. Two climate conditions were considered. Results of the adoption of infrared coatings revealed positive performance in reducing the cooling need. In particular, the application of IR reflective coatings decreased the temperatures of building outer surfaces and thus the heat transfer into the building. Moreover, also the visual compatibility was assured, as well as the conservation of the cultural value of the architecture. Further study must test other behaviors, such as the anti-bacterial and anti-pollutant characteristics. Finally, even if very interesting, this is an emerging technology and thus it was not included in this investigation.

1) Retrofit with a cool roof

A cool roof technology helps in reducing the outer temperature of the building roof and thus the summer heat gains and cooling loads. It can also limit the urban heat island effects and the ambient overheating because of the capacity to reflect solar radiation. Besides an extremely high solar reflectance, cool coatings have a high value of thermal emissivity in the infrared spectrum, which allows the roof to release heat to the surrounding environment, by thermal radiation. The Italian Ministerial Decree 26/06/2015 [134], Annex 1, establishes a mandatory verification of the effectiveness of cool coatings in terms of cost-benefits and assumes a solar reflectance value not lower than 0.65 for new or deeply refurbished flat roofs. The proposed cool coating has the following thermal characteristics:

- Infrared emissivity: 90%;
- Solar absorbance: 16%;
- Visible absorbance: 16%.

Figure 3.10 shows the constructive details of the roof slab, with the addition of the reflective layer. The transient energy analysis, by means of BPS (building performance simulation) proves a summer primary energy reduction of 2.0% (1222 kWh_p and, conversely, a winter increment of primary energy demand for the space heating, of around 0.8% (588 kWh_p).

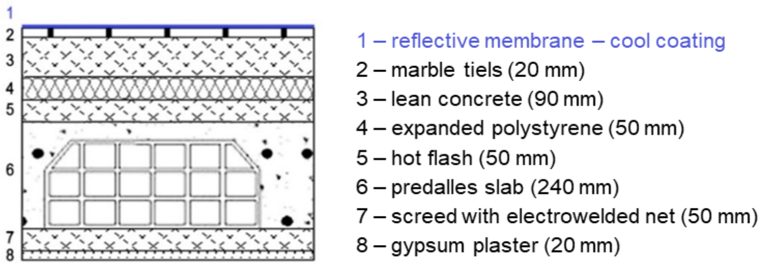

Figure 3.10 - Roof covering with the addition of cool roof layer.

These outcomes can be seen in Figure 3.11. The results reveal a limited, but positive effect during the hot season due to a lower surface temperature caused by the reflection of the solar radiation. Conversely, during the winter, the roof absorption of the solar radiation would be a favorable heat gain but, in case of cool roof, this effect is reduced too.

By assuming that the present coating has a satisfactory maintenance level, from the economic point of view, the investment cost is about 14’000 € (15 €/m^2 for the painting, 5 €/m^2 in addition, for taking into account a light preparation of the slab, including installation, transport of materials and labor costs). This type of intervention, during the occupied hours, when the cooling system is available and runs, does not imply a relevant increment of the indoor thermal comfort. Conversely, as it was seen, a reduction of heat gain and thus of the cooling load would be achieved.

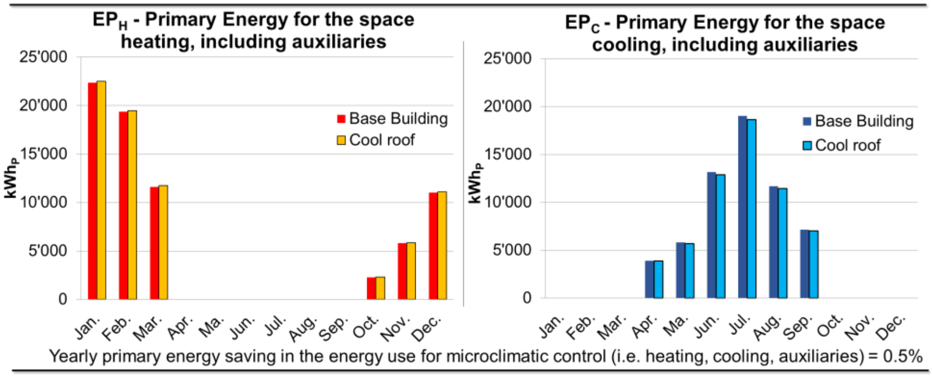

Figure 3.11 - HVAC Heating and cooling primary energy demand, before and after the cool roof installment.

2) Evaluation of a green roof

This is a complex technological system, whereby the plant layer becomes an integral part of the roof slab. Green vegetation provides numerous advantages, including the improvement of the internal microclimate and energy savings in both heating and cooling seasons, as well as large-scale benefits such as, for instance, the reduction of urban heat islands, enhancement of air quality, reduction of urban pollution due to the filtration of particulate matters and, moreover, also attenuation of peak loads on the sewage systems during the peaks of raining. The aforementioned Italian Ministerial Decree 26/06/2015 [134] makes explicit reference to this technology; in detail, at the point 3 of the requirements in Annex 1, it establishes a mandatory evaluation in terms of cost-benefits of passive air conditioning technologies such as green roofing. These roofs are characterized by a cropped layer of different plant species, which require minimal maintenance, for the extensive roof, and medium-high maintenance for intensive roofs.

The proposed intervention involves the installation of an intensive type roof, characterized by a stomatal resistance (depending on the opening and closure of the stomata) equal to 120 s/m, a leaf area index (indicative of leaf density) of 3.5 m^2/m^2 and vegetation with a height of 40 cm. The current building has as horizontal envelope, a “predalles” slab, whose total thermal transmittance is equal to 0.37 W/m^2K. The suggested intervention reduces the thermal transmittance of the envelope, reaching the value of 0.32 W/m^{2}K, according to the minimum requirements proposed by the Ministerial Decree of 26/06/2015 [134]. This reduction of U_{factor} was achieved because of the addition of some centimeters of soil and other layers that characterize a typical green roof, as represented in Figure 3.12. No increasing of thermal insulation was applied. It should be noted that the installation of intensive green roofs often requires a structural verification.

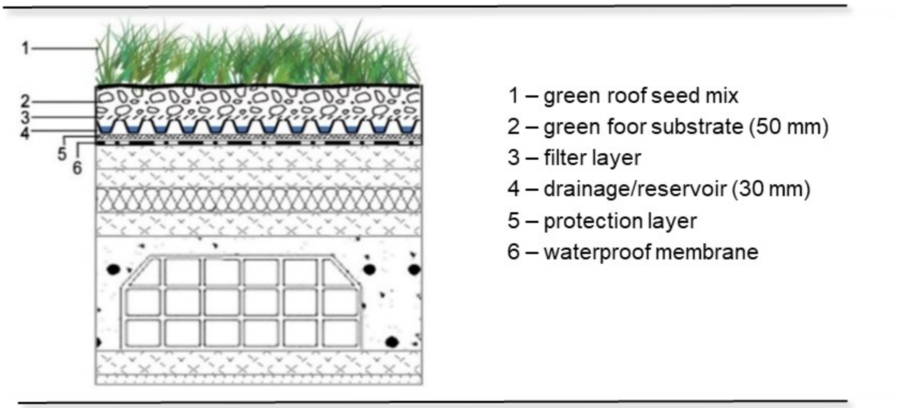

Figure 3.12 - Roof covering with the addition of an intensive green roof.

From the energetic point of view, the addition of the “green roof” layer, produces a summer primary energy reduction of 1.6% (993 kWh_p), and a winter primary energy reduction of 0.6% (443 kWh_p) (Figure 3.13). In summer, the improvement is due to the evaporative cooling while, in winter, benefits are achieved because of the lower thermal transmittance and the lower convection, linked to the low speed of air in the canopy. Obviously, the reduction of solar absorptance is a winter contrasting effect.

The estimated investment cost associated with the proposed EEM was determined on the basis of European market trends, and by the metrics of similar works. All told, the calculated investment is equal to 120 €/m^2, including installation of an intensive green roof, transport of materials, labor and maintenance costs. The surface object of intervention is around 700 m^2, so, the total cost is about € 84’000.

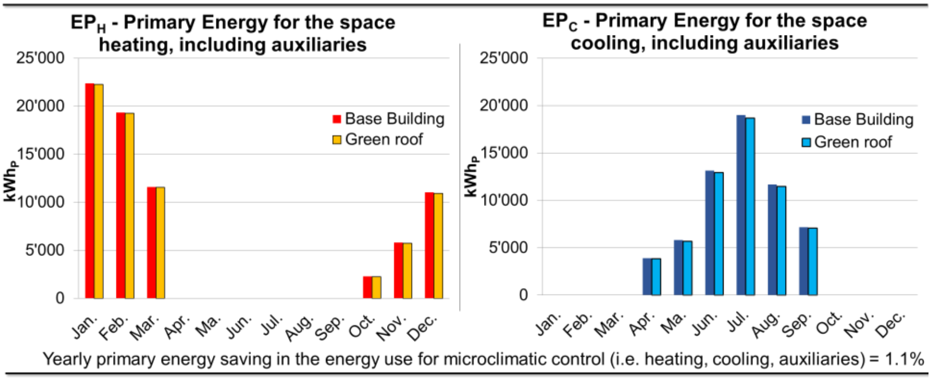

Figure 3.13 - HVAC Heating and cooling primary energy demand, before and after the green roof addition.

According to the present Italian legislation, public Institutions—but also private stakeholders—can benefit from incentives for energy efficiency measures that imply energy savings. In detail, the incentive is paid by the Italian manager of electric system, the GSE energy services manager), and the so-called "Thermal Account" ("Conto Termico" in Italian) [135] establishes that for thermal insulation of the opaque building envelope, a refunding of 40% of the total intervention cost within the expenditure of € 400'000 can be achieved. In this specific case, it was tried to test the chance to achieve that incentive also for green roofs that, usually, are equipped with a significant layer of thermal insulation. In this case, the thermal insulation was not added, being the building roof already thermally-insulated, so that the U_{value} reduction until a value of 0.27 W/m^{2}K was not achieved and thus incentive cannot be obtained. Finally, the cost of investment is entire, without economic benefits or incentives from funding programs.

3) Thermal insulation for the vertical opaque envelope

The building is an example of educational edifice built in Italy in the second half of the 1900s. This means that, as typical, the structural frame is made of reinforce concrete and the walls are made of a double layer of bricks, with a quite low thermal conductivity, with an interposed air gap. This provides a satisfactory level of thermal resistance, so that, during the 2005 refurbishment, the thermal vertical envelope was not improved by means of insulation. At this stage, by considering the aims of this investigation, however, a further addition of thermal insulation for walls was considered, in order to reduce the thermal losses in winter and the thermal gains in summer, during the daytime and when the outdoor temperatures and solar radiation are high. It should be specified, however, that in summer, it is quite important the thermal capacity, besides the thermal insulation. Indeed, high masses or materials with high specific heat allow to accumulate heat without increasing the indoor temperatures. This is the common sensible storing of building components that provides attenuation and time lag of the heat transfer.

The building is in the climatic zone C, and the thermal transmittance of the vertical envelope is 0.67 W/m^{2}K. Still with reference to the energy performance of the building envelope, the Ministerial Decree 26/06/2015 [134] defines the limit values of thermal transmittance for buildings object of energy refurbishment. In particular, the reference thermal transmittances for refurbished buildings should be 0.36 W/m^{2}K. The reduction of thermal transmittance requires 8 cm of insulation material on the external side of the vertical envelope as represented in Figure 3.14 (expanded polyurethane, λ = 0.026 W/m^{2}K, density ρ = 35 kg/m^3, specific heat c_p = 1464 J/kgK), and the achieved U_{value} is 0.22 W/m^{2}K. This value is significantly lower than the aforementioned threshold (i.e., 2021 limit) of thermal transmittance for refurbished buildings. The energetic analysis shows a yearly reduction of primary energy demand of 1.9% (from 260’853 kWh$_p$/m^{2}y to 255’794 kWh$_p$/m^{2}y) referred to the whole facility and all energy uses. Specifically, as Figure 3.15 shows, the positive effects on energy consumption of HVAC system, are evident during winter season (reduction of HVAC energy demands for the active heating of about 6.9%), while these are not relevant during summer, and are similar to the percentage variation of a simulative error. The installation cost is 59.6 €/m^2, including materials, labor and scaffolding, and so the total investment is 128’140 €. For the economic analysis, to evaluate the convenience of the investment, the incentives paid by the aforementioned “Thermal Account” [135] were taken into account, because these incentives are possible for this kind of energy efficiency measure. To access the incentive, in the case of thermal insulation of opaque surfaces, the maximum allowable cost in relation to the perimeter walls is 80 €/m^2, and the incentivized percentage corresponds to 40% of the total investment, as long as it does not exceed € 400'000. In the specific case of the proposed redevelopment, the total incentive is 51'256 €, paid in annual cashflow of € 10'251/year, for five years. Of course, this incentive can be achieved, because the final U_{value} is lower than the threshold established by the funding program, equal to 0.30 W/m^{2}K for the climatic zone C.

In this study, by considering that the building is heated and cooled during the occupied hours, there aren't significant changes in indoor thermal comfort due to the refurbishment by means of additional insulation. Conversely, as it was seen, there will be a significant reduction in energy demand for heating.

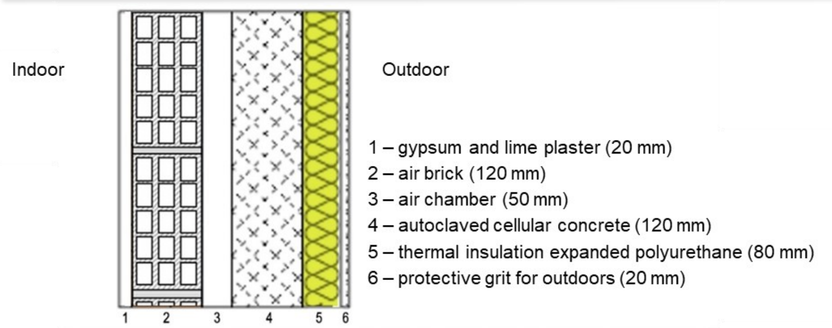

Figure 3.14 -. Wall stratigraphy with thermal insulation.

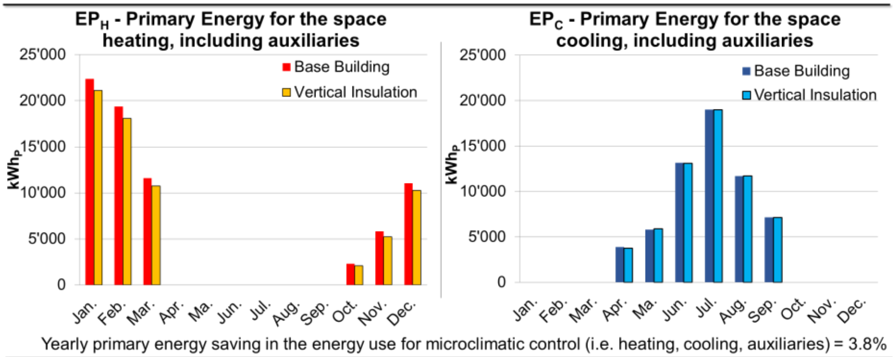

Figure 3.15 - HVAC heating and cooling primary energy demand, before and after the thermal insulation addition.

4) Application of a Phase Change Material (PCM) Plaster

Phase change materials are a promising building technology, being able to absorb energy, as latent heat, during the melting process, and to release it during the solidification. In this study, the capability of PCMs was tested, applied on the internal side of external building components, in containing the thermal excursion during the day, by attenuating the indoor thermal levels and so the use of air-conditioning. The simulated PCM exists and is a melting material encapsulated in a plastic film. Initially, in a first simulated configuration, it has a melting temperature of 23 °C and a freezing temperature of 21 °C. Starting from the values of specific heat of the material (985 J/kgK in the solid phase, 2251 J/kgK in the liquid phase), the different values of the enthalpy variation was calculated, following Equation (3.1):

$$Q_{sens} + Q_{lat} = \int_{T_1}^{T_{phase\ change}} m \cdot c_{sol} \cdot dT + \left(m \cdot \Delta H_{sol-liq}\right) + \int_{T_{phase\ change}}^{T_2} m \cdot c_{liq} \cdot dT \quad (3.1)$$

where:

- Q_{sens} and Q_{lat} are the stored sensible and latent heat, respectively,
- m is the mass of the PCM material,
- c_{sol} and c_{liq} are the specific heat in the solid and liquid phase respectively,
- $\Delta H_{sol-liq}$ is the latent heat of fusion,
- T_1, T_2 and $T_{phase-change}$ are the temperatures at the beginning, at the end of transformation and during the phase change, respectively. Of course, in the reality, $T_{phase-change}$ is a small range and not a unique temperature.

The simulated PCM, starting from all characterizations derived from real datasheets, has a reliable thickness of 2 cm, a latent heat storage capacity of 165–200 J/g, a thermal conductivity of 0.7 W/mK, and it was installed in the inner side of the building envelope, as Figure 3.16 shows.

The building performance simulation (i.e., BPS) of PCM in building components must be performed through the conduction finite difference algorithm (Con-FD), with a Crank Nicholson difference scheme. Thus, in this case, a different heat balance algorithm was used, being necessary the Con-

FD instead of the CTF (conduction transfer function) methods. On the other hand, the green roofs previously analyzed can be modeled only by means of CTF and this last algorithm works very properly for the characteristics of the case study here discussed. In the case of PCM, conversely, the conduction finite differences are necessary, being mandatory the knowledge of the nodal temperatures inside the walls.

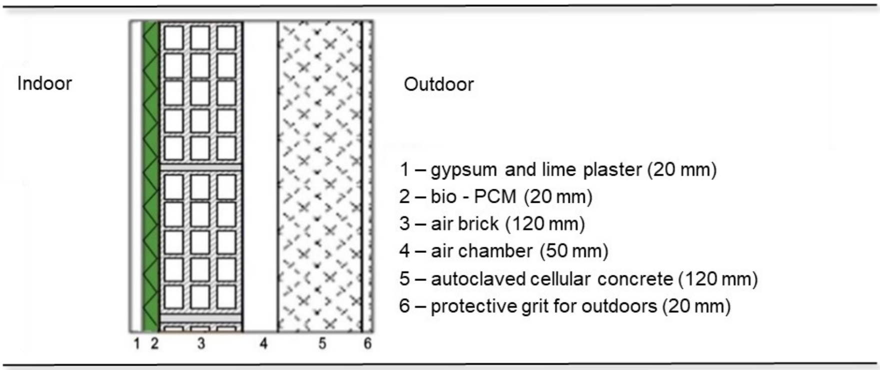

Figure 3.16 - Wall stratigraphy with the PCM-layer.

Finally, being obliged to use two different solution algorithms, and thus CTF (for the base case, cool roof, green roof, addition of thermal insulation and so on) and Con-FD (for the PCM implementation into vertical walls), a further calibration of a second Con-FD base case was performed, with the achieved following indexes MBE_{month} (%) = 2.8, *CV(RMSE)* (%) = 10.9. Again, these values are within the aforementioned M&V limits (i.e., $MBE_{month} \leq \pm 5\%$, $CV(RMSE) \leq 15\%$) and very close to those previously calculated for the building simulated by means of CTF. A summary between Conf-FD and CTF differences was proposed in Table 3.10.

As is clear from Table 3.7, the comparison of “numerical simulations” also gives favorable results in terms of values of calculated energy uses. Once achieved this positive feedback, in order to perceive the difference properly, the effectiveness of the PCMs was evaluated by comparing the building with phase change materials to the base case simulated with the Con-FD.

Table 3.10 - Base Building: Differences in electric energy due to the different simulation algorithm, Conduction Transfer Function (CTF) and Conduction Finite Difference (Cond-FD).

Base building	Heating [kWh$_e$]	Cooling [kWh$_e$]	Fans [kWh$_e$]	Electricity HVAC [kWh$_e$]	Electricity FACILITY [kWh$_e$]
CTF building	26’432	26’349	12’223	65’003	127’296
Con-FD building	26’293	25’482	12’249	64’023	126’218
Δ Energy	0.53%	3.40%	-0.21%	1.53%	0.85%

Figure 3.17 shows the indoor temperature variation of a typical classroom, during a typical summer week (from 03 to 09 July). The constant temperature value, around 26 °C from 8:00 to 18:00 for the first five days, is due to the activation of space cooling by means of the VRV. Instead, for the two last days, Saturday and Sunday (when there is not an active temperature control), the maximum peak without PCM is 29 °C and 28 °C with PCM application.

Definitively, two effects are clear, and thus:

- a significant attenuation of high-temperature peaks (more evident in the weekends, when the cooling system is turned off);
- a consistent decrease of temperatures at the nights, every day.

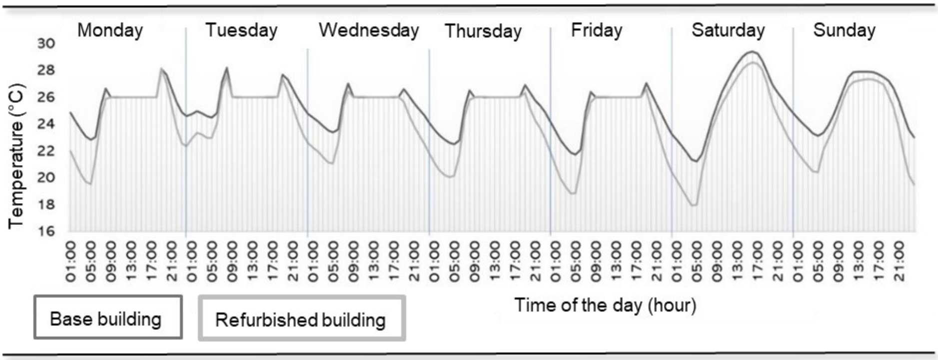

Figure 3.17 - Curves of indoor temperature

The first effect happens during the diurnal hours: the PCM melting allows storage of latent heat, until the melting point of 23 °C, stealing it to the ambient. Conversely, the second effect (i.e., a more accentuated temperature decrease at the night) is contrary to what it can be expected. Indeed, the addition of thermal storage, sensible or latent, produces time lag and attenuation of both hot peaks (and this is verified here) and of low peaks (in this case study, this is not verified). Really, the simulation with PCMs produces lower cold peaks, at the night, because the amount of nocturnal ventilation was incremented, so that during the day, the building avoids overheating thanks to the latent storage while, at the night, the additional nocturnal ventilation, necessary for discharging the phase change material (i.e., the reducing of internal energy and consequent solidification), allows a convective cooling of the building. Finally, the PCM works as thermal mass and thus, during the nocturnal hours, when the building is not occupied, it requires a cool ventilation for the solidification and the discharging process, so that during the following diurnal periods is again ready for storing heat. In any case, it was verified accurately that the beneficial cooling effects are due to the combined effect "PCM plus night cool ventilation" and not merely to this last.

The reduction of summer cooling of the PCM building compared to the base case is relevant and it is around 11.7% (i.e., 6888 kWh_p saved). During the winter season, a small energy-saving occurs too, around 1.6% (1141 kWh_p saved). This positive effect is due to the capability of PCM in storing also the surplus energy (due to internal gains, equipment, endogenous sources and lighting) that sometimes, in the heating season, overheats the indoor space beyond 23 °C (the melting temperature of the PCM). Of course, this happens only in the central hours of the day, with maximum occupancy and solar gains. Moreover, also a second reason for this saving can be found and thus the addition of a layer (the PCM) that contributed to a further reduction of the building U_{value}. In any case, the achieved saving in heating demand is not relevant (Figure 3.18).

Similarly, in the same percentage, the reduction of greenhouse emissions is equal to 1.2 tons of $CO_{2\text{-equiv}}$. In terms of economic profitability and cost analysis, it was considered an investment cost of 29.5 €/m^2 (i.e., 36,875 € in total), including the PCM cost and the plaster reconstruction, with an annual reduction of operating costs of about 784 €. By calculating the global cost according to equation (2.15), it results that C_g is higher, compared to the base building, of about 14,570 € in a calculation period of 30 years. Besides the reduction of energy demands in summer and also in winter, the advantages of this application are also related to the indoor thermal comfort; indeed, the uncomfortable hours from the thermic point of view are 1543 for the base building and 1469 for the refurbished building with the PCM plaster. The positive effects of this energy efficiency measure on thermal comfort are demonstrated by the ASHRAE 55-2004 comfort analysis. Annually, as the results prove, 74 h of "net" thermal comfort were gained (Table 3.9), because 215 h of additional thermal comfort were gained in summer, while, during the heating season, 141 h of comfort were lost. These outcomes depend on the PCM characteristic of storing latent heat, subtracting this from the ambient air.

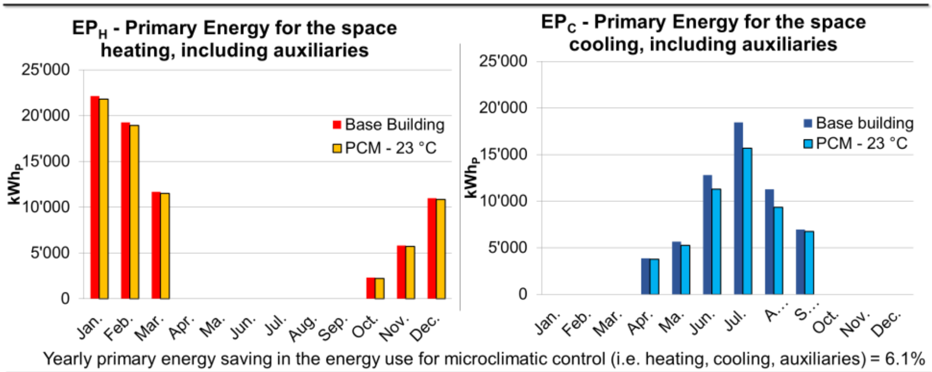

Figure 3.18 - HVAC Heating and cooling primary energy demand, before and after the PCM plaster addition

By considering the aforementioned increment of global cost, it results that, along the lifetime, the cost of one hour of summer comfort regained (i.e., additional) is equal to of 2.25 €/h. This is a quite favorable result, given that, by means of active cooling, a single hour of comfort costs about 6.10 €/h. If both seasons of heating and cooling are considered, as it was said some lines above, the net annual increment of thermal comfort hours is 74, and the cost of one additional hour of comfort as a result of the PCM retrofit measure is 6.56 €/h, in the face of the 7.85 €/h necessary to obtain the same condition of thermal comfort through the use HVAC system. A summary is proposed in Table 3.11.

Table 3.11 - Costs of additional hours of comfort during a year and during the summer

All-Year Analysis		**Summer Analysis**	
Additional Hours of comfort with PCM adoption	74 h	Additional Hours of comfort with PCM adoption	215 h
PCM wallboard: average cost of one hour of additional comfort	6.56 €/h	PCM wallboard: average cost of one hour of additional comfort	2.25 €/h
Use of HVAC: average cost of one hour of comfort	7.85 €/h	Use of HVAC: average cost of one hour of comfort	6.10 €/h

In the specific case of the PCM wallboard, a Fanger thermal comfort analysis was performed too. Particularly, the PMV and PPD indexes were examined for three typical classrooms, one for each story of the building. The PMV is the Predicted Mean Vote, and it depends from the vote of a large number of people about the thermal comfort of an ambient. As it was well-known, it is based on a thermal scale of 7-points, from −3 (very cold) to 3 (very hot), and the values are acceptable when are between −1 and +1 (0 is the thermal neutrality). The PPD is the Predicted Percentage Dissatisfied index and is related to the people's perception of cool or warm. When PMV is ±1, PPD is 25%; when PMV is ±0.5, PPD is 10%; in case of PMV = 0, PPD is 5%.

The PMV and PPD values reported in Figure 3.19 correspond to the three typical classrooms of the University of Molise. As shown, the PCM retrofit intervention reduces considerably the PMV value during the cooling period compared to the value of the base building. It is interesting to underline the results of the PCM application in June. Indeed, in all the three considered rooms, the PMV passes from a positive value (perception of a warm indoor ambient) to a negative one (perception of a cool indoor space), always within the PMV limits of acceptability. This different perception of comfort depends on the PCM behavior. In June, this innovative material reaches the melting point of 23 °C, storing latent heat from the ambient air and avoiding a further heating of the room, so that the classrooms are also a bit cold for the specific season. In other words, the building spaces are even considered "cool". Consistently with the PMV results, the PPD values have the same trends. During the winter season, as Figure 3.19 shows, the PMV of the classrooms with PCM is the same as the reference building and the same happens for the PPD index, of course.

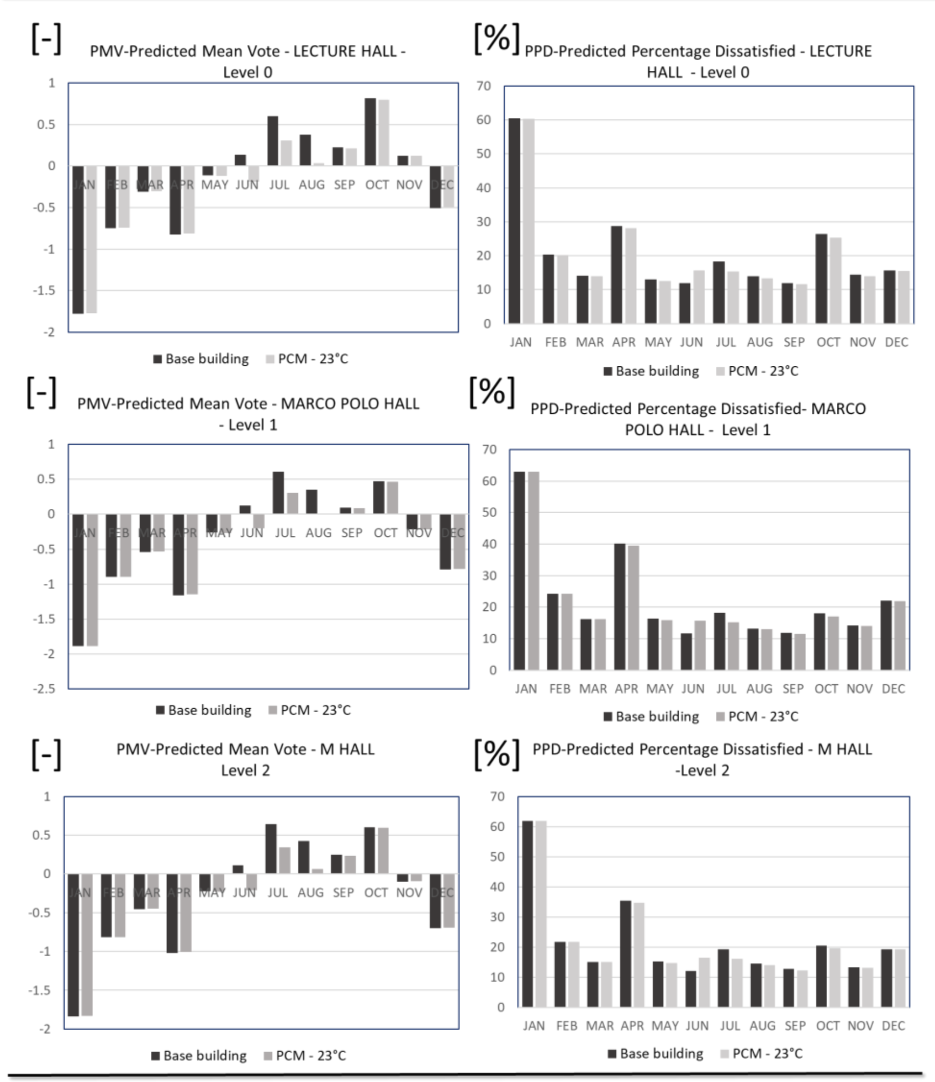

Figure 3.19 - PMV and PPD average month values for three typical rooms during the year

That depends on the melting temperature of the PCM. In fact, the results of thermal analyses show that the PCM does not store latent heat and does not reach the fusion temperature during winter. Please note that the worse values of the PMV-PPD of January are related to the fact that, in many days at the beginning of the month, the University is closed and the HVAC systems are turned off.

In terms of cost analysis, with reference to the PCM, the NPV (net present value) is negative, even if slightly, and this outcome reveals that, merely under the point of view of the costs, the addition of phase change material, for this building, is not repaid along the lifetime. In any case, the difference between the global costs of the PCM refurbished building and the base case building is minimal. The base building has a global cost of 523’748 € and the building with PCM has a G_C of 538’318 €, in a calculation period of 30 years. A difference of 14’570 € probably, for a public Institution involved in having a demonstration role can be accepted, mainly if the better summer and yearly comfort are achieved after the PCM refurbishment. Furthermore, considering the future trends of the increasing earth temperature and the enhancement of the electric energy prices, the PCM retrofit may be a convenient energy conservation measure for the improvement of the building energy efficiency.

3.3.2.1. Optimization of the Phase Change Layer

The design of phase change materials for improving the thermal performance of the building envelope is, as known, a quite delicate issue, being necessary tailored evaluations concerning the melting temperature, enthalpy of fusion, quantity of materials (i.e., thickness, encapsulation, weight), and other physical and constructive characteristics. In this deepening, a wide study is proposed for optimizing the selection of the most proper phase change material to do as more convenient is possible its application in this case study, by considering the building technology, building thermo-physics, building location and its use. It should be noted, moreover, that a further optimization would involve also the PCM layer position inside the wall. Really, in this case, it was supposed the application of the PCM on the inner side of the external walls, to preserve it from too frequent cycles of charging and discharging (typical for application in the external side) and being this kind of application less invasive in the frame of the building retrofit.

To identify the best PCM configuration, and thus the best results in terms of energy consumption, costs, emissions and comfort, different phase change materials were evaluated. Specifically, ten PCMs were tested, according to their melting temperature: from 18 °C to 28 °C. Comparing the results, the energy consumption reduction is quite the same during the cold season. Indeed, even if the melting point is 18 °C or 19 °C, and the corresponding freezing temperature is 16 °C and 17 °C respectively, the heat stored by the PCM would be released during the nocturnal hours when the building is uninhabited, and the systems are turned off. At the same way, with the exception of some hours in few days of the heating periods (when indoor gains are quite high), the ambient air can't reach a higher temperature than 20 °C because the heating set-point is 20 °C, so, if the freezing temperature of the PCM exceeds the 20 °C, it would be always solid and couldn't release the heat stored (there is no phase changing). Finally, the energy consumption reduction of 1.6% during the winter is mainly related to the addition of a layer in the external building wall, which implies the reduction of thermal transmittance. The choice of the PCM was carried out evaluating the summer primary energy reduction of the different applications of PCMs (Figure 3.20).

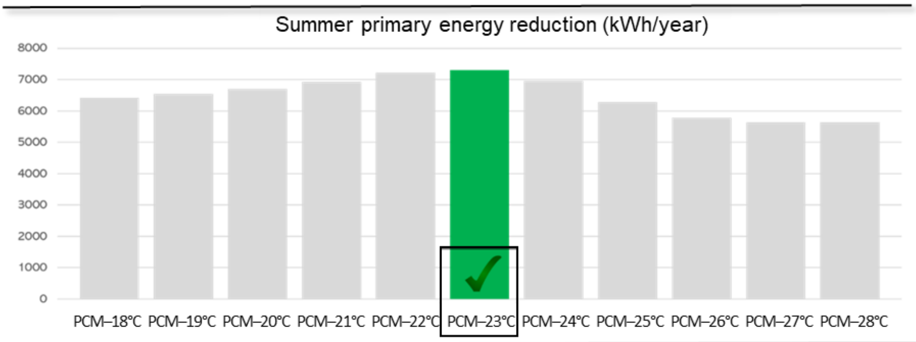

Figure 3.20 - Comparing PCM additions in terms of summer primary energy reduction

The results show a considerable reduction of energy consumption when the melting point of the PCM is 23 °C and growing energy demand when the PCM melting point increases or decreases. The advantages of the PCM building integration occur when the material changes its phase from solid to liquid and vice versa, in order to collect heat, subtracting it to the ambient and releasing it during the solidifying phase. When the PCM melting point is too low (18 °C–20 °C) the material will be melted all the time, instead, when it's too high the PCM will be predominately solid (25 °C–28 °C). For these reasons, the best PCM, for this case study, is the one with a melting temperature of 23 °C and a freezing temperature of 21 °C. Of course, these outcomes are the ones that maximize the cooling energy savings with reference to this peculiar case study, characterized by well-defined constructive technologies, building use, location and specific other boundary conditions.

5) Addition of a second envelope skin: vented façade

Natural ventilation can be used as a cooling passive strategy for buildings. In the specific case of a vented façade, the external air is used to reduce the temperature of a cavity between the thermal insulation material and the external coating. This strategy can dissipate the incident solar radiation and reduce the energy demand of the building, for both heating and cooling purposes. The vented façade proposed is made up of:

- Rockwool thermal insulation material (thickness 8 cm, thermal conductivity 0.035 W/mK, density 60 kg/m^3, specific heat 1030 J/kgK);
- Air cavity of 5 cm;
- Exterior baffle with 6% of openings (thermal emissivity 0.9, solar absorptivity 0.6).

Benefits can be achieved in both the seasons of heating and cooling, because, in winter, the thermal insulation is dry, not affected by rainfall, so that the thermal conductivity does not rise because of water and humidity. Besides the ventilation, the external cavity also allows a better preservation of the wall. In summer, conversely, the ventilation of the cavity, powered by the solar radiation on the baffle, allows the stack effect with a consequent heat dissipation and a lower cooling load of the building. With reference to the educational building of Termoli, the vented façade was added to the present wall. The vented coating was modeled in the software EnergyPlus, through the natural vented cavity and the gap convective radiation as other side conditions model, with input data reported in Figure 3.21.

Field	Units	Obj1
Name		FV 1
Boundary Conditions Model Name		facciata ventilata
Area Fraction of Openings	dimensionless	0.06
Thermal Emissivity of Exterior Baffle Material	dimensionless	0.9
Solar Absorbtivity of Exterior Baffle	dimensionless	0.6
Height Scale for Buoyancy-Driven Ventilation	m	0.05
Effective Thickness of Cavity Behind Exterior Baffle	m	0.05
Ratio of Actual Surface Area to Projected Surface Area	dimensionless	0.97
Roughness of Exterior Surface		MediumRough
Effectiveness for Perforations with Respect to Wind	dimensionless	0.6
Discharge Coefficient for Openings with Respect to Buc	dimensionless	0.8
Surface 1 Name		P1:P1Aula_Wall_2_

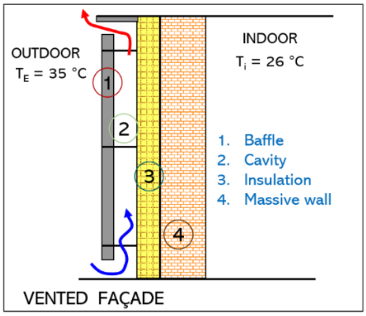

Figure 3.21 - Energy-Plus model of the vented façade.

The application of the vented façade implies a reduction of the primary energy required for the winter heating (4.8%) due to the addition of the thermal insulation layer. During the hot season, conversely, the natural vented cavity reduces the surface temperature of the external wall, but the addition of a thermal insulation material makes its effect negligible. Indeed, even if the daily temperature of the external environment (and thus the cavity temperature) goes down, the high thermal resistance of the cavity does not allow a significant heat dissipation from the inside to the outside. These phenomena can be understood better by analyzing the performances, by comparing the base building (e.g., the present building) with the building refurbished with a rockwool thermal insulation and the building refurbished with rockwool thermal insulation and the vented cavity. The results of the thermo-energetic simulations are shown in Table 3.12. Compared to a simple retrofit with thermal insulation and a new external plaster, the addition of a vented facade reduces the summer energy consumption only of about 0.3%, with no variation of yearly primary energy consumption. For this reason, in this design, that technology was not considered as profitable.

Table 3.12 - Comparison, with respect to the base building, of the retrofit with thermal insulation and the retrofit with thermal insulation and vented façade.

Building with Vented Facade			**ΔENERGY**
Winter Primary Energy Reduction	3472	kWh_p	4.8%
Summer Primary Energy Reduction	1953	kWh_p	3.2%
Yearly Primary Energy Reduction	5425	kWh_p	4.1%
Building with Rockwool Thermal Insulation			
Winter Primary Energy Reduction	3688	kWh_p	5.1%
Summer Primary Energy Reduction	1791	kWh_p	2.9%
Yearly Primary Energy Reduction	5480	kWh_p	4.1%

3.3.3. Energetic and Economic Analysis Results and Discussion

Summarized energy performances of all retrofit measures, proposed and evaluated for the energy requalification of the building, are shown in Table 3.13. More in detail, the following parameters are synthetically reported and thus: energy demands (primary energy) and CO_2 equivalent emissions, as well as their reduction compared to the base building (ΔEP and $ΔCO_2$), the investment costs, return time of the invested capital (SPB and DPB), and the net present value (NPV) associated with each intervention. The evaluation of the different solutions follows the cost-optimal approach described in sub-section 2.2.2. The cost-optimal level corresponds to an energy performance level with the lowest cost, during the economic lifecycle:

- the cost takes into account the investment costs, maintenance and operating costs and disposal costs, where applicable;
- the economic lifecycle is determined by each member state and is the estimated period where the building preserves entirely its energy performance.

In accordance with the EU legislative frame [132], the calculation time of the economic analysis is 30 years. All energy efficiency measures have a lifespan longer than 30 years, so that a second installation is not necessary during the time horizon of the investigation (i.e., no second installation, no residual value). The investment cost generally includes the cost of disposal of the technology; therefore, the cost of rebuilding was not increased by the costs of removal and transport to the landfill.

Comparing the different interventions, it should be noted that:

- The green roof technology determines a reduction in HVAC energy consumption, produces a summer primary energy reduction of 1.6% (993 kWh_p), and a winter primary energy reduction of 0.6% (443 kWh_p). The thermal transmittance of the roof, with and without the green roof are: 0.32 W/m^2K and 0.37 W/m^2K.

  Niachou *et al.* [136] examined different scenarios, comparing the addition of a green roof on a well-insulated building and a non-insulated building, with a typical Mediterranean climate (Loutraki, Greece). For a well-insulated building, and particularly for a roof whose thermal transmittance switches from 0.39 W/m^2K to 0.33 W/m^2K, the energy-saving for heating corresponds to 8%, and the energy-saving for cooling to 0%, with a total energy saving of 2%.

  The performance of the green roof would be better if the thermal transmittance of the roof had been greater than 0.4 W/m^2K. To higher thermal transmittance corresponds a major thermal flux. In this case, the roof is well insulated and, even if the roof surface temperature is reduced by the green roof vegetation, the advantages in terms of energetic saving are not relevant.

  This reduction of energy demand is not enough if analyzed contextually to the investment cost, and therefore the NPV is negative at 30 years. The installation of this technology would allow energy savings not high enough to compensate an investment cost of € 84’000.
- Analogously, the cool roof technology does not produce positive results in economic terms. The primary energy reduction of 0.6% is not enough to get back the investment cost (14,000 €), and the NPV is negative. About this, Synnefa *et al.* [137] focused on the effect of cool roofs in different climatic conditions on energy consumption, but also on the relation between thermal transmittance and cool roof

energy saving. When the thermal transmittance of a roof is low, like the case study here analyzed (0.37 W/m^{2}K), the heat transfer between the roof surface and the indoor ambient is small and the energy saving is not important.

- The thermal insulation layer reduces the energy consumption of 1.1% during a year, but the investment costs are too high. Indeed, the vertical insulation with expanded polyurethane, having a thermal conductivity equal to 0.026 W/m^{2}K, implies an investment cost of € 128’140, but also a return time of the capital higher than 30 years and thus a negative NPV was calculated. These results are in line with those obtained by Ascione *et al.* [138]. The study focused on the application of different measures for the retrofit of a Conference Hall in Naples. In the specific case of the thermal insulation (8 cm of polyurethane), they obtained an annual variation of primary energy of 0.7% and a SPB major than 30 years.
- The cooling strategy through the vented façade is not economically convenient, indeed, even if the primary energy demand for cooling and heating decreases of 4.1%, the investment cost of 344’000 € cannot be repaid before 30 years, and thus the NPV is negative. In terms of energy savings, the simulated solution has results coherent with those obtained by Balocco *et al.* [139]. A vented facade high 14 m, with an air cavity of 7 cm, was tested by the authors, on the southern wall of a building in Florence. The results showed the reduction of energy for cooling of 7% compared to the building without a vented façade. The vented façade here examined, with a height of 13.2 m and an air cavity of 10 cm, could reduce the cooling demand of the University of Molise located in Termoli, of 3.2%. This result is lowest than the case study of Balocco *et al.* because the vented façade was tested on all the walls of the building, differently oriented, and not only on the southern surface. Besides, although comparable, there are certain differences related to the climatic conditions of Florence and Termoli.

- The phase change material offers advantages from the energetic point of view but not actually from the economic point of view. For an investment cost of 36’875 €, the NPV is negative, and the DPB is longer than 30 years. From the energetic point of view, the summer energy saving is 11.7%, instead, the winter energy saving is 1.6%. The results obtained are comparable, although qualitatively, with those provided by Saafi *et al.* [140]. The study focused on the application of a PCM on the internal surface of the building envelope, under the Tunisia Mediterranean climate. A PCM with a melting temperature of 23 °C, guarantees a cooling energy reduction rate of 12%, and a heating energy reduction of 7.8% for freezing temperature of 20 °C.

Really, it should be noted that:

- The present building already has a quite satisfactory level of energy efficiency: it means that the high potential of energy-saving already was exploited during the previous energy retrofit.
- These economic analyses were performed with a particularly low electric energy price. In fact, the University of Molise pays only 0.20 €/kWh$_e$, but considering the certain increase of energy cost, and the future increment of energy demand for active cooling, the innovative PCM intervention can be considered a valuable energy efficiency measure.

Moreover, by considering a large number of stakeholders involved in energy efficiency projects, and thus the community besides the building owners and managers, a macroeconomic analysis was provided too, which takes into account the investment cost but also the maintenance, management, and any additional costs. As established by the aforementioned “Commission Regulation (EU) No. 244/2012 of 16 January 2012” [132], the macroeconomic analysis also considers the costs of greenhouse gas emissions and the residual value of the investment for a calculation period of 30 years (for the redevelopment of residential and public buildings). More in detail, Table 3.14 infers the so-called global costs, and all economic and technical parameters provided by the aforementioned EU Delegated Regulation. As can be seen from Table 3.14 and Figure 3.22, the intervention with the highest overall global cost is the vented façade and is equal to 645’042 €. Conversely, the global cost of PCM intervention is the lowest (538’318 €).

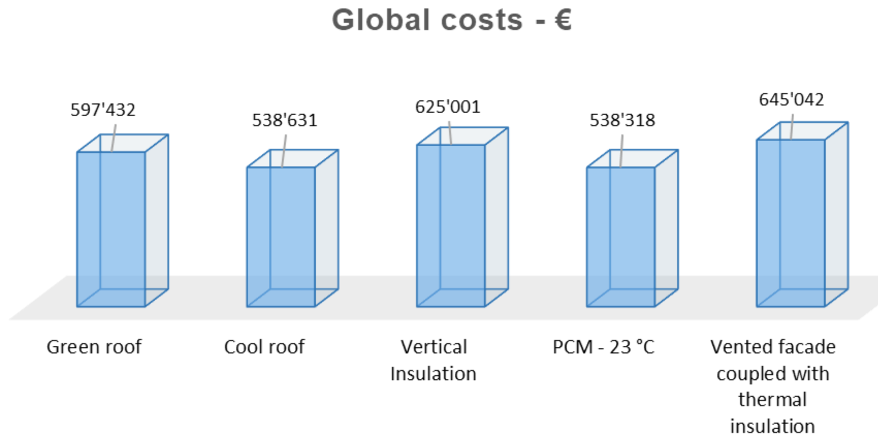

Figure 3.22 - GC global costs of the considered energy efficiency measures—calculation period of 30 years.

Furthermore, to provide some suggestions, the following possible future events can be considered:

- an increase of energy price of 25%,
- funding measures also for energy efficiency strategies devoted to cooling (i.e., 40% of the investments, as already established by the thermal account),
- stagnancy of value of money and thus a discount rate equal to 1% (in this study, the discount rate is imposed as 3%, but really, in the last years, the value of money remained quite constant. Finally, a discount rate of 1% is reliable today),
- reduction of costs of phase change materials because of their diffusion and thus positive economies of scale.

According to these new boundary conditions, that are surely reliable, the payback would be around 12 years.

3.3.4. Conclusive remarks

Very inefficient buildings, and thus ones built after the Second World War (concrete structures, low thicknesses, absence of insulation, large windows), are already the subject of profound refurbishments, mainly to add thermal insulation and reduce the energy demands for heating. Today and for the next years, the challenge is and will be to limit the energy demands for cooling and improving the microclimatic comfort during the hot seasons. Thus, the targets are the buildings built around the 1990s and 2000s, conceived with a good thermal performance for what concerns the winter behavior but without care toward the summer energy comfort. This is the focus of this section (3.3), also according to the aims of the new Directive 844/2018, aimed at a decarbonized building stock in the future decades, starting from the existing buildings. In this regard, guidelines for refurbishing quite recent buildings, mainly to improve the summer conditions and reducing the energy demands for cooling—also by considering the more and more pressing climate change and urban heat island phenomenon, that overheat our cities and communities—are needed and up to date.

The present section (3.3) focused on the energy refurbishment of a public building, one of the main edifices of the University of Molise, located in Termoli (Province of Campobasso, Italy). The retrofit was aimed at reducing the increasing energy demands for the summer space cooling. The energy efficiency measures investigated and optimized in terms of energy, emissions, costs, and thermal comfort have positive effects on the reduction of summer energy demand. Considering the public role of the building, present regulations were taken into account and, in particular, the ones in a matter of energy efficiency of the public buildings were considered, aimed at a low-carbon future through energy savings. The proposed interventions are passive strategies for the building envelope: cool roof and green roof for the horizontal building envelope, thermal insulation, phase change materials and vented façade for the vertical envelope. Firstly, a transient energy model was calibrated, starting from the historical energy consumption; secondly, once having a reliable numerical model of the present scenario, the different solutions were simulated through the software EnergyPlus. Then, all results were analyzed according to different points of view, and thus energy, costs, and emissions analyses. The economic analysis was not limited to the evaluation of operational energy and costs savings, but focuses on the investment assessment, by taking into account the global costs (European Regulation 244/2012 [37]). In the specific case of the PCMs application, different PCMs were compared, varying their melting temperature from 18 °C to 29 °C in order to verify the best solution in terms of microclimatic indoor comfort and reduction of energy consumption. The innovative solution of phase change wallboard with a melting temperature of 23 °C behaves as the best. Indeed, it causes a reduction of primary energy demand during summertime (11.7%), and a consequent decrement of CO_2 emissions. This solution offers advantages in terms of indoor thermal comfort, by increasing the summer indoor comfort of 215 h. According to another comfort model, and thus the Fanger analysis for casual classrooms, a significant improvement of PMV and PPD was achieved during the cooling period and almost no variation during the heating seasons was registered. In terms of costs, the PCM intervention is not actually convenient but considering the future climate evolution and increasing of energy prices, the PCM intervention may be a convenient measure for the improvement of the building energy efficiency. As clear from the results, only an innovative solution as a PCM could improve effectively the thermal comfort and the energy saving of the building. A building like the one analyzed renovated in 2005 and with an envelope with low thermal transmittance, can’t be redeveloped energetically through traditional passive strategies, but only with an innovative solution that influences the apparent thermal capacity (employing the latent heat-storing) of the opaque envelope acting from the inner side. A phase change material can be a valid solution.

Table 3.13 - Results of the energy and economic analyses of the retrofit measures applied to the case study.

Type of Intervention	Primary Energy Demand (HVAC)	Primary Energy Demand (Building)	Tot/m^2	Annual EP saving (HVAC) *	CO_2	Annual CO_2 reduction (HVAC)*	Investment cost	SPB	DPB
Unit of measurement	[MWh]	[MWh]	[kWh/m^2]	[%]	[Ton/year]	[%]	[€]	[years]	[years]
Green roof	131.8	259.4	99.0	1.1%	39.0	1.1%	84’000	> 30 years	> 30 years
Cool roof	132.6	260.2	99.3	0.5%	39.1	0.5%	14’000	> 30 years	> 30 years
Vertical Insulation	128.1	255.8	97.7	3.8%	38.4	3.8%	128’100	> 30 years	> 30 years
PCM wallboard	123.2	250.6	95.7	6.1%	37.7	6.1%	36’900	> 30 years	> 30 years
Vented facade	127.8	255.4	97.5	4.7%	38.4	4.7%	344’000	> 30 years	> 30 years

Table 3.14 - Technical and economical analysis according to the indication EU delegated regulation n. 244/2012; fuel cost 0.20 €/kWh$_e$, discount rate 3.0%, economic lifecycle = 30 years.

Type of Intervention	Investment Costs	Lifetime Discounted Management Costs	Emission Costs	Residual Value	Global Costs
Unit of measurement	[€]	[€]	[€]	[€]	[€]
Green roof	84’000	498’226	29’049	13’843	597’432
Cool roof	14’000	497’800	29’138	2307	538’631
Vertical insulation *	128’140	489’335	28’643	21’117	625’001
PCM plaster	36’875	479’455	28’065	6077	538’318
Vented facade	344’000	329’129	28’602	56’689	645’042

* “Thermal Account” (“Conto Termico”, in Italian) incentives have been considered. The “Thermal Account” establishes a refunding of 40% of the total intervention cost for thermal insulation of the opaque building envelope.

CHAPTER 3 – References

[1] Santamouris, M.; Kolokotsa, D. Passive cooling dissipation techniques for buildings and other structures: The state of the art. Energy Build. 2013, 57, 74–94.

[2] Ascione, F.; Bianco, N.; De Masi, R.F.; De Rossi, F.; Vanoli, G.P. Simplified state space representation for evaluating thermal bridges in building: Modelling, application and validation of a methodology. Appl. Therm. Eng. 2013, 61, 344–354.

[3] Ascione, F. Energy conservation and renewable technologies for buildings to face the impact of the climate change and minimize the use of cooling. Sol. Energy 2017, 154, 34–100.

[4] Alcazar, S.; Olivieri, F.; Neila, J. Green roofs: Experimental and analytical study of its potential for urban microclimate regulation in Mediterranean–continental climates. Urban Clim. 2016, 17, 304–317.

[5] Yaghoobian, N.; Srebric, J. Influence of plant coverage on the total green roof energy balance and building energy consumption. Energy Build. 2015, 103, 1–13.

[6] Ascione, F.; Bianco, N.; de Rossi, F.; Turni, G.; Vanoli, G.P. Green roofs in European climates. Are effective solutions for the energy savings in air-conditioning? Appl. Energy 2013, 104, 845–859.

[7] Ascione, F.; Bianco, N.; De Masi, R.F.; De Rossi, F.; Vanoli, G.P. Technical and economic analysis of green roofs to reduce building cooling needs. In Eco-efficient Materials for Mitigating Building Cooling Needs—Design, Properties and Application; Pacheco-Torgal, F., Labrincha, J., Cabeza, L., Granqvist, C., Eds.; Woodhead Publishing: Sawston, UK, 2015; pp. 349–378.

[8] Gagliano, A.; Detommaso, M.; Nocera, F.; Evola, G. A multi-criteria methodology for comparing the energy and environmental behavior of cool, green and traditional roofs. Build. Environ. 2015, 90, 71–81.

[9] Pisello, A.L.; Piselli, C.; Cotana, F. Thermal-physics and energy performance of an innovative green roof system: The Cool-Green Roof. Sol. Energy 2015, 116, 337–356.

[10] Santamouris, M.; Pavlou, K.; Synnefa, A.; Niachou, K.; Kolokotsa, D. Recent progress on passive cooling techniques: Advanced technological developments to improve survivability levels in low-income households. Energy Build. 2007, 39, 859–866.

[11] Lucchi, E.; Tabak, M.; Troi, A. The "cost optimality" approach for the internal insulation of historic buildings. Energy Procedia 2017, 133, 412–423.

[12] Cao, Z.J.; Liao, W.; Wang, S.X.; Zhao, H.B.; Wang, Y.Z. Polyurethane foams with functionalized graphene towards high fire-resistance, low smoke release, superior thermal insulation. Chem. Eng. J. 2019, 361, 1245–1254.

[13] Cabeza, L.F.; Castell, A.; Medrano, M.; Martorell, I.; Pérez, G.; Fernández, I. Experimental study on the performance of insulation materials in Mediterranean construction. Energy Build. 2010, 42, 630–636.

[14] Stazi, F.; Tomassoni, F.; Vegliò, A.; Di Perna, C. Experimental evaluation of ventilated walls with an external clay cladding. Renew. Energy 2011, 36, 3373–3385.

[15] Marinosci, C.; Semprini, G.; Morini, G.L. Experimental analysis of the summer thermal performances of a naturally ventilated rainscreen façade building. Energy Build. 2014, 72, 280–287.

[16] Kasaeian, A.; Pourfayaz, F.; Khodabandeh, E.; Yan, W.M. Experimental studies on the applications of PCMs and nano-PCMs in buildings: A critical review. Energy Build. 2017, 154, 96–112.

[17] Baetens, R.; Jelle, B.P.; Gustavsen, A. Phase change materials for building applications: A state-of-the-art review. Energy Build. 2010, 42, 1361–1368.

[18] Feldman, D.; Banu, D.; Hawes, D.W. Development and application of organic phase change mixtures in thermal storage gypsum wallboard. Sol. Energy Mater. Sol. Cell. 1995, 36, 147–157.

[19] Theodoridou, M.; Kyriakou, L.; Ioannou, I. PCM-enhanced lime plasters for vernacular and contemporary architecture. Energy Procedia 2016, 97, 539–545.

[20] Sittisart, P.; Farid, M.M. Fire retardants for phase change materials. Appl. Energy 2011, 88, 3140–3145.

[21] Tyagi, V.V.; Kaushik, S.C.; Tyagi, S.K.; Akiyama, T. Development of phase change materials based microencapsulated technology for buildings: A review. Renew. Sustain. Energy Rev. 2011, 15, 1373–1391.

[22] Gil-Baez, M.; Padura, Á.B.; Huelva, M.M. Passive actions in the building envelope to enhance sustainability of schools in a Mediterranean climate. Energy 2019, 167, 144–158.

[23] De Santoli, L.; Fraticelli, F.; Fornari, F.; Calice, C. Energy performance assessment and a retrofit strategies in public school buildings in Rome. Energy Build. 2014, 68, 196–202.

[24] Newton, J.; Gedge, D.; Early, P.; Wilson, S. BUILDING GREENer—Guidance on the Use of Green Roofs, Green Walls and Complementary Features on Buildings; CIRIA Press: London, UK, 2007.

[25] Manso, M.; Castro-Gomes, J. Green wall systems: A review of their characteristics. Renew. Sustain. Energy Rev. 2015, 41, 863–871.

[26] Rakhshandehroo, M.; Yusof, M.; Johari, M.; Deghati Najd, M. Green Façade (Vertical Greening): Benefits and Threats. Appl. Mech. Mater. 2015, 747, 12–15.

[27] Susorova, I. Green facades and living walls: vertical vegetation as a construction material to reduce building cooling loads. In Eco-Efficient Materials for Mitigating Building Cooling Needs. Woodhead Publishing: Cambridge, UK, 2015; pp. 127–153.

[28] Pérez, G.; Rincón, L.; Vila, A.; González, J.M.; Cabeza, L.F. Green vertical systems for buildings as passive systems for energy savings. Appl. Energy 2011, 88, 4854–4859.

[29] Riley, B. The state of the art of living walls: Lessons learned. Build. Environ. 2017, 114, 219–232.

[30] Medl, A.; Stangl, R.; Florineth, F. Vertical greening systems—A review on recent technologies and research advancement. Build. Environ. 2017, 125, 227–239.

[31] Pérez, G.; Coma, J.; Martorell, I.; Cabeza, L.F. Vertical Greenery Systems (VGS) for energy saving in buildings: A review. Renew. Sustain. Energy Rev. 2014, 39, 139–165.

[32] Safikhani, T.; Abdullah, A.M.; Ossen, D.R.; Baharvand, M. A review of energy characteristic of vertical greenery systems. Renew. Sustain. Energy Rev. 2014, 40, 450–462.

[33] Hunter, A.M.; Williams, N.S.G.; Rayner, J.P.; Aye, L.; Hes, D.; Livesley, S.J. Quantifying the thermal performance of green facades: A critical review. Ecol. Eng. 2014, 63, 102–113.

[34] Besir, A.B.; Cuce, E. Green roofs and facades: A comprehensive review. Renew. Sustain. Energy Rev. 2018, 82, 915–939.

[35] Charoenkit, S.; Yiemwattana, S. Living walls and their contribution to improved thermal comfort and carbon emission reduction: A review. Build. Environ. 2016, 105, 82–94.

[36] Susorova, I., & Bahrami, P. Facade-Integrated Vegetation as an Environmental Sustainable Solution for Energy-Efficient Buildings. 2013. MADE Research Journal of Cardiff University: Cardiff, UK, 6–14.

[37] Watson, D.J. Comparative physiological studies in the growth of field crops. I. Variation in net assimilation rate and leaf area between species and varieties, and within and between years. Ann. Bot. 1947, 11, 41–76.

[38] Breda, N.J. Ground-based measurements of leaf area index: A review of methods, instruments and current controversies. J. Exp. Bot. 2003, 54, 2403–2417.

[39] Charoenkit, S.; Yiemwattana, S. Role of specific plant characteristics on thermal and carbon sequestration properties of living walls in tropical climate. Build. Environ. 2017, 115, 67–79.

[40] Koyama, T.; Yoshinaga, M.; Hayashi, H.; Maeda, K.; Yamauchi, A. Identification of key plant traits contributing to the cooling effects of green façades using freestanding walls. Build. Environ. 2013, 66, 96–103.

[41] Pérez, G.; Coma, J.; Sol, S.; Cabeza, L.F. Green facade for energy savings in buildings: The influence of leaf area index and facade orientation on the shadow effect. Appl. Energy 2017, 187, 424–437.

[42] Susorova, I.; Angulo, M.; Bahrami, P.; Stephens, B. A model of vegetated exterior facades for evaluation of wall thermal performance. Build. Environ. 2013, 67, 1–13.

[43] The Guide to Hydrological Practices (WMO No.168), 2008. Available online: https://unstats.un.org/unsd/envaccounting/waterGuidelines/Material/WMO_Guide_168_Vol_I_en_hydrological_practices.pdf. Accessed in November 2021.

[44] Libessart, L.; Kenai, M.A. Measuring thermal conductivity of green-walls components in controlled conditions. J. Build. Eng. 2018, 19, 258–265.

[45] He, Y.; Yu, H.; Ozaki, A.; Dong, N.; Zheng, S. An investigation on the thermal and energy performance of living wall system in Shanghai area. Energy Build. 2017, 140, 324–335.

[46] Consolino, F.; Banfi, E. The Simon & Schuster Guide to Climbing Plants; Simon and Schuster Inc.: New York, NY, USA, 1994; p. 255.

[47] Gianoli, E. Using Ideas from Behavioural Ecology to Understand Plants. The behavioural ecology of climbing plants, 2015, AoB PLANTS 7: plv013. Available online: https://doi.org/10.1093/aobpla/plv013. Accessed in November 2021.

[48] Niklas, K.J. Climbing Plants: Attachment and the Ascent for Light. Curr. Biol. 2011, 21, 199–201.

[49] Turgeon, A.J. Turfgrass Management; Prentice Hall Inc.: Englewood Cliffs, NJ, USA, 1980; p. 418.

[50] Beard, J.B. Turfgrass Science and Culture; Prentice Hall Inc.: Englewood Cliffs, NJ, USA, 1973; p. 658.

[51] Croce, P.; De Luca, A.; Falcinelli, M.; Modestini, F.S.; Veronesi, F. Tappeti Erbosi, Cura, Gestione e Manutenzione Delle Aree Verdi Pubbliche e Private; Edagricole: Calderini, Bologna, Italy, 2006; p. 340.

[52] Whittinghill, L.J.; Rowe, D.B.; Schutzki, R.; Cregg, B.M. Quantifying carbon sequestration of various green roof and ornamental landscape systems. Landsc. Urban Plan. 2014, 123, 41–48.

[53] Wood, A.; Bahrami, P.; Safarik, D. Green Walls in High-Rise Buildings: An output of the CTBUH Sustainability Working Group; Images publishing: Mulgrave, Victoria, Australia, 2014.

[54] Chen, Q.; Li, B.; Liu, X. An experimental evaluation of the living wall system in hot and humid climate. Energy Build. 2013, 61, 298–307.

[55] Kontoleon, K.J.; Eumorfopoulou, E.A. The effect of the orientation and proportion of a plant-covered wall layer on the thermal performance of a building zone. Build. Environ. 2010, 45, 1287–1303.

[56] Manso, M.; Castro-Gomes, J.P. Thermal analysis of a new modular system for green walls. J. Build. Eng. 2016, 7, 53–62.

[57] Mårtensson, L.M.; Wuolo, A.; Fransson, A.M.; Emilsson, T. Plant performance in living wall systems in the Scandinavian climate. Ecol. Eng. 2014, 71, 610–614.

[58] Coma, J.; Perez, G.; de Gracia, A.; Bures, S.; Urrestarazu, M.; Cabeza, L.F. Vertical greenery systems for energy savings in buildings: A comparative study between green walls and green facades. Build. Environ. 2017, 111, 228–237.

[59] Cuce, E. Thermal regulation impact of green walls: An experimental and numerical investigation. Appl. Energy. 2017, 194, 247–254.

[60] Cameron, R.W.F.; Taylor, J.E.; Emmett, M.R. What's 'cool' in the world of green façades? How plant choice influences the cooling properties of green walls. Build. Environ. 2014, 73, 198–207.

[61] Susorova, I.; Azimi, P.; Stephens, B. The effects of climbing vegetation on the local microclimate, thermal performance, and air infiltration of four building facade orientations. Build. Environ. 2014, 76, 113–124.

[62] Mazzali, U.; Peron, F.; Romagnoni, P.; Pulselli, R.M.; Bastianoni, S. Experimental investigation on the energy performance of Living Walls in a temperate climate. Build. Environ. 2013, 64, 57–66.

[63] Wong, N.H.; Tan, A.Y.K.; Chen, Y.; Sekar, K.; Tan, P.Y.; Chan, D.; Chiang, K.; Wong, N.C. Thermal evaluation of vertical greenery systems for building walls. Build. Environ. 2010, 45, 663–672.

[64] Cheng, C.Y.; Ken, K.; Cheung, S.; Chu, L.M. Thermal performance of a vegetated cladding system on facade walls. Build. Environ. 2010, 45, 1779–1787.

[65] Lacasta, A.M.; Penaranda, A.; Cantalapiedra, I.R.; Auguet, C.; Bures, S.; Urrestarazu, M. Acoustic evaluation of modular greenery noise barriers. Urban For. Urban Green. 2016, 20, 172–179.

[66] Perini, K.; Ottelé, M.; Fraaij, A.L.A.; Haas, E.M.; Raiteri, R. Vertical greening systems and the effect on air flow and temperature on the building envelope. Build. Environ. 2011, 46, 2287–2294.

[67] Eumorfopoulou, E.A.; Kontoleon, K.J. Experimental approach to the contribution of plant-covered walls to the thermal behaviour of building envelopes. Build. Environ. 2009, 44, 1024–1038.

[68] Scarpa, M.; Mazzali, U.; Peron, F. Modeling the energy performance of living walls: Validation against field measurements in temperate climate. Energy Build. 2014, 79, 155–163.

[69] Olivieri, F.; Olivieri, L.; Neila, J. Experimental study of the thermal-energy performance of an insulated vegetal façade under summer conditions in a continental Mediterranean climate. Build. Environ. 2014, 77, 61–76.

[70] Haggag, M.; Hassan, A.; Elmasry, S. Experimental study on reduced heat gain through green facades in a high heat load climate. Energy Build. 2014, 82, 668–674.

[71] Razzaghmanesh, M.; Thermal performance investigation of a living wall in a dry climate of Australia. Build. Environ. 2017, 112, 45–62.

[72] Ottelé, M.; Perini, K.; Fraaij, A.L.A.; Haas, E.M.; Raiteri, R. Comparative life cycle analysis for green facades and living wall systems. Energy Build. 2011, 43, 3419–3429.

[73] Mårtensson, L.M.; Fransson, A.M.; Emilsson, T. Exploring the use of edible and evergreen perennials in living wall systems in the Scandinavian climate. Urban For. Urban Green. 2016, 15, 84–88.

[74] Djedjig, R.; Ouldboukhitine, S.; Belarbi, R.; Bozonnet, E. Development and validation of a coupled heat and mass transfer model for green roofs. Int. Commun. Heat Mass Transf. 2012, 39, 752–761.

[75] Dahanayake, K.W.D. K. C.; Chow, C.L. Studying the potential of energy saving through vertical greenery systems: Using EnergyPlus simulation program. Energy Build. 2017, 138, 47–59.

[76] Malys, L.; Musya, M.; Inard, C. A hydrothermal model to assess the impact of green walls on urban microclimate and building energy consumption. Build. Environ. 2010, 73, 187–197.

[77] Djedjig, R.; Bozonnet, E.; Belarbi, R. Modeling green wall interactions with street canyons for building energy simulation in urban context. Urban Clim. 2016, 16, 75–85.

[78] Olivieri, F.; Redondas, D.; Olivieri, L.; Neila, J. Experimental characterization and implementation of an integrated autoregressive model to predict the thermal performance of vegetal facades. Energy Build. 2014, 72, 309–321.

[79] Pulselli, R.M.; Pulselli, F.M.; Mazzali, U.; Peron, F.; Bastianoni, S. Emergy based evaluation of environmental performances of LivingWall and Grass Wall systems. Energy Build. 2014, 73, 200–211.

[80] Vox, G.; Blanco, I.; Schettini, E. Green façades to control wall surface temperature in buildings. Build. Environ. 2018, 129, 154–166.

[81] Victorero, F.; Vera, S.; Bustamante, W.; Tori, F.; Bonilla, C.; Gironás, J.; Rojas, V. Experimental study of the thermal performance of living walls under semiarid climatic conditions. Energy Procedia 2015, 78, 3416–3421.

[82] Feitosa, R.C.; Wilkinson, S.J. Attenuating heat stress through green roof and green wall retrofit. Build. Environ. 2018, 140, 11–22.

[83] Herath, H.M.P.I.K.; Halwatura, R.U.; Jayasinghe, G.Y. Modeling a Tropical Urban Context with Green Walls and Green Roofs as an Urban Heat Island Adaptation Strategy. Procedia Eng. 2018, 212, 691–698.

[84] Hoelscher, M.T.; Nehls, T.; Jänicke, B.; Wessolek, G. Quantifying cooling effects of facade greening: Shading, transpiration and insulation. Energy Build. 2016, 114, 283–290.

[85] De Jesus, M.P.; Lourenço, J.M.; Arce, R.M.; Macias, M. Green façades and in situ measurements of outdoor building thermal behavior. Build. Environ. 2017, 119, 11–19.

[86] Marchi, M.; Pulselli, R.M.; Marchettini, N.; Pulselli, F.M.; Bastianoni, S. Carbon dioxide sequestration model of a vertical greenery system. Ecol. Model. 2015, 306, 46–56.

[87] Othman, R.; Kasim, S.Z.A. Assessment of Plant Materials Carbon Sequestration Rate for Horizontal and Vertical Landscape Design. Int. J. Environ. Sci. Dev. 2016, 7, 410–414.

[88] Paull, N.J.; Irga, P.J.; Torpy, F.R. Active green wall plant health tolerance to diesel smoke exposure. Environ. Pollut. 2018, 240, 448–456.

[89] Prodanovic, V.; Hatt, B.; McCarthy, D.; Zhang, K.; Deletic, A. Green walls for greywater reuse: Understanding the role of media on pollutant removal. Ecol. Eng. 2017, 102, 625–635.

[90] Prodanovic, V.; Zhang, K.; Hatt, B.; McCarthy, D.; Deletic, A. Optimisation of lightweight green wall media for greywater treatment and reuse. Build. Environ. 2018, 131, 99–107.

[91] Masi, F.; Bresciani, R.; Rizzo, A.; Edathoot, A.; Patwardhan, N.; Panse, D.; Langergraber, G. Green walls for greywater treatment and recycling in dense

urban areas: A case-study in Pune. J. Water Sanit. Hyg. Dev. 2016, 6, 342–347.

[92] Brenneisen, S. Space for urban wildlife: Designing green roofs as habitats in Switzerland. Urban Habitats 2006, 4, 27–36.

[93] Oberndorfer, E.; Lundholm, J.; Bass, B.; Coffman, R.R.; Doshi, H.; Dunnett, N.; Gaffin, S.; Köhler, M.; Liu, K.K.Y.; Rowe, B. Green roofs as urban ecosystems: Ecological structures, functions and services. BioScience 2007, 57, 823–833.

[94] Francis, R.A.; Lorimer, J. Urban reconciliation ecology: The potential of living roofs and walls. J. Environ. Manag. 2011, 92, 1429–1437.

[95] Chiquet, C.; Dover, J.W.; Mitchell, P. Birds and the urban environment: The value of green walls. Urban Ecosyst. 2013, 16, 453–462.

[96] Lundholm, J.T. Green Roofs and Facades: A Habitat Template Approach. Urban Habitats 2006, 4, 87–101.

[97] Collins, R.; Schaafsm, M.; Hudson, M.D. The value of green walls to urban biodiversity. Land Use Policy 2017, 64, 114–123.

[98] Gao, X.; Asami, Y. Effect of urban landscape on land price in two Japanese cities. Landsc. Urban Plan. 2007, 81, 155–166.

[99] Des Rosiers, F.; Thériault, M.; Kestens, Y.; Villeneuve, P. Landscaping and house values: An empirical investigation. J. Real Estate Res. 2002, 23, 139–161.

[100] Coma, J.; Solé, C.; Castell, A.; Cabeza, L.F. New green facades as passive systems for energy savings on buildings. Energy Procedia 2014, 57, 1851–1859.

[101] Djedjig, R.; Belarbi, R.; Bozonnet, E. Experimental study of green walls impacts on buildings in summer and winter under an oceanic climate. Energy Build. 2017, 150, 403–411.

[102] Wong, I.; Baldwin, A.N. Investigating the potential of applying vertical green walls to high-rise residential buildings for energy-saving in sub-tropical region. Build. Environ. 2016, 97, 34–39.

[103] Feng, H.; Hewage, K. Energy saving performance of green vegetation on LEED certified buildings. Energy Build. 2014, 75, 281–289.

[104] Perini, K.; Bazzocchi, F.; Croci, L.; Magliocco, A.; Cattaneo, E. The use of vertical greening systems to reduce the energy demand for air conditioning. Field monitoring in Mediterranean climate. Energy Build. 2017, 143, 35–42.

[105] Wong, N.H.; Tan, A.Y.K.; Tan, P.Y.; Wong, N.C. Energy simulation of vertical greenery systems. Energy Build. 2009, 41, 1401–1408.

[106] Tudiwer, D.; Korjenic, A. The effect of living wall systems on the thermal resistance of the façade. Energy Build. 2017, 135, 10–19.

[107] Van Renterghem, T.; Hornikx, M.; Forssen, J.; Botteldooren, D. The potential of building envelope greening to achieve quietness. Build. Environ. 2013, 61, 34–44.
[108] Horoshenkov, K.V.; Khan, A.; Benkreira, H. Acoustic properties of low growing plants. J. Acoust. Soc. Am. 2013, 133, 2554–2565.
[109] Hong-Seok, Y.; Kang, J.; Chris, C. Random-Incidence Absorption and Scattering Coefficients of Vegetation. Acta Acust. United Acust. 2013, 99, 379–388.
[110] Jang, H.S.; Kim, H.J.; Jeon, J.Y. Scale-model method for measuring noise reduction in residential buildings by vegetation. Build. Environ. 2015, 86, 81–88.
[111] Wong, N.H.; Tan, A.Y.K.; Tan, P.Y.; Chiang, K.; Wong, N.C. Acoustics evaluation of vertical greenery systems for building walls. Build. Environ. 2010, 45, 411–420.
[112] Azkorra, Z.; Pérez, G.; Coma, J.; Cabeza, L.F.; Bures, S.; Álvaro, J.E.; Erkoreka, A.; Urrestarazu, M. Evaluation of green walls as a passive acoustic insulation system for buildings. Appl. Acoust. 2015, 89, 46–56.
[113] Fernández-Bregón, N.; Urrestarazu, M.; Valera, D.L. Effects of a vertical greenery system on selected thermal and sound mitigation parameters for indoor building walls. J. Food Agric. Environ. 2012, 10, 1025–1027.
[114] Pérez, G.; Coma, J.; Cabeza, L.F. Nature Based Strategies for Urban and Building Sustainability; Chapter 3.7—Vertical Greening Systems for Acoustic Insulation and Noise Reduction; 2018; pp. 157–165.
[115] Giordano, R.; Montacchini, E.; Perone, A. Living Wall Systems: A technical standard proposal. Energy Procedia 2017, 111, 298–307.
[116] Tedesco, S.; Giordano, R.; Montacchini, E. How to measure the green façade sustainability? A proposal of a technical standard. Energy Procedia 2016, 96, 560–567.
[117] Feng, H.; Hewage, K. Lifecycle assessment of living walls: Air purification and energy performance. J. Clean. Prod. 2014, 69, 91–99.
[118] Manso, M.; Castro-Gomes, J.; Paulo, B.; Bentes, I.; Teixeira, C.A. Life cycle analysis of a new modular greening system. Sci. Total Environ. 2018, 627, 1146–1153.
[119] Perini, K.; Rosasco, P. Cost benefit analysis for green façades and living wall systems. Build. Environ. 2013, 70, 110–121.
[120] Perini, K.; Rosasco, P. Evaluating the economic sustainability of a vertical greening system: A Cost-Benefit, Analysis of a pilot project in mediterranean area. Build. Environ. 2018, 142, 524–533.

[121] Oquendo-Di Cosola, V.; Olivieri, F.; Ruiz-García, L.; Bacenetti, J. An environmental Life Cycle Assessment of Living Wall Systems. J. Environ. Manag. 2020, 254, 109743.

[122] Perez Urrestarazu, L.; Egea, G.; Franco-Salas, A.; Fernandez-Canero, R. Irrigation Systems Evaluation for Living Walls. J. Irrig. Drain. Eng. 2014, 140, 04013024–1/11.

[123] Perini, K.; Ottelé, M.; Haas, E.M.; Raiteri, R. Greening the building envelope, façade greening and living wall systems. Open J. Ecol. 2011, 1, 1.

[124] Sheweka, S.; Magdy, N. The Living walls as an Approach for a Healthy Urban Environment. Energy Procedia 2011, 6, 592–599.

[125] ISPRA Report. Available online: http://www.isprambiente.gov.it/files2018/pubblicazioni/rapporti/R_280_18_Emissioni_Settore_Elettrico.pdf/view. Accessed in November 2021

[126] EnergyPlus simulation software, Version 7.2.0; U.S. Department of Energy: Washington, DC, USA, 2012.

[127] DesignBuilder, Version 3.4; DesignBuilder Software Ltd.: Gloucestershire, UK, 2013.

[128] ASHRAE—American Society of Heating. Refrigerating and Air-ConditioningEngineers, Guideline 14 2002, Measurement of Energy and Demand and Savings; ASHARE: Atlanta, GA, USA, 2002.

[129] U.S. Department of Energy, Federal Energy Management Program (FEMP). M&V Guidelines: Measurement and Verification for Performance-Based Contracts; FEMP: Washington, DC, USA, 2015.

[130] Italian Presidential Decree n 412/1993. D.P.R. 26 august 1993, n. 412. Available online: http://efficienzaenergetica.acs.enea.it/doc/dpr412-93.pdf. Accessed in November 2021

[131] ISPRA Report, Atmospheric Emission Factors of Greenhouse Gases in the National Electricity Sector and in the Main European Countries. Available online: http://www.isprambiente.gov.it/files2019/pubblicazioni/rapporti/R_303_19_gas_serra_settore_elettrico.pdf/view. Accessed in November 2021

[132] Commission Delegated Regulation (EU) No 244/2012 of 16 January 2012. Available online: https://eur-lex.europa.eu/legal-content/EN/TXT/PDF/?uri=CELEX:32012R0244&from=GA. Accessed in November 2021

[133] Becherini, F.; Lucchi, E.; Gandini, A.; Barrasa, M.C.; Troi, A.; Roberti, F.; Bernardi, A. Characterization and thermal performance evaluation of infrared

reflective coatings compatible with historic buildings. Build. Environ. 2018, 134, 35–46.

[134] Ministerial Decree 26/06/2015. Available online: https://www.mise.gov.it/images/stories/normativa/DM_requisiti_minimi.pdf. Accessed in November 2021

[135] GSE—Energy Services Manager. Available online: https://www.gse.it/servizi-per-te/efficienza-energetica/conto-termico. Accessed in November 2021

[136] Niachou, A.; Papakonstantinou, K.; Santamouris, M.; Tsangrassoulis, A.; Mihalakakou, G. Analysis of the green roof thermal properties and investigation of its energy performance. Energy Build. 2001, 33, 719–729.

[137] Synnefa, A.; Santamouris, M.; Akbari, H. Estimating the effect of using cool coatings on energy loads and thermal comfort in residential buildings in various climatic conditions. Energy Build. 2007, 39, 1167–1174.

[138] Ascione, F.; Bianco, N.; De Stasio, C.; Mauro, G.M.; Vanoli, G.P. Building envelope, HVAC systems and RESs for the energy retrofit of a Conference Hall on Naples promenade. Energy Procedia 2015, 75, 1261–1268.

[139] Balocco, C. A simple model to study ventilated facades energy performance. Energy Build. 2002, 34, 469–475.

[140] Saafi, K.; Daouas, N. Energy and cost efficiency of phase change materials integrated in building envelopes under Tunisia Mediterranean climate. Energy 2019, doi: 10.1016/j.energy.2019.115987.

CHAPTER 4.

Energy refurbishment of present buildings through active strategies: implication of the Covid-19 pandemic

This chapter is aimed at providing useful suggestions and guidelines for the renovation of an existing building of educational use, intervening on the active systems. Starting from a real case study, and thus the architectural and technological refurbishment of an Italian University building (Campobasso, South Italy, cold climate), with the aims of improving the classrooms' quality and safety, a comprehensive approach for the retrofit design is proposed. The scope of this investigation is to do University classrooms safe and sustainable indoor places, during the SARS-CoV-2 global pandemic. Classrooms and common spaces must be thought again, for a new "in-presence" life, due to the recent worldwide emergency following the spring 2020 pandemic diffusion of COVID-19. By taking into account the necessary come back to classrooms, experimental studies (monitoring and investigations of the current energy performances) are followed by the coupling of different numerical methods of investigations, and thus building performance simulations, under transient conditions of heat transfer, and computational fluid dynamics studies, to evidence criticalities and potentialities to designers involved in the re-thinking of indoor spaces hosting multiple persons, with quite high occupancy patterns. Both energy impacts, in terms of monthly and annual increase of energy demands due to higher mechanical ventilation, and indoor distribution of microclimatic parameters (i.e., temperature, airspeed, age of air) are here investigated, by proposing new scenarios and evidencing the usefulness of HVAC systems, equipment (e.g., sensible heat recovery, without flows' contamination) and suitability of some strategies for the air distribution systems (ceiling squared and linear slot diffusers) compared to traditional ones. Figure 4.1 shows a graphical summary of the present chapter.

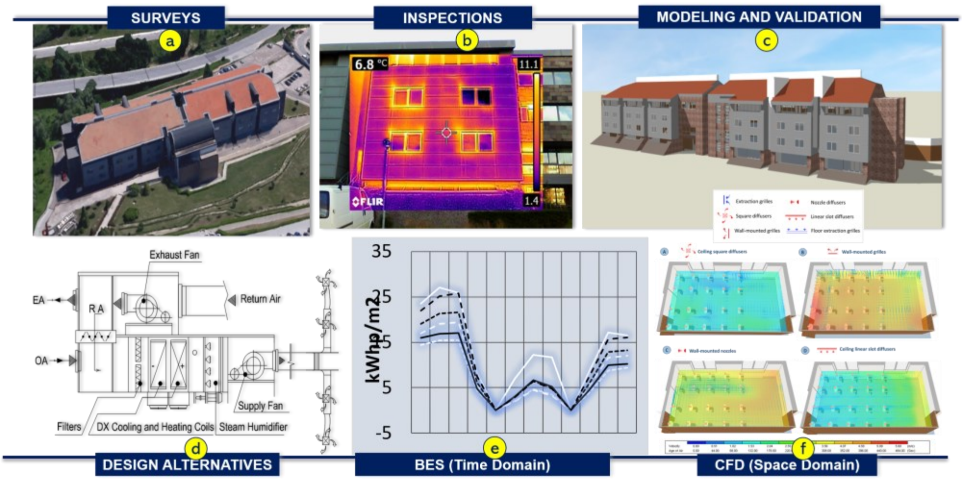

Figure 4.1 – Graphical summary of chapter 4

4.1. State of the art and Research significance

During the first months of 2020, our lives have been shacked up by the pandemic diffusion of the Severe Acute Respiratory Syndrome CoronaVirus 2 (SARS-CoV-2) that, really at a global level, has had an exponential diffusion, by involving heavily quite all countries, with around 33 million of global cases, almost 1 million global deaths, about 204’700 victims in the U.S., 141’700 in Brazil, 94’600 in India, 76’400 in Mexico, around 42’100 in U.K. (COVID-19 Dashboard, at Johns Hopkins University, 28 September 2020). Both contagions and deaths are probably many more than those of official data. The World learned a new word: lockdown. A large part of the population had to change, suddenly, habits, daily activities, sport, and hobbies, besides new modalities for working and learning and, where the lockdown has been too light, tardive, short, or uncoordinated, the pandemic resumed or did not slow down its spread, so that diffusion and complications, especially in the older segment of the population, have had a serious impact on society. The pandemic COVID-19 heavily destabilized all aspects of normal life, with a violent and sudden re-organization of every-day activities in “remote mode”, from the smart working to the educational (i.e., scholastic and university) web-learning.

In this investigation, only a small part of the global issue can be addressed, a huge problem that concerns our future normality, the sustainability of our lives, the need to renew economies, incomes, lost jobs, and salaries. Even before the COVID-19, the World had big and unacceptable differences of possibilities among countries and persons of the same nations, cities, and districts. Now, everything has been exasperated, and the digital divide, for instance, is only a new and terrible face of the 2020 energy poverty.

The aim of this chapter is the proposition of a novel contribute toward the recovery of normal life, and then try to rethink what we do every day: teaching in the presence of students, learning in presence of teachers, by guaranteeing the reciprocal safety in the place in which family and society invest in the future. In particular, the study here proposed deals with the issue of ventilation in university classrooms of a real educational building and its impact on energy demands, costs, and emissions for the micro-climatic control. This investigation regards the redevelopment of an educational building that, in the second half of 2019, was involved by the re-design of indoor spaces, to create new classrooms and which, in the midst of the pandemic, is currently designed again, with a series of reflections. New systems and equipment were planned to allow safety, comfort, flexibility, airflows compatible with the need of containing the transmission of the virus, and, if possible, also with a view to energy savings, linked to lower polluting and climate-changing emissions and thus to a cleaner ambient.

The investigation concerns a building of the University of Molise (South Italy, city of Campobasso, Apennines backcountry), namely some large spaces of the Faculty of Agriculture, and, in particular, it begins with the calibration of a calculation model, deeply defined with regard to input data (i.e., direct inspections and surveys on building components, thermal images, etc.) derived from in-field surveys. Then, the outcomes of the transient energy simulation (BPS) were compared to the monitored energy consumptions, through the organization and comparisons of historical bills of the energy supply contracts (natural gas and electricity). Furthermore, by correcting some input when necessary, the model was calibrated. Once available a reliable numerical model of the whole building, to reduce the computational effort, a simplified model was developed and tested for what concerns its capability in predicting the real energy demands.

Then, the architectural modifications were applied, with the definition of seven new classrooms and, regarding the new spaces, alternative configurations of air conditioning systems were proposed. In particular, a mixed air-water system, with fan coil units and primary air, and several all-air systems (Constant Air Volume, dedicated outdoor air systems, or even with a partial recirculation) were tested, with and without installation of sensible heat recovery. In particular, the capabilities of the sensible heat recovery (cross plate heat exchanger of aluminum, and not rotary systems, to avoid possible contamination between exhausted air and external air) were tested, in terms of effectiveness in reducing the energy demands. After the energy, economic and environmental study, a deepening concerned one of the new classrooms of the building: in particular, one of the possible and suitable HVAC (Heating, Ventilating and Air Conditioning) configuration, deeply analyzed through BPS (building performance simulation, in the domain of the time), was modeled also for what concerns the air diffusion performance of several strategies of supply and extraction of the air in the room. Thus, several air diffusers configurations and air distribution strategies were designed and simulated in a suitable CFD environment (Computation Fluid Dynamics, in the domain of the space). Various configuration of inlet systems of ceiling (square, linear) and wall-mounted (grilles and nozzles) diffusers, as well as different types of extraction grilles, were firstly designed according to the ASHRAE ADPI method, and then analyzed as regards the implications on the indoor environment, in terms of thermal and flow fields, air velocity, mean age of air.

The chapter is organized as follows: after an introduction section, with recent referenced studies in the matter of measures and habits for limiting contagions, with a special focus on the role of the HVAC systems and thus heating, cooling, and ventilation; section 4.2 introduces the study methodology and the advanced modeling of building energy performance; in section 4.3, the architectural and technological refurbishment of one of the main building of the University of Molise is presented. The need of flexibility and management of increased outdoor air, that emerged during the last months, has implied the energy, economic and environmental tests of HVAC systems' alternatives, shown in section 4.4, evaluated with hourly energy studies, according to transient energy simulations, with a deepening on the air diffusion performances in one of the new classrooms, by means of a CFD investigation (section 4.5), firstly by establishing the social distancing. Some additional remarks and future topics to develop are proposed in section 4.6.

The main objective and novelty of this study, from the point of view of technicians involved in the architectural engineering and the energy efficiency of buildings, is to propose a comprehensive approach and methodology for sustainable and safe educational activities, by renovating spaces, air conditioning, and ventilation systems, also with consideration of the air distribution strategy in classrooms.

4.1.1. COVID-19 and role of Heating, Ventilating, and Air Conditioning in Buildings

COVID-19 is an abbreviation of Coronavirus Disease 2019, appeared in China at the end of 2019 and, in few weeks, diffused in the entire world, with millions of contagions, hundreds of thousands of deaths, many of these not calculated in statistics. COVID-19 can have many different evolutions in different persons, given the large variability of the reaction of the human body, and thus it can imply quite light infections not showing symptoms or, on the opposite extreme, very heavy complications, illness, respiratory acute affections, cardiac pathologies and, often, mortality. All possible effects (and affected organs, e.g., lungs, kidneys, heart, brain) are probably still unknown. Surely, the mortality rate among unvaccinated people is high, and the risk of severe complications for a huge part of infected people is common as well. In general, from available data, it results that the weakest part of the population is constituted by the older persons, with an age higher than 60 years, even if often also young and very young persons can be seriously affected with dramatic implications. The SARS-CoV-2 is highly contagious, with a high rate of reproducing itself. The mathematical indicator more common for evaluating a pandemic risk is the parameter R0, the so-called “basic reproduction number”. This index counts how many persons, starting from one infected case, become infected: an R0 higher than 1 means that the infection is outbreaking, and this can lead to a pandemic. An analogous meaning is expressed by Rt, even if this is dynamic and thus, differently from R0, is referred to the second phase of the pandemic, after the adoption of anti-contagion policies and measures. SARS-CoV-2 is transmitted from the infected person to another person through infectious agents, disseminated by the airborne transmission via the large droplets emitted with coughing, sneezing, the act of speaking, and given the close contacts among persons. During the first months of Covid-19 pandemic, a large debate among scientists started for what concerns the airborne transmission due to the exhaled air and thus related to tiny droplets. Indeed, small particles and droplets, in the respirable size, remain in the air or can be transported by the air movements or by other solid suspended contaminants and, in this way, can reach other persons: presently, the airborne transmission route is under investigation and requires a better understanding. The contagion requires direct contact from pathogens, coming from an infected person to another person. These pathogens are the microorganisms, transmitted with airborne droplets, aerosols, or present on a surface that, after contact with mouth and nose, enter into the respiratory tract of the person that could become infected. Eyes can be also a route for the virus. Thus, some key factors must be taken into account for limiting contagions, and these involve many behaviors and practices.

In this chapter, only the HVAC-related operations for reducing the transmission are investigated. On the other hand, non-HVAC-related good practices and measures (e.g., the necessary social distancing, frequent sanitizing of rooms and surfaces, cleaned hands, use of surgical, FFP2, or KN95 facial filters, frequent opening of windows for removing pathogens in naturally ventilated buildings) here are not discussed. These habits, behaviors and practices - first of all the avoiding of too-close contacts, i.e., less than 1-2 m, for achieving the so-called social distancing - must be suitable and correct.

In the view of restarting in-presence activities, among which the educational ones, one common question among the technicians involved in the topic of building engineering but also very common among persons and workers, was the following one: Which can be the impact of HVAC systems as regards the spreading of the virus, with the risk of contagious and contamination by the SARS-CoV-2? Worldwide, many associations of technicians involved in the building energy study and design of building systems and equipment, for instance, ASHRAE (the Position Document on Infectious Aerosols [1]) in the USA, REHVA (COVID-19 guidance document [2]) in Europe, AiCARR [3], [4] in Italy answered to the first questions. Several useful documents and guidelines were published from the Indoor Environmental Quality – Global Alliance (IEQ-GA), that join many world associations involved in study and research concerning the indoor environmental comfort. At the IEQ website, several documents are suggested for understanding the role of ventilation and HVAC systems about the containment of COVID-19 transmission (https://ieq-ga.net/covid-19/information-center/).

Epidemiology Science has underlined that closed environments (i.e., the indoor spaces) are much more dangerous, in terms of risks of contagions, compared to open spaces, first of all given the lack of spacing among people. Really, ventilation, and thus a suitable renovation of air inside buildings, is an efficient strategy to fight the indoor contamination. Indeed, ventilation is a way of diluting the concentration of pathogens. There are no doubts that the building ventilation is necessary and, mainly in overcrowded indoor environments (i.e., high occupancy, such as common in working or studying places), air change rates must be intense, even if, of course, this implies a higher ventilation thermal load and thus higher air-conditioning-related energy and economic (and even “environmental”) costs.

Common events (breathing and sneezing, toilet flushing, or, for instance, during the use of medical equipment, like in a dental clinic) spread pathogens into the indoor air, in form of large droplets and aerosols, characterized by a different behavior [1]. Large respiratory droplets are responsible for the short-range transmission, while the smaller aerosols, due to the evaporation of droplets, can infect secondary persons without direct contact with the primary one, also traveling for long distances:

- "respiratory droplets" are those with a diameter > 5-10 μm, and these tend to fall on pavement or surfaces because of gravity so that the infection can be limited by maintaining a threshold distance among people. This is why social distancing is necessary for limiting the contagions due to close contacts (probably, the main cause of contagions).
- "droplet nuclei", with a < 5 μm diameter, and thus the dried residua of droplets, and aerosols can settle and travel in the air for a long time and distance; these are responsible for the airborne transmission, can remain suspended in the air and also can travel for several meters, with the related risk of transmission. This is why indoor ventilation is important.

The World Health Organization [5] has considerd the respiratory droplets and the direct contact as the primary via for the virus transmission. Moreover, the WHO considers the airborne transmission possible, mainly under circumstances related to activities generating aerosols (i.e., some medical procedures cited in [5]).

According to the American ASHRAE, "Ventilation and filtration provided by heating, ventilating, and air-conditioning systems can reduce the airborne concentration of SARS-CoV-2 and thus the risk of transmission through the air. Unconditioned spaces can cause thermal stress to people that may be directly life-threatening and that may also lower resistance to infection. In general, disabling of heating, ventilating, and air-conditioning systems is not a recommended measure to reduce the transmission of the virus" (literally, from the ASHRAE website (https://www.ashrae.org/technical-resources/resources). Thus, three facts can be evidenced:

- ventilation is suitable for diluting and for removing the indoor infection pathogens;
- filtration can reduce the indoor contamination, of course, it requires suitable positions, maintenance, and replacement of proper High-Efficiency Particulate Air (HEPA) filters.
- a suitable thermal and hygrometric environment can reduce the thermal stress, and thus it can allow the strengthening of the individual resistance to infections.

Finally, besides the aforementioned good practices, surely flexible and suitable air-conditioning and ventilation systems must be commissioned, designed and managed for reducing the risk of contaminations. Really, HVAC systems can be an important partner to contrast the infections and the ASHRAE position paper [1] underlines the need of perfect design and maintenance of these, by respecting for instance the requirements of relevant design standards and handbooks (ASHRAE Fundamentals [6], Application [7], Systems and Equipment 2020 [8]). This document specifies - besides the need of suitable air changes for dilutions – the importance of suitable airflow patterns, thermal and hygrometric fields in the indoor environment (temperature and humidity distribution) and filtration, also through the ultraviolet germicidal irradiation (UVGI). Minimum standards to fulfill are the ANSI/ASHRAE Standards 62.1 [9] (in the matter of Indoor Air Quality - IAQ), ANSI/ASHRAE Standards 62.2 [10] (IAQ in residential low-rise buildings), ANSI/ASHRAE/ASHE Standard 170 [11] (ventilation in Healthcare facilities).

The following two statements have been approved by the ASHRAE, specifically for what concerns the transmission of SARS-CoV-2, and thus:

- concerning the airborne transmission, a suitable operation of building and facility, that includes proper management and use of air-conditioning, can limit and reduce the airborne exposure, and thus it can contribute in controlling the virus transmission.

- about the airborne concentration, specifically, ventilation and filtration can have a positive effect in reducing the concentration of virus in the air and thus in reducing the risk of transmission through the air.

According to several papers, among which [1] and the recent study of Correia *et al*. [12], large droplets, with a diameter > 10 μm and emitted as a consequence of coughing and sneezing, fall to the floor and on surfaces in a distance of about 1-2 m from the infected person. This is why close contacts must be avoided, just for reducing such modality of respiratory infection, as discussed by Chen *et al*. [13]. Of course, large droplets, once emitted, evaporate too, by becoming an aerosol, and, to control the virus transmission, the management of the aerosol is different being capable of traveling for meters and tens of meters, as stated by Morawska and Cao [14]. The authors, during the first phase of studies in the matter of COVID-19, underlined that the predecessor of SARS-CoV-2 (i.e., the SARS-CoV-1) has had the main transmission route just in the air.

As cited, large droplets are affected by gravity, and thus the via of the infections related to these is the close contact, directly from person to person. On the other hand, ventilation and air conditioning operations may affect the diffusion and distribution of droplet nuclei and aerosol. As evidenced by Correia *et al*. [12], the infection route via aerosol connected to the use of centralized air-conditioning systems may be possible and requires attention, so proper HEPA filters, that can remove pathogens, must be adopted. In this regard, air handling units can have a positive effect because of air filtration, which improves the quality of air supplied into the indoor spaces. Differently, channels and air ducts, without HEPA filters, may spread the virus. In the same study [12], the example of the Diamond Princess Cruise Ship was inferred. Finally, the wrong management of ventilation systems can be dangerous.

In the study of Yao *et al*. [15], it has shown, on large statistics, a negative association between confirmed COVID-19 and ambient levels of ozone and a positive association between the confirmed COVID-19 and the average ambient relative humidity. The same investigation, also based on previous studies, evaluated that large droplets in closed environments evaporate fast into fine aerosols. Finally, fine aerosols require deep attention, to manage viral particles. Here again it is underlined the important role that HVAC systems can play.

According to [1]): “Directional airflow can create clean-to-dirty flow patterns and move infectious aerosols to be captured or exhausted”. This is what will be proposed in the second part of this investigation, by accurately designing air distribution systems (method ASHRAE ADPI – Air Diffusion Performance Index), by evaluating thermal and flow fields inside the classrooms, together with other parameters related to thermal comfort and air diffusion performance (e.g., local age of air).

In a matter of the role of ventilation systems and airflow purification and directions for controlling the transmission of diseases and viruses, some authoritative studies are here briefly cited. First studies in a matter of management of ventilation in buildings to face contagions and spread of COVID-19 are, obviously, related to health care facilities, hospitals, and special buildings.

Firstly, the variation of indoor pressure can be a lever for protecting an indoor space from surrounding spaces:

- a positive pressure, for instance, can be designed where immunodeficient persons are hosted;
- a negative pressure, conversely, is suitable for spaces hosting infective patients.

Finally, negative and positive pressures are important strategies that can be adopted in designing particular building wards. About it, authoritative indications, worldwide, were already inferred in previous studies, among which [16], [17].

In 2018, a wide review proposed by Quian and Zheng [18] testified the importance of ventilation, both natural and mechanical, to dilute contaminants. The study refers to the most known respiratory affections from 2003 to 2013 (e.g., SARS, H1N1, MERS). As testified by the many cited studies, even if natural ventilation, enhanced by enlarging the size of the windows, can improve the indoor air quality, the ventilation system of a hospital, general wards or even negative pressure wards, has to both dilute contaminants and, at the same time, allow the supply of pathogen-free air into the indoor environments. At the same time, the airflow direction must be controlled, from the clean zones to the dirty areas and this is fundamental to reduce the transmission of contaminated aerosols between rooms. This study is referred to hospitals but, the same notes can be transferred also to other spaces, especially those with a high occupancy rate.

Linch and Goring [19] outlined, for the long-term care facilities, some points for improving the safety of the environments against possible transmission of the Sars-CoV-2, and these involve the modification of patients’ rooms to negative pressure, for limiting the contamination of other spaces. These key points concern the suitable evaluation of space volumes, ventilation requirements and differential pressure, the installation of additional exhaust fans, the increment of the overall air filtration efficiency, the correct management of doors (i.e., closed doors between corridors and wards, open doors between wards and bathroom, if here the exhaust air is extracted), the respecting of all guidelines for the prevention of infections as proposed by the dedicated Centres for Disease Control and Prevention (CDC).

Still on the matter of hospital settings, Zhao *et al*. [20] cited an important study of the WHO [21], in which a ventilation flow rate of 288 m^3/h per person is recommended to control the airborne transmission. Really, [21], in the matter of natural ventilation in hospitals, proposes an average ventilation rate of 160 l/s/patient for airborne precaution rooms, with a minimum value of 80 l/s/person, while lower values are needed for general wards (i.e., 60 l/s/patient); regarding corridors and spaces without a fixed number of the persons, a ventilation rate of 2.5 l/s/m^3 is cited. According to [20], natural ventilation is dependent by weather and architectural features and, existing ventilation systems often are not capable in providing such ventilation rates: therefore, they underlined that the use of indoor purifiers provided with HEPA filters is recommended, because such systems generally are enough efficient for removing such virus-laden aerosols, given their size range (the peak concentration of Sars-CoV-2 aerosols is in two size range, sub-micron between 0.25 μm and 1.0 μm, and super-micron > 2.5 μm). The efficiency of filtration of HEPA is higher than 95% and around 100% concerning the aforementioned particles' ranges. Such air purifiers can be used also in dwellings, in which quarantined persons are hosted. Specifically, as regards to the COVID-19 hospitals created in Wuhan just during the peak of the pandemic (January 2020) and thus the Huoshenshan and Leishenshan hospitals, Luo *et al*. [22] presented the lesson learned from these design and construction, ultra-rapid to be ready in less than 12 days for facing the sanitary emergency in Hubei. By means of a BIM approach, and thus an integrated, architectural, engineering and service design, the Leishenshan Hospital was designed for having wards in negative pressure compared to the surroundings, to isolate the pathogens. Mechanical ventilation was largely used to dilute the contamination, and the air circulation was carefully designed for fulfilling relevant standards. In the same vein proposed in other works (in the next sections), also regarding the Leishenshan Hospital, various solutions of air supply and extraction were simulated, during the design phase, to select the air distribution and return strategy most suitable for preventing the contagions. This design is very interesting also for the high care to the issue of discharging the filtered exhaust air into the surrounding environment, aimed at avoiding secondary pollution.

Concerning dental clinics, using accurate CFD simulations, Chen *et al*. [23] studied the capability of the air cleaner in controlling the dispersions of droplets and aerosol particles, emitted by patients and exposing the dental healthcare workers at high risks. All boundary conditions were properly modeled, by taking into account the kind of ventilation systems, and thus even the airflow, temperature, and supply velocity, to evaluate the efficiency of air cleaners. The simulation results revealed that the use of air cleaners can be effective for reducing the exposure of workers to both airborne droplets and aerosol particles. In addition, the directions of airflow and the relative location between positions of the air cleaner and sources of droplets/aerosol are important. Dental settings are extremely serious environments, with a high risk of cross infections between dentists, operators, and patients, because of aerosols and droplets, and this is evidenced in the wide review of Shah [24], in which available studies are discussed, about new protocols and guidelines for the management of patients, the dental activities, new organization models and practices for facing the risks of transmission during the COVID-19 pandemic. On the other hand, poor indoor ventilation can be a factor of contagions. In this regard, for several countries of the Middle East, a deep review of Amoatey *et al*. [25] revealed that the indoor ventilation in buildings is often not sufficient, and the indoor pollution can have various health effects, and thus respiratory affections and sick syndrome buildings. More in-depth, ventilation levels not fulfilling the ASHRAE standards are verified in most buildings and, as cited in [26] (some of the same authors), this can have effects also on the transmission of COVID-19, so that specific studies are required. Really, where ambient temperatures and relative humidity are extreme, often ventilation in the building is limited, for reducing the consumption of the HVAC systems, usually working with very low setpoint temperatures. These two conditions, and thus a poor air change rate (around 5 liters per second per person, instead of 8, as suggested by ASHARE) and the low indoor air temperature can favor the transmission of respiratory diseases, as the COVID-19. This can happen in airports, shopping malls, mosques, offices, and residential buildings and, to acquire scientific data and knowledge, the authors underline the necessity of study concerning the building ventilation rate for avoiding virus transmission via respiratory droplets and maybe aerosols. A deep study in the matter of university classrooms is not available in the literature and, in this vein, the study here proposed is going to give a contribution to the field.

Again, concerning the filtration importance, it is very interesting the notation of Shiu *et al*. [27], that underline, in the case of measles, the necessity of protecting from nosocomial infections, and thus the necessity of adoption of HEPA filters also in the outlet exhaustion ducts. This is a very interesting notation also in the matter of studies concerning air-conditioning operation for reducing the COVID-19 transmission. About the airflow purifications, the role of ultraviolet germicidal disinfection, and its contribution was deeply investigated by Memarzadeh *et al*. [28] and testing procedures are provided in [29].

Really, as cited, even if a large part of the population is currently vaccinated, to limit and nullify the risk of contagious, the HVAC-related strategies must be, obviously, complementary to non-HVAC containment operations, and the most important are the social distancing, a frequent cleaning of surfaces, correct behaviors of persons, and thus the use of facial winters, the avoiding of contact of hands with mouth, nose, eyes and of each self-inoculation into mucous membranes. These aspects are deepened by Morawska *et al*. [30]. The need for precautions, suitable behaviors, practices, and systems for avoiding transmission is evidenced also by Faridi *et al*. [31]. The authors collected air samples in hospital wards hosting persons affected by COVID-19, at distances of 2 to 5 m from beds, and the samples resulted in negative. Therefore, the study evidenced that close contacts are those very dangerous, and thus the healthcare workers must be surely equipped with stringent levels of personal protection systems. Kumar and Morawska [32] evidence also the necessity, for indoor environments characterized by a high density of occupancy, to minimize the virus-laden as possible, and thus ventilation is an important strategy. The risk of infection rises if the indoor air is stagnant and this happens when the ventilation is not efficient. The study specifically cites the case of hospitals, malls, shops, schools, public transport, and others. On the other hand, mechanical ventilation must be effective, because in some cases this can also induce a worsening of stagnancy in some zones. Once again, the importance of HVAC systems for effective indoor-outdoor air exchange is underlined, together with other individual good practices.

The risks related to a crowded indoor environment, for instance, classrooms and educational buildings, are evidenced by Franco and Leccese [33] and, in the view of an increase with the in-presence activities, a punctual evaluation of the occupancy is important. The authors proposed a study in which, at the University of Pisa, the CO_2 concentration was measured to evaluate the real number of occupants, and thus to manage the ventilation strategy in terms of DCV (demand control ventilation); this can be useful for controlling both thermal comfort and energy costs. Besides direct measurements of contaminants, also the numerical modeling of indoor environments, through advanced studies, such as the Computational Fluid Dynamic (CFD) analyses, can be useful in sensible buildings. A wide discussion about the potentialities of CFD for understanding the mechanisms of transmission of pathogens (virus and bacteria) and the role of ventilation, with reference to different buildings (among which hospitals and teaching applications), is proposed in the recent study of Peng *et al*. [34], with a wide review of many papers involving different applications of CFD analyses.

This investigation, by taking into account all these studies and the available literature, proposes a novel overview in the matter of increased outside flowrate and total supply mass flowrate supplied into classrooms, by evaluating the impacts on energy demands, costs, emissions and analyzing the indoor spatial distribution of microclimatic parameters, with an original contribution coupling different numerical methodologies.

4.2. Materials and Method

4.2.1. A coupled approach: Building Energy Simulations and Computational Fluid Dynamics Simulations

This investigation proposes a coupled approach of two complementary numerical investigations on building energy performances, and thus a time-dependent study (BES – Building Performance Simulation, based on transient energy balances, performed by assuming sub-hourly time steps) and a space-dependent investigation (CFD – Computational Fluid Dynamic, based on the solution of conservation equations and adoption of turbulence model concerning a 3D discretization of the spatial domain).

The coupling a CFD simulation with a BES provides more detailed information on the building indoor air conditions and improves the accuracy of the energy results [35]. A BES allows the evaluation of the building energy demand, on an hourly or sub-hourly basis for a reference period or even the whole year. Therefore, an analysis of the cooling, heating, and ventilation systems and the indoor environmental conditions is performed, with the assumption that the air is in conditions of 'perfect mixing', i.e., one computational node is representative of the whole zone. Conversely, by taking into account the real volume of the zone, a CFD simulation makes a prevision of the indoor temperature distribution, of the air velocity, humidity, and contaminant concentration, and it allows the evaluation of the local thermal comfort, usually with reference to a specific instant. A large deepening of the methodology adopted is reported in CHAPTER 2, section 2.1.

The importance of air purification and indoor ventilation is one of the main topics in this serious emergency period. Filtration, ventilation and air conditioning systems could contribute to mitigate the diffusion of particles and droplets, and therefore the infection transmission, especially in crowded buildings. Ventilation systems, properly designed, which provide outdoor air, highly filtered, could reduce the exposure to contaminated air. The use of CFD to verify the indoor conditions of environments at risk of contagion was widely demonstrated, especially in hospital rooms [36], [37].

Thus, the use of a coupled CFD and BES analysis can be the right approach to investigate the indoor building environment together with the building energy demand. In the proposed investigation, the coupled approach was applied to a case study: this is a University Faculty located in Campobasso (Italy), which hosts the Department of Agriculture, Environment and Food. The investigation starts with the calibration of the building energy model, based on real and measured data, continues with the comparison of different HVAC configurations from the point of view of energy demands, costs, and emissions, and ends with a CFD analysis of a typical classroom, with the aim of limiting the energy request and improving the indoor microclimatic quality (i.e., PMV/PPD, air temperature, flow fields and mean age of air). Methodology and development of the study are shown in Figure 4.2, then accurately described in the following sections.

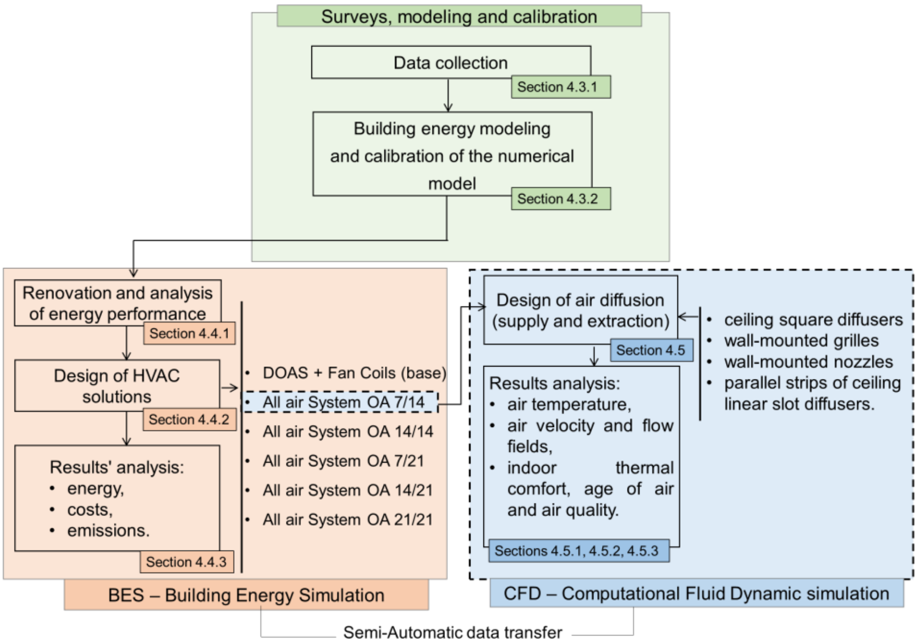

Figure 4.2 - Outline of adopted methodology, HVAC configurations and air diffusion strategies are described in section 4.4 and 4.5, respectively

4.2.2. The building energy simulation

As previously described in CHAPTER 2, after a survey and data collection step, to perform a reliable dynamic energy simulation, the numerical model of the building must be calibrated and validate. Once it is calibrated, the energy efficiency measures proposed can be evaluate. So, in this study, various solutions for the HVAC system were proposed, as detailed in section 4.4.2, for some new classrooms subject to upcoming renovation. The possible configurations were compared in terms of primary energy demands per unit of area for the space heating, cooling and for the annual space conditioning (respectively: EP_H, EP_C and EP_{SC}, kWh_p/m^2), achievable primary energy saving (ΔEP), economic costs for the space conditioning and its variation, avoided carbon dioxide equivalent emissions ($\Delta CO_{2\text{-}eq}$).

In order to compare the energy performance, common primary energy factors (PEF_e) were used, and thus 1.95 for the electricity (i.e., the considered non-renewable average efficiency of thermo-electric Italian system is 0.51) and, concerning the natural gas, a PEF_g equal to 1.05 is chosen, as suggested nationally [38].

Furthermore, in this study:

- emission factor for natural gas is 0.24 tons CO_{2-eq}/MWh [39] (LCA approach emission factor);
- emission factor for electric energy is 0.424 tons CO_{2-eq}/MWh [39] (LCA approach emission factor);
- electricity cost (including non-recoverable taxes) is 0.16 €/kWh (from real energy bills and contracts);
- natural gas cost (including non-recoverable taxes) is 0.062 €/kWh (from real energy and contracts).

The prices of natural gas and electricity are those paid, averagely, by the University of Molise in 2019. Regarding the energy models, as aforementioned, these are geometrically built in DesignBuilder [41], the same software used also for defining the thermo-physics of the building envelope, HVAC system and lighting equipment. Other specifications and schedules of facility's plants and HVAC systems have been implemented and/or modified in EnergyPlus [40], the well-known program for the whole building energy simulations, operating under transient conditions of heat transfer, whose capabilities have been discussed in a very wide scientific literature. Before the modeling of the building as renovated, also a simplification of the original model was provided, in order to reduce the computational effort. Obviously, against the billings and the previous calibrated model, also the new simplified model was tested and validated.

Other particular simulation parameters are described in the section 4.3

4.2.3. The Computational Fluid Dynamic simulation

For understanding the thermal and flow fields and the air quality in the breathing zones of the indoor environment, some common configurations for the supply and the extraction of air were designed for a selected typical classroom. In particular, four air distribution configurations referred to the “All Air systems OA 7/14” (section 4.5), and thus one of the proposed HVAC solutions, were compared through CFD simulations. These will be described in the following lines.

The CFD is an investigation methodology widely used in many studies to evaluate the indoor thermal conditions of different types of environments and buildings, such as lecture rooms [42], museums [43], residential spaces [44] hospitals, offices and schools. As for the case here treated, Buratti *et al*. [45] evaluated the indoor thermal comfort in a university classroom, through CFD simulations. Méndez *et al.* [46] optimized the organization of a hospital room by considering, at the same time, the better ventilation at the patient site and the cost of execution. The authors analyzed the age and the velocity of air inside the room and verified some modifications in the location and geometry of the air inlet and outlets, and the dimension of the partitions.

This investigation, conversely, compares some types of supply and extraction systems of the air through CFD simulations in order to bring out differences in terms of thermal comfort and air purity and quality. Following the provisions of Italian Government [47] and therefore to simulate the real situation that will occur at the resumption of the “in presence” educational activities (in the next weeks, in Italy), the number of occupants for the classroom under consideration was halved, to ensure the minimum spacing of 1 meter between the students. In non-emergency conditions, and therefore for the calibrated model, the number of occupants considered corresponds to the number of seats in the classroom and to the provisions of the Italian Ministerial Decree 18-12-1975.

All diffusers’ configurations were designed by taking into account the ADPI (Air Diffusion Performance Index) method [6], [48]. This index, developed for evaluating the air diffusion performance in the cooling-mode operation, establishes a relation among the type of diffusers, isothermal throw distances, layout of air terminals, characteristic length of the room, and it is referred to a typical range of cooling loads. Higher is the ADPI, the higher is the achievable performance by the air distribution systems in terms of thermal comfort and reduction of the discomfort due to air draft inside the room. According to ASHRAE Fundamentals 2017 [6], [48], most air distribution systems is designed for achieving an ADPI higher than 80%.

For what concerns the CFD simulations, the boundary conditions were directly acquired from the previous BES model, while, convergence criteria, turbulence model, mesh, resolution methods, were defined and implemented in the CFD numerical model. The numerical method to solve the set of partial differential equations (PDEs) describing the transport of momentum, energy and turbulence quantities is the finite volume method (FVM), while the grid which discretized the room space is a computational mesh of non-overlapping adjoining rectilinear cells (finite volume grid), 30 cm spacing. An up-wind discretization scheme was adopted for the convection term and a standard k-ε turbulence model was selected ("k" is the turbulent kinetic energy and ε is its dissipation rate). The convergence criteria were set with a termination residual of 10^{-5}. All the boundary conditions, and thus the interface data, were automatically assumed by the hourly dynamic simulation of the building. The used code is DesignBuilder [41].

4.2.4. Thermal comfort and indoor air quality

In order to compare the different air distribution configurations, the thermal comfort and the indoor air quality were deepened. The analysis of the thermal comfort for the indoor environment was performed through the Fanger approach [49], and thus through the PMV and PPD indices, respectively the Predicted Mean Vote and the Predicted Percentage of Dissatisfied. In addition, some other parameters were investigated to evaluate the indoor thermal comfort, namely the vertical temperature stratification and the air velocity. An excessive vertical temperature stratification, indeed, in addition to implying a greater energy consumption in the period of heating, could produce a feeling of discomfort (heat in the head, cold in the feet). The UNI EN ISO 7730 standard [49] establishes that this temperature difference, at 0.1 m and 1.1 m (sitting people), must not be above 3 °C. This means accepting one maximum percentage of dissatisfied equal to 5%. To evaluate the temperature uniformity in the indoor environment, the temperature difference ($T_{max} - T_{min}$) was calculated for the central area of the occupied volume, both in the horizontal and vertical sections. The aim was to evaluate both the presence of local thermal discrepancies and the presence of high temperature differences between the lower part and the breathing area of the environment (see section 4.5.1).

For what concerns the air velocity, as conventionally assumed in the summer regime, an air movement within 1 m/s was not considered uncomfortable, while, in the winter regime, even an airspeed above 0.20 m/s was considered as a cause of local discomfort (see section 4.5.2).

This investigation does not aim to evaluate merely the indoor thermal comfort depending on the adopted air terminal solutions, but would also evaluate the parameters which affect the local air quality and rate of renewal, such as the movement of the indoor air, flow fields, and mean age of the air which depends on the number of diffusers, their position, the airspeed and the position of the extraction grilles (insights in the sections 4.5.2 and 4.5.3). Obviously, the occupant number affects the air quality, indeed, the human respiration and transpiration release components such as water vapor, bio-effluents and carbon dioxide (CO_2) which, in large quantities, makes the air unhealthy. Suitable air changes to ensure the healthiness of the indoor environments was defined starting from the Italian Standard UNI 10339 [50] and then were adopted in the energy model of the building. By considering the COVID-19 emergency, as a precaution, different HVAC configurations were then proposed in the study, in which the outside flow rate was doubled or tripled (section 4.4.2). Moreover, as aforementioned, in the CFD simulation, the number of people was halved in compliance with very recent national guidelines [47], to reduce the number of persons, by lowering the spread of pathogens in the air and mainly for allowing the necessary social distancing.

4.3. The case study: The University building of Campobasso

Campobasso, where the case study University building is located, is a city of Italian backcountry, in the south, near the Apennine Mountains and characterized by a quite cold climate, classified Cfb according to the Köppen-Geiger method. The average annual temperature is of about 12.3 °C; all main information about the statistical weather conditions are provided in Figure 4.3.

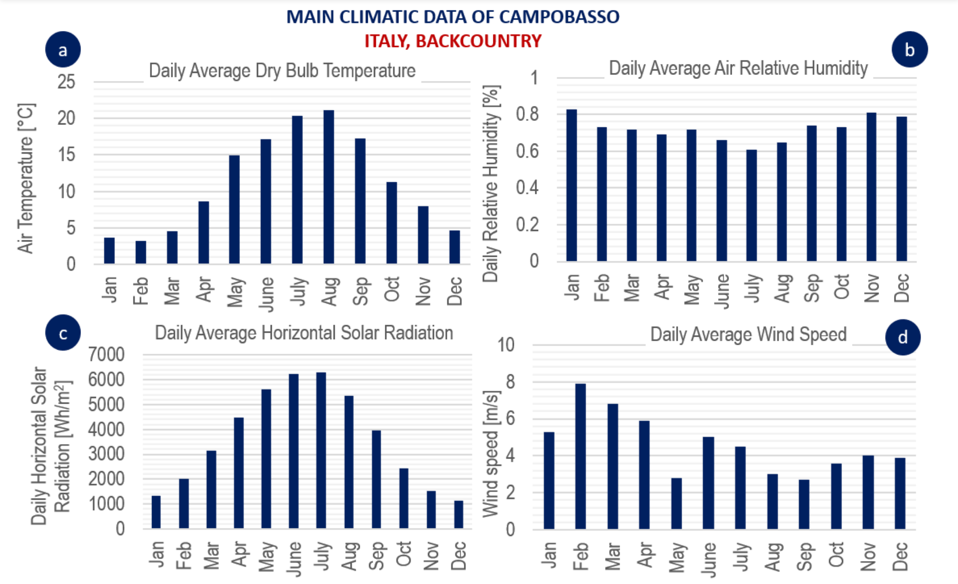

Figure 4.3 - Climate of Campobasso, south Italy: a) monthly profiles of air temperature, b) relative humidity, c) average daily global solar radiation and d) wind speed

4.3.1. Energy Audit

The building was built in the early ‘90s; it is characterized by two blocks (namely, I and II in Figure 4.4), with a rectangular shape and six floors joined by means of an atrium covered with a cupola. The whole surface to volume ratio (S/V) is 0.37 m^{-1}.

Figure 4.4 - Case study: Map of Campobasso and building position

The most important information about the climatic conditions, the thickness (s) and the thermo-physics of the building envelope are summarized in Table 4.1. Herein, the value of thermal transmittance (U) was calculated according to [51] and [52] and the periodic thermal transmittance (Y_{IE}) according to [54] starting from the available datasheets. During the 2018, accurate thermal images were also acquired in order to check eventual lack of uniformities in thermal characteristics and presence of significant thermal bridges or air infiltrations (Figure 4.5).

Regarding the building envelope, it is composed by different types of opaque and transparent components. The main wall types have aerated concrete blocks, with mineral fiber insulation and external aluminum panels (Figure 4.5a) or hollow bricks with air gap and external “porfido” stones (Figure 4.5b). The structural slabs of ceilings are made with pre-stressed reinforced concrete, with different types of finishing and insulation level. Through a comparison of the values reported in Table 4.1 and the ones established by Italian legislation for new and refurbished buildings, it results that, currently, the case study building has not optimal U_{values}. Indeed, current reference values of thermal transmittances are 0.28 W/m^{2}K and 0.24 W/m^{2}K for vertical walls and roof slab, respectively. This causes quite high heat losses and then a negative impact on heating needs and on the comfort conditions for occupants. For Y_{IE}, and thus the periodic thermal transmittance, to limit the diurnal indoor overheating, the current normative reference values are 0.10 W/m^{2}K and 0.18 W/m^{2}K, for vertical and horizontal building components, respectively. The current building envelope values are suitable.

Moreover, because of the high occupancy rate and large windows, during the summer, the building cannot prevent indoor overheating.

Several types of windows were identified. The first one is a laminated glass-wall, used in the south-west façade, at the entrance (ground floor) and for the hallway of the first floor (Figure 4.5c). The second type of transparent envelope consists of glass blocks. Finally, all other windows are clear, double-glazed (6mm glass/12mm air/6mm glass), with aluminum frames and most of these has an inner shading system, with vertical white slats.

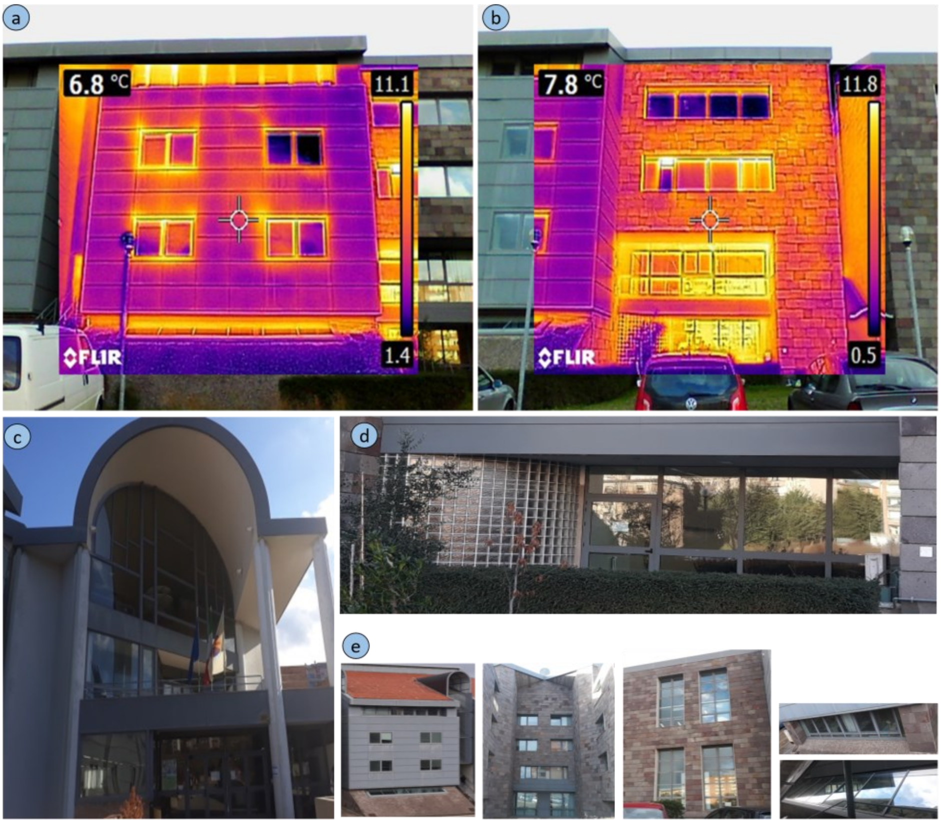

Figure 4.5 - Building envelope: a) Wall with aluminium panel; b) Wall with porfido stone; c) glass walls; d) Glass blocks; d) others window types

Table 4.1 - The main features of the site, building and facility

CAMPOBASSO SITE							
Elevation	701 m		Latitude	41°33'36''		Longitude	14°39'37''
Winter Design Day	Temperature		-4 °C			Relative humidity	48.8
Summer Design Day	Temperature		29 °C			Relative humidity	50.0
Heating degree-days (calculation baseline 20°C)	2346		Horizontal monthly average irradiance (maximum value)				307 W/m^2
BUILDING GEOMETRY AND ENVELOPE AND HEAT AND COOL GENERATORS							
Total building floor area (m^2)	11070			Total volume (m^3)			43062
Net conditioned floor area (m^2)	10498			Conditioned total volume (m^3)			34483
Building Geometry	Total			North	East	South	West
Gross wall area (m^2)	9289.5			2152.9	2576.4	2230.6	2329.6
Window opening area (m^2)	1244.9			217.2	381.8	273.7	372.2
Net window-wall ratio (%)	13.40			10.1	14.8	12.3	16.0
Opaque envelope	T (m)	U_{value} (W/m^{2}K)	Y_{IE} (W/m^{2}K)	Opaque envelope	T (m)	U_{value} (W/m^{2}K)	Y_{IE} (W/m^{2}K)
Wall with alum. panel	0.460	0.324	0.097	Cupola	0.200	0.407	0.250
Internal wall	0.300	0.964	0.498	Attic floor	0.580	0.454	0.020
Floor	0.610	0.412	0.010	External roof	0.480	0.524	0.046
U_{value} Glass walls and Glass Doors	3.26 and 3.67 W/m^{2}K			U_{value} of all other windows	2.97 and 3.28 W/m^{2}K		
Central Heating Generator	Hot water boilers 2 * 766 kW			Boiler Efficiency at rated conditions			0.76
Central Cooling Generator	Air cooled 735 kW + 438 kW			Chiller EER at rated conditions (Wh_t/Wh_e)			3.00

The occupancy rate of classrooms was established according to provisions of the aforementioned Italian Laws. As regards the air conditioning systems of the building, all offices, lecture rooms, bar, circulation zones and most classrooms are served by a mixed air/water system, given by a combination of fan-coil and air handling units (AHU). Classrooms and corridors of the ground floor of the II block have heavy cast-iron radiators, and a centralized AHU for balancing latent loads and providing ventilation. The bigger “Mendel” classroom, the library and the main central hall are air-conditioned by an all-air system, which provides both heating, cooling and ventilation necessities. Two traditional boilers with nominal power equal to 766 kW (each one) and two vertical storage boilers (1500 l) allow the hot water generation, also for sanitary use. Moreover, two electrical air-cooled chillers provide the cold water: a first chiller (nominal power of 735 kW, refrigerant R404A) is dedicated to the II block II (Figure 4.4) and the hall, a second one (484 kW, R134A) produces cold water for the block I. Eight air handing units are placed in the attic, with pre- and post-heating coils, humidifiers and cooling coil. For the library, the AHU is simpler, equipped merely with heating and cooling coils. The AHUs of the II block have also a static cross flow recovery system that operates during the winter period. The flow rates managed by the AHU were censed, and these range from 7000 m^3/h to 21’000 m^3/h. A dedicated air handling unit is used for the chemical laboratory, with an airflow of 2700 m^3/h.

The lighting systems consist of fluorescent lamps of 36 W, with an average installed power of 5 W/m^2 for offices, meeting rooms, library and corridors, and of about 7 W/m^2 in the laboratory and 11 W/m^2 in the classrooms.

Regarding the thermal zone’s characterization, the use of each room has been verified. In the block I, the ground floor and the 1st floor host the library, some laboratories a big classroom, some offices, the university entrance desk and reception. On the 2nd and 3rd floors, there are the department secretary, offices, chemistry, physics and informatics laboratories. In the block II, on the ground floor, there are classrooms and information point, while on the first floor there are student secretary, offices and laboratories; the 2nd and 3rd floors host classrooms and some administrative offices (as the Director's one). During the carried-out inspections, to verify the thermal zones distribution, questionnaires have been proposed to office occupants and students, in order to describe, as accurately as possible, the real conditions inside the building. More in detail, questions concerned: a) how many hours are spent in the building daily, b) how many hours are spent by working at a computer or other equipment, c) conditions of comfort or discomfort felt by occupants, about the indoor microclimate and d) main criticalities about the air quality. All information and data were used to provide accurate modeling of the thermal zones. Some punctual measurements were carried out for evaluating the illuminance level (I, lux) on working desk, by considering two different scenarios: 1) at the center of the teacher's desk at a height of around 90 cm and 2) in the center of student's desk placed in the middle of the third row. In a day of overcast sky and under the operation of the artificial lighting system (consisting of 32 lamps of 36 W for this classroom), the maximum (I_{max}), minimum (I_{min}) and average (I_{mean}) values recorded during a sampling time are 309 lux, 299 lux and 307 lux, respectively. According to the standard UNI EN 12464-1 [54], that recommend 300/500 lux for classrooms/offices, it was verified the suitability of these measured values.

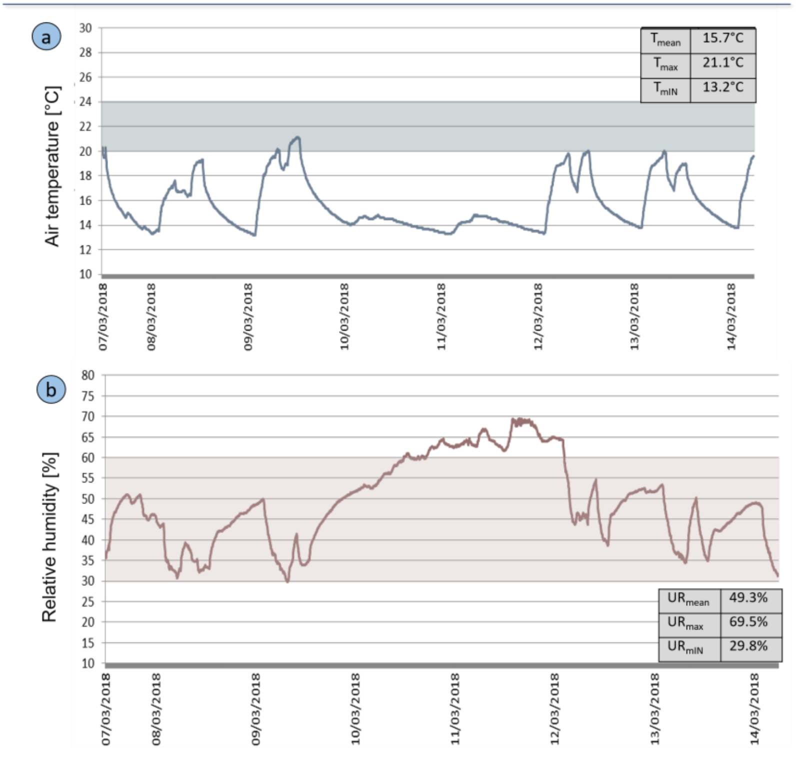

Figure 4.6 - a) monitoring of air temperature, b) monitoring of relative humidity

Finally, the last step of energy audit was an accurate analysis of the historical energy requests, by collecting data of electricity and natural gas demands of the last three years. In some rooms and with reference to winter typical days, the indoor conditions of temperature and relative humidity were measured (Figure 4.6), by revealing a satisfactory thermal comfort, analyzed by means of the traditional PMV and PPD indices [49].

4.3.2. BES - Energy modeling and calibration

All acquired information and boundary conditions concerning the building use were considered for building modeling (Figure 4.7). The following parameters and boundary conditions for simulations were assumed (please, note that only the main ones are here cited):

- Weather File: ITA_Campobasso.162520_IGDG, Lat. 41.33°, Long. 14.39°, Elev. 701 m.
- Heat Balance Algorithm: Conduction Transfer Functions (CTF), 2 timestep/hour.
- Surface Convection Algorithm Inside: TARP, variable natural convection based on temperature differences.
- Surface Convection Algorithm Inside: DOE-2, correlation from measurements for rough surfaces.
- Maximum HVAC iterations: 20.

In the simulation model, to describe as accurately as possible the real conditions inside the building, several typologies of thermal zones were created and these were detailed according to the specific uses, in terms of occupancy rate, installed power and use of the equipment, according to the characteristics identified during the surveys.

The operation schedules were created according to managers and occupant information. According to the Italian legislation, for that climatic zone, the heating period is between 15 October and 15 April, while the common operation of these buildings establishes the space cooling in the period 15 June – 30 August. The ventilation is always turned on. The operational period goes from 7:00 to 18:00 and there is the possibility to turn on the heating system when the external temperature is too low during the night, while during the weekends and holiday periods, all systems were considered turned off. In April and October, the operating schedule is from 7:00 to 12:00 and from 15:00 to 18:00.

Figure 4.7 - a) real building and rendered from DesignBuilder; b) Rendering of simulation model (north-east side)

Figure 4.8 shows the comparison between the energy requests of the real building and those calculated by simulation, with reference to electricity (Figure 4.8a) and natural gas (Figure 4.8b): also the indexes MBE and CV(RMSE) are provided. It can be observed that the numerical model represents suitably the real building, with a good agreement of energy demands.

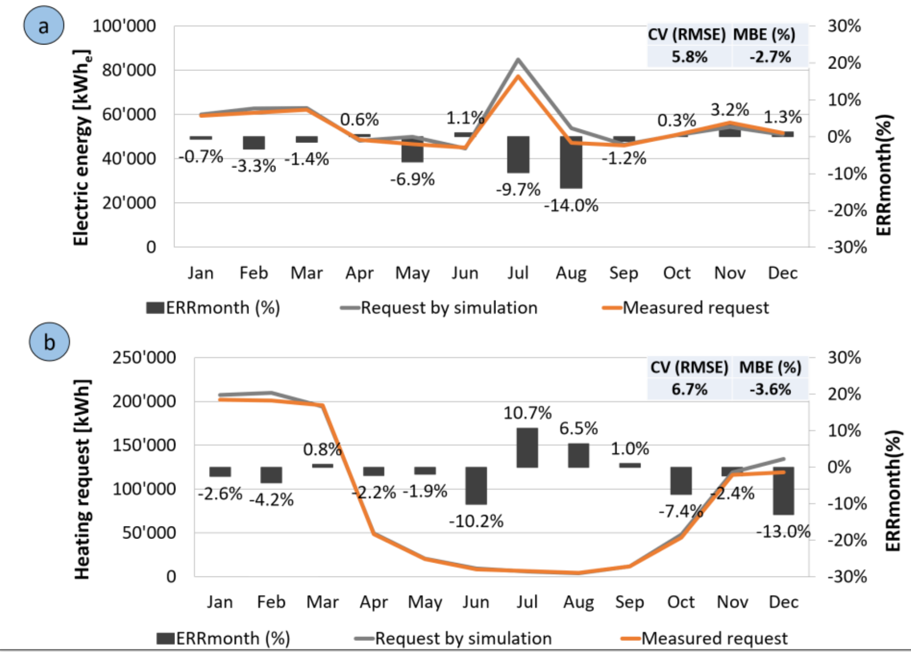

Figure 4.8 - Model calibration: a) total electricity; b) natural gas for heating

Finally, a powerful numerical model for performing further simulations, to test possible alternatives for improving building performance, microclimatic control and energy efficiency, is available. In the present configuration, according to the energy model, the requests of electricity and natural gas are 661 MWh and 928 MWh, respectively.

4.4. The building renovation, HVAC performance, and analysis of design alternatives

4.4.1. The architectural refurbishment, the new classrooms and energy performance simulations

The investigated building will be interested, by an architectural refurbishment, to provide a new distribution of the indoor spaces, and specifically for having 7 new classrooms and thus for strengthening the capability in offer 'face-to-face' didactics. With reference to the 1st floor, current and new plans are depicted in Figure 4.9.

Figure 4.9 - 1st floor of the block II: Current plan (A) and architectural renovation (B) designed for having 7 new classrooms (1 at the ground floor, 6 at the first floor)

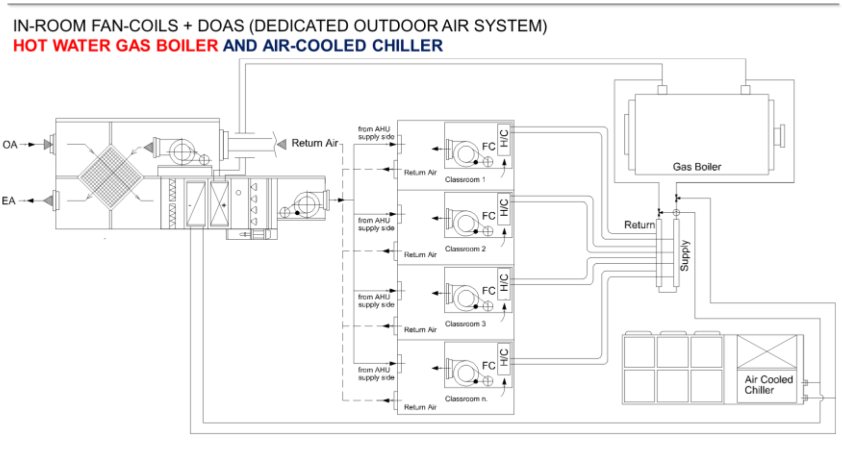

Figure 4.10 - The mixed air water systems, with in-room fan-coils (heating or cooling coil, according to the season) and centralized AHU, originally designed for the new classrooms

In the previous design, approved by University offices *before* the COVID-19 pandemics, a standard HVAC system was proposed for the new classrooms, and this consisted of a mixed air-water system (and thus a centralized dedicated outdoor air system, connected to gas boiler and chiller, and in-room fan coils), capable in providing heating, cooling and ventilation, as schematically depicted in Figure 4.10. The design and management of HVAC system is based on a simple rule: balancing thermal loads and ensuring adequate ventilation of outside air (OA), for improving the indoor air quality.

4.4.2. BES – Building Energy Simulations: energy analysis of alternative HVAC systems

To reduce the risks of contamination from a room to another one of the same building, served by the same HVAC systems, the recirculation in centralized air conditioning systems should be avoided. Indeed, recirculation air in a centralized air handling unit, without a correct operation of suitable filters, could provide transportation of pathogens from a contaminated ambient to another one. Moreover, used along with other best practices recommended by the aforementioned and cited Institutions and Centers for Disease Control and Prevention, increasing ventilation, and thus the amount of outdoor air, can be part of a plan to protect occupants by contagions of diseases. Indeed, for reducing every risk of potential airborne viral transmission - by reducing exposure to virus-laden aerosols – and also for reducing the chance for particles to settle and remain on surfaces (desks, chairs, furniture), the main HVAC-related strategy is the increasing of ventilation for removing and diluting the pathogens, as discussed in the previous sub-sections. Finally, with the aim to refurbish both classrooms and didactic activities, a strategic plan is under evaluation, together with technicians of the University of Molise.

For what concerns the HVAC systems, the plan is based on the conversion, for the new 7 classrooms (Figure 4.9) of the existing mixed air-water system into an all-air system, with some variants concerning total airflow rate, outside air, kind of handling in the AHU. Of course, the aims are:

- suitable ventilation of the indoor environment;
- high capability in the microclimatic control;
- achievement, when possible, of energy savings;
- reduction of emissions and limitation of the climatic impacts.

The comparison among possible configurations is performed under the points of view of energy, economic and emission savings. In the second phase of this study (i.e., the CFD simulation, section 4.5), also a reduction of the number of students, to fulfill the need of social distancing, is supposed.

The modification of HVAC operation concerns the classrooms of the block II. One of these is placed on the ground floor (originally, designed for 117 students), the other ones are located at the first floor, with a number of seats ranging from 40 to 120 (Figure 4.9). In the original design, these classrooms would be conditioned by an air-water system in which the outdoor ventilation is regulated according to the minimum OA rate required by the Italian Standard UNI 10339 [50] and thus, in each classroom, the ventilation rate is 0.007 m^3/s person. More in deep, the designed HVAC system (already described and depicted in Figure 4.10) couples fan coils, in a variable number depending on the size of the classroom, to an all-air system without recirculation, equipped with a flat plate sensible heat recovery. The centralized DOAS (Dedicated Outdoor Air System) is the same for all classrooms. The heating and cooling coils, in the Air Handling Unit, are fueled by the hot water and chilled water produced by a centralized gas boiler (efficiency η, at rated conditions, equal to 0.76) and by an air-cooled chiller (EER, at rated conditions, equal to 3 Wh_t/Wh_e), respectively. These are the heat and cool generators already installed in the building. The DOAS is equipped with sensible heat recovery (efficiency, at rated conditions, 0.7). This HVAC system will be shortly called FC + DOAS.

Really, the following considerations and aims motivated the thinking of some design alternatives:

a) avoiding centralized systems, at least for the new classrooms. Indeed, even if the recirculation of air is not provided (the designed one is a dedicated outdoor air system), anyway the air channels can be a route for airborne transportation, from a classroom to another one;
b) avoiding in-room terminals allows simplification of design (e.g., no need of collecting water condensed by fan-coils);
c) flexibility in the use of single HVAC systems. Given that this is a low-rise building, with sufficient technical spaces, dedicated rooftop HVAC systems, with DX (direct expansion) heating and cooling coils can be installed;
d) a dedicated rooftop for each classroom allows the perfect management of ventilation, microclimatic control, operation of recirculation, heat recovery, management of thermodynamic conditions of the supply air.

Finally, new different HVAC systems were designed and modeled, whose difference is the installation of a heat recovery system, merely "sensible" (efficiency 0.75) and consisting of a flat plate metal matrix, in order to avoid any possible contamination between outside air and recirculation air. At the rated conditions, the COP and ERR of the DX heating and cooling coils are 2.75 Wh_t/Wh_e and 3.00 Wh_t/Wh_e, respectively. It should be noted that, for the seven new classrooms, seven dedicated rooftop AHUs are designed. Thus, no multizone systems are considered. The new tested HVAC systems, without (A) and with (B) the heat recovery, are depicted in Figure 4.11. Before commenting the results, two notes: a) the impact of humidification was neglected (no humidification set-point was assigned), b) the ventilation during the intermediate season (no cooling, no heating) was neglected. These choices are motivated by the fact that the impact of ventilation loads on the space conditioning would be evidenced, and conditions that will alter the comparison are not modeled.

Each HVAC system has been designed with different characteristics, in terms of total (mixed) air flow rate (TA) and outside ventilation air (OA), according to Table 4.2. Total air (TA) is the sum of outside air (OA) and recirculating air (RA). The ACH is referred to the total mixed supply air (TA, and thus OA+RA).

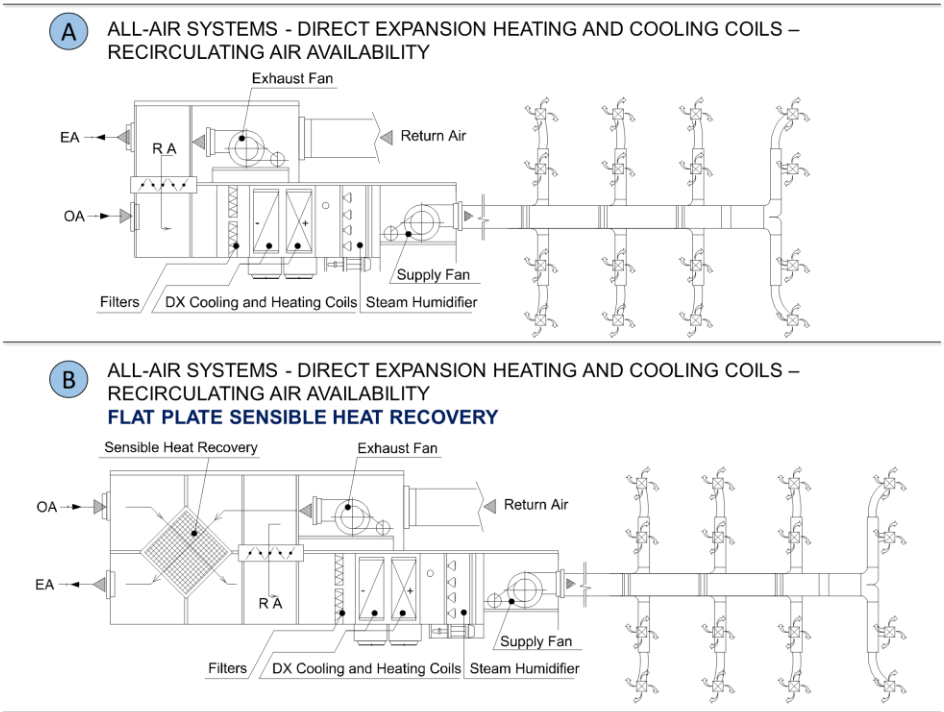

Figure 4.11 - The new designed all-air systems, without (A) and with (B) the sensible heat recovery

Thus, it means that, alternatively to the configuration 0 (the DOAS + FC, Figure 4.10), 5 further HVAC system typologies are modeled, based on the nominal occupancy of the classrooms:

1. All air System OA 7/14: an outside flow rate of 0.007 $m^3/(s\ pers)$ is imposed, with a total mixed supply flor rate of 0.014 $m^3/(s\ pers)$. Thus, OA is 50% of TA.
2. All air System OA 14/14: an outside flow rate of 0.014 $m^3/(s\ pers)$ is imposed, with a total mixed supply flor rate of 0.014 $m^3/(s\ pers)$. Thus, OA is 100% of TA.

3. All air System OA 7/21: an outside flow rate of 0.007 $m^3/(s\ pers)$ is imposed, with a total mixed supply flor rate of 0.021 $m^3/(s\ pers)$. Thus, OA is 33% of TA.
4. All air System OA 14/21: an outside flow rate of 0.014 $m^3/(s\ pers)$ is imposed, with a total mixed supply flor rate of 0.021 $m^3/(s\ pers)$. Thus, OA is 67% of TA.
5. All air System OA 21/21: an outside flow rate of 0.021 $m^3/(s\ pers)$ is imposed, with a total mixed supply flor rate of 0.021 $m^3/(s\ pers)$. Thus, OA is 100% of TA.

All five HVAC alternative systems are available in both configurations of Figure 4.11, and thus without and with (“Sens Rec”) Sensible Heat recovery.

Table 4.2 - Peculiarities of classrooms and designed alternatives for the HVAC systems here installed

	Main peculiarities of the Classrooms			**1) All Air System OA 7/14**				**2) All Air System OA 14/14**			
				OA = 0.007 $m^3/(s\ p)$, TA = 0.014 $m^3/(s\ p)$				OA = 0.014 $m^3/(s\ p)$, TA = 0.014 $m^3/(s\ p)$			
	Floor [n]	Seats [-]	Volume [m^3]	OA [m^3/s]	TA [m^3/s]	TA [m^3/h]	ACH [h^{-1}]	OA [m^3/s]	TA [m^3/s]	TA [m^3/h]	ACH [h^{-1}]
Room GF	ground floor	117	835.8	0.8	1.6	5896.8	7.1	1.6	1.6	5896.8	7.1
Room 1F-1	first floor	120	620.9	0.8	1.7	6048.0	7.3	1.7	1.7	6048.0	7.3
Room 1F-2	first floor	40	220.4	0.3	0.6	2016.0	7.5	0.6	0.6	2016.0	7.5
Room 1F-3	first floor	60	384.6	0.4	0.8	3024.0	6.5	0.8	0.8	3024.0	6.5
Room 1F-4	first floor	80	403.7	0.6	1.1	4032.0	7.9	1.1	1.1	4032.0	7.9
Room 1F-5	first floor	40	215.8	0.3	0.6	2016.0	7.7	0.6	0.6	2016.0	7.7
Room 1F-6	first floor	39	204.1	0.3	0.5	1965.6	7.9	0.5	0.5	1965.6	7.9

	3) All Air System OA 7/21				**4) All Air System OA 14/21**				**5) All Air System OA 21/21**			
	OA = 0.007 $m^3/(s\ p)$, TA = 0.021 $m^3/(s\ p)$				OA = 0.014 $m^3/(s\ p)$, TA = 0.021 $m^3/(s\ p)$				OA = 0.021 $m^3/(s\ p)$, TA = 0.021 $m^3/(s\ p)$			
	OA [m^3/s]	TA [m^3/s]	TA [m^3/h]	ACH [h^{-1}]	OA [m^3/s]	TA [m^3/s]	TA [m^3/h]	ACH [h^{-1}]	OA [m^3/s]	TA [m^3/s]	TA [m^3/h]	ACH [h^{-1}]
Room GF	0.8	2.5	8845.2	10.6	1.6	2.5	8845.2	10.6	2.5	2.5	8845.2	10.6
Room 1F-1	0.8	2.5	9072.0	10.9	1.7	2.5	9072.0	10.9	2.5	2.5	9072.0	10.9
Room 1F-2	0.3	0.8	3024.0	11.3	0.6	0.8	3024.0	11.3	0.8	0.8	3024.0	11.3
Room 1F-3	0.4	1.3	4536.0	9.7	0.8	1.3	4536.0	9.7	1.3	1.3	4536.0	9.7
Room 1F-4	0.6	1.7	6048.0	11.9	1.1	1.7	6048.0	11.9	1.7	1.7	6048.0	11.9
Room 1F-5	0.3	0.8	3024.0	11.5	0.6	0.8	3024.0	11.5	0.8	0.8	3024.0	11.5
Room 1F-6	0.3	0.8	2948.4	11.9	0.5	0.8	2948.4	11.9	0.8	0.8	2948.4	11.9

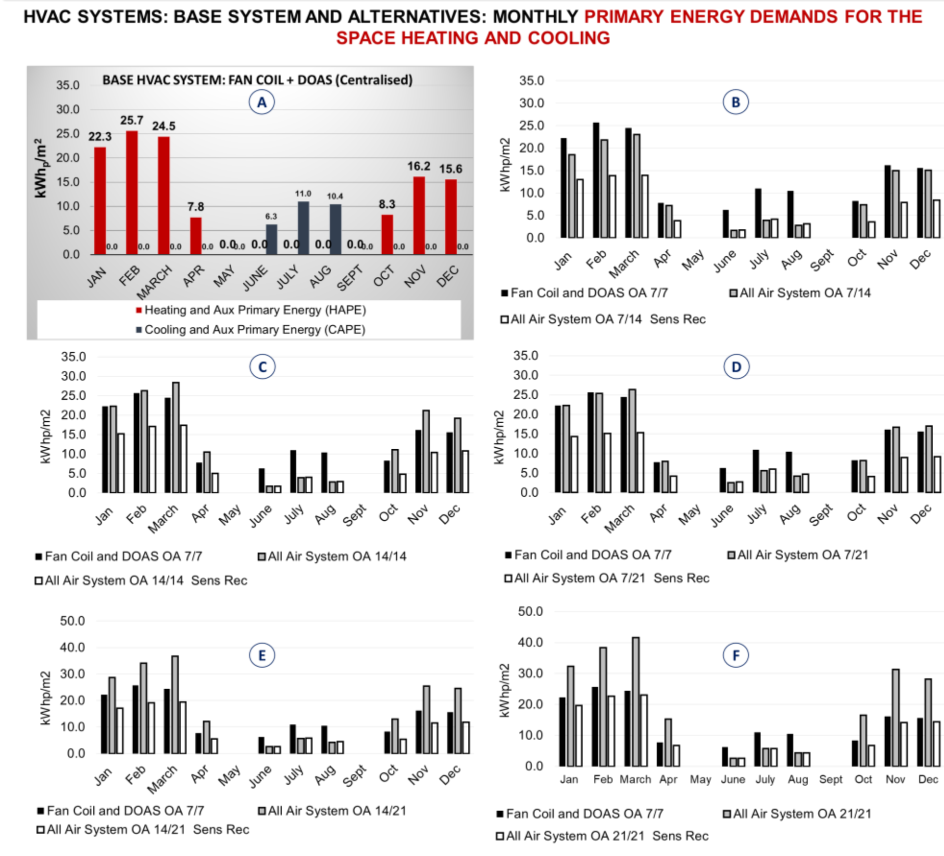

Figure 4.12 - Monthly primary energy demands for the space conditioning of each analyzed HVAC configuration, compared to the base case (FC + DOAS), with and without heat recovery in the same picture

As shown in Table 4.2, configurations 1, 2 e 3 handle, depending on the specific classroom, from 6.5 ACH (classroom 1F-3) to 7.9 ACH (classroom 1F-4 and 1F-6), while configurations 4 and 5 determine from 9.7 ACH (classroom 1F-3) to 11.9 ACH (classroom 1F-4 and 1F-6). These differences are due to the number of seats and/or different volumes of the rooms. In Figure 4.12, the primary energy demands of the base system and of the design alternatives are shown. In Figure 4.12A, the base system (FC + DOAS) is detailed and then compared, in the other part of the figure (from B to F), to the energy demands of the design alternatives, with and without the heat recovery system, in the same picture.

The base system has primary energy demands (i.e., mean values for the whole building) equal to 1122 MWh_p for the space heating and 147 MWh_p for the space cooling, and it corresponds to an EP_H and EP_C (primary energy demands/m^2 for the space heating and cooling, respectively) equal to 94.7 kWh/m^2y and 12.4 kWh/m^2y.

With reference to the new classrooms, and thus by excluding the remaining part of the building (not involved by consideration of design alternatives), the following results have been calculated (the subscripts H means "Heating", C = "Cooling", SC = "Annual Space Conditioning") and the comparisons are always referred to the base case (FC + DOAS).

- 0 Base Case (Configuration 0) FC + DOAS: EP_H = 120.2 kWh_p/m^2y, EP_C = 27.7 kWh_p/m^2y, EP_{SC} = 148.0 kWh_p/m^2y.
- 1 Configuration, All Air System OA 7/14: EP_H = 108.1 kWh_p/m^2y, EP_C = 8.4 kWh_p/m^2y, EP_{SC} = 116.5 kWh_p/m^2y. The PES (primary energy saving) is of 31.4 kWh/m^2y, and thus around the 21%.
- 1BIS Configuration, All Air System OA 7/14 Sens Rec: EP_H = 64.4 kWh_p/m^2y, EP_C = 9.1 kWh_p/m^2y, EP_{SC} = 73.5 kWh_p/m^2y. The PES is of 74.5 kWh/m^2y, and thus the 50%.
- 2 Configuration, All Air System OA 14/14: EP_H = 139.2 kWh_p/m^2y, EP_C = 8.5 kWh_p/m^2y, EP_{SC} = 147.6 kWh_p/m^2y. There is a slight annual PES, almost neglectable, 0.3 kWh/m^2y (0.2%).
- 2 BIS Configuration, All Air System OA 14/14 Sens Rec: EP_H = 80.7 kWh_p/m^2y, EP_C = 8.7 kWh_p/m^2y, EP_{SC} = 89.4 kWh_p/m^2y. The PES is of 58.5 kWh/m^2y, and thus the 40%.
- 3 Configuration, All Air System OA 7/21: EP_H = 123.8 kWh_p/m^2y, EP_C = 12.4 kWh_p/m^2y, EP_{SC} = 136.2 kWh_p/m^2y. The PES is of 11.7 kWh/m^2y, and thus the 8%.
- 3 BIS Configuration, All Air System OA 7/21 Sens Rec: EP_H = 71.3 kWh_p/m^2y, EP_C = 13.4 kWh_p/m^2y, EP_{SC} = 84.7 kWh_p/m^2y. The PES is of 63.3 kWh/m^2y, and thus the 43%.

- 4 Configuration, All Air System OA 14/21: EP_H = 174.8 kWh_p/m^2y, EP_C = 12.4 kWh_p/m^2y, EP_{SC} = 187.1 kWh_p/m^2y. There is an increase of energy demands, +39.2 kWh/m^2y (+26%).
- 4 BIS Configuration, All Air System OA 14/21 Sens Rec: EP_H = 89.9 kWh_p/m^2y, EP_C = 12.9 kWh_p/m^2y, EP_{SC} = 102.8 kWh_p/m^2y. The PES is of 45.1 kWh/m^2y, and thus the 30%.
- 5 Configuration, All Air System OA 21/21: EP_H = 203.6 kWh_p/m^2y, EP_C = 12.5 kWh_p/m^2y, EP_{SC} = 216.0 kWh_p/m^2y. There is an increase of energy demands, +68.1 kWh/m^2y (+46%).
- 5 BIS Configuration, All Air System OA 21/21 Sens Rec: EP_H = 107.4 kWh_p/m^2y, EP_C = 12.6 kWh_p/m^2y, EP_{SC} = 119.9 kWh_p/m^2y. The PES is of 28.0 kWh/m^2y, and thus the 19%.

All other results, in terms of energy demands, are provided in Table 4.3. It is quite clear that the use of heat recovery, in the cold climate of Campobasso, is necessary. Indeed, the high occupancy rate implies a high amount of ventilation air. By taking into account the opportunity of increasing - doubling or even tripling - this amount (i.e., 14 l/s and 21 l/s per person of ventilation air, during the first phases of recovery of the face-to-face didactics, can be suitable for removing and diluting eventual pathogens), the sensible heat recovery is very useful. It should be noted that all configurations equipped with heat recovery determine primary energy savings compared to the base case, and this PES ranges from 19% (All Air System OA 21/21 Sens Rec) to 50% (All Air System OA 7/14 Sens Rec).

Even if without the sensible heat recovery, the configurations All Air System OA 7/14 and All Air System OA 7/21 provide a more safe indoor air quality compared to the base case (or, at least, higher flexibility) because the OA flow rate is the same but there is no risk connected to a centralized system (i.e., air channels, mainly when the system is turned off, could be a route for tranfer of virus-laden aerosols), without an increment of energy demands. Furthermore, having a dedicated system for each classroom (where the building geometry allows it) simplifies the management. Obviously, the investment costs of single separated systems could be higher. Conversely, the increase of the OA flow rates (14 l/s pers and 21 l/s pers), with wide ACHs and without heat recovery, induces a rising of energy demands for the annual space conditioning, and thus +26% (All Air System OA 14/21) and +46% (All Air System OA 21/21).

Table 4.3 - Primary Energy Demands for Heating (EP_H), Cooling (EP_C), space conditioning (EP_{SC}) for all HVAC systems

		EP_H [kWh_p/m^2y]	EP_C [kWh_p/m^2y]	EP_{SC} [kWh_p/m^2y]	PES [kWh_p/m^2y]	PES [%]
Base Case	Fan Coil and DOAS OA 7/7	120.2	27.7	148.0	----	----
Configuration 1	All Air System OA 7/14	108.1	8.4	116.5	31.4	21%
Configuration 1 BIS	All Air System OA 7/14 Sens Rec	64.4	9.1	73.5	74.5	50%
Configuration 2	All Air System OA 14/14	139.2	8.5	147.6	0.3	0.2%
Configuration 2 BIS	All Air System OA 14/14 Sens Rec	80.7	8.7	89.4	58.5	40%
Configuration 3	All Air System OA 7/21	123.8	12.4	136.2	11.7	8%
Configuration 3 BIS	All Air System OA 7/21 Sens Rec	71.3	13.4	84.7	63.3	43%
* Configuration 4	All Air System OA 14/21	174.8	12.4	187.1	-39.2	-26%
Configuration 4 BIS	All Air System OA 14/21 Sens Rec	89.9	12.9	102.8	45.1	30%
* Configuration 5	All Air System OA 21/21	203.6	12.5	216.0	-68.1	-46%
Configuration 5 BIS	All Air System OA 21/21 Sens Rec	107.4	12.6	119.9	28.0	19%

** A negative PES means an increase of energy demand*

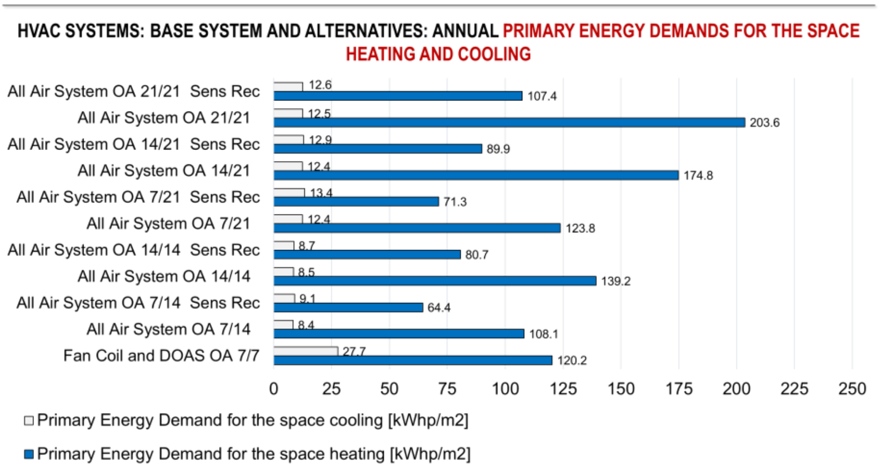

Figure 4.13 - Annual primary energy demand EP_H and EP_C for the base case and each analyzed HVAC configuration

A summary of annual energy demands, in terms of primary energy, is provided in Figure 4.13, where it can be seen the large variability that concerns the energy demands for the space heating while, with reference to the cooling season, no large variations occur. This is mainly due to the coldness of the site, Campobasso, in which the cooling period is very short, and to the use of the building that, as common in Italy, is scarcely occupied in July and August. Because of these reasons, energy demand for the summer air-conditioning is not so intensive.

In order to allow an immediate understanding of the impacts of the sensible heat recovery, the monthly values of energy demand for air-conditioning are provided in Figure 4.14, with reference to the base case compared to all configurations without heat recovery (A), and with reference to the design alternatives equipped with the heat exchanger (B). Here, it is quite evident that, with reference to all months of the heating period, the presence of the sensible heat recovery is the discriminant: with this component, the energy impacts of the increase of the outside airflow can be limited significantly. Thus, as depicted in Figure 4.13, it could be more convenient to provide 21 l/s of outdoor air per person (EP_H = 107.4 kWh/m^{2}y) than 7 l/s (EP_H = 108.1 kWh/m^{2}y), if the recovery of sensible energy from the exhaust air is applied in the first case and not in the second one. In addition, too many air changes (21 l/s per person instead of 14 l/s per person), even if allow a high capability and short time required by the HVAC for repristinating the indoor design conditions at the early morning or after impulsive variations of heating loads, anyway these increase the energy requests for the air movement and thus the electric energy required by fans. Finally, the configuration 7/14 and 14/14 - with air changes ranging from 6.5 to 7.9 h^{-1}, depending on the specific classroom (see Table 4.2) - are enough to maintain the desired microclimate. On the other hand, even if energy demands for ventilating and ventilation are higher, the configuration 21/21 allows a higher indoor air quality and higher velocity of the systems in limiting the oscillation of indoor conditions. Moreover, under critical conditions, such as during an epidemic, this configuration allows wide management of OA.

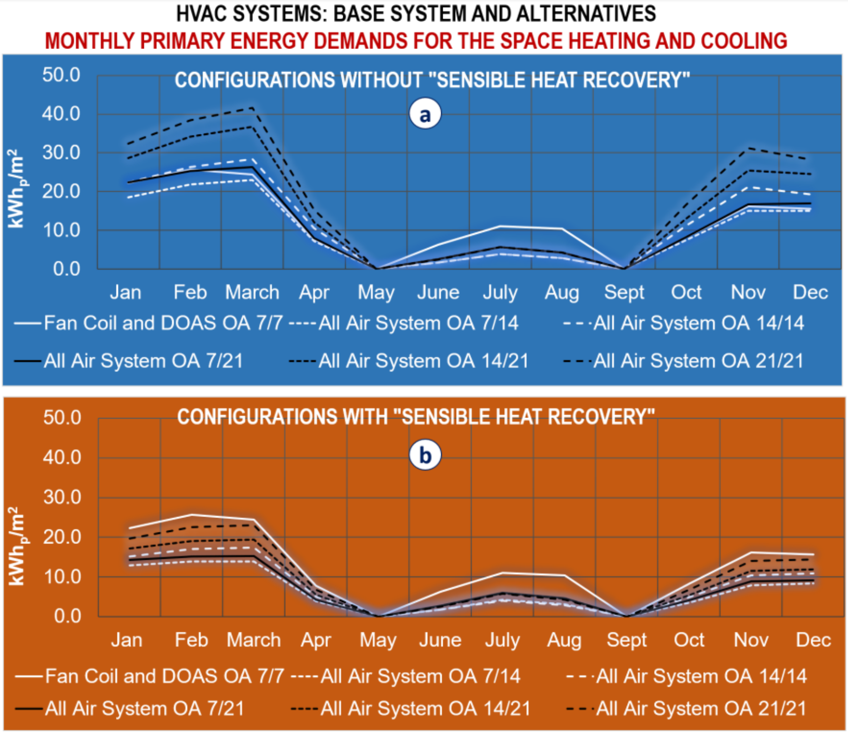

Figure 4.14 - Monthly primary energy demands for space conditioning of the HVAC alternatives, without (A) and with (B) heat recovery

4.4.3. Annual operating costs and environmental study

A last study derived from BES is the evaluation of annual costs for air-conditioning, by varying the HVAC systems configurations, and also the variation of environmental impacts and GHG emissions. In Figure 4.15, a summary is proposed. In order to provide numbers easily understandable, whose order of magnitude is quite typical, the annual costs of air-conditioning and the tons of $CO_{2\text{-}eq}$ emissions are referred to 100 m^2 of new classrooms.

The economic costs of the winter heating and ventilation range from 585 €/100m^2 to more than 1650 €/100m^2. About the cost of cooling, the outcomes are very similar for all HVAC configurations, and only the base case system, equipped with fan coils and a DOAS, shows higher energy demands (and thus higher costs), but this depends on the fan coil regulation. Anyway, the cooling energy demand is quite low and thus the percentage differences and the simulation error can be significant.

Of course, by confirming the results achieved for what concerns the energy analysis, by evaluating the year-around costs for the space conditioning, once again it emerges that energy savings are achieved when heat recovery systems are installed and, also in the case of a 100% OA, with high (i.e., 14/14 l/s person, ACH from 6.5 to 7.9 h^{-1}) or very high (21/21 l/s person, ACH from 9.7 to 11.9 h^{-1}) outside air changes, the economic expenditures are lower or similar compared to the base case (FC + DOAS). With reference to the annual microclimatic control, the costs range from 603 €/100m² (minimum) to 1768 €/100m² (maximum), connected to the adoption of the All Air System OA 7/14 Sens Rec and the All Air System OA 21/21, respectively.

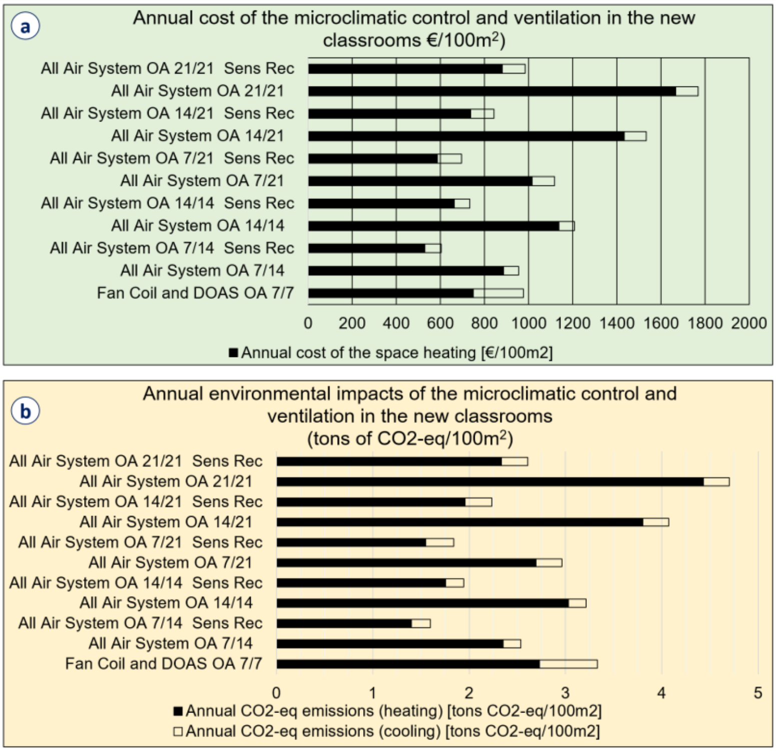

Figure 4.15 - Economic and Environmental (B) studies: economic costs and environmental emissions related to each analyzed HVAC configuration

In terms of GHG emissions, the outcomes are even more significant. Indeed, given the increasing share of renewables in the electricity conversion, the $CO_{2\text{-eq}}$ emission factor connected to the use of electricity is decreasing, as testified by the tables inferred in [39] (Annex I, Table A.I.6, LCA emission factor of electric energy). In the same study provided by the Covenant of Majors (table A.I.1 [39]), it emerges that the LCA emission factor of natural gas has been quite constant in the last years. This supports the energy transition towards electricity. Finally, by varying the HVAC systems, the emissions for annual air conditioning of 100 m^2 of new classrooms can vary from 1.6 tons of $CO_{2\text{-eq}}$ to 4.7 tons of $CO_{2\text{-eq}}$, and thus the environmental GHG emissions can be triplicated. Also in this case, with reference to the heating period, the use of sensible heat recovery, for all configurations, reduces the environmental impacts from 40 to 50%, compared to the same HVAC system without a sensible heat exchange between exhaust air and outside air.

4.5. CFD simulation: Air diffusion strategies, thermal and flow fields, air velocity, and age of air

In this sub-section, some common configurations for the supply and the extraction of air from the indoor environment have been designed, to evaluate the thermal fields in the various areas of the classrooms and, mainly, for understanding the thermal and flow fields and the age of the air in the breathing zones. Definitively, the air diffusion performances of four distribution configurations referred to the all air systems - and thus the new and suitable HVAC systems analyzed in the previous sections - are here examined.

The analyzed room is the 1F-2, a typical classroom of 81.6 m^2, which in the pre-COVID-19 period (according to the design idea) could accommodate 40 people: at today, by taking into account the necessary "social distancing" as a preventive anti-contagion measure [47], it is estimated an occupancy by 20 persons (Figure 4.16, the number has been halved compared to the normal occupancy capacity), which, obviously, are sources of endogenous heat gains, due to the specific metabolic activity.

About the configuration of HVAC systems here modelled, this is the aforementioned All Air System OA 7/14 and thus system that provides, according to Table 4.2, ACH equal to 7.5 h^{-1} for the classroom 1F-2, with 50% OA and 50% RA. In a CFD study, the presence of the heat recovery systems does not have influence, and also the air recirculation does not affect the outcomes: indeed, besides the boundary conditions, the incident parameters are the total supply flow rate and its thermodynamic conditions. In the CFD model, by acquiring boundary conditions from the previous BES investigations, the following schemes for the air-conditioning ventilation (supply and extraction = 0.56 $m^{3/}s$) have been implemented and simulated:

- 6 ceiling square diffusers (directional 4 ways),
- 4 wall-mounted grilles, placed on the upper zone of the vertical walls,
- 10 wall-mounted nozzles, high turbulence, placed on the upper part of one of the two short sides of the room,
- 6 parallel strips of ceiling linear slot diffusers.

By excluding a lateral strip, useful dimensions for the arrangements of air diffusers were a length of 11.6 m and a width of 6.5. All configurations (Figure 4.16) have been designed through the ADPI (Air Diffusion Performance Index) method [6],[48] Regarding the extraction systems, this consists of extraction grilles, place on the floor, or in the lower part of the building walls (it depends by the configuration of the supply).

The choice of the diffusers arrangement, firstly, has been based on qualitative considerations and experience, in order to obtain uniform microclimatic conditions within the environment, by taking into account the volumetric flow rates, the distance between the terminals, the distance between diffusers and walls, as common in design practice.

Starting from typological distribution schemes, the ADPI method allowed the determination of the throw and thus the designing the specific air terminals: then, the CFD simulation is performed, by evaluating indoor uniformity, but also the flow vectors, preferring – for instance – a vertical movement of the indoor air, so that air exhaled by persons (with possible pathogens) does not invest other students but can be mainly directed towards the extraction grilles.

The description begins from the air diffusion configuration with square diffusers, six and placed on the false ceiling. As shown in Figure 4.16A, the distance between each diffuser is 3.3 – 3.9 m while the distance from the nearest wall is 1.6 – 1.9 m. The air extraction is guaranteed by 4 extraction grilles (30x50 cm) placed in the lower part of the short walls. Each extraction grill is defined in the numerical CFD code by shape, size, and volumetric flow rate. The extraction airflow rate is 100% of that supplied into the environment, and thus, the resolution of Navier-Stokes equations (namely, the mass continuity) is not perturbed (i.e., no exfiltration air was assumed). The total volume flow released in room 1F-2 is 560 l/s, and thus 93 l/s are supplied by each diffuser, while 140 l/s are extracted by each extraction grill.

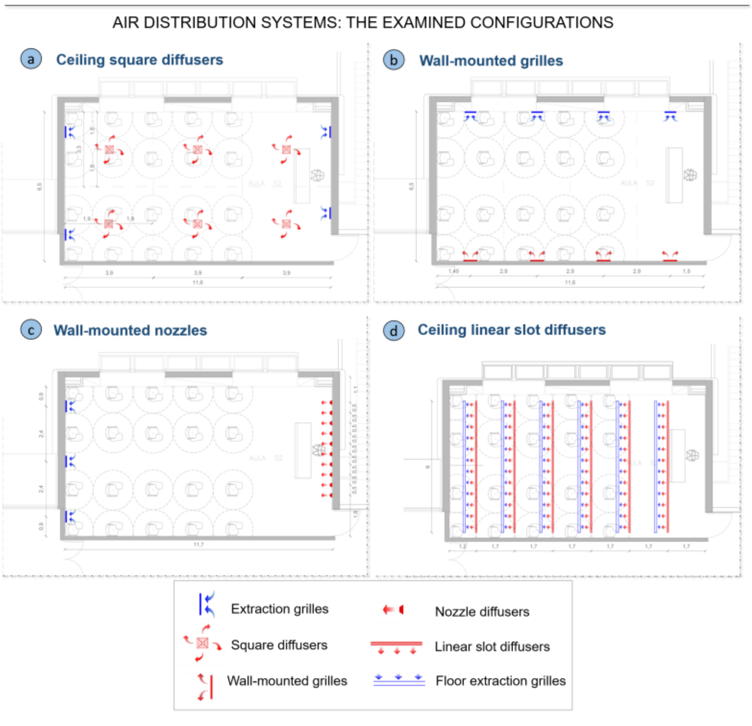

Figure 4.16 - Air distribution system schemes: ceiling square diffusers (a), wall-mounting grilles (b), wall-mounted nozzles (c), ceiling linear slot diffusers (d)

The design criterion of the air terminals started from the definition of the isothermal throw (T) (i.e., the distance covered by the flow between the center of the diffuser axis and the point where the airspeed decreased to the predetermined value of 0.25 m/s) and the characteristic length of the room (L) (i.e., the minimum distance between the diffuser and the closest obstacle, wall or interference with the throw of another diffuser). After a distribution hypothesis of the air terminals, the ambient thermal load was estimated, in the summer regime and design conditions. The throw of the diffuser, by considering a terminal speed of 0.25 m/s, was obtained by multiplying the ratio $T_{0.25}/L$ (0.8 for ceiling square diffusers [6]) by the characteristic length of the room (L). In the case of square diffusers, this length is equal to 1.9 m, therefore the throw distance (T_d) is equal to 1.56 m. Having the volumetric flow rate, the air jet velocity, and the throw, it was possible to determine, from technical catalogs, the discharge velocity and the diffuser model. Given that the rooms of the second floor have common indoor heights, with the idea of considering also sloped platforms, low discharge velocities are established. In Table 4.4, all data for the air terminal design are reported, to deeply describe the configurations represented in Figure 4.16: in the last two lines, the necessary data to model the air terminals for CFD models are detailed.

Table 4.4 - Data for air terminal design, input and output of the ADPI method

		Square diffusers	**Wall mounted grilles**	**Wall mounted nozzles**	**Linear slot diffusers**
L - characteristic length	[m]	1.9	6.5	11.6	2.7
$T_{0.25}/L$*	[-]	0.8	1.5	1.5	0.3
Throw distance	[m]	1.56	9.8	17.4	0.84
Supply flow rate	[l/s]	560	560	560	560
Air diffusers' number	[-]	6	4	10	6
Supply flow rate/diffuser	[l/s]	93	140	56	93
Maximum ADPI*	[-]	93	85	85	92
Cooling Load**	[W/m^2]	65	65	65	65
Discharge air velocity	[m/s]	1.3	1.6	2.86	1.76
Dimensions	[m]	0.35x0.35	0.43x0.22	0.16x0.16	6x0.05

** the values refer to the ADPI tables, and differ according to the air terminal type*

*** the thermal load reported is a reference value of the ADPI tables, and it is close to that calculated for the room 1F-2*

In the configuration B (Figure 4.16B), the air is supplied by 4 wall-mounted grilles, located on the upper part of the longest wall, spaced by 2.9 m, while the extraction is performed by four extraction grilles (30x50 cm) located at the lower part of the opposite wall. Configuration C has ten wall-mounted nozzles, located at the upper part of the shortest wall. The three extraction grilles (30x50 cm) are positioned on the opposite wall and have a mutual distance of about 2.4 m each other (Figure 4.16C). Finally, Figure 4.16D shows the last configuration: 6 slot linear diffusers located on the false ceiling and spaced by 1.7 m, with 6 extraction grilles (600x10 cm) on the floor. The position of the linear diffusers and extraction grilles was accurately designed to guarantee the uniform distribution of the indoor air and the immediate extraction of the air exhaled by the seated people. The air diffusers were defined for the CFD simulation as follow:

- ceiling square diffusers: four-way supply with a discharge angle of 60° (angle between the jet and the downward-pointing normal);
- wall-mounted grilles: two-way supply with a discharge angle of 0° (the flow is perfectly orthogonal to the wall where the grill is positioned);
- wall-mounted nozzles: one-way supply with a y-discharge angle of -5° (angle between the inward-facing normal to the surface and the local surface Y-axis);
- ceiling linear slot diffuser: one-way supply with a x-discharge angle of 20° (angle between the inward-facing normal to the surface and the local surface X-axis).

The CFD studies were performed by considering a typical winter day, the 4th of February, at 12:00 o'clock, and thus a common condition of lessons. The inlet air temperature (23°C) was deduced from the dynamic simulation (BES). The CFD simulations were performed only during the winter period. The summer period was neglected in the CFD study, because, considering the Campobasso summer temperatures reported in Figure 4.3, the building energy demand for cooling is quite low and thus the cooling service and energy demands are secondary.

Really, this study wants to be merely indicative, to propose a methodology for evaluating which is, in every specific design context, the best way for approaching the air distribution and diffusion scheme, in order to improve the indoor air quality in the breathing zone and for having feedback (in addition to the use of the ADPI) on the air distribution system quality, also in terms of comfort and thermal gradients and asymmetry. In the following sub-sections, the results of each configuration are examined, with a focus on the uniformity of thermal–hygrometric parameters in the volume, the airspeed, the vertical thermal stratification, and finally the indoor thermal comfort and the age of the air in the occupied zones.

4.5.1. Air Temperature

Vertical temperature gradients may occur in the indoor environment, since, for reasons related to the lower density, the warmer air tends to stratify upwards. For each configuration, the temperature gradient ($T_{max} - T_{min}$) was calculated for the central room volume, both in the horizontal and vertical sections, to verify the presence of local thermal discrepancies (see deepening in section 4.2.4). In all cases, the air diffusion configurations guarantee good indoor temperature uniformity: indeed, the maximum temperature gradient is 1.3 °C and it concerns the solution A, in the plant view (Figure 4.17).

Similarly, the vertical temperature stratification is almost uniform for all configurations, as clear in Figure 4.18 and Figure 4.19. A negligible vertical temperature gradient was found in sections B and D, namely for the wall-mounted grille ($T_{max} – T_{min}$ = 0.7 °C) and ceiling linear slot diffuser ($T_{max} – T_{min}$ = 1.1 °C) configurations. Anyway, the vertical and horizontal temperature conditions are quite uniform, and these avoid localized discomfort and uncomfortable vertical differences.

As Figure 4.17, Figure 4.18 and Figure 4.19 show, the mean air temperature in all the examined configurations is between 21-22 °C, and thus fully acceptable and coherent for a heated classroom in winter.

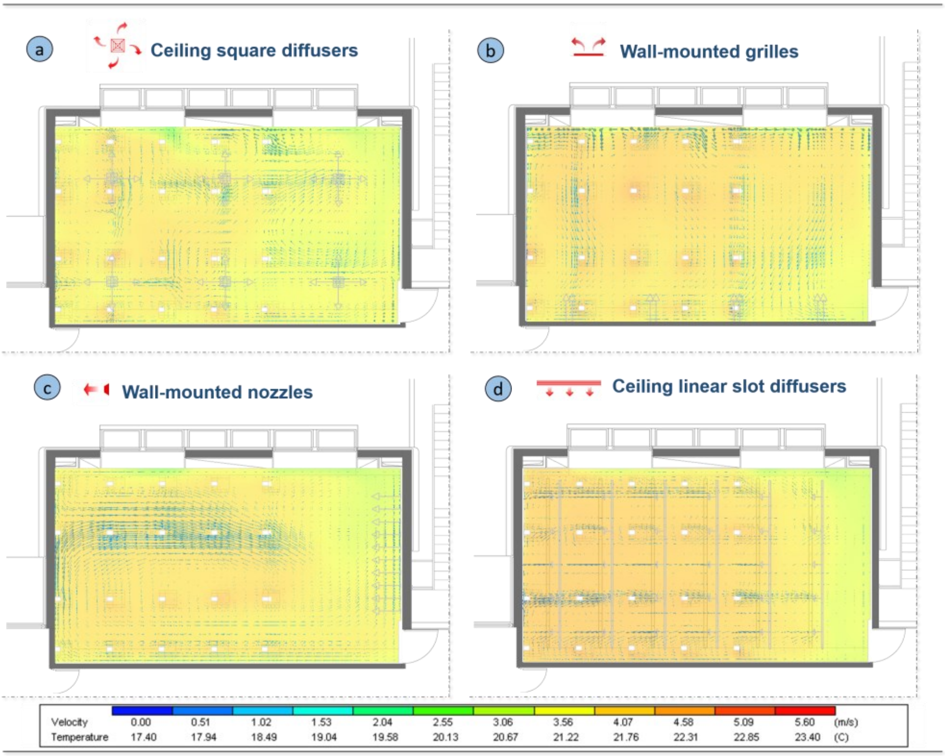

Figure 4.17 - CFD section at student head level, temperature and air speed for the following cases: ceiling square diffusers (a), wall-mounting grilles (b), wall-mounted nozzles (c), ceiling linear slot diffusers (d)

4.5.2. Air velocity and flow fields

The obtained values of airspeed for all the examined air distribution configurations are suitable for the occupant thermal comfort, in all examined cases. Generally, in the summer regime, an air movement within 1 m/s is not excessively annoying, while, in wintertime, even the slightest perception of draught (air with speeds above 0.20 m/s) can be a cause of local discomfort. As clear in the Figure 4.18 and Figure 4.19, the airspeed in the occupied zone (from 0 to 1.1 m for seated people) is less than 0.2 m/s for the configurations A, B, and D, while, for the configuration C, the airspeed in the center of the breathing zone is about 0.5 m/s. This condition could cause a localized discomfort to the students sitting in the central part of the room. Excluding partly case C, all the solutions assure acceptable indoor airspeed.

Another interesting element to examine is the air movement in the occupied area. As particularly evident in Figure 4.17 and Figure 4.18, configurations A, B, and C involve a whirling air movement and the breathed air moves from one student to another. In the case D, on the other hand, the movement of the air is almost vertical (Figure 4.19D), so that the exhaled air is then directly extracted in by the grilles positioned on the floor. This could be a valid solution to reduce the transportation of droplets from one person to another one.

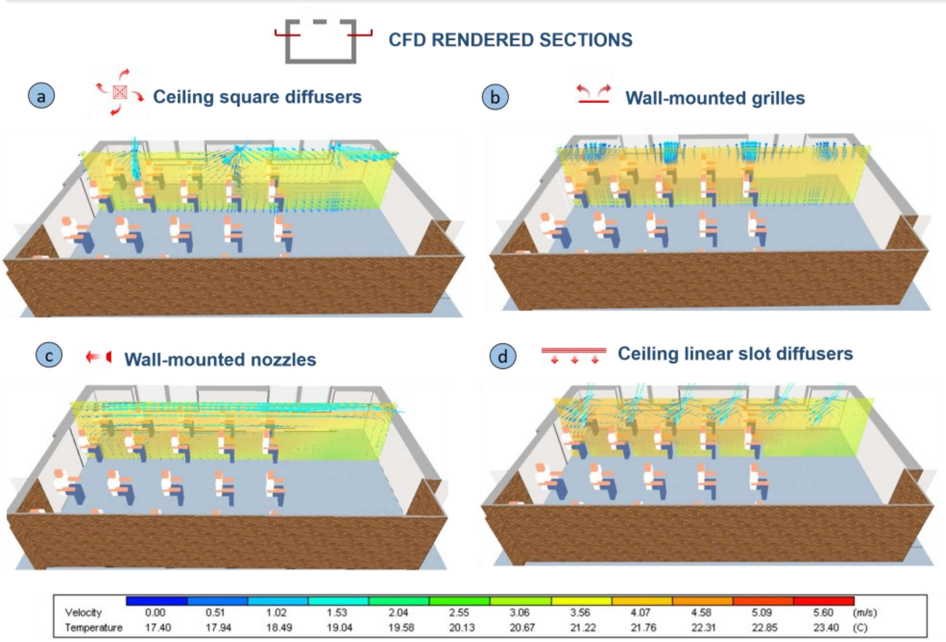

Figure 4.18 - CFD longitudinal section. Temperature and air velocity for the following cases: ceiling square diffusers (a), wall-mounting grilles (b), wall-mounted nozzles (c), ceiling linear slot diffusers (d)

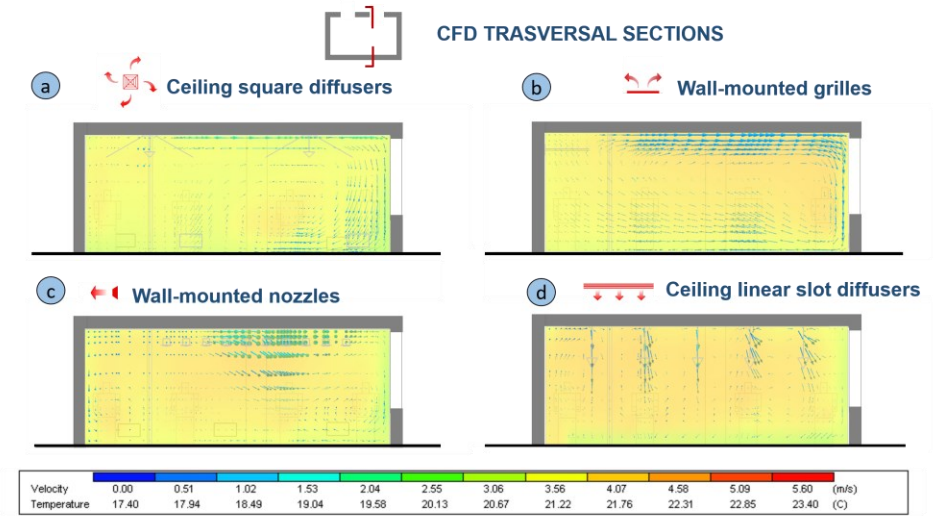

Figure 4.19 - CFD transversal section. Temperature and air velocity for the following cases: ceiling square diffusers (a), wall-mounting grilles (b), wall-mounted nozzles (c), ceiling linear slot diffusers (d)

4.5.3. Indoor thermal comfort, age of air and air quality

The different configurations were compared in terms of comfort according to the Fanger approach [49], and thus by calculating the PMV (Predicted Mean Vote) and PPD (Percentage of person dissatisfied) indexes. Some assumptions were done: the clothing resistance is equal to 1 clo, the metabolic energy equal to 1.20 met, typical for seated people, the relative humidity is equal to 50%. The airspeed, the mean radiant temperature, and the air temperature were automatically assumed from the CFD simulation and, as for the temperature, the air velocity and the age of the air were calculated for the entire classroom volume. Assuming a monitoring point near the first line of students, in case A, the PMV index is equal to -0.20, while the PPD index is 7% (Table 4.5). The PMV value falls perfectly in the range of moderate indoor environments (-1<PMV<1), while the percentage of dissatisfied is very low. In the configuration C, the PPD and PMV are quite the same (PMV= -0.23; PPD = 7%).

Table 4.5 - PMV and PPD for the analyzed configurations for a monitoring point

	(A) Square diffusers	(B) Wall mounted grilles	(C) Wall mounted nozzles	(D) Linear slot diffusers
PMV [-]	-0.20	-0.12	-0.23	-0.06
PPD [%]	7	6	7	5.5

The most significant difference emerges by comparing the configuration C with D. In the latter case, the PMV is equal to -0.06, with a consequent PPD of 5.5%, confirming a perfect condition of indoor thermal comfort. All results demonstrate the effectiveness of the designed solutions for the HVAC system and air terminals, in terms of thermal comfort.

Really, it is important to underline that this investigation does not aim to evaluate the correctness of the simulated air terminals, in terms of thermal comfort merely, but also it wants to evaluate the movement of the indoor air, flow fields, the mean age of the air, which are closely linked to the number of diffusers, their position, the airspeed and the position of the extraction grilles. Indeed, looking at Figure 4.20, the differences between the proposed configurations emerge.

In Figure 4.20 (breathing zone), the range of age of air considered is between 0 and 484 s. Of course, the lower the age of the air, the fresher it is: the more it tends to blue color, the fresher it is. The age of air is “the length of time that some quantity of outside air has been in a building, zone, or space” [6] and it is directly correlated to the air quality. This indicator is useful for understanding the effectiveness of the ventilation systems designed and for identifying the solution that better meets the needs of air purity and freshness. Thus, this parameter can be useful also for contagions' prevention. As shown in Figure 4.20, the configurations which have a lower average age of air are the A and D, both characterized by ceiling diffusers. In particular, the solution with ceiling square diffusers (A), has a maximum age of the air of about 176 s, while a minimum of about 88 s. In the configuration with linear slot diffusers (D), the minimum age of the air is similar to the previous one, but the maximum is around 300 s. This occurs only in the entrance area of the classroom and depends on the position of the extraction grills and the inclination of the inlet air jet (x-discharge angle of 20°), as shown in the section of Figure 4.18D. The two other configurations can be considered less valuable from the point of view of air quality, and particularly this is true for the one with wall mounted grilles. In this case, the maximum age of the air is 484 s and concerns the back of the classroom penalizing the last line of students, while the minimum is around 300 s. As clear, the air distribution is not uniform, and the air quality can be considered worse compared to the other configurations. These results are in line with those of Ascione *et al*. [43] which showed a better air quality for a museum room with ceiling diffusers compared to the case with wall air terminals.

More in general, it can be concluded that, for the room under consideration, all air terminal configurations give satisfactory results in terms of comfort and air quality. The configuration which guarantees better results regarding the uniformity of the air distribution and its purity, as well as optimal comfort conditions, is the one with linear slot diffusers (solution D). Indeed, this configuration guarantees a vertical displacement of the breathed air, and therefore reduces the possibility of diffusion of contaminants throughout the whole indoor environment. In addition, it could be noted that the airspeed in rooms with common heights is an issue requiring attention.

Here, the aim is not to propose universal solutions. Indeed, the analyses involved only a classroom and merely common air diffusers, in common configurations. On the other hand, each diffuser can be valid or unsuitable, depending on the whole air diffusion configuration and features of the room, building, facility and thermal loads. Conversely, the proposed approach is the main result. Finally, also a correct, deeply-investigated, checked air diffusion strategy could be a valid tool for allowing air movement from clean zones to dirty ones, and thus for supporting in preventing the spread of contagions.

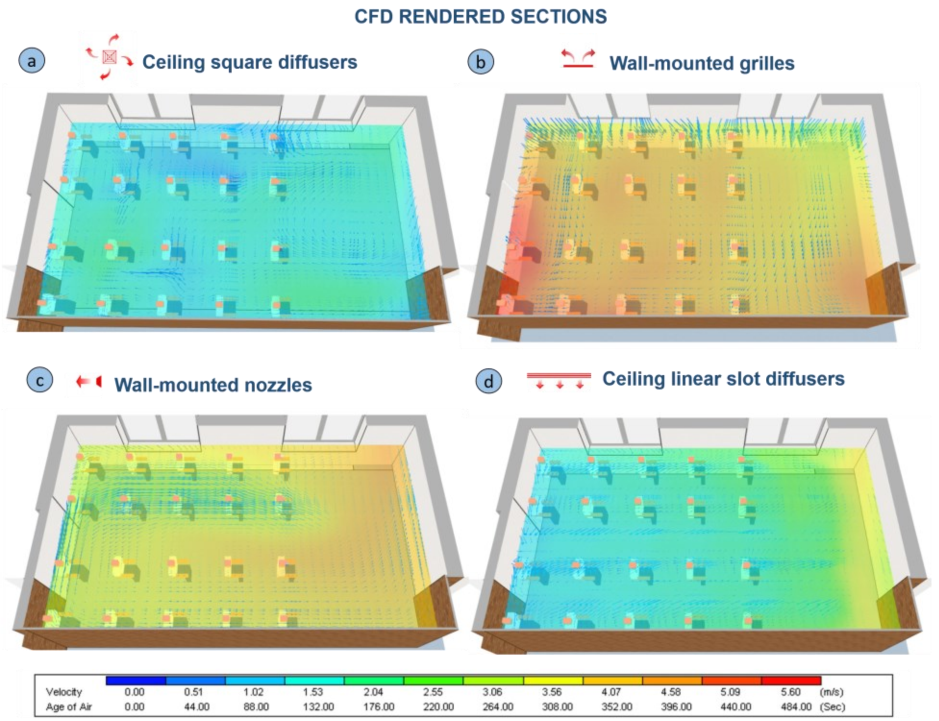

Figure 4.20 - CFD rendered sections at student breathing zone. Air speed and mean age of air for the following cases: ceiling square diffusers (a), wall-mounting grilles (b), wall-mounted nozzles (c), ceiling linear slot diffusers (d)

4.6. Additional remarks and future studies

The lesson learned in the last two years will remain impressed in our minds. The catastrophic impacts of a pandemic for persons, economies, social equalities are evident. Really, further food for thought can be found, starting from the positive effect of the lockdown on the earth's environmental conditions, ambient air, and water quality, with a decrease of pollution, even related to the reduction of energy intensity and use of fossil fuels. This was evidenced in many studies, for instance [55] and [56] for China, concerning VOCs and many pollutants, and, in Europe, by [57] and [58], with investigations concerning the environmental benefits of lockdown respectively in locations of Spain and Italy. These and other studies, once again, underline that the impact of human activities on earth conservation is enormous: all citizens, by living their life, must play their part toward sustainability. Of course, many and many topics and issues must be addressed, starting from a global journey involving “all countries towards a more sustainable and equitable world” (literally from Oldekop *et al*. [59]). According to these authors, key challenges concern: a) the global value chains, b) the need for digitalization, c) the issue of debt and public finances and, d) climate change. The answer is the local and global cooperation, a multi-scalar approach, and it involves both the global North and South of the World, with important challenges concerning the human global rights (the contrast to poverty, the issue of migration, social protection, sustainability, affordable houses and cities, right jobs, food availability livelihoods, etc.).

Here, we need to remain in the field of energy efficiency of the built environment, and thus safe, secure, sustainable buildings and cities. Some key issues, already evidenced in the last decades by members of scientific organization, are now evident for everybody and thus the mandatory need of:

- sustainable buildings, suitable for life, including activities among which the personal care and wellness, the study and the work, at home and in remote ways. This implies that the current indices and parameters (for instance concerning the occupancy rate in social housing, or the standard equipment of standard houses) must be revised, by including also targets related to the wellbeing [60], [61];
- technological integration of systems and equipment for improving the environmental comfort in buildings, including flexible systems for allowing suitable indoor air quality, microclimatic control, high thermal and hygrometric comfort [62] (with special attention to passive technologies [63]) and with high care to the acoustical and visual characteristic of environments;
- resilient urban cities and districts, with attention paid to urban quality and comfort, to face the energy poverty [64], the climate change, the extreme climate events and also to restore a sane relationship between nature and urbanization [65];

- energy supply, conversion, and self-use even over the boundary of the single building [66], and thus the development of energy communities, at the building, district, and city levels, where all functions can cooperate (e.g., construction sectors, industry, transport), being each stakeholder both “consumer” and “prosumer”, and thus by sharing the energy surplus and providing virtuous cooperation among citizens, toward progressive decarbonization with the highest share of renewables [67].

Regarding the aforementioned topics, the attention must be paid to both new urbanization and the built environment, and thus, as recently underlined by EU guidelines, the nearly zero-energy targets must concern both new constructions (Directive 2010/31/EU [68]) and the retrofit of existing buildings (Directive EU 844/2018 [69]).

4.7. Conclusive remarks

The proposed investigation coupled several methodologies of the architectural and technological engineering, for renovating classrooms of an Italian Educational building, with a view to the necessities of safety and healthiness. In the first semester of 2020, suddenly the World discovered a fragility with respect to pandemics. The modern economies and lifestyles are based on complete globalization and interchanges of people, things, information. In a few months, at the World scale, the COVID-19 caused hundreds of thousands of deaths, officially, but it is quite accepted that the statistics are greatly underestimated. Lockdowns interested most countries and now, we are slowly acquiring new different normality, approaching again the “in-presence” activities. These face-to-face activities are now a reality, supported by a strengthening of e-learning and telematic activities. At the same time, university and educational buildings, given the high occupancy rates, must be safe and secure, and thus architectural and technological retrofits are necessary in order to contrast and avoid contagions of COVID-19 and other severe syndromes. Good practices in the matter of hygiene, social distancing, good habits and behaviors, frequent cleanings of hands and surfaces are mandatory, mainly to avoid direct affections. On the other hand, secondary transmission routes, related to nuclei droplets and small aerosols are possible and require dilution of pathogens, filtrations (also of the exhaust air), strong ventilation. Here, with reference to the already planned architectural renovation of a Department of the University of Molise (Italy), in which new classrooms will be built, a new investigation that couples two different numerical approaches - and thus a) building energy performance (BES) simulation, 0-D and in the domain of the time and with sub-hourly calculations extended to the whole year, and b) computational fluid dynamic (CFD) analysis, 3-D and referred to specific hours – is proposed.

The investigation begins with an accurate audit of the present building, with surveys on building components and energy systems, by monitoring the indoor conditions and acquiring the historical metered energy demands. Then, based on the available information, a suitable energy model has been defined by using a whole program for the building energy simulation, calibrated against the real energy demands from bills. After a model simplification to reduce the computational effort, the current building was modified, with reference to the digital model, for defining the new architectural distribution, with the design of the new seven classrooms.

With reference to the building energy analysis, starting from the originally designed HVAC system, a mixed air-water system with in-room fan-coils and an AHU handling merely outdoor air (i.e., a dedicated outdoor air system), then other configurations are investigated, and thus an all-air system with and without the sensible heat recovery from the exhaust air, with variable amount of outdoor air (from 33% to 100%, with a minimum of 7 l/s pers of OA) and air change rates varying from 6.5-7.9 h^{-1} (configurations with total supply air of 14 l/s person) to 9.7-11.9 h^{-1} (configurations with total supply air of 21 l/s person). The main outcomes reveal that:

- By considering the new classrooms, the annual primary energy demand for the space heating (EP_H) ranges from 64.4 kWh_p/m^2 (OA 7 l/s pers, activation of sensible heat recovery and recirculation air) to 203.6 kWh_p/m^2 (21 l/s pers, 100% OA, bypass of the heat recovery).

- The heat recovery, in the cold climate of Campobasso (Italy, backcountry), is very effective in reducing the additional energy demands connected to the strong increase of outdoor air. Thus, AHUs must be equipped with flat plate heat exchangers, without contamination of the outdoor air with the exhaust air (in this way, if there is the need of operating at 100% OA, sensible heat recovery can be effectively used).
- The use of sensible heat recovery allows significant energy saving. Indeed, also in case of high ACH (from 9.7 to 11.9 h^{-1}), the energy impact by varying the amount of OA, and thus 7, 14 or 21 l/s person, is limited, with EP_H equal to 71.3 kWh_p/m^2, 89.9 kWh_p/m^2 and 107.4 kWh_p/m^2, respectively. Of course, the same trend is achieved for the annual economic costs for the space conditioning and annual HVAC-related $CO_{2\text{-eq}}$ emissions, with differences also of 1165 €/100m^2 and 3.1 tons $CO_{2\text{-eq}}$/100m^2, respectively, by considering the HVAC design alternatives requiring the lowest and highest energy demands, respectively.
- The increase of OA implies higher energy demands but also better indoor air quality, and thus a lower values of CO_2 concentration and lower ages of air. According to Wargocki *et al*. (2020) [81], this will have a positive impact on students' performances, in terms of rapidity of reasoning and right answers to questionnaires, better learning and daily attendance.
- All design alternatives have similar energy demands for cooling, with EP_C from 8 kWh/m^2 to 12.9 kWh/m^2 and the role of the heat recovery, in this climate and building use, is marginal during the cooling period.

Then, by considering the social distancing, the number of persons was halved in each classroom (i.e., from 120 to 60, from 40 to 20 and so on); A CFD model of a specific classroom was created, and, by achieving all necessary boundary conditions from the previous BES simulations, a CFD study was performed, by investigating the air diffusion performances of four configurations (allowing 7.5 h^{-1} air changes per hour): 6 ceiling square diffusers, 4 wall-mounted grilles, 10 wall-mounted nozzles (high turbulence), 6 parallel strips of ceiling linear slot diffusers. All configurations have been designed by means of the ASHRAE ADPI method, and also suitable air extraction systems were modeled. The following conclusions can be inferred:

- All air terminal configurations give satisfactory results in terms of thermal comfort, but the configuration which guarantees better results regarding uniformity of the air distribution and its purity, as well as optimal comfort conditions, is the one with linear slot diffusers.
- In terms of uniformity of air temperature, age of air and flow and thermal fields, with reference to the specific case studies, optimal microclimatic conditions were achieved by using linear slot diffusers, in six strips, parallel to the students' row. This evaluation considers the following aspects: the indoor uniformity, the PMV according to the Fanger approach, the air movement directed by the person to the extraction grilles, so that the air breathed and exhaled by persons is then directed towards the grilles positioned on the floor and at the lower part.

Finally, according to the authors, the proposed study shows the importance of a correct HVAC system design, not limited to evaluations of different HVAC configurations in terms of energy, economy, and emissions, but also in terms of comfort and IAQ. It is essential to analyze the different air diffusion strategies so that suitable air quality, lack of stagnancy zones and overall thermal comfort can be guaranteed, with a view to the uniformity throughout the indoor environment. However, this design effort must also be accompanied by an important contribution in the maintenance of the system, such as control and replacement of filters (HEPA) and in the sanitization and correct ventilation of the rooms. The ventilation, indeed, is necessary for diluting and removing indoor pathogens and proper filters can reduce indoor contamination.

Really, what is noteworthy, more than the specific achieved results (i.e., these can vary, by changing the use of the building or the climate, but also with varying the classroom geometry or loads), is the method. Flexibility and accuracy in predictions, also by means the use of advanced numerical methods and coupled experimental (surveys, monitoring, audits) and numerical approaches (also of multiple nature, such the BES and CFD studies here presented), can support a conscious design. With this study, still ongoing, a contribution to the recovery of normal life is given, trying to rethink what we do every day: teaching and learning in the presence of students and teachers.

CHAPTER 4 – References

[1] ASHRAE Position Document on Infectious Aerosols Approved by ASHRAE Board of Directors April 14, 2020, American Society of Heating Refrigerating and Air-Conditioning Engineers, Atlanta, GA, USA.

[2] REHVA COVID-19 guidance document, April 3, 2020, REHVA, Federation of European Heating, Ventilation and Air Conditioning Association, Brussels, Belgium.

[3] AiCARR AiCARR Position Paper on HVAC systems operation during SARS-CoV2-19 emergency. AiCARR, Associazione Italia Condizionamento dell'Aria, Riscaldamento e Refrigerazione, Milano, Italia. Available online: https://www.aicarr.org/Pages/Normative/FOCUS_COVID-19_IT.aspx. Accessed in November 2021

[4] AiCARR Protocol for risk reduction of SARS-CoV2-19 diffusion with the aid of existing air conditioning and ventilation systems. AiCARR, Associazione Italia Condizionamento dell'Aria, Riscaldamento e Refrigerazione, Milano, Italia. Available online: https://www.aicarr.org/Pages/Normative/FOCUS_COVID-19_IT.aspx. Accessed in November 2021

[5] WMO, Modes of transmission of virus causing COVID-19: implications for IPC precaution recommendations, World Health Organization 2020. WHO reference number: WHO/2019-nCoV/Sci_Brief/Transmission_modes/2020.2.

[6] ASHRAE Handbook - Fundamentals 2017, American Society of Heating Refrigerating and Air-Conditioning Engineers, Atlanta, GA, USA.

[7] ASHRAE Handbook - HVAC Applications 2019, American Society of Heating Refrigerating and Air-Conditioning Engineers, Atlanta, GA,

[8] ASHRAE Handbook - HVAC Systems and Equipment 2020, American Society of Heating Refrigerating and Air-Conditioning Engineers, Atlanta, GA, USA.

[9] ANSI/ASHRAE Standard 62.1-2019, Ventilation for Acceptable Indoor Air Quality. Atlanta: ASHRAE. ASHRAE.

[10] ANSI/ASHRAE Standard 62.2-2019, Ventilation and Acceptable Indoor Air Quality in Low-Rise Residential Buildings.

[11] ANSI/ASHRAE/ASHE Standard 170-2017, Ventilation of Health Care Facilities. Atlanta: ASHRAE.

[12] G. Correia, L. Rodrigues, M. Gameiro da Silva, T. Gonçalves, Airborne route and bad use of ventilation systems as non-negligible factors in SARS-CoV-2

transmission, Medical Hypotheses, Volume 141, 2020, 109781, ISSN 0306-9877, https://doi.org/10.1016/j.mehy.2020.109781.

[13] W. Chen, N. Zhang, J. Wei, H.-L. Yen, Short-range airborne route dominates exposure of respiratory infection during close contact. Build. Environ., 176 (2020), p. 106859

[14] L. Morawska, J. Cao, Airborne transmission of SARS-CoV-2: the world should face the reality. Environ. Int. (2020), p. 105730.

[15] M. Yao, L. Zhang, J. Ma, L. Zhou, On airborne transmission and control of SARS-Cov-2, Science of The Total Environment, Volume 731, 2020, 139178, ISSN 0048-9697, https://doi.org/10.1016/j.scitotenv.2020.139178.

[16] L. Stefanutti, Applicazioni di impianti di climatizzazione. Hospital, Tecniche Nuove Editor (Chapter 14), 1996.

[17] AIA – American Institute of Architects, Guidelines for Design and Construction of Hospital and Healthcare Facilities, American Institute of Architects Press, Washington, DC, 2006.

[18] H. Qian, X. Zheng, Ventilation control for airborne transmission of human exhaled bio-aerosols in buildings, Journal of Thoracic Disease, 2018;10(Suppl 19):S2295-S2304.

[19] R.M. Lynch, R. Goring, Practical Steps to Improve Air Flow in Long-Term Care Resident Rooms to Reduce COVID-19 Infection Risk. Journal of the American Medical Directors Association, JAMDA 21 (2020), pp. 893-894.

[20] B. Zhao, Y. Liu, C. Chen, Air purifiers: A supplementary measure to remove airborne SARS-CoV-2, Building and Environment, Volume 177, 2020, 106918.

[21] Y. Chartier, Y., and C. L. Pessoa-Silva. *Natural ventilation for infection control in health-care settings*. World Health Organization, 2009.

[22] H. Luo, J. Liu, C. Li, K. Chen, M. Zhang, Ultra-rapid delivery of specialty field hospitals to combat COVID-19: Lessons learned from the Leishenshan Hospital project in Wuhan, *Automation in Construction*, 2020, 103345.

[23] C. Chen, B. Zhao, W. Cui, L. Dong, N. An, X. Ouyang, The effectiveness of an air cleaner in controlling droplet/aerosol particle dispersion emitted from a patient's mouth in the indoor environment of dental clinics, Journal of the Royal Society Interface 7.48 (2010), pp. 1105-1118.

[24] S. Shah, COVID-19 and paediatric dentistry- traversing the challenges. A narrative review, Annals of Medicine and Surgery, 2020, Volume 58, pp. 22-33.

[25] P. Amoatey, H. Omidvarborna, M.S. Baawain, A. Al-Mamun, A. Bari, W.B. Kindzierski, Association between human health and indoor air pollution in the Gulf Cooperation Council (GCC) countries: a review. *Reviews on Environmental Health*, *1*(ahead-of-print), 2020.

[26] P. Amoatey, H. Omidvarborna, M.S. Baawain, A. Al-Mamun, Impact of building ventilation systems and habitual indoor incense burning on SARS-CoV-2 virus transmissions in Middle Eastern countries. *Science of The Total Environment*, 2020, 139356.

[27] Shiu EYC, Leung NHL, Cowling BJ. Controversy around airborne versus droplet transmission of respiratory viruses. Curr Opin Infect Dis [Internet]. 2019 Aug;32(4):372–9. Available online: https://pubmed.ncbi.nlm.nih.gov/31259864/. Accessed in November 2021

[28] Memarzadeh F, Olmsted RN, Bartley JM. Applications of ultraviolet germicidal irradiation disinfection in health care facilities: Effective adjunct, but not stand-alone technology. Am J Infect Control [Internet]. 2010;38(5 SUPPL.):S13–24. Available from: Doi: 10.1016/j.ajic.2010.04.208.

[29] ASHRAE Standard 185.2-2014 -- Method of Testing Ultraviolet Lamps for Use in HVAC&R Units or Air Ducts to Inactivate Microorganisms on Irradiated Surfaces, American Society of Heating Refrigerating and Air-Conditioning Engineers, Atlanta, GA, USA.

[30] L. Morawska, J.W. Tang, W. Bahnfleth, P.M. Bluyssen, A.Boerstra, G.Buonanno, J. Cao, S. Dancer, A. Floto, F. Franchimon, C.Haworth, J. Hogeling, C. Isaxon, J. L. Jimenez, J. Kurnitski, Y. Li, M. Loomans, G. Marks, L. C. Marr, L. Mazzarella, A. K. Melikov, S. Miller, D. K. Milton, W. Nazaroff, P.V. Nielsen, C.Noakes, J. Peccia, X. Querol, C. Sekhar, O. Seppänen, S. Tanabe, R. Tellier, K.W. Tham, P. Wargocki, A. Wierzbicka, M. Yao, How can airborne transmission of COVID-19 indoors be minimised?, Environment International, Volume 142, 2020,105832, ISSN 0160-4120, https://doi.org/10.1016/j.envint.2020.105832.

[31] S. Faridi, S. Niazi, K. Sadeghi, K. Naddafi, J. Yavarian, M. Shamsipour, N. Zahra S. Jandaghi, K. Sadeghniiat, R. Nabizadeh, M. Yunesian, F. Momeniha, A. Mokamel, M. Sadegh Hassanvand, T. Mokhtari Azad, A field indoor air measurement of SARS-CoV-2 in the patient rooms of the largest hospital in Iran, Science of The Total Environment, Volume 725, 2020, 138401.

[32] P. Kumar, L. Morawska, Could fighting airborne transmission be the next line of defence against COVID-19 spread?, City and Environment Interactions, 2019, Volume 4, 100033

[33] A. Franco, F. Leccese, Measurement of CO2 concentration for occupancy estimation in educational buildings with energy efficiency purposes, Journal of Building Engineering, 2020, 101714.

[34] S. Peng, Q. Chen, E. Liu, The role of computational fluid dynamics tools on investigation of pathogen transmission: Prevention and control, Science of The Total Environment, 2020, 142090.

[35] Srebric, J., Chen, Q., & Glicksman, L. R. (2000). A coupled airflow and energy simulation program for indoor thermal environmental studies. Massachusetts Inst. of Tech., Cambridge, MA (US).

[36] Yang, J., Sekhar, C., Wai, D. C. K., & Raphael, B. (2013). Computational fluid dynamics study and evaluation of different personalized exhaust devices. HVAC&R Research, 19(8), 934-946.

[37] Cho, J., Woo, K., & Kim, B. S. (2019). Removal of Airborne Contamination in Airborne Infectious Isolation Rooms. ASHRAE Journal, 61(2), 8-21.

[38] Italian Government, Decreto interministeriale 26 giugno 2015, Applicazione delle metodologie di calcolo delle prestazioni energetiche e definizione delle prescrizioni e dei requisiti minimi degli edifici. [in Italian]

[39] Covenant of Mayors for Climate and Energy: Default emission factors for local emission inventories (2017). European commission publications. Available online: https://publications.jrc.ec.europa.eu/repository/bitstream/JRC107518/jrc_technical_reports_-_com_default_emission_factors-2017.pdf: Accessed in November 2021

[40] U.S. Department of Energy. EnergyPlus simulation software, 960 Version 8.1.0.

[41] DesignBuilder v. 4.6. Available online ⟨http://www.designbuilder.co.uk/⟩. Accessed in November 2021

[42] Noh, K. C., Han, C. W., & Oh, M. D. (2008). Effect of the airflow rate of a ceiling type air-conditioner on ventilation effectiveness in a lecture room. International journal of refrigeration, 31(2), 180-188.

[43] Ascione, F., Bellia, L., & Capozzoli, A. (2013). A coupled numerical approach on museum air conditioning: Energy and fluid-dynamic analysis. Applied energy, 103, 416-427.

[44] Ghadikolaei, F. M., Ossen, D. R., & Mohamed, M. F. (2020). Effects of wing wall at the balcony on the natural ventilation performance in medium-rise residential buildings. Journal of Building Engineering, 101316.

[45] Buratti, C., Palladino, D., & Moretti, E. (2017). Prediction of indoor conditions and thermal comfort using CFD simulations: A case study based on experimental data. Energy Procedia, 126, 115-122.

[46] Mendez, C., San José, J. F., Villafruela, J. M., & Castro, F. (2008). Optimization of a hospital room by means of CFD for more efficient ventilation. Energy and Buildings, 40(5), 849-854.

[47] Piano scuola 2020-2021, Documento per la pianificazione delle attività scolastiche, educative e formative in tutte le Istituzioni del Sistema nazionale di Istruzione. Available online: https://www.miur.gov.it/documents/20182/2467413/Le+linee+guida.pdf/4e4bb411-1f90-9502-f01e-d8841a949429?version=1.0&t=1593201965918. Accessed in November 2021

[48] ASHRAE. Method of testing for rating the performance of air outlets and inlets. ANSI/ASHRAE Standard 70-1991; 1991.

[49] ISO 7730:1994. Moderate thermal environments — Determination of the PMV and PPD indices and specification of the conditions for thermal comfort, 1994.

[50] UNI 10339 - Italian Organization for Standardization. Norma UNI 10339: Impianti areaulici ai fini di benessere. Generalità, classificazione e requisiti. Regole per la richiesta di offerta, l'offerta, l'ordine e la fornitura. [in Italian]

[51] UNI – Italian Unification Body. UNI 10351 Materiali e prodotti per l’edilizia – Proprietà termoigrometriche –Procedura per la scelta dei valori di progetto. 2015. (In Italian).

[52] ISO – International Organization for Standardization. ISO 6946: Building components and building elements – Thermal resistance and thermal transmittance – Calculation methods. 2017.

[53] UNI – Italian Unification Body. UNI EN ISO 13786 Thermal performance of building components - Dynamic thermal characteristics - Calculation methods. 2018.

[54] UNI – Italian Unification Body. UNI EN 12464-1: Luce e illuminazione – Illuminazione dei posti di lavoro – Parte 1: Posti di lavo interni. (In Italian), 2011.

[55] L. Li, Q.Li, L.Huang, Q.Wang, A.Zhu, J.Xu, Z. Liu, H.Li, L.Shi, R.Li, M.Azari, Y.Wang, X. Zhang, Z. Liu, Y. Zhu, K. Zhang, S. Xue, M.C.G. Ooi, D.Zhang,

A.Chan, Air quality changes during the COVID-19 lockdown over the Yangtze River Delta Region: An insight into the impact of human activity pattern changes on air pollution variation, Science of The Total Environment, Volume 732, 2020, 139282, ISSN 0048-9697, https://doi.org/10.1016/j.scitotenv.2020.139282.

[56] Rui Bao, Acheng Zhang, Does lockdown reduce air pollution? Evidence from 44 cities in northern China, Science of the Total Environment, Volume 731, 2020, 139052, ISSN 0048-9697, https://doi.org/10.1016/j.scitotenv.2020.139052.

[57] J.M. Baldasano, COVID-19 lockdown effects on air quality by NO2 in the cities of Barcelona and Madrid (Spain), Science of The Total Environment, 2020, 140353, ISSN 0048-9697, https://doi.org/10.1016/j.scitotenv.2020.140353.

[58] B. Rugani, D. Caro, Impact of COVID-19 outbreak measures of lockdown on the Italian Carbon Footprint, Science of The Total Environment, Volume 737, 2020, 139806, ISSN 0048-9697, https://doi.org/10.1016/j.scitotenv.2020.139806.

[59] J.A. Oldekop, R. Horner, D. Hulme, R. Adhikari, B. Agarwal, M. Alford, O. Bakewell, N. Banks, S. Barrientos, T. Bastia, A.J. Bebbington, U. Das, R. Dimova, R. Duncombe, C. Enns, D. Fielding, C. Foster, T. Foster, T. Frederiksen, P. Gao, T. Gillespie, R. Heeks, S. Hickey, M. Hess, N. Jepson, A. Karamchedu, U. Kothari, A. Krishnan, T. Lavers, A. Mamman, D. Mitlin, N. M.Tabrizi, T.R. Müller, K. Nadvi, G. Pasquali, R. Pritchard, K. Pruce, C. Rees, J. Renken, A. Savoia, S. Schindler, A. Surmeier, G. Tampubolon, M. Tyce, V. Unnikrishnan, Y. Zhang, COVID-19 and the case for global development, World Development, 2020, Volume 134, 105044.

[60] Z. Li, D.H.C Chow, D. Ding, J. Ying, Y. Hu, H. Chen, W. Zhao, The development and realisation of a multi-faceted system for green building planning: A case in Ningbo using the fuzzy analytical hierarchy process, Energy and Buildings, 2020, Volume 226, 110371.

[61] A. Santangelo, S. Tondelli, Occupant behaviour and building renovation of the social housing stock: Current and future challenges, Energy and Buildings, 2017, Volume 145, pp. 276-283.

[62] D. Kolokotsa, M. Santamouris, Review of the indoor environmental quality and energy consumption studies for low income households in Europe, Science of The Total Environment, 2015, Volume 536, pp. 316-330.

[63] F. Ascione, Energy conservation and renewable technologies for buildings to face the impact of the climate change and minimize the use of cooling, Solar Energy, 2017, Volume 154, pp. 34-100.

[64] M. Santamouris, Innovating to zero the building sector in Europe: Minimising the energy consumption, eradication of the energy poverty and mitigating the local climate change, Solar Energy, 2016, Volume 128, pp. 61-94.

[65] J. Tai Kim, M. S. Todorovic, Towards sustainability index for healthy buildings—Via intrinsic thermodynamics, green accounting and harmony, Energy and Buildings, 2013, pp. 627-637,

[66] R. Gupta, A. Bruce-Konuah, A. Howard, Achieving energy resilience through smart storage of solar electricity at dwelling and community level, Energy and Buildings, 2019, Volume 195, pp. 1-15.

[67] D. Chiaramonti, K. Maniatis, Security of supply, strategic storage and Covid19: Which lessons learnt for renewable and recycled carbon fuels, and their future role in decarbonizing transport?, Applied Energy, 2020, Volume 271, 115216.

[68] EU Commission and Parliament, Directive 2010/31/EU of the European Parliament and of the Council of 19 May 2010 on the energy performance of buildings (EPBD Recast). Off. J. Eur. Union 2010, Available online: https://eurlex.europa.eu/LexUriServ/LexUriServ.do?uri=OJ:L:2010:153:0013:0035:EN:PDF. Accessed in November 2021

[69] Directive (EU) 2018/844 of the European Parliament and of the Council of 30 May 2018. Available online: https://eur-lex.europa.eu/legal-content/EN/TXT/PDF/?uri=CELEX:32018L0844&from=IT. Accessed in November 2021

[70] Wargocki, P., Porras-Salazar, J.A., Contreras-Espinoza, S., Bahnfleth, W. The relationships between classroom air quality and children's performance in school (2020) Building and Environment, 173, art. no. 106749.

CHAPTER 5.

Energy refurbishment of the building/HVAC system

Previous chapters (CHAPTER 1 and CHAPTER 4) have illustrated the refurbishment of different case studies, in the first case through passive strategies for the building envelope, in the second case intervening on the systems for the microclimatic control even evaluating the improvement of indoor air quality. This chapter will show the energy refurbishment of the whole building/HVAC systems for a case study in Greece – a student dormitory that belongs to the National and Kapodistrian University of Athens (NKUA) – and for three different Italian residential buildings, representative of the building typologies of the Italian building stock, belonging to different climates and construction ages. Finally, the last section reports some overviews about how the occupants' wrong habits could affect the results of a BES, evidencing the importance of considering a non-standard occupant profile in energy simulations. This investigation has been partly developed during a third-year 6-month PhD period, just under the guidance of professors from the NKUA.

5.1. The scientific and normative background

The energy efficiency of buildings is a key factor of the international policy actions, to favor the transition to a green society. As widely narrated in CHAPTER 1, starting from 2002, the EU guidelines have progressively introduced the mandatory standard of high performing buildings, for what concerns the energy performance, by establishing firstly the mandatory refurbishment of the existing building stock when renovated partly or globally (Directive 2002/91/EU [1]), then the cost-optimal methodology for choosing the best trade-off between energy performance and investments, followed by the mandatory fulfillment of nearly zero-energy standard for new public (2019) and private buildings (2021) (Directive 2002/91/EU [2] and Delegated

Regulation 244/2012 [3]), then the exemplary role of the public hand in refurbishing the owned buildings of at least the 3% yearly (Directive 2012/27/EU [4]), and finally by extending the nZEB target to the overall building stock, for a decarbonized built environment within 2050 (Directive 844/2018/EU [5]).

From the technical point of view, there are several studies focused on building energy conservation through energy demand reduction based on building envelope interventions [6], [7] also by considering the application of innovative materials as mineral fiber insulation panels [8], vacuum insulation panels [9], hemp-lime mortar [10], thermochromic coatings [11].

Several authors focused their researchers on the optimization of the heating and cooling system configurations [12], [13]also considering the cost-effectiveness of smart thermostat systems [14] and the integration of renewable energy system with some innovative technologies as the organic transparent photovoltaics [14], [15] or the photovoltaic-thermoelectric-battery wall system [16]. Really, the reduction of energy needs for what corners the building envelope, can be achieved in two different ways, and thus by “defending” the buildings from the surrounding environment (here, the word “insulation”) or by determining a favorable interaction with this (i.e., the so-called “bioclimatic technologies”). A wide discussion of both traditional and innovative building envelope technologies is proposed in [17], together with an overview of several passive and active possible exploitation of renewables. Really, currently, the real challenge is to provide not merely an energy-efficient construction sector, but also to allow livability of the built environment, for what concerns healthiness, comfortable conditions of temperature and relative humidity, noise conditions, and indoor air quality. One of the side dramatics effects of the 2020 worldwide pandemic was the lockdown for millions of persons, where houses were not so comfortable to host suitably people all day long, mainly where the energy poverty and the so-called “digital divide” exacerbated an irrelated living condition. The mandatory attention to the improvement of living conditions for people, by retrofitting deeply the building sector, and thus allowing reduction of energy demands, improve indoor air quality, mitigate the overheating of our cities (that, dramatically, increases mortalities due to uncomfortable conditions), eradication of energy poverty are all issues urgent and challenging, as admirably shown by Santamouris [18].

During the COVID-19 pandemic, the necessity of healthy and safe spaces has become prominent, and this means design effective mechanical ventilation systems to control the indoor air quality. Therefore, the approach for a building energy refurbishment must consider both the building envelope and the active systems for the microclimatic control, to guarantee the reduction of the energy demand but also livability and healthiness of spaces. In the following sections (5.2 and 5.3), different energy refurbishments will be presented for different case studies, intervening on all three levers of energy efficiency: passive and active systems, and plants from renewable energy sources.

5.2. A student dormitory in Athens: a complete renovation

This section investigates the theoretical assessment of the performance of applied energy retrofit and seismic enhancement measures for a student dormitory belonging to the National and Kapodistrian University of Athens This study is part of a wider investigation for the European research project *“Proactive synergy of integrated Efficient Technologies on buildings’ Envelopes (Pro-GET-OnE)”* - H2020-EE-2016-2017/H2020-EE-2016-PPP [19]. The building case study is located within the University Campus (37.97°N 23.76°E) and it was built in 1986. The structure, in reinforced concrete, is characterized by a rectangular shape (56.6 m × 15.4 m), with four floors above ground and a basement, with an overall gross building area of approximately 3642 m^2. Each floor, with an area of 725 m^2, hosts 36 single-bed rooms for students, with the exception of the ground-floor, which hosts 30 rooms (Figure 5.1). As shown in the energy audit carried out for this building [20], interventions to improve energy efficiency and student’s comfort conditions are necessary.

Figure 5.1 - Location (a), aerial view (b) and façade (c) of the building under investigation.

Starting from a calibrated numerical model of the building state of fact, carried out in [20], the present investigation deeply examines selected renovation measurements to evaluate the building refurbishment both under energy and environmental point of view. Moreover, thermal and visual comfort are also evaluated, in accordance with the aim of Pro-GET-onE project. More in detail, the application of different inteGrated Efficient Technologies (GET) will be presented considering different types of solutions such as the addition of *Extra Room* (ER), *Sun-Spaces* (SS) and *Balconies* (BAL). The simulation tools used for the purposes of this study are EnergyPlus v. 9.2 [21] and DesignBuilder v. 6.1 [22], providing the graphical definition of geometry, dimensions and positions of the thermal envelope.

A detailed description of each selected solution is presented in terms of:

- Geometry and spaces reorganization.
- Compositions (i.e., materials, thicknesses and layers) of the opaque and transparent building envelope elements.
- HVAC types and their operation.

In the following sub-section (5.2.1), the methodological approach is presented to highlight all the improvements and variations that occurred for the post-retrofit cases compared to the existing ones. Thus, the outcomes of this investigation could be used as a starting point for further comparison with the in-field measures which will be carried out in the next steps of the Project.

5.2.1. The methodological approach for the post-retrofit evaluation

Energy and environmental impact

The post-retrofit scenario of the building is evaluated by means of Building Energy Performance Simulations (BEPS), a transient energy analysis, widely presented in section 2.1.1. The analysis was necessary to obtain the results in terms of the primary energy demand for different end-uses or the energy consumptions for different energy carriers, normalized on the net conditioned building area.

The values of the primary energy conversion factors refer to the local legislation in force (*KENAK* in Greece [23]) and are 0.345 for electricity and 0.953 for natural gas. Regarding the environmental impact of energy consumptions, all data are expressed in terms of CO_2 emissions, and the emission factors refer to the Greek legislation [23], and are 0.196 $tCO_{2\text{-}eq}$/MWh for natural gas and 0.989 $tCO_{2\text{-}eq}$/MWh for electricity.

Finally, a monthly trend of the annual amount of electricity from Photovoltaic (PV) and thermal energy produced by solar panels is also reported, only for the post retrofit scenario. Their percentage of coverage with respect to the energy carriers is also provided.

Thermal and visual comfort

Thermo-hygrometric comfort and daylight analysis were investigated on an hourly basis and with the use of a room by room approach since global data referred to the whole building are not very significant and are also difficult to be interpreted. Thus, an in-depth analysis of hourly data for various rooms is shown. In this way, any effect on the occupant's comfort conditions can be directly highlighted by the application of different GET-systems. The rooms chosen for this analysis are located on the ground, first and second floor and in two different orientations, East and West. They are double rooms for which either ER, SS, or BAL solutions are applied. In this way, it is possible to have a general overview of the application of the three different scenarios proposed in Pro-GET-onE project.

To evaluate the thermal comfort conditions within the indoor environment, the international standard ISO 7730 [24] was taken into consideration. This latter presents a method for predicting the general thermal sensation and the percentage of thermal dissatisfaction of people exposed to moderate thermal environments. More precisely, it enables a numeric determination and interpretation of thermal comfort levels by using the calculation of PMV (Predicted Mean Vote) and PPD (Predicted Percentage of Dissatisfaction) indices. According to the recommended comfort requirements, for people occupying spaces, the PPD must be less than 10% which corresponds to -0.5 <PMV <+ 0.5. In this investigation, both the passive effect of the new building envelope on the indoor thermal comfort and the effects of the addition of a cooling system on the thermal sensation of the occupants are described.

Concerning visual comfort analysis, the daylight illuminance contour plots and average daylight factor (DF) are generated for each selected room. For all calculations, the Radiance ray-tracing simulation engine through the DesignBuilder software [22] was used. It is considered that light can be transmitted through exterior and interior windows. Moreover, the shading and reflective effect of local shading devices along with component/assembly blocks are included. Window shading options such as slatted and diffusing blinds are not included in Radiance calculations. It is important to annotate that Radiance operates by using a statistical Monte Carlo approach, meaning that the results cannot be repeatable. In this study, standard settings are used such as the number of ambient bounces equal to 2 (maximum number of diffuse bounces computed by the indirect calculation). The height of the "working plane" (i.e., the considered reference surface) above the floor level for each zone in the daylight simulation is set at 0.7 m. The sky model selected is an overcast day with illuminance at the Zenith equal to 10000 lux (overcast model).

5.2.2. The building renovation

In this subsection, a detailed description of the GET-implementation and HVAC system replacement is presented for the case study. The refurbishment of the dormitory consists of four main interventions:

- The addition of new volumes.
- The replacement of the heating, cooling, and Domestic Hot Water (DHW) systems.
- The addition of thermal insulation for the building envelope.
- The addition of two renewable energy systems.
- The replacement of the electrical equipment and lighting system.

In the following paragraphs, a detailed description of the interventions is provided in comparison with the current state of the building.

Modification of space geometry

With reference to the present case study, a re-distribution of the internal spaces and therefore, of the thermal zones, was carried out in order to provide additional individual space for the inhabitants. Figure 5.2 and Figure 5.3 depict the layout of the living spaces before and after the renovation actions. The common areas are marked in blue color, the individual spaces in orange and the private spaces, added due to the application of different GET systems, in yellow. These systems are: *Extra-Room* (ER), *Sun-Space* (SS) and *Balcony* (BAL). In total, the gross floor area was increased by around 35%. Initiating from the available vectorial plans and prospects, the geometrical features of all elements of the building were drawn for the refurbished case. In Figure 5.4, the rendered view of the building model is presented, for both the pre and post-retrofit stages. The surrounding buildings have been also modelled in order to take into account any possible shadow on the examined building. The main geometrical information and data about the opaque and transparent surfaces of the building envelope are shown in Table 5.1. The window-wall ratio increases from 36% to 44%, approximately.

Figure 5.2 - Plans of the ground floor, before (a) and after (b) the renovation.

Figure 5.3 - Plans of the first floor, before (a) and after (b) the renovation

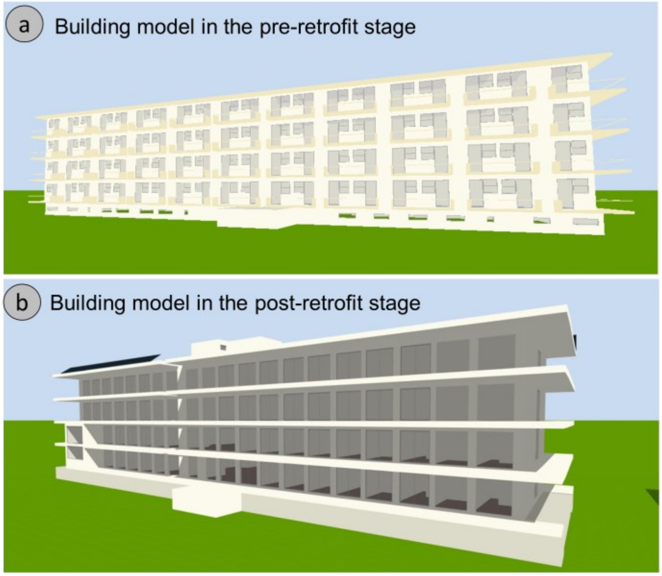

Figure 5.4 - Rendered views of the building model in the pre-retrofit (a) and post retrofit (b) stage.

Table 5.1 - Opaque and transparent building envelope areas.

Pre-retrofit stage	Total	North	East	South	West
Gross Wall Area [m^2]	2009.63	207.39	797.60	207.75	796.88
Above Ground Wall Area [m^2]	1808.96	180.52	724.06	180.72	723.67
Window Opening Area [m^2]	649.38	53.86	271.18	51.93	272.42
Gross Window-Wall Ratio [%]	32.31	25.97	34.00	24.99	34.19
Above Ground Window-Wall Ratio [%]	35.90	29.83	37.45	28.73	37.64
Post-retrofit stage					
Gross Wall Area [m^2]	2373.73	263.57	923.30	263.48	923.38
Above Ground Wall Area [m^2]	2019.49	219.98	789.80	219.87	789.83
Window Opening Area [m^2]	884.40	30.21	407.49	31.56	415.13
Gross Window-Wall Ratio [%]	37.26	11.46	44.13	11.98	44.96
Above Ground Window-Wall Ratio [%]	43.79	13.73	51.59	14.35	52.56

Thermo-physical properties of the new building envelope

Thermal insulation of the building envelope was applied to the external walls, slabs and the stair block. In particular, the opaque envelope of the refurbished building demonstrates the following thermo-physical properties:

- The external walls have a thermal transmittance (U_{value}) of 0.29 W/m^{2}K (pre-retrofit U_{value}= 1.69 W/m^{2}K) and consist, starting from the outside, of 1 cm of inner plaster, 10 cm of thermal insulation (thermal conductivity 0.034W/mK), 18 cm of brick and 1 cm of exterior plaster.
- The underground walls are made of 6 cm of polystyrene thermal insulation, 23 cm of reinforced concrete and 2.5 cm of plaster, with a total thermal transmittance equal to 0.48 W/m^{2}K (pre-retrofit U_{value}= 1.69 W/m^{2}K).
- The ground floor (U_{value} = 0.29 W/m^{2}K), starting from the inside, has the following layers: 2 cm of ceramic tiles, 6 cm of concrete, 10 cm of polystyrene thermal insulation, 20 cm of reinforced concrete(pre-retrofit U_{value}= 2.07 W/m^{2}K).
- The flat roof has a thermal transmittance of 0.28 W/m^{2}K (pre-retrofit U_{value}= 1.06 W/m^{2}K).and is composed of 1 cm of ceramic tiles, 15 cm of concrete, 10 cm of polystyrene thermal insulation, 15 cm of reinforced concrete and 2 cm of internal plaster.

Referring to the transparent envelope, windows have an aluminum frame with thermal break (U_{value} = 2.2 W/m^{2}K) and double glasses (U_{value} = 1.7 W/m^{2}K) with a Solar Factor (g) of 0.57 and a Light Transmission of 0.75.

Table 5.2 - Thermo-physical properties of the building envelope

U-value of:	**Pre-retrofit stage**	**Post-retrofit stage**	**Percentage variation**
External walls [W/m^{2}K]	1.69	0.29	-83%
Ground floor [W/m^{2}K]	2.07	0.30	-86%
Flat roof [W/m^{2}K]	1.06	0.28	-74%
Underground walls [W/m^{2}K]	1.69	0.49	-71%
Window frames [W/m^{2}K]	5.87	2.2	-63%
Window glass [W/m^{2}K]	5.87	1.7	-71%

Table 5.2 summarizes all thermal transmittances, before and after the retrofitting works, along with the respective percentages of variation. It is

important to note that for all building elements, a percentage reduction of more than 50% is achieved and the new values fall within the limits imposed by the local legislation in force [23].

HVAC system and operation

The plant's configuration consists of two main parts:

- Autonomous systems serve the two double rooms with ER placed on the ground floor and the two double rooms with SS on the first floor.
- A centralized system that serves the other rooms and the common areas.

Regarding the centralized plant, a mixed air-water system will be installed. For heating and cooling purposes four air-to-water heat pumps (HP), one for each floor, are available, characterized by a COP of 3.20 and by an EER of 2.95. The electric HP treats the heat transfer fluid (water) which is sent to each room through 2 pipe Fan Coil Units (FCU), with a constant water flow and variable speed fan. These air to water HP are also connected, per couple, to two water storages with a capacity of 500 L each. Within the bathrooms and common areas, for heating services, hot water radiators fueled by a gas heating boiler will be installed. The DHW will be provided by a gas boiler connected to a solar collector system (38 panels), south exposed, with 45° tilt and positioned on the rooftop. Finally, in each zone, a decentralized mechanical ventilation system, equipped with heat recovery and air filtration, can provide five different fresh air flows on the basis of five different fan speeds. The heat exchanger with double-crossed flow offers sensible and latent heat recovery, with a relative efficiency of up to 82%. A triple filter eliminates particulate matter (up to 98% of PM2.5 and all PM10), together with pollen, dust mites, spores and bacteria larger than 0.4 μm. A summary of the main technical data of the plant components is demonstrated in Table 5.3. Four autonomous systems will be installed in the two double rooms of the ground floor and in the two double rooms of the first floor, respectively. Those air-to-air HP provide warm air during winter and cold air during summer. The same systems also provide dehumidification and are equipped with an electronic filter (ePM1 90%, according to ISO 16890) to purify the air before supplying it into the rooms. Moreover, these compact systems are equipped with active thermo-dynamic heat recovery. This means that there is an interaction between the airflow taken from the external environment and the exhaust air taken from the indoor environment. The main technical features are summarized in Table 5.4. The systems here described replace the systems installed in the pre-retrofit building, widely specified in [20].

Table 5.3 - Technical data of HVAC centralized system.

	Characteristics	Manufacturer	Model	Zone
Heating and cooling services				
4 air to water HP connected to in-room FCU	Heating capacity: 53.0 kW; COP: 3.20; Cooling capacity: 53.3 kW; EER: 2.95.	CLIVET	ELFOEnergy Storm EVO; ELFOspace WALL 3	Rooms; common areas
2 water storage	Capacity: 500 l	FIORINI		
Gas heating boiler connected to hot water radiators	low-temperature boiler (92/42/EEC) Nominal capacity: 285 kW	WOLF	MKS 250	Common areas; bathrooms
DHW service				
Gas boiler connected to solar collectors	Efficiency of the gas boiler: 0.95 Number of solar collectors: 38 Area of a single solar collector: 1.8 m^2 Azimut: south Tilt angle: 45°			Common areas; bathrooms
Ventilation service				
Controlled mechanical ventilation with heat recovery and air filtration	5 fan speeds Air flow: 15 ÷ 41 m^3/h Thermal efficiency: 82 ÷ 69% Absorbed power 4.6 ÷ 20.6 W	THESAN	AIRCARE ES	Rooms
Controlled mechanical ventilation with heat recovery and air filtration	Air flow: 590 m^3/h			Common areas

Table 5.4 - Technical details of HVAC autonomous systems.

	Characteristics	Manufacturer	Model	Zone served
Heating and cooling services				
4 air to air HP	Heating capacity: 3.18 kW; SCOP: 3.83; Cooling capacity: 2.14 kW; SEER: 2.95.	CLIVET	ELFOPack CPAR	2 double rooms at ground floor and 2 double rooms at the first floor.
Ventilation service				
Controlled mechanical ventilation with heat recovery and air filtration	Total flow air provides to each room: 400 m³/h Recirculated flow air from each room: 100 m³/h Absorbed power 1.16 kW			

The schematic visualization of the HVAC system, developed in the building's numerical model through *DesignBuilder* software [22], is depicted in Figure 5.5, with reference to both the pre and post-retrofit stages.

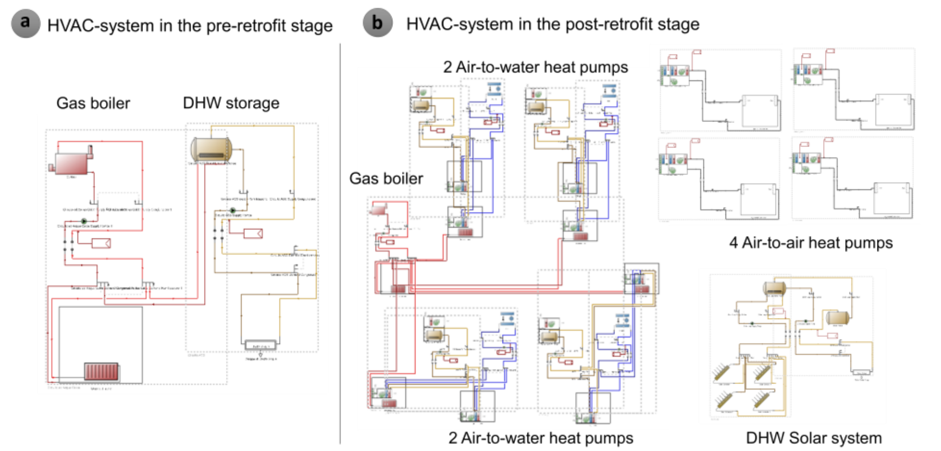

Figure 5.5 - Schematic visualization of the HVAC system.

The high-temperature boiler with low efficiency, present in the current state, has been replaced by new and more efficient systems. The old radiators have been replaced by FCU in the bedrooms and common spaces, which allow the occupants to achieve adequate thermal comfort conditions more quickly. Moreover, the addition of two new energy services, i.e. ventilation and cooling, contributes to the occupant's well-being. The net conditioned building area increases from 2584 m^2 (in the existing state) to 2681 m^2 (after the renovation).

Table 5.5 - Boundary conditions for the energy simulation of the building's post-retrofit stage

<table>
<tr><th colspan="6">INTERNAL GAINS</th></tr>
<tr><td rowspan="2">Lighting system [W/m^2]</td><td>7.5</td><td>Bedrooms and common areas – fluorescent lights</td><td colspan="2" rowspan="2">Occupancy [person/m^2]</td><td rowspan="2">0.05</td></tr>
<tr><td>4.0</td><td>Bathrooms – led lights</td></tr>
<tr><td colspan="3">Maximum use of artificial lighting is scheduled during the evening hours, a reduced use during the earlier morning and late afternoon, null in the remaining hours of the day and night</td><td colspan="3">The maximum occupancy in the building is scheduled until 8:00 am and from to 5:00 pm to 10:00 pm. During the diurnal daily hours, the building occupancy, is reduced by 75% and during the evening of 25%.</td></tr>
<tr><td colspan="3" rowspan="2">Light control according to the daylight illuminance (linear correlation)</td><td rowspan="2">Electric equipment [W/m^2]</td><td>4</td><td>Bedrooms and common areas</td></tr>
<tr><td>1</td><td>Bathrooms</td></tr>
<tr><th colspan="6">NATURAL VENTILATION AND INFILTRATION</th></tr>
<tr><td colspan="3">Natural ventilation</td><td colspan="3">0.56 ACH (scheduled as maximum during the diurnal hours, reduced of 50% during the evening and null during the night)</td></tr>
<tr><td colspan="3">Infiltration</td><td colspan="3">0.2 ACH – for 24h/day</td></tr>
<tr><th colspan="6">SET POINT TEMEPRATURE</th></tr>
<tr><td colspan="2">Heating setpoint [°C]</td><td>20</td><td colspan="2">Cooling setpoint [°C]</td><td>26</td></tr>
<tr><th colspan="6">AVAILABILITY</th></tr>
<tr><td colspan="6">Heating period</td></tr>
<tr><td colspan="3">Bedrooms and common areas – air to water HP</td><td colspan="3">From 7:00 am to 9:00 am, from 5 pm to 10 pm, from November 1st to March 31st</td></tr>
<tr><td colspan="3">Bathrooms and common areas – gas heating boiler</td><td colspan="3">From 7:00 am to 11 am, and form 6:00 pm to 10:00 pm, from November 1st to March 31st</td></tr>
<tr><td colspan="3">Ground floor and first floor double rooms – air to air HP</td><td colspan="3">From 7:00 am to 9:00 am, from 5 pm to 10 pm, from November 1st to March 31st</td></tr>
<tr><td colspan="6">Cooling period</td></tr>
<tr><td colspan="3">Bedrooms and common areas - air to water HP</td><td colspan="3">From 12:00 pm to 8:00 pm, from June 1st to September 30th</td></tr>
<tr><td colspan="3">Ground floor and first floor double rooms – air to air HP</td><td colspan="3">From 12:00 pm to 8:00 pm, from June 1st to September 30th</td></tr>
<tr><td colspan="6">Mechanical ventilation activation</td></tr>
<tr><td colspan="3">Bedrooms</td><td colspan="3">From 7:00 am to 9:00 am, from 5:00 pm to 10:00 pm, from November 1st to March 31st
From 12:00 pm to 8:00 pm, from April 1st to October 31st</td></tr>
</table>

Regarding the integration of Renewable Energy Sources (RES), three PV strings with a total power of 14.4 kW$_{peak}$ will be installed on the rooftop. In

detail, two strings with 5.7 kW_{peak} each will be placed to the southeast and northwest orientation, while one 3.0 kW_{peak} string is on the northeast. With reference to all of them, a tilt angle of 35° is selected. In The high-temperature boiler with low efficiency, present in the current state, has been replaced by new and more efficient systems. The old radiators have been replaced by FCU in the bedrooms and common spaces, which allow the occupants to achieve adequate thermal comfort conditions more quickly. Moreover, the addition of two new energy services, i.e. ventilation and cooling, contributes to the occupant's well-being. The net conditioned building area increases from 2584 m^2 (in the existing state) to 2681 m^2 (after the renovation).
Table 5.5, the main boundary conditions along with the operating mode used for the simulations are presented.

5.2.3. Results and discussion

In this subsection, all the results will be presented in comparison with the ones referred to the current state of the building, in order to achieve a clear overview of the benefits of the deep renovation process.

Energy and environmental analysis

An overview of the building's energy status, in terms of energy demand and greenhouse gas emission, is provided. More specifically, in Figure 5.6, the normalized primary energy demand for different end-uses over the whole year is shown. The normalized values refer to the net conditioned building area, which is 2584 m^2 (in the existing state) and 2681 m^2 (after renovation). It should be noted that the energy demand of auxiliaries has increased (+86%) if compared to the existing state, due to the addition of a mechanical ventilation system. The cooling demand has been also added. If on one hand, this leads to an increase of energy in such end-use, on the other hand, it contributes to the occupant well-being.

The values in Figure 5.6 represent the demand to satisfy each energy service, without taking into account the electricity converted by the PV system. If this latter is considered, the total primary energy savings reach 337’627 kWh/y, with a reduction of 51%.

Figure 5.7 depicts the amount of the required energy, considering the two different energy sources (electricity & natural gas) by taking into account merely the building as control volume. Thus, Figure 5.7a illustrates the electricity demand, deducting the amount produced by PV for the case of the post-retrofit stage; on the other hand, Figure 5.7b, shows the amount of natural gas. The percentages of reduction concerning the pre-retrofit stage are also illustrated.

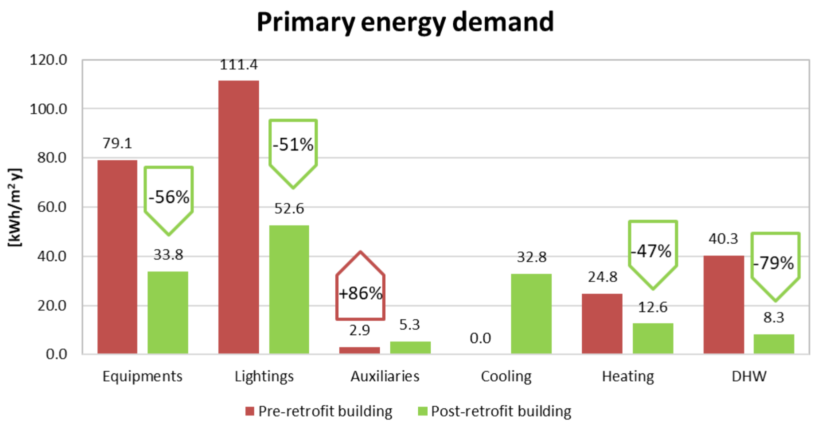

Figure 5.6 - Normalized primary energy demands

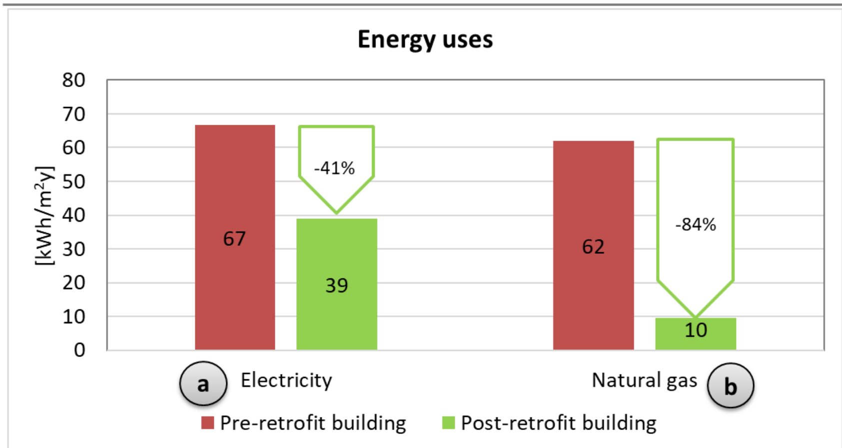

Figure 5.7 - Energy uses: electricity (a) and natural gas (b).

Focusing on the energy conversion systems enhanced by RES (present only in the post-retrofit scenario), Figure 5.8 shows the comparison between the electricity demand and the PV coverage. Moreover, in Figure 5.9, the total annual amount of electricity from PV and thermal energy from solar panels is reported. These latter are the energy vectors directly available and usable by the building. From the BEPS results, over one year, the PV system is able to cover 20% of the electricity demand, while the solar panels 50%, approximately.

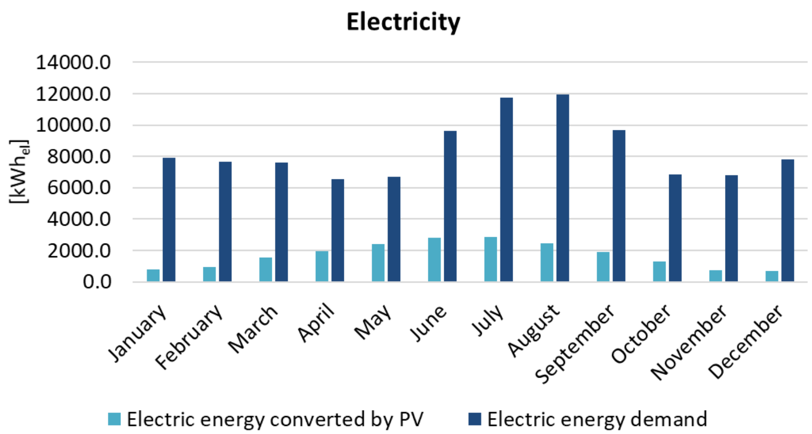

Figure 5.8 - Monthly amounts of electricity in the post-retrofit stage

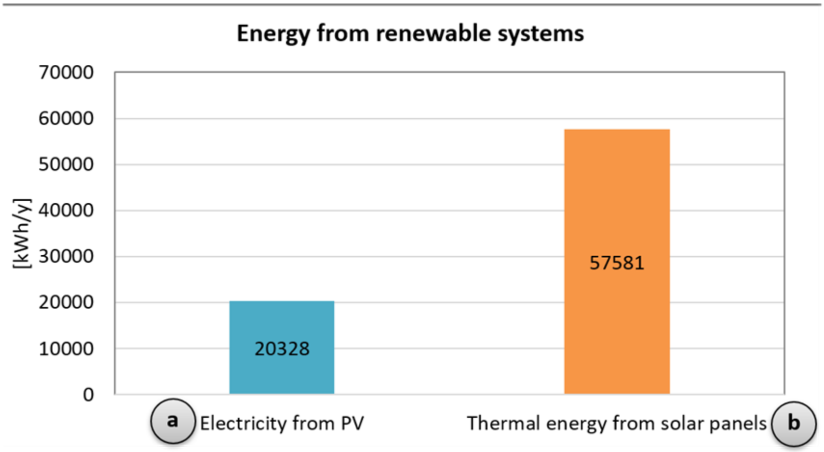

Figure 5.9 - Annual amounts of energy from renewable systems in the post-retrofit stage

Finally, referring to the CO_2 emissions, Figure 5.10 shows the comparison between the pre-retrofit and post-retrofit stages. It should be noticed that the electricity converted by PV has been considered. Throughout the whole year, the building refurbishment involves a reduction of 48% of CO_2 emissions among the existing building.

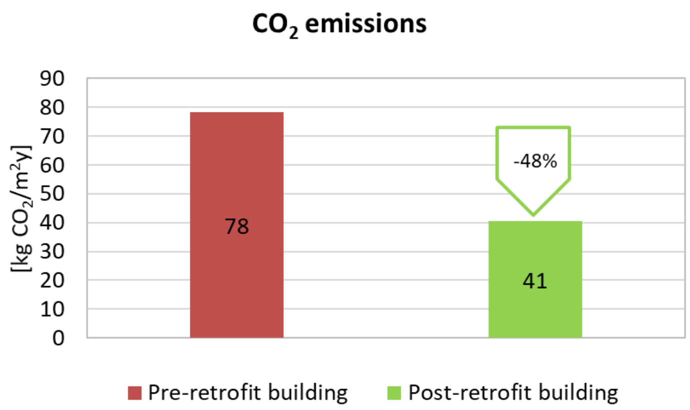

Figure 5.10 - CO_2 emissions for pre and post-retrofit stages

According to Greece the reference law Y.A. RIS / DEPEA / 85251 / 27.11.2018 “Approval of the National Plan for increasing the number of nearly zero energy buildings” (Government Gazette B '5447/2018) [25], the Athens dormitory meets the nZEB requirements. The Greek law establishes that a building can be considered nZEB if it is:

- at least A class, for new buildings and,
- at least B+, for an existing building - partial/deep renovation.

In this case, the asset rating evaluation was developed using the calculation with semi-stationary boundary conditions conducted by the constructor partners of Pro-GET-onE [19]. It was shown that the refurbished building under investigation will be classified in energy category B +, and so, as an existing building, it meets the nZEB requirements

Thermal and visual comfort

As mentioned above, indoor thermal comfort analysis is performed for some representative rooms located on the ground, first and second floor and in two different orientations, East and West (Figure 5.11). Those are the double rooms for which either the ER, SS, or BAL solutions were applied, in order to achieve a general overview of the application of the three different scenarios proposed by Pro-GET-onE [19]. In particular, the double rooms with ER are located on the ground floor and the ones with SS and BAL, on the first and second floor, respectively. The double rooms of the third floor were not considered in this analysis because they have balconies similar to those of the second floor and thus, thermal and visual comfort analysis would demonstrate similar results.

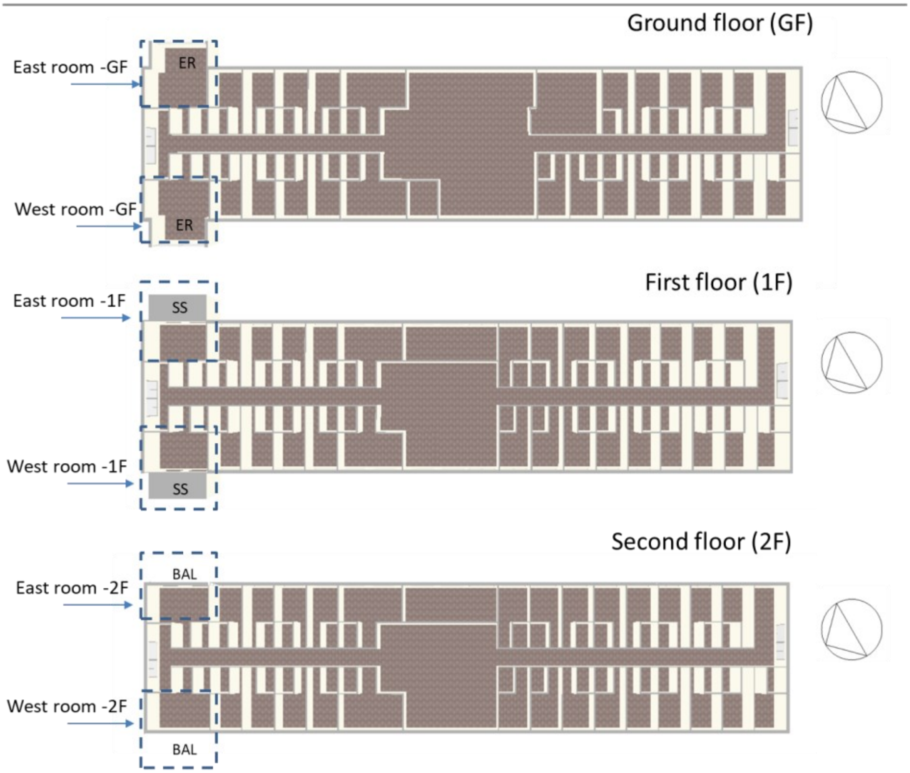

Figure 5.11 - Selected rooms for the investigation of thermal comfort conditions.

Regarding the application of ISO 7730 [24] thermal comfort model for warm months, the thermal resistance of clothing is set equal to 0.5 Clo while for cold months equal to 1.0 Clo. The metabolic rate for the students in the bedrooms is 140 W/person (mainly resting). For a suitable analysis, the PMV values must be shown on an hourly basis and thus, two days of interest were chosen for this study:

- *October 31st:* on which the heating systems are turned off, to examine the passive effect of the new building envelope on the indoor thermal comfort.
- *July 1st*: during which the cooling systems are operating (refurbished phase), to investigate how the addition of the cooling system can affect indoor comfort levels.

Concerning the selected days, the hourly trend of the PMV is depicted in Figure 5.12 for the ground floor, in Figure 5.13 and in Figure 5.14 for the first and second floor, respectively. The application of the ER (Figure 5.12), during the warm day ensures a reduction of the PMV, from about 2 (warm sensation) to less than 1, so relatively close to the desired thermal comfort zone (- 0.5 <PMV <+ 0.5). During the cold day, the difference between the pre and post retrofit stage is significant in the Western room, with an average difference equal to 0.5.

Furthermore, the application of SS (Figure 5.13) and BAL (Figure 5.14) during the warm day demonstrated values of PMV within or close to the desired comfort zone, due to the horizontal projections. It should be underlined that the sunspaces are considered as “open spaces”, therefore demonstrating a thermal behavior similar to the BAL solution. For those cases, PMV index is decreasing from 3 (hot) to ± 0.5 (around the thermal neutrality). In addition, for the cold day, SS or BAL solutions can provide a neutral thermal sensation among the slightly cool and cool sensations (-1 & -2) of the pre-retrofit stage.

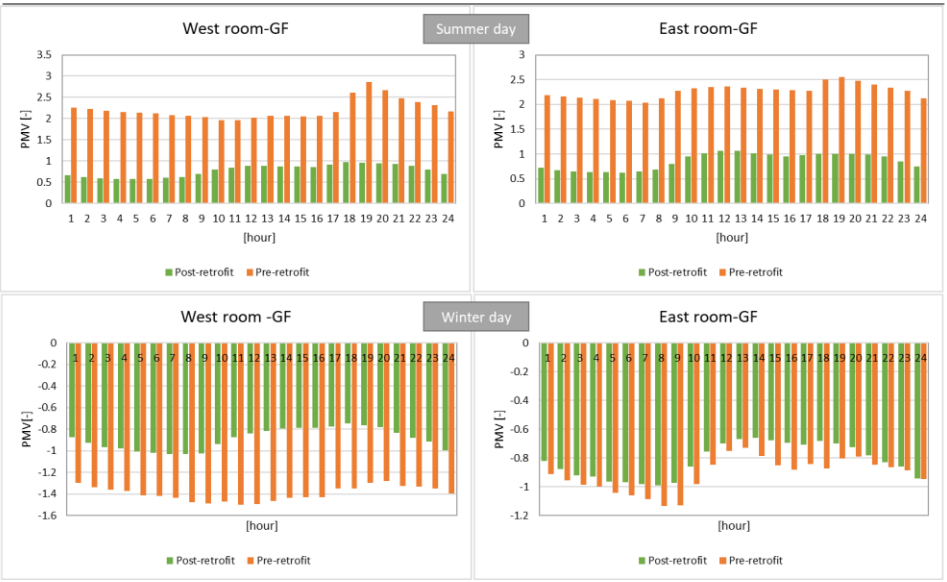

Figure 5.12 - PMV trends in the rooms of the ground floor (GF)

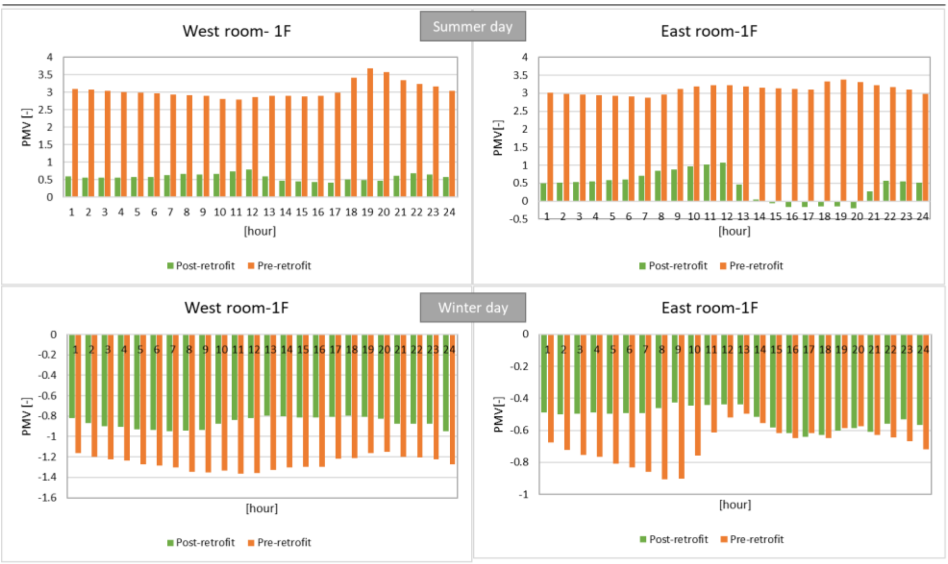

Figure 5.13 - PMV trends in the rooms of the first floor (1F)

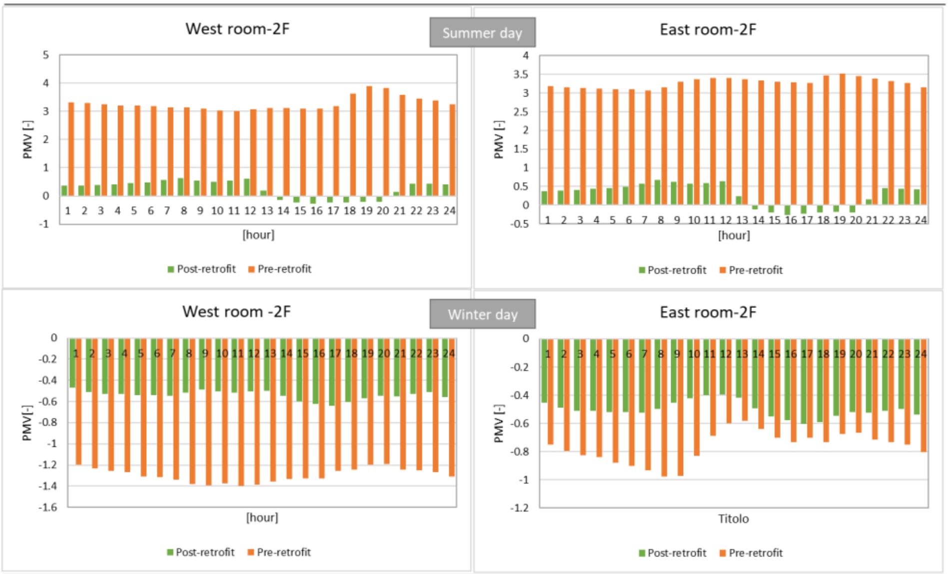

Figure 5.14 - PMV trends in the rooms of the second floor (2F)

The above results show that the developed GET solutions could be considered passive building envelope systems during cold months since they can guarantee thermal comfort of the occupants even when the HVAC systems are not switched on, thus determining energy savings related to the HVAC operation.

For warm days, it was found that the installation of a cooling system strongly affects the achievement of thermal comfort which otherwise would not be achieved. These results are also enhanced from Figure 5.15, which presents the PMV trends in the examined rooms during the whole warm period (June – September). Moreover, the presence of four compact HP (ELFOPack) in the rooms of the ground and first floor can achieve less fluctuant values of PMV if compared to the rooms of the second floor.

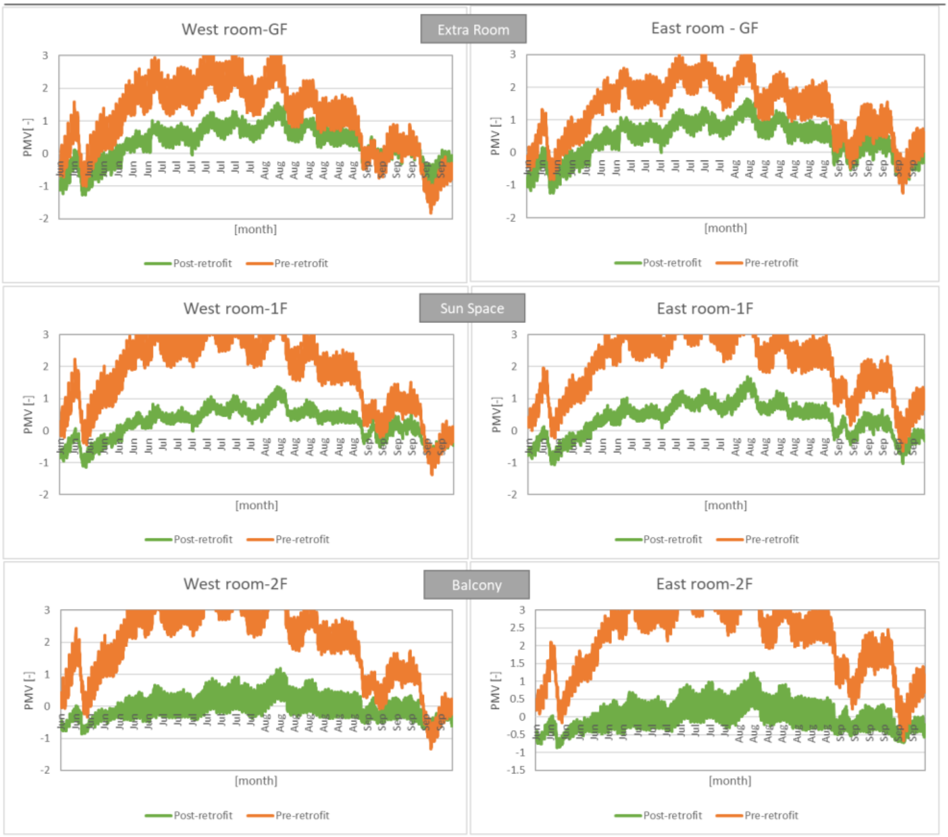

Figure 5.15 - PMV trends during the warm season (June – September)

Concerning daylight conditions simulated for the refurbished building, Figure 5.16 and Figure 5.18 illustrate the daylight contour maps of the six representative rooms. Those Figures depict the daylight distribution on the working plane (0.7 m). Grey color represents the areas with a DF lower than 2%. Comparing the daylight results of the rooms of the second floor in Figure 5.18, with those of the ground and first floor (Figure 5.16 and Figure 5.17, respectively) a remarked difference can be noticed. Indeed, for the second floor, the daylight illuminance levels are lower than those of the ground and first floor, because of the presence of the balconies.

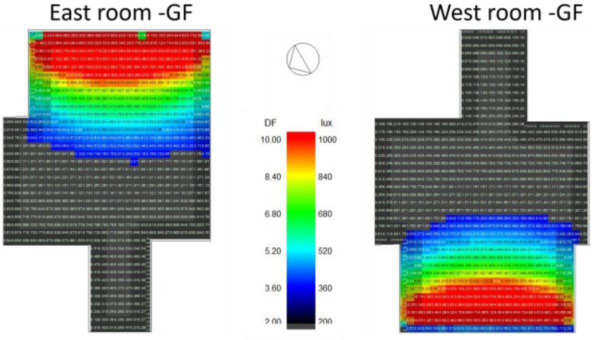

Figure 5.16 - Daylight distribution contour map of double rooms of the ground floor

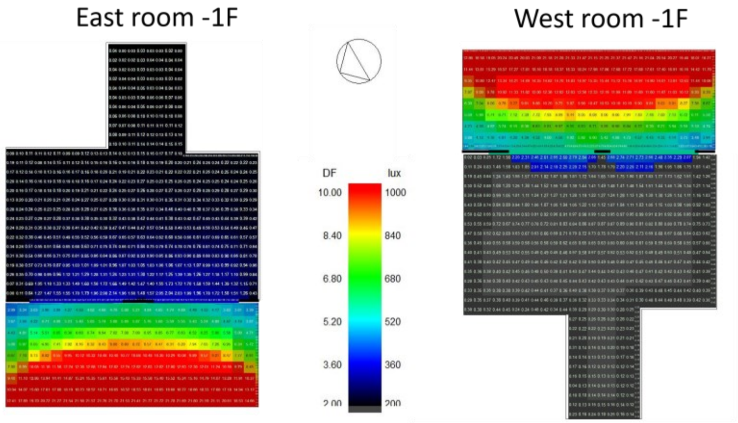

Figure 5.17 - Daylight distribution contour map of double rooms of the first floor

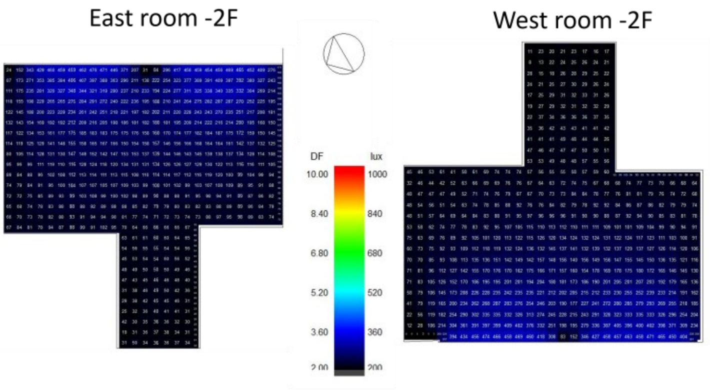

Figure 5.18 - Daylight distribution contour map of double rooms of the second floor

To compare pre and post-retrofit results, Table 5.6 demonstrates the average DF related to the six different rooms. The SS area was considered for the calculation since it could be occupied by the students. With the implementation of ER and SS, the average DF remains almost the same or increases, while the application of the BAL decreases the levels of DF. However, it should be emphasized that this calculation refers only to the illumination due to natural light. Nevertheless, all GET system solutions will be equipped with state-of-the-art lighting and control systems which will allow a suitable level of illumination to all users.

Table 5.6 - Average daylight factor (DF) in the pre and post-retrofit stage

Average Daylight Factor [%]			
	PRE-RETROFIT	POST-RETROFIT	
West room - GF	3.1	3.3	ER
East room - GF	3.0	4.0	
West room - 1F	3.2	3.2	SS
East room - 1F	3.0	3.5	
West room - 2F	3.3	1.3	BAL
East room - 2F	3.0	1.5	

5.2.4. Conclusive remarks

Section 5.2.3 has evidenced the benefits in terms of energy saving, reduction of CO_2 emissions, and visual and thermal comfort of seismic and energy redevelopment of the building/HVAC system for a selected construction site in Athens. In this case, the building renovation has interested also the building geometry and shape, indeed, new spaces (ER and SS) and balconies (BAL) were added according to the Pro-GET-onE [19].

The results, from an energy and environmental point of view, were found to be very promising. Indeed, the total primary energy saving is reaching 341’146 kWh/y, with a reduction of 51% while the CO_2 emissions will be reduced by approximately 49%. Moreover, the addition of two new energy services (i.e., the ventilation and the cooling systems), if on one hand determines an increase in energy demand only for that end-use, on the other hand, it contributes to the occupant’s well-being. This latter has been also demonstrated through an extensive thermal comfort analysis. Indeed, during the cooling season, in the pre-retrofit building, the occupants are constantly facing discomfort conditions (with slightly warm to hot sensation) while in the post-retrofit scenario the comfort sensation index PMV is close to the neutral range. Moreover, the results show that the developed GET solutions could be considered passive building envelope systems during cold periods since they can guarantee thermal comfort for the occupants even when HVAC systems are not switched on. Finally, the daylight analysis has shown that ER and SS, BAL solution could lead to a decrease of the average DF in the post-retrofit configuration. However, it should be noticed that all GET solutions will be equipped with state-of-the-art lighting and control systems which will allow an adequate level of illumination to all users.

In the following section (5.3), the energy refurbishment of three Italian residential buildings is reported. The study will show the energy benefits of the interventions but also the economic profitability taking into account the tax deduction planned by the "Recovery Decree" enacted in Italy as a social policy to face the COVID-19 emergency.

5.3. Residential buildings in Italy: Energy efficiency promotion and funding measures for green investments in buildings

COVID-19 pandemic brought economic crisis, significantly in the building sector, with also an increase of energy consumption in the residential sub-sector due to the more intensive energy use. The strategic plans put in place by the European Union to face this crisis aimed at environmental sustainability, by identifying buildings as a key perspective. In Italy, in 2020, it has been established a tax deduction of 110% (divided into 5 annual quotas) aimed at promoting energy efficiency measures for existing buildings, even for fulfilling the new requirements of the energy efficiency in buildings and cities provided by the Directive EU 844/2018. This section proposes a critical analysis of several passive and active energy efficiency measures for residential buildings, belonging to different climates and construction ages, employing both semi-stationary and dynamic approaches. Considering the energy, environmental and economic indicators, it is shown how the new funding program, widely described in sub-section 1.2.1, can boost the diffusion of energy efficiency measures characterized by the best energy performance, and not by the best cost/benefit ratio. Furthermore, the understanding of how the incentive scheme works can help in implementing any adjustment for supporting the diffusion of the nearly zero energy building standard among the various stakeholders involved in the construction sector and city sustainability.

5.3.1. The building case studies

The dynamic and steady-state analysis to investigate the funding program, was performed for different buildings, representative of typical typologies of the Italian building stock: a single-family building, named A, a four-story building, named B, and a ten-story building (high rise example), named C. In the following paragraphs, a detailed description is reported.

The single-family house (Building A)

The first building typology investigated is a single-family house of the 1980s, located in Italy. It is developed on three levels: a semi-basement floor (i.e., the garage) and two floors above the ground, as shown in Figure 5.19, with a total area of 230 m^2 and a surface to volume ratio of 0.71 m^{-1}. To define a case study representative of the Italian building stock, the TABULA WebTool has been used [26].

The building envelope has a structural frame in reinforced concrete. Walls are made of hollow masonry blocks, floor and roof slabs have mixed reinforced concrete and hollow bricks. The main features of the building are described in Table 5.7; the opaque building envelope is characterized by the following materials:

- Starting from the outside, the external walls are made up of 2 cm of plaster, 12 cm of aerated bricks, 3 cm of insulation, 10 cm of the air gap, 12 cm of aerated bricks, and 2 cm of lime plaster. The total thickness is 41 cm and the thermal transmittance (U_{value}) is 0.73 W/m^2K.
- The roof slab with a thickness of 27 cm and a thermal transmittance of 1.15 W/m^2K is made up of an external waterproofing coating of 3 cm, reinforced concrete and hollow blocks mixed slab of 22 cm, and a lime plaster of 2 cm.
- The slab between the garage and the floor above the ground has a thermal transmittance of 1.161 W/m^2K and a thickness of 0.38 cm (1.5 cm of tiles, 2 cm of lightweight concrete, 32 cm of reinforced concrete and hollow blocks mixed slab, 2 cm of lime plaster).

The windows are double glazed with an air gap (U_g = 2.80 W/m^2K) and wooden frames (U_f = 2.31 W/m^2K). There are no shading systems and the total solar factor (g_{gl}) is 0.75. The microclimatic control in the heating season and the production of DHW are provided by a centralized gas boiler. Efficiencies of the generation and distribution subsystem are low (0.72 and 0.86, respectively). In-rooms hot water radiators are installed, and the indoor temperature control is centralized for the whole building. The building is not provided with mechanical cooling.

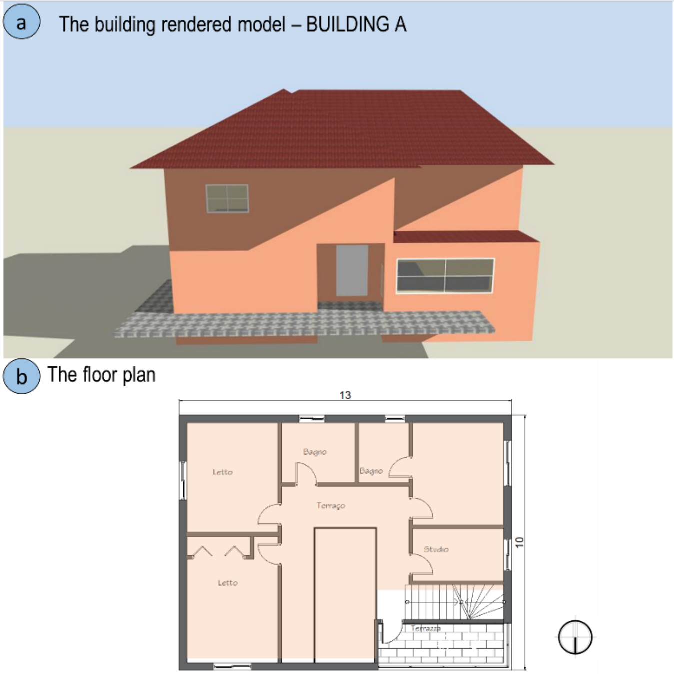

Figure 5.19 - The single-family house: a) Rendered view of the building, b) Indoor distribution of the building for the first floor

Table 5.7 - Main building features – BUILDING A

BUILDING GEOMETRY					
Total Building Area [m^2]	230	Total building Volume [m^3]			601
Net Conditioned Building Area [m^2]	223	Conditioned total volume [m^3]			586
Gross Roof Area [m^2]	198	Surface to volume ratio [1/m]			0.71
CONDITIONED AND UNCONDITIONED ZONES					
Number of conditioned zones 12		Number of unconditioned zones		1	
ENVELOPE - WINDOW TO WALL RATIO					
	Total	North	East	South	West
Gross Wall Area [m^2]	254	70	57	70	57
Window Opening Area [m^2]	21	6	4	5	6
Gross Window-Wall Ratio [%]	8	9	7	7	10
DHW SYSTEM					
The DHW is provided by the centralized gas boiler					
THERMAL TRANSMITTANCE					
External walls [W/m^{2}K]	0.73	Floor [W/m^{2}K]			1.62
Roof floor [W/m^{2}K]	1.15				
Glass (windows) [W/m^{2}K]	2.80	Frame (windows) [W/m^{2}K]			2.31

The four-floors building (Building B)

The second building case study is a four-floor building, built during the nineties. The overall height is 13.2 m and the floor plan is quite rectangular. The total area is 1.318 m^2 and the volume is 3986 m^3. Each floor has four apartments, equally distributed and with only one front naturally lightened. The flats, having an inter-floor height of 3 m, are connected by a staircase facing the northwest. The longest façade of the building, 30 m long, is exposed to the northwest and southeast, while the blind façades, 13 m long, to the northeast and southwest as evident in Figure 5.20.

For what concerns the building envelope, the following opaque components are present:

- The external walls have a thermal transmittance of 0.51 and a thickness of 34 cm (external plaster 2 cm, hollow bricks 14 cm, rock wool insulation 4 cm, hollow bricks 12 cm, and internal lime plaster 2 cm)
- The ground slab has a U equal to 0.46 W/m^2K and a thickness of 36 cm (reinforced concrete and hollow blocks mixed slab of 23 cm, extruded polystyrene insulation of 4 cm, lightweight concrete of 8 cm, and floor tiles)
- The roof slab has a U_{value} of 0.47 W/m^2K and a thickness of 38 cm (asphalt covering, polystyrene insulation 4 cm, waterproofing membrane, lightweight concrete of 5 cm, reinforced concrete and hollow blocks mixed slab of 23 cm, and internal lime plaster 2 cm).

In addition, windows are made of double glasses with an air gap (U_{value} = 2.72 W/m^2K) and old wooden frames (U_{value} = 2.31 W/m^2K).

During the heating period, the indoor microclimate is managed by a gas boiler with a thermal efficiency of 0.92, connected to in-room hot water radiators. The DHW is guaranteed by a gas water heater with an efficiency of 0.85. There is no mechanical cooling system for allowing microclimatic control in summer. All main features of the building and installed systems are described in Table 5.8.

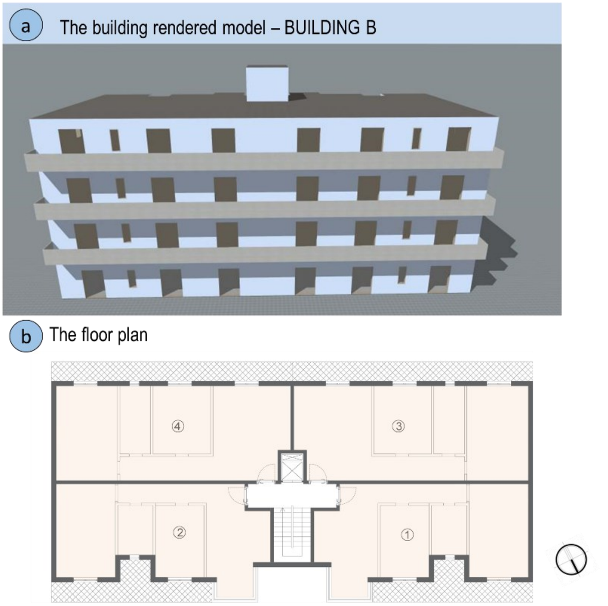

Figure 5.20 - The four floors building: a) Rendered view of the building, b) Indoor distribution of an intermediate floor

Table 5.8 - Main building features – BUILDING B

BUILDING GEOMETRY					
Total Building Area [m^2]	1318	Total building Volume [m^3]			3986
Net Conditioned Building Area [m^2]	1234	Conditioned total volume [m^3]			3739
Gross Roof Area [m^2]	374	Surface to volume ratio [1/m]			0.99
CONDITIONED AND UNCONDITIONED ZONES					
Number of conditioned zones 32		Number of unconditioned zones		5	
ENVELOPE - WINDOW TO WALL RATIO					
	Total	North	East	South	West
Gross Wall Area [m^2]	1328	405	259	405	259
Window Opening Area [m^2]	227	88	25	89	25
Gross Window-Wall Ratio [%]	17	22	10	22	10
DHW SYSTEM					
Gas water heater			systems efficiency: 0.85		
THERMAL TRANSMITTANCE					
External walls [W/m^{2}K]	0.51	Ground floor [W/m^{2}K]			0.46
Roof floor [W/m^{2}K]	0.47	Floor internal partitions [W/m^{2}K]			0.71
Glass (windows) [W/m^{2}K]	2.72	Frame (windows) [W/m^{2}K]			2.31

The ten floors building (Building C)

The third case study is a typical building of a residential district built during the sixties. The building is composed of two rectangular blocks staggered by about 2 m, and each of them has a staircase that connects three apartments for floors. The total height is 33 m and the ten floors have a common internal distribution with an internal net height of 3 m. The longest facades of the building are about 60 m long and these are oriented to south and north respectively, while the shortest ones are 11 m long and are oriented to west and east, as shown by Figure 5.21. The total building area is 6080 m^2 and the volume is 18'327 m^3. The conditioned zones are 60 and these correspond to the building apartments. The values of thermal transmittance of the building envelope and its features are coherent with those of the UNI TS 11300-1/2008 (abacus A3) [27] (the Official Italian Application of the ISO EN 13790 [28]) and the CTI recommendation R03/3 of Italian Thermo-technical Committee (abacus A5) [29].

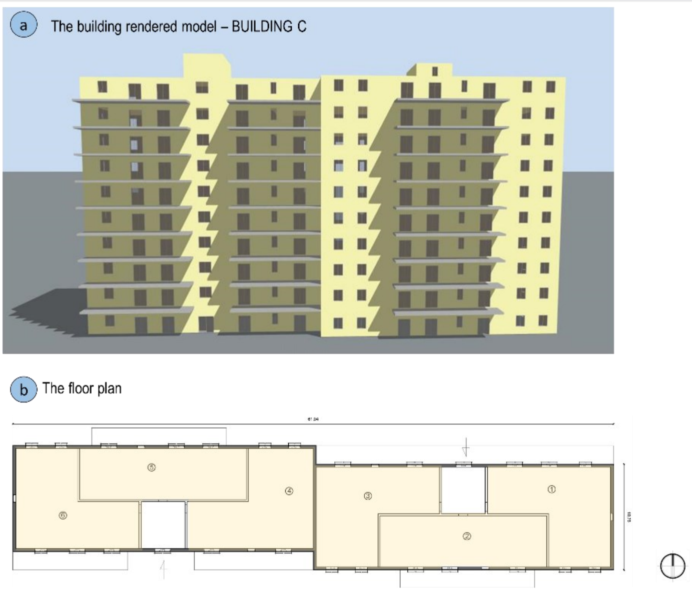

Figure 5.21 - The ten floors building: a) Rendered view of the building, b) Indoor distribution of an intermediate floor

The opaque envelope is here described in detail:

- the external walls, starting from the outside, have an external cement-based plaster of 3 cm, aerated bricks of 12 cm, an air gap of 5 cm, lapillus block of 8 cm, and lime plaster of 2 cm. The overall thickness is 30 cm and the thermal transmittance is 0.95 W/m^{2}K;
- the roof slab has a total thickness of 36 cm and U_{value} equals 0.94 W/m^{2}K (bituminous waterproofing membrane, lightweight concrete 10 cm, 2% reinforced concrete 5 cm, reinforced concrete, and hollow tiles mixed slab 18 cm, and lime internal plaster 2 cm);
- the ground floor consists of 5 layers: tiles, lightweight concrete 5 cm, 2% reinforced concrete 5 cm, reinforced concrete, and hollow tiles mixed slab 18 cm, and bitumen felt. The total thickness is 30 cm and the thermal transmittance is 0.98 W/m^{2}K.

According to the abacus A.3. of the relevant standard UNI TS 11300-1/2008 [27], the thermal transmittance of the building envelope after 1950 is around 1.0 W/m^{2}K, depending on the thicknesses, and thus the values here reported are perfectly coherent. The heating control is guaranteed by a gas boiler with an efficiency of 0.79 W/m^{2}K connected to in-room hot water radiators, while the DHW is provided by an electric water heater (system efficiency 0.9). There is no mechanical cooling. The main features of this building are reported in Table 5.9.

Table 5.9 - Main building features – BUILDING C

BUILDING GEOMETRY					
Total Building Area [m^2]	6.080	Total building Volume [m^3]			18.327
Net Conditioned Building Area [m^2]	5.573	Conditioned total volume [m^3]			16.810
Gross Roof Area [m^2]	658	Surface to volume ratio [1/m]			0.49
CONDITIONED AND UNCONDITIONED ZONES					
Number of conditioned zones 60		Number of unconditioned zones		22	
ENVELOPE - WINDOW TO WALL RATIO					
	Total	North	East	South	West
Gross Wall Area [m^2]	4989	451	2043	451	2044
Window Opening Area [m^2]	796	11	387	11	387
Gross Window-Wall Ratio [%]	16	3	19	3	19
DHW SYSTEM					
Electric water heater			systems efficiency: 0.9		
THERMAL TRANSMITTANCES					
External walls [W/m^{2}K]	0.95	Ground floor [W/m^{2}K]			0.98
Roof floor [W/m^{2}K]	0.94	Floor internal partitions [W/m^{2}K]			1.02
Glass (windows) [W/m^{2}K]	5.78	Frame (windows) [W/m^{2}K]			5.88

5.3.2. The methodological approach for the investigation

To calculate the energy demands of the complex system constituted by the building and the installed facilities, two approaches can be used. The first one is based on a set of algebraic equations that describe the interaction between the building and the external environment from a macroscopic point of view. It is a simplified or semi-stationary method. The second approach consists of the dynamic thermo-energetic simulation that considers all those transitory phenomena that significantly affect the performance of the building-system (external weather conditions, lighting system, thermal inertia of the building envelope, performance of air conditioning systems in partial load conditions, regulation etc.). Both approaches are used for the evaluation of the efficiency measures on the presented case studies to critically compare the profitability from both energy and economical point of view.

In the next paragraphs, the energy efficiency interventions are reported (and the two approaches, semi-stationary and dynamic, used to analyze the measures proposed, are described.

Energy efficiency and conservation measures

It was chosen to place the buildings in three different Italian cities (Naples, Ancona and Turin), representative of the three most frequent climatic zones: C, 1034 HDD; D, 1688 HDD; and E, 2617 HDD (baseline 20°C). These cities are positioned in the south, in the center, and the north of Italy, respectively, to carry out the analysis of the application of tax reduction for the various climatic contexts and building markets.

The EEMs concerned two macro-categories, following the two main “driving measures”:

- measures on building envelope (ETICS): insulation of walls and roof slab, in addition to the replacement of windows and solar shading installation.
- replacement of the heat generator or refurbishment of the entire system (generation, distribution, regulation, and emission) in addition to the integration of a solar thermal system.

In all cases, the thermo-physical thresholds required by Decree-Law 06/08/2020, Annex E [30], different among the climate zones, have been fulfilled and the heating and solar thermal systems comply with the requirements of the same Decree [31]. Table 5.10, Table 5.11, and Table 5.12 summarize both “driving” and “driven” Energy Efficiency Measures for the three different buildings, with their short name too, and the total investment costs that are within the cost limits reported in Annex I of the Decree-Law 06/08/2020 [32]. The cost of each EEM includes the cost of materials and installation and was determined by considering the Italian market trend and comparable works.

In this tables, λ is the thermal conductivity of the adopted insulation material, U_g and U_f are the thermal transmittances of glass and frame, respectively, $\eta_{(LHV)}$ and $\eta_{(HHV)}$ are boiler efficiency at rated conditions, by considering the Lower Heating Value and the Higher Heating Value, respectively.

Table 5.10 - The energy efficiency measures and relative costs – BUILDING A

Building A				
EEM code	Italian country	EEM description	EEM performance	EEM costs
D1 Driving 1 (ETICS)		**Wall insulation**	λ= 0.034 W/mK	
	Naples	thickness 0.08 m	U= 0.27 W/m²K	26’185 €
	Ancona	thickness 0.09 m	U= 0.25 W/m²K	26’770 €
	Turin	thickness 0.11 m	U= 0.22 W/m²K	27’729 €
		Roof insulation	λ= 0.034 W/mK	
	Naples	thickness 0.10 m	U= 0.26 W/m²K	24’477 €
	Ancona	thickness 0.13 m	U= 0.22 W/m²K	25’452 €
	Turin	thickness 0.15 m	U= 0.19 W/m²K	26’089 €
W windows replacement	**Triple low-emission glass** with Argon and aluminium frame with thermal break		U_g=0.90 W/m²K U_f=1.10 W/m²K	8'400 €
D2 Driving 2	**Condensing boiler**			
	Naples	22 kW$_t$	$\eta_{(LHV)}$= 97.5 % (80-60°C) $\eta_{(HHV)}$= 104.8 % (50-30°C)	3’000 €
	Ancona	27 kW$_t$		3’200 €
	Turin	30 kW$_t$		3’700 €
	Single room regulation with thermostatic valves			
SC solar collectors	**Glazed collectors**			
	Naples	net area of 2.0 m² (in all cities)	Inclination of 45° south facing	2'600 €
	Ancona			
	Turin			

Table 5.11 - The energy efficiency measures and relative costs – BUILDING B

Building B				
EEM code	Italian country	EEM description	EEM performance	EEM costs
D1 Driving 1 (ETICS)		**Wall insulation**	λ= 0.034 W/mK	
	Naples	thickness 0.05 m	U= 0.29 W/m^{2}K	161'461 €
	Ancona	thickness 0.08 m	U= 0.23 W/m^{2}K	170'830 €
	Turin	thickness 0.10 m	U= 0.21 W/m^{2}K	177'147 €
		Roof insulation	λ= 0.034 W/mK	
	Naples	thickness 0.06 m	U= 0.26 W/m^{2}K	42'296 €
	Ancona	thickness 0.10 m	U= 0.20 W/m^{2}K	46'048 €
	Turin	thickness 0.12 m	U= 0.18 W/m^{2}K	47'258 €
W windows replacement		**Triple low-emission glass** with Argon and aluminium frame with thermal break	U_g=0.90 W/m^{2}K U_f=1.10 W/m^{2}K	90'780 €
D2 Driving 2	**Condensing boiler**			
	Naples	70 kW$_t$	$\eta_{(LHV)}$= 97.5 % (80-60°C) $\eta_{(HHV)}$= 104.8 % (50-30°C)	10'500 €
	Ancona	80 kW$_t$		11'500 €
	Turin	90 kW$_t$		12'200 €
	Single room regulation with thermostatic valves.			
SC solar collector	**Glazed collectors**			
	Naples	net area of 18 m^2 (in both Naples and Ancona)	Inclination of 45° south facing	23'400 €
	Ancona			
	Turin	net area of 20 m^2		26'000 €

Table 5.12 - The energy efficiency measures and relative costs – BUILDING C

Building C				
EEM code	Italian country	EEM description	EEM performance	EEM costs
D1 Driving 1 (ETICS)		**Wall insulation**	λ= 0.034 W/mK	
	Naples	thickness 0.08 m	U= 0.29 W/m^{2}K	679'857 €
	Ancona	thickness 0.10 m	U= 0.25 W/m^{2}K	704'994 €
	Turin	thickness 0.12 m	U= 0.22 W/m^{2}K	721'245 €
		Roof insulation	λ= 0.034 W/mK	
	Naples	thickness 0.10 m	U= 0.25 W/m^{2}K	80'985 €
	Ancona	thickness 0.12 m	U= 0.22 W/m^{2}K	83'113 €
	Turin	thickness 0.14 m	U= 0.19 W/m^{2}K	85'257 €
W windows replacement	Naples	**Triple low-emission glass** with Argon and aluminium frame with thermal break	U_g=0.90 W/m^{2}K U_f=1.10 W/m^{2}K	296'036 €
	Ancona			
	Turin			
D2 Driving 2	**Condensing boiler**			
	Naples	400 kW$_t$	$\eta_{(LHV)}$= 97.5 % (80-60°C) $\eta_{(HHV)}$= 104.8 % (50-30°C)	51'600 €
	Ancona	460 kW$_t$		53'000 €
	Turin	540 kW$_t$		61'500 €
	Single room regulation with thermostatic valves.			
SC solar collector	**Glazed collectors**			
	Naples	net area of 78 m^2	Inclination of 45° south facing	85'800 €
	Ancona	net area of 80 m^2		88'000 €
	Turin	net area of 90 m^2		99'000 €

The EEMs were also combined, indeed, the “driving” measures were coupled with the “driven” measures [33], for a total of 5 energy efficiency interventions:

- D1: the ETICS (i.e., “External Thermal Insulation Composite System”) insulation of walls and roof slab.
- D1 + W: the ETICS driving measure was coupled with the replacement of windows.
- D2: the replacement of the heating system with a new style condensing boiler, with also improvement of the heating system regulation.
- D2+SC: the previous driving measure was combined with the addition of a solar collector system.
- D1+W+D2+SC: all the driving and driven measures were coupled with each other.

Table 5.13 - The solar collector systems and the integration in the DHW production

Italian country	DHW need yearly	Percentage of solar collectors’ integration	DHW integrated by solar collectors yearly
	kWh_p	%	kWh_p
Building A			
Naples	4829.0	73%	3525.1
Ancona		61%	2945.7
Turin		55%	2655.9
Building B			
Naples	31561.8	77%	24302.6
Ancona		65%	20515.2
Turin		65%	20515.2
Building C			
Naples	248264.4	75%	186197.7
Ancona		64%	158888.7
Turin		66%	163854.0

The technical features of the EEMs are reported in Table 5.10, Table 5.11, and Table 5.12. As said before, the energy efficiency interventions were applied in each building (Buildings A, B, and C) located in each one of the three Italian cities (Naples, Ancona, and Turin). In particular, the replacement of the heating system with a new stile condensing boiler differs according to the building thermal loads and the different Italian climatic zone. The solar collector systems, for all buildings and all the climatic zones, were designed with an inclination of 45°, azimuth 0°, and by considering a DHW need of 40 l/day per person. In all cases, the number of panels, and thus the area of the solar thermal systems, was chosen according to the Italian Decree-Law 28/2011 [34]. This Decree establishes that, in the case of new buildings or building refurbishment, the DHW need must be covered by renewable energy sources to the extent of at least 50%. Table 5.13 report the solar collectors' integration in the DHW production for all buildings in each Italian country.

The steady state calculation method

The Italian Ministerial Decree of 26/06/2015 [35] on the "Application of the energy performance calculation methods and establishment of buildings' prescriptions and minimum requirements" establishes the minimum energy performance requirements of buildings and units through a calculation process based on the definition of the reference building and on minimum rate of renewable energy sources. In compliance with this Decree, during the design phase, many parameters must be checked, ranging from the features of single components to the energy performance of the whole building. More in detail, the building global energy performance is calculated by means of "non-renewable primary energy need index" ($EP_{gl,nren}$) that quantifies the amount of energy actually consumed or estimated to meet the different needs associated with standardized use of the building, that includes, for residential building, heating, hot water, cooling and ventilation. According to the value of this index, the energy label system classifies the energy demands on a scale from A4 to G, defined starting by a specific reference building [36], [37] according to the procedure of the European Delegated n° 244/2012 [3]. Briefly, the reference building is an ideal version of a building, geometrically identical to the original one, placed in the same geographical coordinates and with the same orientation. The reference building's energy demands are calculated by applying standard boundary conditions and defined characteristics for the building, according to the climate zone of the project, comprehensives of structural and geometrical thermal bridges. This procedure is in agreement with the European Standard 15217 [38] and EN ISO 52003-1 [39].

The determination of the non-renewable primary energy need index requires the solution of the energy balance on the building-HVAC system according to the methodology proposed in the UNITS 11300 technical series, starting from the first part [27]. Actually, these require a quasi-steady state calculation method that simplifies the solution of a complex heat transfer problem where several dynamic phenomena are involved.

As known, the simplest building energy calculation is a steady-state approach, in which all building parameters are fixed. This type of calculation is used to determine peak thermal loads. However, external and internal parameters, as well as the operating parameters of building systems and plants change over time. Thus, a quasi-steady state method tries to improve the static calculations by performing a series of calculations at various conditions. The adopted time step is monthly variation. This provides 12 distinct "states" in a year. In this method, the simulation is executed monthly for one typical day characterized by standardized building use and climate data. It is assumed that the operating conditions of the typical day are constant for all reference months. The dynamic behavior of external forcing is considered by means of some adjustment parameters as well as for the inertial behavior of building envelope and plant systems.

The energy model of the building is defined according to an asset rating approach. The standard evaluation starts from the input data provided into the technical documentation of the building design or achieved by means a real inspection and survey of the architecture, both as regards the building envelope and the technical systems. All other boundary conditions are standardized. More in detail, the determination of the heating and cooling seasons is done considering the relations between external climates and free gains, and for the wintertime also considering such as established by the Italian Presidential Decree 412/93 [40]. Furthermore, as regards the indoor air setpoint temperature, the value of 20°C must be considered in wintertime and 26°C during the summer. The UNI 10349-1 [41] provides the monthly conventional climatic data to be used for the determination of energy performance of buildings. As regards the people and installed equipment schedules, the standardized approach imposes that, for residential buildings, the mean internal gains must be calculated considering the mean heat gains (provided by the standard and expressed in watt) and the net surface area of the building.

More specifically, concerning the case studies, the $EP_{gl,nren}$ index includes only the heating and hot water energy services. Thus, its calculation requires the calculation of the heating performance index $EP_{H,nren}$ (primary energy for heating) and of the hot water performance index $EP_{W,nren}$ (primary energy need for hot water) obtained by the calculation of the energy need (final energy) and of the energy losses and recoveries of the plants. The definitions of the building envelope characteristics and uses are necessary in order to evaluate the energy need for heating, due to the energy transfers through the building shell for transmission (diffusive heat exchange) and for ventilation (convective heat exchange). The energy losses due to the building ventilation have been calculated, according to the Italian standard, with a simplified approach, by assuming a mean air change equal to 0.5 Vol/h. The calculation of the positive endogenous contributes has been done assuming for the internal gains the value of 450 W. For the solar gains, the radiation heat transfer phenomenon for the transparent and glazed building surfaces has been considered. Briefly, these contributions depend on the collecting area, the solar irradiance and the shading reduction factor. Each one of the above-defined parameters can be calculated adopting the relations contained into the UNITS 11300-1 [27]. For instance, in the case of transparent surfaces, the collecting area depends on the amount of glazed area of the building, by the solar energy transmittance of the transparent surfaces and by the shading reduction factor due to the presence of movable window blinds. The positive contributes (endogenous and solar on the glazed surface) have been opportunely reduced in order to operate in safety conditions and to take into account the dynamic behaviors of the building envelope. In particular, a reduction factor has been calculated, for each case study, month and climate for the computation of the winter energy free gains in order to avoid an over-estimation of the overall thermal energy need. For instance, this parameter, for building A, varies from 0.93 to 0.99 in the different considered cities and months. In order to evaluate the primary energy request for heating, the system efficiencies, as well as the energy losses, have been calculated, according to UNITS 11300-2 [42], considering several sub-systems: generation equipment; distribution of fluid devices; emitters into the indoor environment; control devices. Each one determines energy losses, so that the transferred energy is progressively reduced. Considering the base case, the average seasonal efficiency varies from a minimum of 0.52 (building A in the case of Ancona and Naples) and a maximum of 0.68 (building B, Turin). The same procedure has been applied for the evaluation of primary energy for hot water.

For the case studies, these calculations have been performed by means of software accredited by the Italian Thermo-Technical Committee, named TERMUS [43].

The transient energy analysis

A transient energy analysis is a time-dependent simulation, based on energy balances in a continuous thermal transient regime, performed by assuming sub-hourly time-steps and by resolving transfer functions. The numerical models for the transient energy simulations were built through a 3D geometrical model and by defining the location, the orientation, the thermophysical properties of the building envelope, the activity, and operation parameters. For each building models were defined in detail: materials of the building envelope as defined in sub-section 5.3.1, the temperature setpoints, the climatic weather data file, and also, unlike the steady-state model, real conditions of use of the buildings. Indeed, occupancy, lighting, and electrical equipment were defined with proper schedules. The operational conditions of the heating system and the hours of activation were set according to the climatic Italian zone as established by the Italian Presidential Decree n

74/2013 [44]. For what concerns the infiltration rate, it was progressively reduced according to the thermophysical quality of the windows, the minimum is 0.3 h^{-1} in building B, with a window glasses transmittance of 2.72 W/m^2K and wooden frames, while the maximum is 0.7 h^{-1} for building C with a window glasses transmittance of 5.78 W/m^2K and aluminum frames. Also, the salutary opening of windows was considered, by modeling a time-dependent natural ventilation rate, to a maximum of 4 h^{-1}. For what concerns the electrical gains, the lighting system was modeled by defining a typical schedule for residential use and a daylight illuminance control: a maximum use during the evening, and a minimum use during the first hours of the morning. In this way, the real managing of artificial lights from occupants was defined. The use of electrical equipment, such as computers, electrical heaters, or kitchen appliances, was planned as intensive during the hours of use of kitchens. The occupancy was scheduled as typical in dwellings, and thus with greater crowding during the night, earlier morning, and evening. These conditions of use of the building are usual for residential buildings. In any case, unordinary conditions, such as those of the COVID-19 pandemic which markedly increased the number of hours spent at home every day, and therefore the traditional energy consumption of residential buildings, were not contemplated.

The data, necessary for the definition of the transient numerical model, some of which are specific to each building and others common to all three, are reported in Table 5.14.

As previously said, the heating demand of the three buildings is satisfied by hot water boilers which supply in-rooms hot water radiators. To build real building models, the nominal capacity of the generator systems was adopted according to the Italian climatic zone. Depending on the building thermal loads, the nominal capacity is higher for the Italian countries with severe winters. Table 5.15 reports the technical features of the heating systems before the building energy refurbishment. No mechanical cooling is available.

The validation of the energy results of the building numerical models was performed taking into account the energy consumptions of real reference buildings. In particular, according to the year of construction of the building, on which depend the thermophysical properties of the building envelope, the type of systems for the microclimatic control and the production of DHW, the building energy demand can considerably vary.

Table 5.14 - Input parameters, operational and performance data for the definition of the building numerical models

INTERNAL GAINS			
Lighting system [W/m^2 every 100 lux]	2	Occupancy [person/m^2]	0.04
Maximum use of artificial lighting is scheduled during the evening hours, a reduced use during the earlier morning and late afternoon, null in the remaining hours of the day and night		The maximum occupancy in the building is scheduled from 8:00 pm to 8:00 am. During the diurnal daily hours, the building occupancy, is reduced by 50%	
Light control according to the daylight illuminance (dimming)		Electric equipment [W/m^2]	4
BOUNDARY CONDITIONS			
Heating setpoint [°C]	20	Cooling setpoint [°C]	26
Natural Ventilation			
Natural ventilation (time-dependent, till a maximum of 4 h^{-1}) is activated when both summer conditions occur:		a) the zone air temperature is higher than 27 °C b) the outdoor temperature is at least 2°C lower than indoor one	
Infiltration rate			
Building A: 0.5 h^{-1}	Building B: 0.3 h^{-1}	Building C: 0.7 h^{-1}	
SIMULATION PARAMETERS			
Solution Algorithm		Conduction Transfer Function	
Surface Convection Algorithm - inside	TARP	Surface Convection Algorithm - outside	DOE - 2
CONVERSION FACTORS, COSTS AND EMISSIONS			
Primary Energy Factor of Natural Gas	1.05	Primary Energy Factor of Electricity	1.96
Natural Gas Cost [€/kWh$_g$]	0.073	Electricity Cost [€/kWh$_e$]	0.223
Natural Gas LCA emission factor [kg CO_{2-eq}/kWh$_g$]	0.24	Electricity LCA emission factor [kg CO_{2-eq}/kWh$_e$]	0.424
WEATHER DATA			
Naples		NAPLES - ITA IWEC Data WMO#=162890	
Ancona		Ancona - ITA IGDG WMO#=161910	
Torino		TORINO - ITA IWEC Data WMO#=160590	
HEATING PERIOD			
Naples		10 hours a day, from November 15th to March 31st	
Ancona		12 hours a day, from November 1st to April 15th	
Torino		14 hours a day, from October 15th to April 15th	

For this reason, the energy results were compared with the energy bills of real original buildings and it was verified, even if on annual basis, that the Mean Bias Error [45] was between ± 5%. The same methodology was described in detail by Ascione *et al*. [46].

Table 5.15 - The hating systems of the buildings before the refurbishment.

BUILDING A HEATING SYSTEM – GAS BOILER		
	Generation systems efficiency [-]	Nominal capacity
Naples		22 kW_t
Ancona	0.72	27 kW_t
Turin		30 kW_t
BUILDING B HEATING SYSTEM – GAS BOILER		
	Generation systems efficiency [-]	Nominal capacity
Naples		70 kW_t
Ancona	0.92	80 kW_t
Turin		90 kW_t
BUILDING C HEATING SYSTEM – GAS BOILER		
	Generation systems efficiency [-]	Nominal capacity
Naples		400 kW_t
Ancona	0.79	460 kW_t
Turin		540 kW_t

5.3.3. Results and discussion

In this sub-section, the simulation results are discussed. More in detail, the following indicators are used for comparing the proposed configurations:

- the global non-renewable energy performance index, $EP_{gl,nren}$ and the Energy label;
- the percentage difference (Δ) compared to the “BC” (base case, described for what concerns $EP_{gl,nren}$ and CO_2 emissions;
- the ISI index defined as the “the investment cost” to the “annual primary non-renewable energy saving”;
- the Net Present Value (NPV_{20}) (lifespan of 20 years) and the discounted pay-back period (DPB).

The NPV_{20} and the DPB are calculated by considering a discount rate of 3% yearly, according to [3]. Reference prices are 0.19 €/kWh and 0.67 €/Sm^3 for electricity and natural gas, respectively [47]. By simplifying, tax reduction considers three possible scenarios (SC):

- SC1: 110% tax saving, over 5 years based on the new “Super-bonus” incentive mechanism.

- SC2: tax saving of 50-65% in 10 years based on the previous “Eco-bonus” incentive, here simplified (50% for envelope EEMs and 65% for heating system EEMs).
- SC3: no incentives are considered.

The acronym “NA” means that the tax reduction is “not applicable” because the improvement of two energy classes is not achieved.

The steady-state analysis results

Figure 5.22, referred to the Building A, proposes the comparison of adopted energy and environmental indices for the base case (BC) and for all EEMs.

In the BC, the maximum values of both indices ($EP_{gl,nren}$ and CO_2 emissions) are achieved in Turin (65.1 kg CO_2/m^2y), followed by Ancona (44.7 kg CO_2/m^2y) and Naples (35.4 kg CO_2/m^2y). This is attributable to the most severe design weather conditions in Turin, where the heating demand is higher than in the other considered cities. However, in all cases, considering the respective reference building, the worst energy class is achieved.

The insulation intervention (D1) seems the most interesting measure, since it allows the improvement of two energy classes and the helving (or more) of the $EP_{gl,nren}$ index that is only further slightly reduced when also the window’s replacement is considered. The ΔCO_2 is comparable with the energy saving, since it has mainly length to the reduction of natural gas request. Moreover, it can be noted that the magnitude of energy and environmental energy saving is comparable for all considered climates and thus the first driving measure seems to be effective under different weather conditions, also in Naples where there is a typical cooling dominated climate.

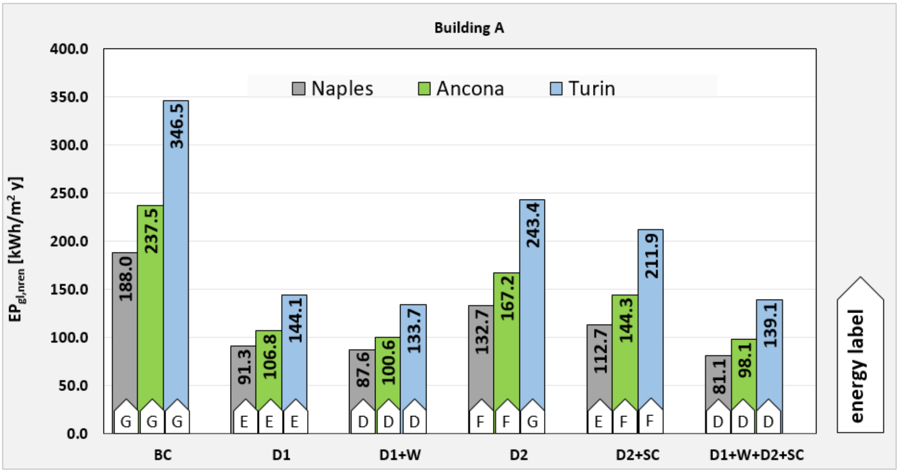

		D1	D1+W	D2	D2+SC	D1+W+D2+SC
$\Delta EP_{gl,nren}$	Naples	-51%	-53%	-29%	-40%	-57%
	Ancona	-55%	-58%	-30%	-39%	-59%
	Turin	-58%	-61%	-30%	-39%	-60%
ΔCO_2	Naples	-51%	-53%	-29%	-40%	-57%
	Ancona	-55%	-58%	-29%	-39%	-58%
	Turin	-58%	-61%	-30%	-39%	-60%

Figure 5.22 - Energy and Environmental results of the steady-state analysis - Building A

The EEM applied to the heating system is not sufficient to obtain the improvement of two energy classes also if the energy saving is around 30% in all cities. For Turin, the D2 does not guarantee any improvement in the energy label. This is essentially due to the fact that D2 involves merely the replacement of the boiler and the improvement of regulation and control of the heating system (regulated on the basis of the temperatures measured in each single room), which has to operate with the existing radiators, and so with a heat transfer fluid at high temperature. In these operating conditions, there are no significant energy benefits deriving from the application of a condensing boiler. Also adding the installation of solar collector, in Ancona and Turin, it is not achieved the increase of two energy classes. In these cities, the hot water consumption could be covered by solar production respectively for 55% and 61%. Conversely, for Naples this integration rises up 73% and the energy class becomes “E” as in the case of D1 scenarios. To obtain even better energy performance, the generation sub-system should be replaced by a different type of plant (e.g., a heat pump). Finally, combined

EEMs on envelope and systems have been applied. For this case, in all the cities, maximum reduction of $EP_{gl,nren}$ and CO_2 emissions is achieved. However, it can be noted that, mainly in Turin, these reductions are comparable to those obtained with only the 1st driving measure (D1). This result indicates that the economic analysis is fundamental for establishing the feasibility of the proposed energy efficiency measures. Figure 5.23 shows the economic impacts and indicators of the various EEMs.

By analyzing the ISI, opposite results are obtained. The EEM that ensures the lowest value (i.e., the best one) is D2, and thus replacement of the boiler, in all cities. This EEM is also the one that brings the shortest DPB, without funding incentives (SC3). In this scenario, all other EEMs have a DPB higher than 15 years. However, the energy analysis suggests that the obtainable saving does not allow a significant improvement of the whole behavior since the energy class remains very low.

When it is possible to access to the SC1, by considering the profitability of the energy retrofit on the basis of the NPV_{20}, for Naples and Ancona, it was found that the most profitable EEM is a combined package involving envelope and heating system (D1+W+D2+SC), followed by the EEMs concerning the envelope alone (D1+W), and thus those ones that bring the greater energy saving. In Turin, the best intervention is the insulation of the building envelope and the replacement of the windows. If SC2 is applied, the most profitable EEM is D2+SC.

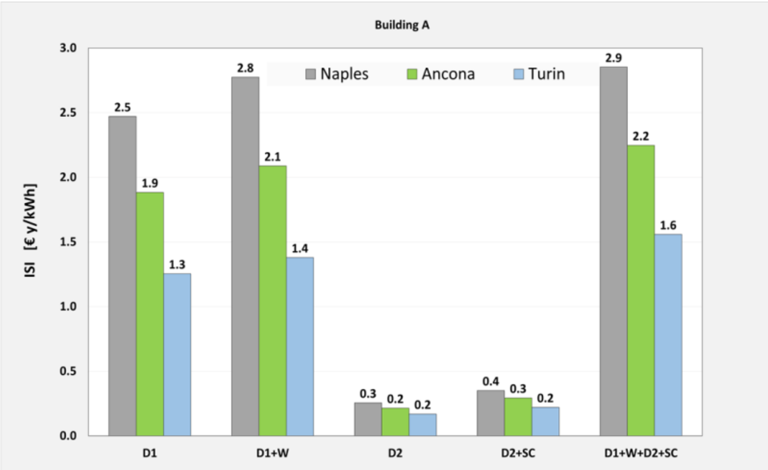

			D1	D1+W	D2	D2+SC	D1+W+D2+SC
NAPLES	SC1	NPV_{20} - €	24424	25404	NA	18531	26873
		DPB - years	5	5	NA	3	5
	SC2	NPV_{20} - €	-5012	-8912	12285	15994	-9981
		DPB - years	>20	>20	3	4	>20
	SC3	NPV_{20} - €	-26619	-34103	10622	12889	-38276
		DPB - years	>20	>20	4	5	>20
ANCONA	SC1	NPV_{20} - €	32891	34490	NA	NA	34938
		DPB - years	5	5	NA	NA	5
	SC2	NPV_{20} - €	2549	-732	15887	20320	-2912
		DPB - years	18	>20	3	4	>20
	SC3	NPV_{20} - €	-19724	-26588	14113	17104	-31984
		DPB - years	>20	>20	3	4	>20
TURIN	SC1	NPV_{20} - €	50685	53327	NA	NA	51785
		DPB - years	4	4	NA	NA	4
	SC2	NPV_{20} - €	19415	17177	23722	30307	12781
		DPB - years	11	13	2	3	14
	SC3	NPV_{20} - €	-3539	-9360	21670	26813	-17249
		DPB - years	>20	>20	3	4	>20

Figure 5.23 - Economic indicators of the steady-state analysis – Building A

Figure 5.24 shows the energy and environmental indices for Building B. In this case, the base case is characterized by better performance due to a medium insulation level of the building envelope and higher efficiency of the boiler. This is advisable by the energy class that in Naples is “B” where the equivalent emissions are 16.6 kg CO_2/m^2y. In Ancona and Turin, the energy class is “C” and the emissions are respectively 21.2 kg CO_2/m^2y and 29.6 kg CO_2/m^2y.

The findings in terms of energy savings bring to different conclusions compared with the Building A. In Naples, only the combination of all considered EEMs allows the improvement of two energy classes and thus can be considered for the application of the new incentive mechanism. The scenario D1 brings the lower energy saving (-10%) and the behavior compared to the reference building does not improve. When also the replacement of the windows is considered the energy saving slightly increases and the energy class becomes A1. The intervention on the heating system seems to be more interesting mainly if also the solar collectors are applied; this allows to cover, during the whole year, the 77% of the hot water demand. These results, according to energy and environmental indicators, suggest that for a mild to hot climate, a further increase of insulation of the opaque and glazed envelope is not a good solution but the efficiency of plants and the renewable integration should be preferred. For the design conditions of Turin, the combination D1+W should be considered according to the energy and environmental indices. Indeed, in this case it is also possible to reach the A1 energy class. Considering Ancona, the EEMs indicated as D1+W allows the improvement of two energy class also if the $\Delta EP_{gl,nren}$ is lower than in the case of D2+SC; in this last case, the energy class becomes B. However, for all cities, the maximum energy saving is achievable when all proposed measures are applied and the obtained $\Delta EP_{gl,nren}$ is comparable for the different climates. Due to the important contribution of solar collector, in Naples, also with the lower $\Delta EP_{gl,nren}$, it is possible to reach the best energy class (A2).

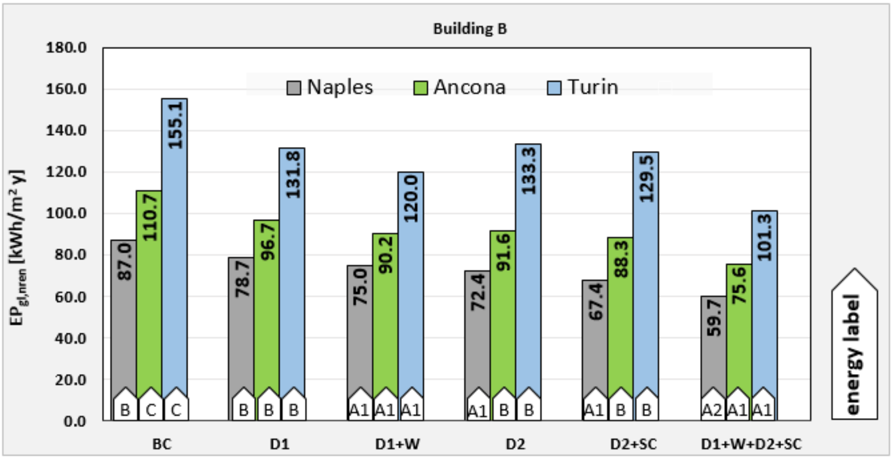

		D1	D1+W	D2	D2+SC	D1+W+D2+SC
$\Delta EP_{gl,nren}$	Naples	-10%	-14%	-17%	-23%	-31%
	Ancona	-13%	-18%	-17%	-20%	-32%
	Turin	-15%	-23%	-14%	-17%	-35%
ΔCO_2	Naples	-9%	-13%	-16%	-22%	-30%
	Ancona	-12%	-18%	-17%	-20%	-31%
	Turin	-15%	-22%	-14%	-16%	-34%

Figure 5.24 - Energy and Environmental results of the steady-state analysis – Building B

The economic analysis for the building B is reported in Figure 5.25. Also in this case, the most profitable EEM, according to ISI, is D2 but, without the incentive (SC3), it is less convenient than for building A; indeed, the DPB is 9 years in Naples and 7 years in the other cases.

Few scenarios can access to the SC1 mechanism and it is remarkable that, for all cities, the selection of D1+W+D2+SC (higher energy saving) is profitable, according to the NPV_{20}, only if the new incentives are provided. The economic analysis suggests that, for this type of building, the introduced incentive mechanism is a fundamental strategy for supporting the diffusion of refurbishment interventions. Indeed, the tax reduction can boost the renovation market since the owners can consider really facilitated in supporting the expense.

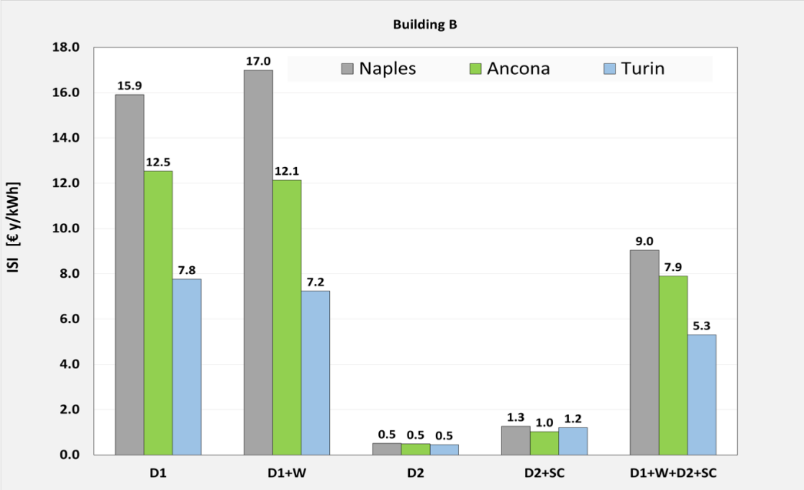

			D1	D1+W	D2	D2+SC	D1+W+D2+SC
NAPLES	SC1	NPV_{20} - €	NA	NA	NA	NA	41733
		DPB - years	NA	NA	NA	NA	5
	SC2	NPV_{20} - €	-69979	-116738	16402	12902	-109997
		DPB - years	>20	>20	6	10	>20
	SC3	NPV_{20} - €	-191645	-277123	10581	-5895	-289179
		DPB - years	>20	>20	9	>20	>20
ANCONA	SC1	NPV_{20} - €	NA	32018	NA	NA	52971
		DPB - years	NA	5	NA	NA	5
	SC2	NPV_{20} - €	-67100	-109739	22407	16421	-104598
		DPB - years	>20	>20	5	10	>20
	SC3	NPV_{20} - €	-196601	-277959	16030	-2930	-292169
		DPB - years	>20	>20	7	>20	>20
TURIN	SC1	NPV_{20} - €	N	53382	NA	NA	80149
		DPB - years	NA	5	NA	NA	5
	SC2	NPV_{20} - €	-56537	-91464	25788	19537	-82004
		DPB - years	>20	>20	5	9	>20
	SC3	NPV_{20} - €	-190532	-264178	19024	-1644	-275899
		DPB - years	>20	>20	7	>20	>20

Figure 5.25 - Economic indicators of the steady-state analysis – Building B

Figure 5.26 refers to energy and environmental results for Building C, for which the base case is characterized by emissions of around 43.3 kg CO_2/m^2y in Turin, 30.8 kg CO_2/m^2y in Ancona and 25.5 kg CO_2/m^2y in Naples. As for Building A, the building envelope has very low performance and the gas boiler has a quite low efficiency. This configuration is characterized by very low energy class that seems mainly influenced by the window's replacement. Indeed, in case of D1, the energy saving ranges around 20%

and the energy class improves only by one step. Conversely, when also the windows are replaced (D1+W), in all cities the C class is reached and the energy and environmental exceeds 30%.

The intervention on the heating and hot water system brings important reduction of energy request and emissions but the energy label is not greatly affected by the proposed choice; for instance, in Naples, also if the solar collectors cover 77% of the hot water request, in the scenario D2+SC, the achievable energy class is D. The best configuration, as in the others case studies, is D1+W+D2+SC, since the energy demand is halved as well as the emissions and the energy class is greatly improved.

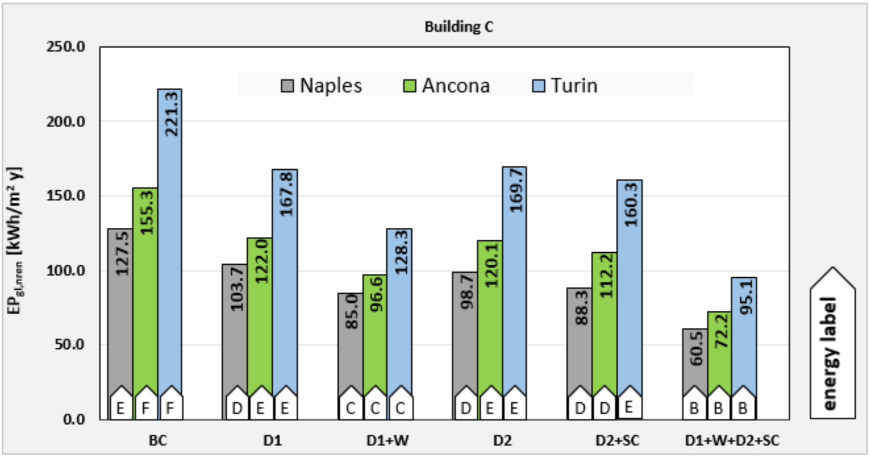

		D1	D1+W	D2	D2+SC	D1+W+D2+SC
$\Delta EP_{gl,nren}$	Naples	-19%	-33%	-23%	-31%	-53%
	Ancona	-21%	-38%	-23%	-28%	-54%
	Turin	-24%	-42%	-23%	-28%	-57%
ΔCO_2	Naples	-17%	-31%	-21%	-30%	-51%
	Ancona	-20%	-36%	-21%	-27%	-52%
	Turin	-34%	-40%	-22%	-27%	-55%

Figure 5.26 - Energy and Environmental results of the steady-state analysis – Building C

Figure 5.27 proposes the economic analysis for Building C. As in the other cases, the low investment for the boiler replacement influences the economic profitability in terms of low value of ISI for D2 and also for D2+SC. Indeed, these are the EEMs that also without incentives are characterized by positive net present values and acceptable discounted pay back. The insulation intervention is not profitable in all considered scenarios also because it cannot benefit of the new incentive mechanism. The package D1+W, also if interesting according to the previous analysis, is profitable only taking advantage from the tax reduction (SC1), with the same DPB in all cities and a very high NPV_{20} in Turin, where there is an important reduction of the operating costs for the space heating.

The high cost for the windows negatively influences the economic analysis of SC2, where the combined effect of operating cost reduction and incentives is not enough to balance the investment costs.

The combination D1+W+D2+SC, in Naples and Ancona, has positive economic analysis only for SC1 and thus also this case study confirms the importance of introduced support measures.

In summary, the semi-stationary analysis has indicated that the introduced incentive mechanism can boost the transition of building market to sustainable refurbishment. Indeed, only with this support, the owners can find profitability in the selection of the energy efficiency packages that assure the maximum energy saving and polluting emissions reduction. On the other hand, without this support, the economic analysis could suggest the selection of the cheapest efficiency measure that has a limited incidence on the building behavior (low $\Delta EP_{gl,nren}$ and energy class) as the replacement of the existing heating system and improvement of the regulation system. The insulation intervention seems to be a good choice for a single dwelling with very low energy performance, but it is usually not profitable, without incentives, for multi-storey buildings for which only a global refurbishment of building-HVAC system can assure high energy savings and positive economic indicators. In all case studies, the DPB for the whole package of measures, when the new incentive mechanism is accessible, becomes 5 years and the conventional energy demand is more than halved.

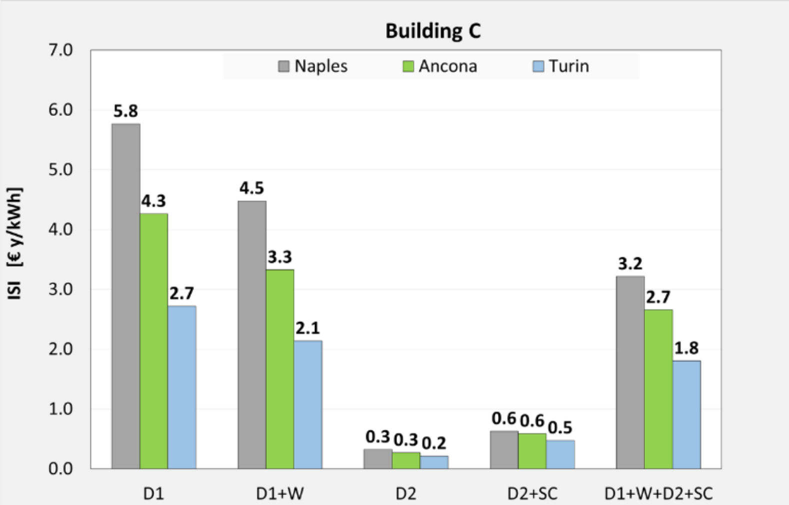

			D1	D1+W	D2	D2+SC	D1+W+D2+SC
NAPLES	SC1	NPV_{20} - €	NA	284221	NA	NA	474382
		DPB - years	NA	5	NA	NA	5
	SC2	NPV_{20} - €	-152078	-200049	163555	223724	-72140
		DPB - years	>20	>20	4.0	6.0	>20
	SC3	NPV_{20} - €	-606388	-780621	134944	147541	-728895
		DPB - years	>20	>20	5.0	9.0	>20
ANCONA	SC1	NPV_{20} - €	NA	389608	NA	303848	572243
		DPB - years	NA	5	NA	3	5
	SC2	NPV_{20} - €	-101047	-105852	204389	239965	12899
		DPB - years	>20	>20	3	6	>20
	SC3	NPV_{20} - €	-571637	-702705	175003	161785	-662133
		DPB - years	>20	>20	4	8	>20
TURIN	SC1	NPV_{20} - €	NA	612033	NA	NA	855665
		DPB - years	NA	5	NA	NA	5
	SC2	NPV_{20} - €	22174	109023	306613	350888	279937
		DPB - years	19	16	3	5	13
	SC3	NPV_{20} - €	-459400	-498814	272514	261897	-416891
		DPB - years	>20	>20	3	7	>20

Figure 5.27 - Economic indicators of the steady-state analysis – Building C

The transient energy analysis results

This paragraph describes in detail the results of the transient energy results and compares them with the results of the steady-state analysis. Figure 5.28, shows the energy and environmental indices for the base case and for all the EEMs, in the case of Building A. The results are coherent with those of the steady-state analysis, both in terms of emissions and energy saving, but, in this case, the $EP_{gl,nren}$ for the intervention on the building envelope is almost halved. This is due to the different calculation approaches: indeed, the steady-state simulation is executed monthly, by considering average climatic conditions and building uses. The temperatures of the indoor environments are constant at the set point value (20 °C), and it means a constant availability of the heating system operation, 24 h/day. This causes an overestimation of the real building energy consumption and obviously of the pollutant emissions. For what concerns the intervention D2+SC (replacement of the heating system coupled with the installation of solar collectors), the incidence of DHW in the transient regime, is higher than the steady state calculation, because, compared to the overall primary energy demand of the building, the transient regime, trying to simulate reality as accurately as possible, considers a limited number of heating hours, so the energy demand for microclimatic control is less than semi-stationary calculation, in which the plants are always operative. Conversely, the use of DHW is the same in both calculation methods (40 l/day/person), and thus, in the overall energy demand, it has a greater impact. Therefore, the intervention aimed at reducing the energy demand to produce DHW, which provides the installation of the solar system, is particularly effective under dynamic conditions.

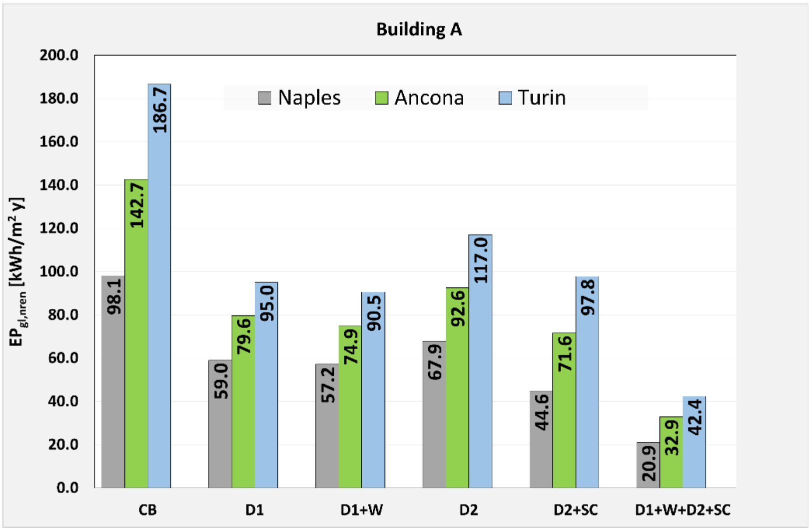

		D1	D1+W	D2	D2+SC	D1+W+D2+SC
$\Delta EP_{gl,nren}$	Naples	-40%	-42%	-31%	-55%	-79%
	Ancona	-44%	-48%	-35%	-50%	-77%
	Turin	-49%	-52%	-37%	-48%	-77%
ΔCO_2	Naples	-40%	-42%	-31%	-55%	-79%
	Ancona	-44%	-48%	-35%	-50%	-77%
	Turin	-49%	-52%	-37%	-48%	-77%

Figure 5.28 - Energy and Environmental results of the transient analysis – Building A

Coherently to the results of Figure 5.22, for interventions D1 (thermal insulation of the envelope) and D1+W (thermal insulation plus windows replacement), the energy-saving progressively is higher in the countries with colder winters (Ancona and Turin).

The most interesting measure is the replacement of the heating system coupled with the installation of solar collectors (D2+SC), which involve an $EP_{gl,nren}$ reduction of around 50% for all the cities, but slightly less in the climatic zones where the solar collector production is lower. Indeed, in Naples (climatic zone C) the D2+SC measure causes an $EP_{gl,nren}$ saving of 55%, while in Ancona (climatic zone D) the $\Delta EP_{gl,nren}$ is 50%, and in Turin (climatic zone E) is 48%. Conversely, the replacement of just the heating system (D2) has more energy and environmental benefits in the climatic zones with colder winters, and thus in Turin and Ancona. Finally, combined EEMs on envelope and systems have been applied. The results show that for all the cities, maximum reduction of $EP_{gl,nren}$, and CO_2 emissions is achieved, the percentage of around 80% both for energy and environmental terms.

The economic analysis was performed also for the transient energy analysis and the results, for Building A, are reported in Figure 5.29. The ISI, as in the steady-state calculation, is the lowest for the intervention D2 (replacement of the boiler) in all the cities and this EEM is also the one that brings the shortest DPB, without funding incentives (SC3). Besides the D2+SC interventions, in the SC3 scenario, all the EEMs have a DPB higher than 20 years. When the SC1 funding incentive is accessed, all the EEMs for all the cities have a DPB lower than 20 years and obviously a positive NPV20. In this scenario, the most profitable EEM is a combined package involving envelope and heating system (D1+W+D2+SC), followed by the EEMs concerning the replacement of the heating system coupled with the installation of the solar collector system (D2+SC) both in Naples and Ancona. In Turin, the D2+SC intervention doesn’t access the SC3 funding program because it doesn’t allow the improvement of at least two energy classes. Finally, this analysis shows that the two calculation approaches could have different results in the economic evaluation of the EEMs. Indeed, according to the steady-state analysis, the most profitable EEM in Turin was the D1+W intervention in the scenario SC1, while, for the transient energy analysis, it was the combined package involving envelope and heating system (D1+W+D2+SC).

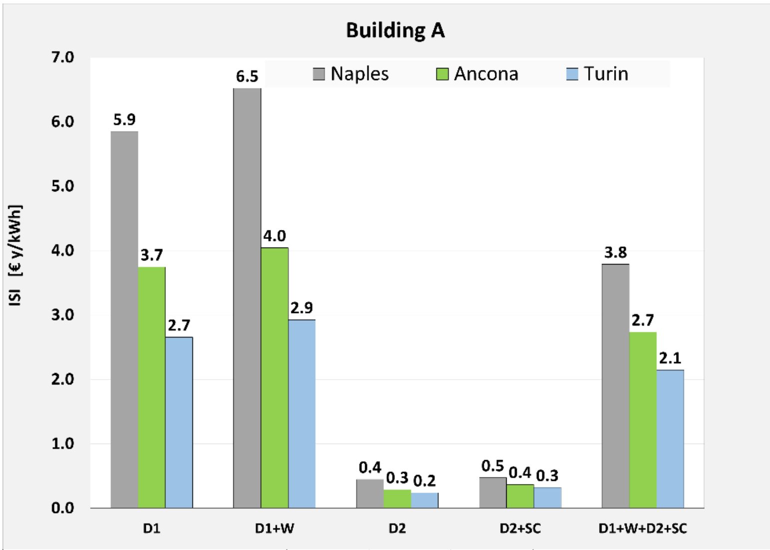

			D1	D1+W	D2	D2+SC	D1+W+D2+SC
NAPLES	SC1	NPV_{20} - €	9329	9801	NA	12249	18115
		DPB - years	5	5	NA	3	5
	SC2	NPV_{20} - €	-20106	-24515	5573	9712	-18739
		DPB - years	>20	>20	5	5	>20
	SC3	NPV_{20} - €	-41714	-49705	3910	6607	-47034
		DPB - years	>20	>20	7	8	>20
ANCONA	SC1	NPV_{20} - €	14790	15943	NA	NA	25565
		DPB - years	5	5	NA	NA	5
	SC2	NPV_{20} - €	-15552	-19280	10001	13541	-12286
		DPB - years	>20	>20	4	5	>20
	SC3	NPV_{20} - €	-37825	-45136	8227	10325	-41357
		DPB - years	>20	>20	5	6	>20
TURIN	SC1	NPV_{20} - €	21344	22429	NA	NA	33463
		DPB - years	5	5	NA	NA	5
	SC2	NPV_{20} - €	-9925	-13721	14234	17476	-5541
		DPB - years	>20	>20	3	4	>20
	SC3	NPV_{20} - €	-32879	-40258	12183	13983	-35571
		DPB - years	>20	>20	4	5	>20

Figure 5.29 - Economic indicators of the transient analysis – Building A

For what concerns Building B, as shown by Figure 5.30, the less convenient intervention is the replacement of the heating system (D2). Indeed, differently compared to the Building A, the gas boiler of the base building was not so inefficient (generation system efficiency is equal to 0.92) and thus its replacement has not provided a substantial energy saving. If compared to Building A, the thermal insulation of the building envelope (D1 scenario), and the coupled intervention D1+W (thermal insulation plus windows replacement), produce energy-savings, and consequent reductions of the pollutant emission, considerably lower, because the thermophysical properties of the envelope of the base Building B are better than those of the base Building A. The most interesting EEM is D2+SC which involves the highest energy saving in Naples, where there is an important contribution of the solar collector productivity. However, with reference to all cities, the maximum energy saving is achievable when all proposed measures are applied (i.e., D1+W+D2+SC).

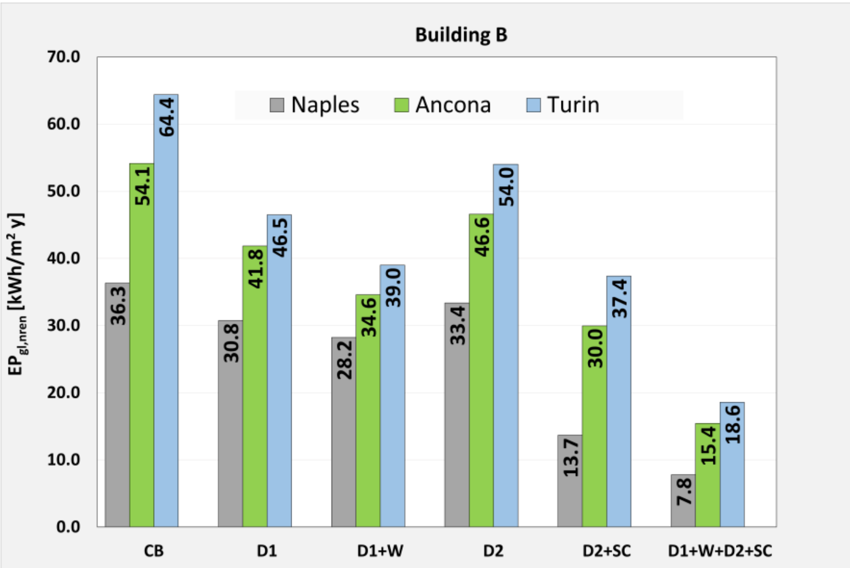

		D1	D1+W	D2	D2+SC	D1+W+D2+SC
$\Delta EP_{gl,nren}$	Naples	-15%	-22%	-8%	-62%	-79%
	Ancona	-23%	-36%	-14%	-45%	-71%
	Turin	-28%	-39%	-16%	-42%	-71%
ΔCO_2	Naples	-15%	-22%	-8%	-62%	-79%
	Ancona	-23%	-36%	-14%	-45%	-71%
	Turin	-28%	-39%	-16%	-42%	-71%

Figure 5.30 - Energy and Environmental results of the transient analysis – Building B

The economic analysis for Building B is shown in Figure 5.31. In this case, the proposed scenario which has the lowest ISI is the D2+SC intervention, indeed, the ISI value for all the three countries is around 1 €/y kWh. Even if this indicator shows the economic profitability, as clarified in the previous sub-section, this refurbishment intervention does not allow the upgrade of two energy classes, therefore, as it happens also with reference to D2, the funding program of scenario 1 cannot be accessed. In any case, the funding program of the second scenario can be achieved, and the D2+SC intervention has a DPB of 10 years in Naples and Ancona, and 9 years in Turin. This EEM results more convenient in Turin where, because of the colder winters, the replacement of the heating boiler has a higher impact on the reduction of the building energy demand. This is also confirmed by the economic analysis for the D2 intervention. By considering the same funding scenario (SC2), case D2 has the lowest DPB in Turin. The highest ISI value, and thus the less convenient EEMs, are D1 (thermal insulation of the building envelope) and D1+W (thermal insulation plus windows replacement) in Naples. These EEMs are not as effective as with reference to Building A. Indeed, the reduction of the building energy demand is not significant and thus the economic indicators are poor. More than the other cases, this building, built during the ’90s, shows that the new funding program issued in Italy (SC1) promotes the energy refurbishment of the whole system “building-HVAC plants”. The singular or coupled EEMs in many cases do not update the energy classes of at least two and thus cannot allow the economic incentive of SC1.

The energy and environmental results for Building C are depicted in Figure 5.32. This building has poor envelope performances and, for this reason, by comparing the results with those of Building B, the reduction of the building energy demand due to the envelope refurbishment (D1 and D1+W) is more consistent. The intervention which gives the lowest $EP_{gl,nren}$ is obviously the total energy refurbishment (D1+W+D2+SC) but an interesting result is even reduction of the energy demand caused by the D2+SC measure (i.e., replacement of the heating boiler, upgrading of regulation systems and solar collectors). Coherently to the previous building case studies, this intervention has the biggest incidence in the city where the productivity of the solar thermal system is higher (Naples).

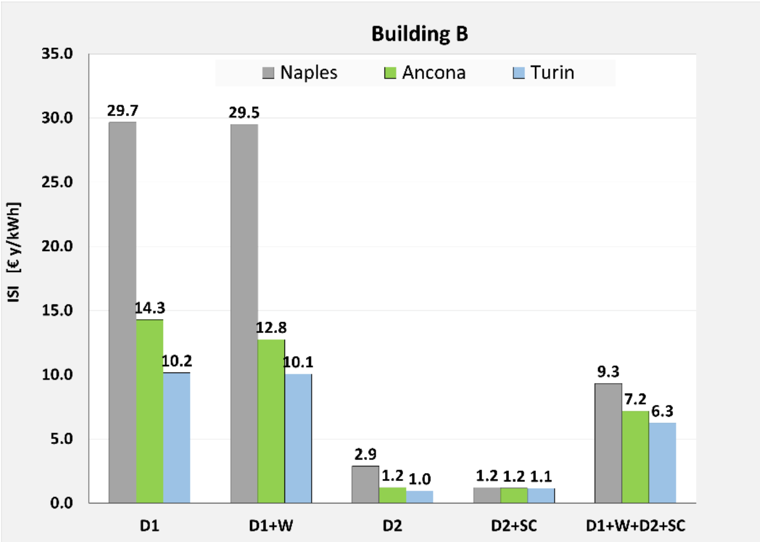

			D1	D1+W	D2	D2+SC	D1+W+D2+SC
NAPLES	SC1	NPV_{20} - €	NA	NA	NA	NA	38809
		DPB - years	NA	NA	NA	NA	5
	SC2	NPV_{20} - €	-74999	-123847	-928	13714	-112922
		DPB - years	>20	>20	>20	10	>20
	SC3	NPV_{20} - €	-196666	-284231	-6750	-5082	-292103
		DPB - years	>20	>20	>20	>20	>20
ANCONA	SC1	NPV_{20} - €	NA	27225	NA	NA	51859
		DPB - years	NA	5	NA	NA	5
	SC2	NPV_{20} - €	-71713	-114532	4499	15235	-105710
		DPB - years	>20	>20	10	10	>20
	SC3	NPV_{20} - €	-201214	-282752	-1878	-4116	-293281
		DPB - years	>20	>20	>20	>20	>20
TURIN	SC1	NPV_{20} - €	NA	34720	NA	NA	60995
		DPB - years	NA	5	NA	NA	5
	SC2	NPV_{20} - €	-67620	-110126	7791	17368	-101159
		DPB - years	>20	>20	8	9	>20
	SC3	NPV_{20} - €	-201615	-282840	1026	-3812	-295053
		DPB - years	>20	>20	18	>20	>20

Figure 5.31 - Economic indicators of the transient analysis – Building B

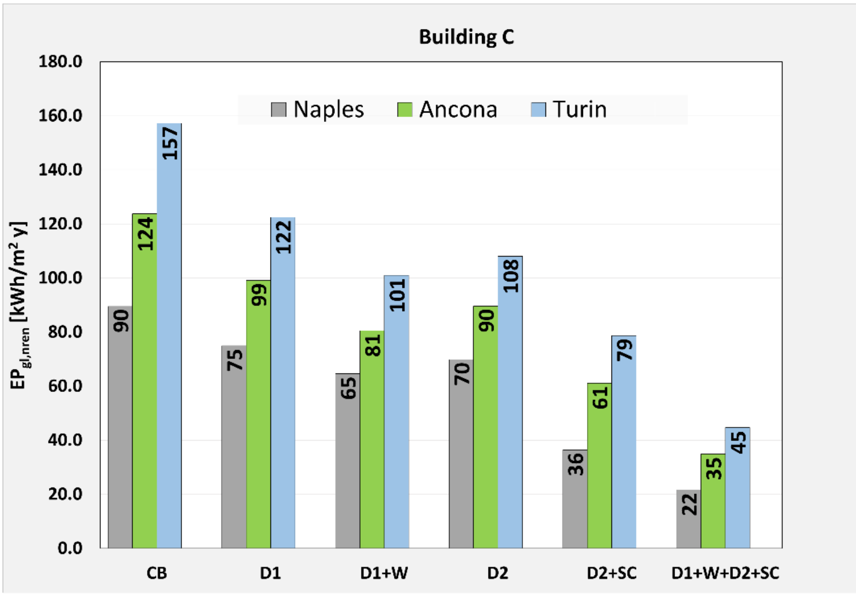

		D1	D1+W	D2	D2+SC	D1+W+D2+SC
$\Delta EP_{gl,nren}$	Naples	-16%	-28%	-22%	-59%	-76%
	Ancona	-20%	-35%	-28%	-51%	-72%
	Turin	-22%	-36%	-31%	-50%	-72%
ΔCO_2	Naples	-17%	-29%	-23%	-59%	-76%
	Ancona	-20%	-36%	-28%	-50%	-72%
	Turin	-22%	-36%	-32%	-50%	-72%

Figure 5.32 - Energy and Environmental results of the transient analysis – Building C

The economic analysis for Building C is proposed in Figure 5.33. In this case, the interventions D2 and D2+SC are very convenient, indeed, the DPBs are all acceptable also without incentives (SC3). This confirms the results obtained by means of the steady-state analysis. Indeed, the DPBs related to the replacement of the heating system (D2) are similar for both approaches, but in the steady-state analysis these are underestimated (and thus the EEM results in a more convenience). In this case too, even if the thermophysical quality of the base building envelope is low, the interventions of thermal insulation and replacement of the windows (D1 and D1+W) are not economically viable except with an economic incentive.

Generally, the economic analysis of the transient simulation has shown that the DPB are underestimated and NPV20 are overestimated in the steady-state simulations, so the energy retrofits seem better than these are in the reality. In general, even if the most convenient interventions are the same for both analyses, a transient simulation is necessary to obtain the real energy demand and environmental emissions of the building, and thus also the real economic indicators. Finally, the steady-state analysis is necessary to understand the energy class of the building and the class update after a building refurbishment, but a transient analysis is equally necessary to suggest to any investor the real economic return of the intervention.

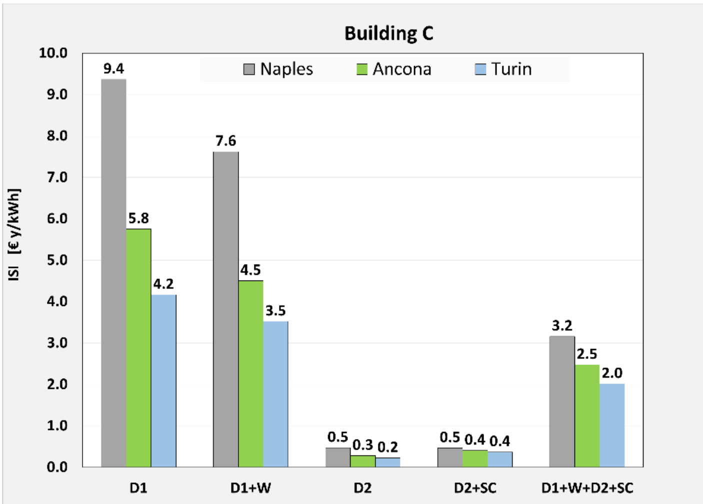

			D1	D1+W	D2	D2+SC	D1+W+D2+SC
NAPLES	SC1	NPV_{20} - €	NA	151050	NA	NA	521685
		DPB - years	NA	5.0	NA	NA	5.0
	SC2	NPV_{20} - €	-222689	-333220	90258	366516	-24838
		DPB - years	>20	>20	5.0	4.0	>20
	SC3	NPV_{20} - €	-676999	-913792	61648	290332	-681593
		DPB - years	>20	>20	8.0	5.0	>20
ANCONA	SC1	NPV_{20} - €	NA	256604	NA	465516	624457
		DPB - years	NA	5	NA	3	5
	SC2	NPV_{20} - €	-176131	-238857	172480	401633	65113
		DPB - years	>20	>20	3	4	17
	SC3	NPV_{20} - €	-646722	-835709	143093	323453	-609919
		DPB - years	>20	>20	4	5	>20
TURIN	SC1	NPV_{20} - €	NA	331571	NA	NA	764660
		DPB - years	NA	5	NA	NA	4
	SC2	NPV_{20} - €	-124985	-171440	255206	487844	188932
		DPB - years	>20	>20	3	4	14
	SC3	NPV_{20} - €	-606559	-779276	221107	398853	-507896
		DPB - years	>20	>20	4	5	>20

Figure 5.33 - Economic indicators of the transient analysis – Building C

The next sub-section summarizes the main findings of the study, by providing a critical comparing of the results of both analyses, steady-state and transient.

Main findings of the study

The outcomes of both analyses indicate that the best energy and environmental performance is achieved if retrofits involve the whole building-HVAC system. Indeed, the energy request is helved according to semi-stationary approach and it is reduced of more than 70% when a dynamic tool is used. However, this design configuration becomes economically profitable only if the new incentive mechanism is applicable. In this case, the obtained DPB is 5 years with both approaches, meanwhile different values of the NPV_{20} are obtained. In case of Building A, the main differences have been obtained; more in detail, the semi-stationary analysis seems overestimate the economic benefit. This is due, probably, to different boundary conditions that gives higher weight to the positive gains and also to different operating hours for the heating system.

In any case, both analyses confirm that, for a building of the 1990, the refurbishment interventions on the building envelope are not as convenient as for a building of the eighties or sixties. This applies to all climate zones considered, and representative of the Italian climate. The replacement of the heating system, or the coupled intervention on the heating system and installation of the solar collector system are generally more profitable than the interventions on the building envelope as evidenced by the very low values of ISI index.

Even if with both calculation methods the most economically advantageous interventions coincide, a transient analysis is necessary to understand the real economic indicators. Indeed, the DPB and NPV_{20} values are realistic only if a dynamic calculation is performed, by considering tailored boundary conditions, starting from the real (or reliable) management of buildings and equipment here installed.

5.3.4. Conclusive remarks

This section has investigated, from energy, environmental and economic points of view, the new funding incentives of the Italian Government, following the COVID-19 emergency, in comparison with the previous funding measures for energy retrofit. With a benefit of 110% of the investment cost, the energy efficiency measures that would be chosen from an energy point of view (i.e., insulation of opaque building envelope, replacement of windows and heating system) is also the most economically profitable, having an NPV_{20} equal to € 21’700 for Naples, € 27’000 for Ancona and € 37’800 in Turin, with an energy-saving and avoided CO_2 emissions of about 60%, by considering a single-family building of about 200 m^2.

With the application of the previous incentive mechanism (tax deduction between 50 and 65%), or in case of absence of incentive, the most convenient choice is the cheaper one (that is also the less efficient) and thus the mere replacement of old gas boilers. It has been highlighted that the best energy and environmental performance is achieved if the retrofits involve the whole building-HVAC system. The Italian funding system leads to prefer EEMs characterized by the best energy performance and not by the best cost/benefit ratio.

This allows economic advantages for building owners and environmental benefits for all. The new funding program is complex and fiscally articulated and this can be a barrier: a wide re-organization of professionals and construction companies is required.

5.4. The role of the occupant behaviors in affecting the feasibility of energy refurbishment of buildings

The occupant behavior could have a considerable impact on building energy demand and on indoor thermal comfort conditions. This depends on the heterogeneous ways of using building and energy systems and on the occupants' capability of adapting to the indoor environment. The two main user's actions, which affect the building energy demand, are the adaptive and non-adaptive ones [48]. In the first case, the occupants try to adapt themselves to the indoor environment, diversifying clothing, or moving through the apartment. In addition, they engage actions to adapt the surrounding environment to their preferences, such as opening or closing windows, modifying the thermostat setpoint, or adjusting shadings. The non-adaptive actions concern the addition of electric equipment which affects the electric load of the building. The motivations of these behaviors are both physical and social. About that, Ajzen & Madden [49] conceptualized the "*Theory of planned behavior"* and considered the individual agency (e.g., perception of comfort, relationship with the environment, personal abilities…) as the main cause of the individual behavior. Strengers and Maller [50] applied a social practice theory to analyze the cooling practices of Australian householders and underlined how the ability to respond to heat depends on the practical knowledge, the understandings about air-conditioners, and the available housing infrastructures. These theories were the base to develop a behavior model for residential buildings in the study of Samaratunga *et al*. [51]. They identified a discrepancy between the predicted energy performance and the measured data and recognized the prevailing causes in consumer behavior and in the building construction. A detailed analysis was performed, and the collected data were used as a base to develop a behavior model to support sustainability policies, the BASIX tool, and governmental education programs.

Moreover, many other authors considered fundamental the modeling of the user's behavior to evaluate the building energy demand for heating and cooling. Gucyeter [52] analyzed the impact of three different behavioral patterns in an office building. A typical office building was modeled, with integrated occupancy patterns, by distinguishing the Inactive Occupant (IO), the Slightly Active Occupant (SAO), and the Active Occupant (AO) models. Each pattern had various occupancy schedules and different use of the lighting system and of the thermostat (i.e., changing heating and cooling setpoints). The results demonstrated the necessity of a proper interaction of the occupants with the building systems. Indeed, switching on the lighting system without adjusting it according to the external lighting conditions, determines excessive gains, i.e. 38.5% and 44.7%, during the heating and cooling seasons, respectively, compared to active occupant models. In addition, the constant presence of people in the office, and thus the increment of heat due to the metabolic activity, causes the growth of internal gains in both heating and cooling periods.

Coherently, the study of Azar and Menassa [53] investigated the effects of the extreme energy use by users in a commercial building. They underlined the importance of encouraging the occupants to energy conservation practices, also by the increase of the extremists' acceptance of new behaviors of energy uses. In [54], the same authors quantified the operation-related energy saving potential for a commercial building. The human actions hugely affect the energy demands and thus the possibility of energy conservation for the commercial building stocks, and thus energy policies must support operation-focused solutions.

Pisello and Asdrubali [55] demonstrated that human-based energy retrofit can be a cost-effective alternative to classic retrofit solutions. The authors integrated numerical and experimental studies about occupant practices of energy saving, in a residential village in Italy, and developed a model for the dynamic simulation of building energy performance. Two different sets of simulations were developed: the first was about the reduction in the use of electricity, the second, diversely, regarded the energy savings obtained by adjusting temperature setpoints. The results showed, in the cases of reduction in the electricity use of 0.5 h/day, 1 h/day, and 1.5 h/day, a primary energy saving of 4.4%, 8.9%, and 13.3%, respectively. The related cost savings, by considering a constant electricity price of 0.25 €/kWh$_e$, were of 10.8 €/year, 21.6 €/year and 32.4 €/year, for each occupant. For what concerns the second group of simulations, the heating setpoint, progressively lowered from 21 °C to 19 °C during the heating season, implied energy savings around 24%. During the cooling season, the maximum energy saving corresponded to 4% at the scale of the village; in this study, the cooling setpoints were set at 25°C, 26°C and 27°C, increasing progressively. In conclusion, the study showed how occupant actions could replace energy retrofit interventions, in terms of energy and costs.

The novel investigation here proposed and largely deepened in [56], compared to the cited studies, shows an original assessment of the impact of users' behavior on a typical residential building from the cost, emission, and energy points of view. The results reported in the following section (5.4.2) refers only to the energy analysis, while the outcomes of the environmental and economic analysis are widely described in [56].

The evaluation outlined in subsections 5.4.1 and 5.4.2, was carried out with reference to a refurbished building with energy efficiency measures incentivized by the consolidated tax relief in Italy (ETICS thermal insulation of walls and flat roof, replacement of window frames with thermal break windows and low-emissive glass), and then reliable changes of behavior were applied in the use of the lighting, heating and cooling systems, in the schedules of windows' opening and in the use of shadings, according to common habits of occupants.

The study demonstrated how a convenient investment in energy terms could turn into a less convenient scenario, due to the wrong actions of the users. The effectiveness of energy efficiency measures can be negatively undermined by the wrong habits of the occupants.

Assessing the impact of the occupant behavior on building energy performance could give a contribution to current policies, to make them more aware and restrictive, and could be the right way to raise awareness among investors, owners, habitants, and all involved stakeholders.

5.4.1. Typical wrong habits for residential buildings: the case study of a Neapolitan building

The occupants try to achieve thermal and visual comfort in different manners which not always correspond to convenient behaviors, under energy and/or economic point of views. Social and environmental conditions could affect occupant actions on gains and loads that result in the energy demand of the building.

Thus, following a literature review, the possible actions of the users were identified and appropriately modeled. The way that occupants deal with energy is influenced by many factors, some objectives and other subjective [57]. The first ones can depend on environmental conditions such as temperature, air velocity, climate, or noise. The subjective factors depend on the personal perception of comfort, which can be affected by age, metabolic activity, particular mood, habits, sensations, social interaction. Other aspects affect occupant actions such as the social or economic conditions. In general, to obtain the comfort conditions, the users perform adaptive or non-adaptive actions [48], as said in the previous lines. In this study, the attention was paid on the adaptive and non-adaptive actions, namely:

- the occasional opening/closing of the windows,
- the increment or decrement of the heating setpoint,
- the adjustment of the shading systems,
- the addition of electric equipment,
- the energy-intensive use of the lighting system.

The main ways of modeling the occupant behaviors in the BPS (building performance simulation) are three: a ‘deterministic’, ‘stochastic’, and ‘user types & behavior styles’ approach [58].

According to Stazi *et al*. [58], the ‘deterministic’ approach refers to a uniform behavior of the occupant. In this case, it is assumed that all users have the same actions and make the same modifications to the systems. The ‘stochastic’ approach depends on the variability in the interaction with the systems by the users. Each occupant, influenced by a different boundary conditions, tries to adapt himself or the surrounding environment in a personal way. Therefore, this approach takes into account the probability that certain actions will occur. Finally, the ‘user type & behavior style’ approach is based on the energy consumption of the occupants, that could be waster, normal or conscious, and on the frequency of interaction with equipment (active, medium, or passive).

The reference modeling approach in the current study is the deterministic one, and the aim is to demonstrate the extent of the occupant actions on building energy demand.

The investigated building is a typical residential edifice located in Naples (Tyrrhenian coastline, Italic Climate C). It is a construction of the sixties and seventies of eight floors (Figure 5.34) and it is characterized by a reinforced concrete structural frame and uninsulated walls. The thermophysical properties of the building and its main technical characteristics are detailed in [56].

Figure 5.34 - Buildings similar to the investigated one, in the same city (A), rendered view of the building model (B).

The energy refurbishment of the building consists of two different energy efficiency interventions. In detail, common energy conservation measures for the retrofit of the residential building stock in Naples were considered:

- the thermal insulation of the opaque building envelope (walls and flat roof). The achieved values of thermal transmittance fulfill the prescriptions of the Italian Ministerial Decree 26/06/2015 (U_{value} = 0.30 W/m^{2}K for the vertical envelope and 0.29 W/m^{2}K for the roof).

- The replacement of the old wood frames and the single glasses (U_g = 5.9 W/m^{2}K) with an aluminum frame with thermal break and a Low-E double glass 6/13/6, with argon-filled cavity (U_g = 1.5 W/m^{2}K).

These interventions affect predominately the building energy demands for space heating, which, has a higher impact on the overall energy request (42%).

To analyze the impact of the occupant behavior on building energy performance, the users' actions were integrated into the simulation building model of EnergyPlus [21]. The changes were made on the refurbished building in order to achieve, in the presence of wrong behaviors of the occupants, two information, namely concerning:

- expected energy performance of the refurbished building not so satisfactory;
- a poor energy improvement in comparison to the base building.

In Figure 5.35, the actions actuated by the occupants and the performed investigations of related effects are shown

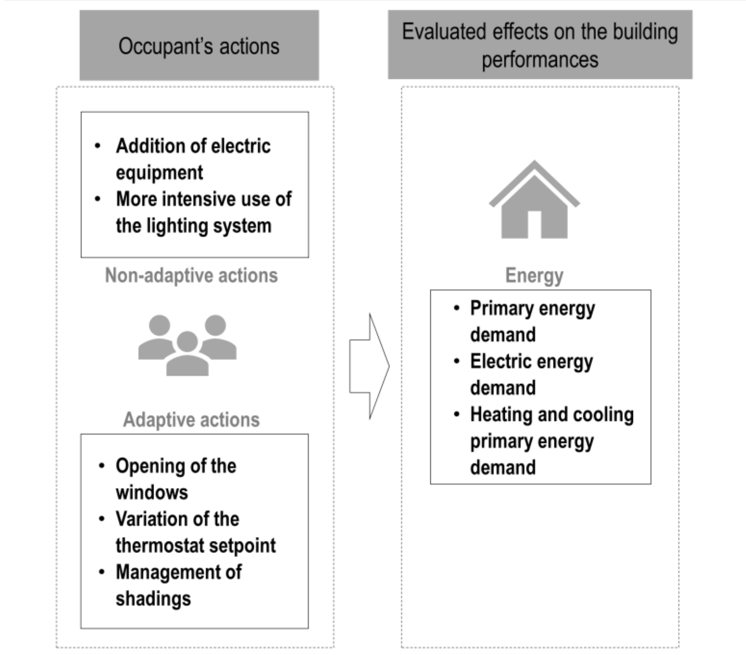

Figure 5.35 - Actions of users and evaluation of their effects

The investigation compares the simulation results of the base building with calibrated energy demand, with those of the refurbished building with standard users and of the refurbished building with energy-intensive users (Figure 5.36). The occupants' behaviors were integrated into the simulation model of EnergyPlus, according to the indications explained in [56]. and summarized in Figure 5.37.

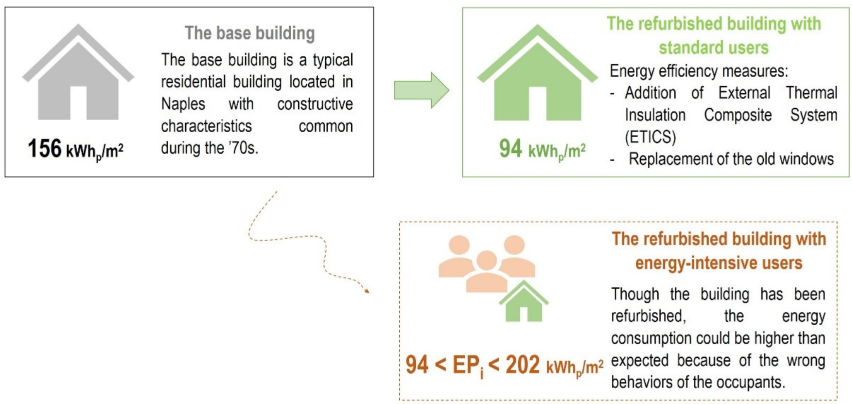

Figure 5.36 - Summary diagram of the simulation models compared

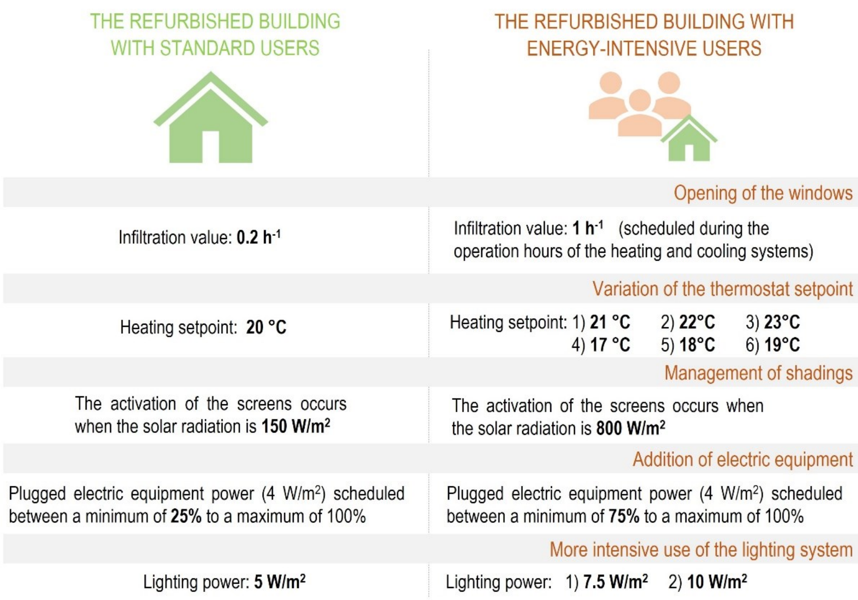

Figure 5.37 - Schematic modeling of the occupant behavior

5.4.2. Results and main outcomes of the study

The results of the analysis show that the energy consumption of the base building, whose numerical model was calibrated and validate according to the real conditions of use, is 156 kWh/m^2. The energy refurbishment involves an energy saving of 42%, and thus the yearly energy demand is reduced to 94 kWh/m^2. The energy results of the simulated wrong habits are summarized in Table 5.16. The table reports the results of the wrong habits examined singularly, and also those of the configuration which added them up all together.

Evaluating the overall results of the wrong habits considered, the behavior that has the most negative impact on the building energy consumption, is the energy-intensive use of electric equipment. The yearly energy demand of the refurbished building, but with an energy intensive use of the electric equipment, is 130 kWh$_p$/m^2, a lower energy demand compared to the base building (156 kWh$_p$/m^2) but the greater energy demand among all those referred to the refurbished buildings (standard use = 94 kWh$_p$/m^2) with wrong habits. The addition and more intense use of equipment nullifies the need for heating (the corresponding value is 0.3 kWh/m^2) but causes the increase of the cooling energy demand from 13 kWh$_p$/m^2 to 16 kWh$_p$/m^2 if compared to the reference refurbished building. In the same way, when the lighting system has a nominal power of 10 W/m^2, the yearly energy demand is 129 kWh$_p$/m^2 and the electric energy demand of the refurbished building passes from 78 kWh$_p$/m^2 to 113 kWh$_p$/m^2. The occupant behavior which does not lead to an increase in annual energy demand is the deactivation of the shading system. In this case, the cooling demand increases but the energy demand for electricity decreases following the reduction in the use of artificial lights. Of course, a sapient use of shadings systems (automatic) will provide undebatable thermal and energy benefits.

Finally, when all the wrong actions were taken into account in their more energy-intensive version (e.g., the heating setpoint was set at 23°C and the power of the lighting system was set at 10 W/m^2) the yearly energy demand results equal to 202 kWh$_p$/m^2, which corresponds to a higher value compared to both the refurbished standard building (94 kWh_p/m^2) and the base building before the refurbishment (156 kWh_p/m^2). It is interesting to note that, even if the overall energy demand is the highest, the heating energy demand is greater than the reference refurbished building but lower than the base building. Conversely, the cooling energy demand has a higher value both with respect to the base case and the refurbished reference building. Thus, more in general, the wrong occupant behaviors have a more significant impact on the cooling demand rather than the heating demand. The combination of energy-intensive behaviors is an extreme condition, which could only occur if users simultaneously assume all the wrong habits. The energy demand of this building typology could be considered as the maximum primary energy demand of a refurbished residential building in Naples. Therefore, the tailored, dynamic and reliable building energy demand of a refurbished building (with no actions on the heating and cooling systems, and without considering the domestic hot water need) could vary from a maximum of 202 kWh_p/m^2 to a minimum of 94 kWh_p/m^2 depending on user's behavior.

Table 5.16 - Results in terms of primary energy demand of the energy-intensive use of the building

	Yearly Overall Energy Demand			**Heating Energy Demand**			**Cooling Energy Demand**			**Electric uses**		
	kWh_p	kWh_p/m^2	% of the BB	kWh_p	kWh_p/m^2	% of the BB	kWh_p	kWh_p/m^2	% of the BB	kWh_p	kWh_p/m^2	% of the BB
Base building (BB)	604’978	156	(100%)	256’442	66	(100%)	50’122	13	(100%)	298’415	77	(100%)
Refurbished building (standard user)	363’738	94	60%	12’708	3	5%	49’686	13	99%	301’345	78	101%
Refurbished building, wrong opening of windows	476’974	123	79%	120’980	31	47%	54’649	14	109%	301’345	78	101%
Refurbished building, heating setpoint 17 °C	351’107	91	58%	75	0	0%	49’687	13	99%	301’345	78	101%
Refurbished building, heating setpoint 23 °C	412’666	106	68%	61’629	16	24%	49’693	13	99%	301’345	78	101%
Refurbished building, deactivated shadings	364’630	94	60%	6729	2	3%	63’371	16	126%	294’530	76	99%
Refurbished building, increased equipment	503’844	130	83%	1151	0	0%	60’608	16	121%	442’084	114	148%
Refurbished building, increased lighting (power 7.5 W/m^2)	429’553	111	71%	5309	1	2%	54’325	14	108%	369’919	95	124%
Refurbished building, increased lighting (power 10 W/m^2)	499’108	129	83%	1709	0	1%	58’906	15	118%	438’493	113	147%
Refurbished building, sum of the wrong behaviors	781’900	202	129%	126’227	33	49%	90’070	23	180%	565’602	146	190%

CHAPTER 5 - References

[1] EU Commission and Parliament Directive 2002/91/EU of the European Parliament and of the Council of 16 December 2002 on the energy performance of buildings. Off. J. Eur. Union 2003. Available online: https://eur-lex.europa.eu/LexUriServ/LexUriServ.do?uri=OJ:L:2003:001:0065:0071:EN:PDF. Accessed in November 2021

[2] EU Commission and Parliament, Directive 2010/31/EU of the European Parliament and of the Council of 19 May 2010 on the energy performance of buildings (EPBD Recast). Off. J. Eur. Union 2010, Available online: https://eur-lex.europa.eu/LexUriServ/LexUriServ.do?uri=OJ:L:2010:153:0013:0035:IT:PDF. Accessed in November 2021

[3] EU Commission, Commission Delegated Regulation (EU) No 244/2012 of 16 January 2012 supplementing Directive 2010/31/EU of the European Parliament and of the Council on the energy performance of buildings. Off. J. Eur. Union 2012, Available online: https://eur-lex.europa.eu/legal-content/EN/TXT/PDF/?uri=CELEX:32012R0244&from=GA. Accessed in November 2021

[4] EU Commission and Parliament, Directive 2012/27/EU of the European Parliament and of the Council of 25 October 2012 on the energy efficiency. Off. J. Eur. Union 2012, Available online: https://eur-lex.europa.eu/legal-content/EN/TXT/PDF/?uri=CELEX:32012L0027&from=IT. Accessed in November 2021

[5] Directive (EU) 2018/844 of the European Parliament and of the Council of 30 May 2018. Available online: https://eur-lex.europa.eu/legal-content/EN/TXT/?uri=uriserv%3AOJ.L_.2018.156.01.0075.01.ENG. Accessed in November 2021

[6] Ascione, F., De Masi, R.F., de Rossi, F., Ruggiero, S., Vanoli, G.P., Optimization of building envelope design for nZEBs in Mediterranean climate: Performance analysis of residential case study, Applied Energy, 2016, 183, pp. 938–957.

[7] H. Li, S. Wang, Coordinated robust optimal design of building envelope and energy systems for zero/low energy buildings considering uncertainties, Applied Energy 265 (2020) 114779

[8] E. Moretti, E. Belloni, F. Agosti, Innovative mineral fiber insulation panels for buildings: Thermal and acoustic characterization, Applied Energy1 69 (2016) 421-432

[9] De Masi, R.F., Ruggiero, S., Vanoli, G.P., Multi-layered wall with vacuum insulation panels: Results of 5-years in-field monitoring and numerical analysis of aging effect on building consumptions, Applied Energy, 2020, 278, 115605

[10] Parcesepe, E., De Masi, R.F., Lima, C., G.M. Mauro, Pecce, M.R., Maddaloni, G., Assessment of mechanical and thermal properties of hemp-lime mortar, Materials, 2021, 14(4), pp. 1–24, 882

[11] Afaq A.Butt, Samuel B.de Vries, Roel C.G.M.Loonen, Jan L.M.Hensen, A. Stuiver, J. E.J.van den Ham, Bart S.J.F.Erich, Investigating the energy saving potential of thermochromic coatings on building envelopes, Applied Energy 291 (2021) 116788

[12] A. Arteconi, A. Mugnini, F. Polonara Energy flexible buildings: A methodology for rating the flexibility performance of buildings with electric heating and cooling systems Applied Energy 251(2019) 113387

[13] E. Schito, P. Conti, L. Urbanucci, D. Testi, Multi-objective optimization of HVAC control in museum environment for artwork preservation, visitors' thermal comfort and energy efficiency, Building and Environment 180 (2020) 107018

[14] D. Schäuble, A. Marian, L. Cremonese, Conditions for a cost-effective application of smart thermostat systems in residential buildings, Applied Energy 262 (2020) 114526

[15] A. Anctil, E. Lee, R. R. Lunt, Net energy and cost benefit of transparent organic solar cells in building-integrated applications, Applied Energy 261 (2020) 114429

[16] Y. Luo, L. Zhang, Z. Liu, J. Yu, X. Xu, X. Su, Towards net zero energy building: The application potential and adaptability of photovoltaic-thermoelectric-battery wall system, Applied Energy 258 (2020) 114066.

[17] F. Ascione, Energy conservation and renewable technologies for buildings to face the impact of the climate change and minimize the use of cooling, Solar Energy 154 (2017), pp. 34-100.

[18] Mat Santamouris, Innovating to zero the building sector in Europe: Minimising the energy consumption, eradication of the energy poverty and mitigating the local climate change, Solar Energy, 128 (2016), pp. 61-94.

[19] Proactive synergy of integrated Efficient Technologies on buildings' Envelopes (Pro-GET-OnE) — H2020. Available online: https://www.progetone.eu/project/. Accessed in November 2021

[20] Assimakopoulos, M. N., De Masi, R. F., Fotopoulou, A., Papadaki, D., Ruggiero, S., Semprini, G., & Vanoli, G. P. (2020). Holistic approach for energy retrofit with volumetric add-ons toward nZEB target: Case study of a dormitory in Athens. Energy and Buildings, 207, 109630.

[21] U.S. Department of Energy. EnergyPlus simulation software v. 9.2.0 https://energyplus.net/. Accessed in November 2021

[22] DesignBuilder v.6.1.0 http://www.designbuilder.co.uk/. Accessed in November 2021

[23] KENAK, 2010. Greek Regulation on Energy Performance of Buildings, Ministerial Decision Δ6/Β/οικ.5825/30-03-2010 ΦΕΚ Β' 407 (in Greek).

[24] ISO 7730:2005 Ergonomics of the thermal environment – Analytical determination and interpretation of thermal comfort using calculation of the PMV and PPD indices and local thermal comfort criteria

[25] Greek national plan "National plan for increasing the number of nearly zero-energy buildings". Available online: https://ec.europa.eu/energy/sites/ener/files/documents/greece_en_version_2017.pdf. Accessed in November 2021

[26] TABULA WebTool; 2016. (Accessed 26/10/20).

[27] Italian Committee for Standardization. Standard UNI TS 11300 part 1: 2008, Energy performance of buildings: Evaluation of energy need for space heating and cooling, 2008.

[28] European Committee for Standardization. Standard ISO EN 13790: 2008, Energy performance of buildings – Calculation of energy use for space heating and cooling, 2008.

[29] Italian Thermo-technical Committee CTI – CTI Recommendation R03/3, Energy Performance of building. Winter heating and domestic hot water, 2003.

[30] Annex E "Requisiti degli interventi di isolamento termico" (In Italian), Decree law 06/08/2020. Available online: https://www.gazzettaufficiale.it/do/atto/serie_generale/caricaPdf?cdimg=20A0539400500010110001&dgu=2020-10-05&art.dataPubblicazioneGazzetta=2020-10-05&art.codiceRedazionale=20A05394&art.num=1&art.tiposerie=SG. Accessed in November 2021

[31] Annex H “Solar collectors” Decree law 06/08/2020. Available online: https://www.gazzettaufficiale.it/do/atto/serie_generale/caricaPdf?cdimg=20A0539400800010110001&dgu=2020-10-05&art.dataPubblicazioneGazzetta=2020-10-05&art.codiceRedazionale=20A05394&art.num=1&art.tiposerie=SG. Accessed in November 2021

[32] Annex I, “Massimali specifici di costo per gli interventi sottoposti a dichiarazione del fornitore o dell’installatore ai sensi dell’Allegato A” (In Italian), Decree law 06/08/2020. Available online: https://www.gazzettaufficiale.it/do/atto/serie_generale/caricaPdf?cdimg=20A0539400900010110001&dgu=2020-10-05&art.dataPubblicazioneGazzetta=2020-10-05&art.codiceRedazionale=20A05394&art.num=1&art.tiposerie=SG. Accessed in November 2021

[33] Annex B “Tabella di sintesi degli interventi” (In Italian), Decree law 06/08/2020. Available online: https://www.gazzettaufficiale.it/do/atto/serie_generale/caricaPdf?cdimg=20A0539400200010110001&dgu=2020-10-05&art.dataPubblicazioneGazzetta=2020-10-05&art.codiceRedazionale=20A05394&art.num=1&art.tiposerie=SG. Accessed in November 2021

[34] D.Lgs. 28/2011, Italian Lesgilsative Decree 28/2011 “Attuazione della direttiva 2009/28/CE sulla promozione dell'uso dell'energia da fonti rinnovabili, recante modifica e successiva abrogazione delle direttive 2001/77/CE e 2003/30/CE”, (In Italian), 2011.

[35] DM 26/06/2015, Italian Ministerial Decree, “Applicazione delle metodologie di calcolo delle prestazioni energetiche e definizione delle prescrizioni e dei requisiti minimi degli edifici”, (In Italian), 2015.

[36] ISO – International Organization for Standardization. ISO 13786: Thermal performance of building components- Dynamic thermal characteristics - Calculation methods. 2007.

[37] DM 26/06/2015, Italian Ministerial Decree, “Adeguamento linee guida nazionali per la certificazione energetica degli edifici”, (In Italian), 2015.

[38] European Standard. EN 15217: Energy performance of buildings - Methods for expressing energy performance and for energy certification of buildings. 2007.

[39] European Standard. EN ISO 52003-1: Energy performance of buildings - Indicators, requirements, ratings and certificates - Part 1: General aspects and application to the overall energy performance. 2017.

[40] DPR 412/1993, Italian Presidential Decree, “Regolamento recante norme per la progettazione, l'installazione, l'esercizio e la manutenzione degli impianti termici degli edifici ai fini del contenimento dei consumi di energia, in attuazione dell'art. 4, comma 4, della legge 9 gennaio 1991, n. 10.” (in italian)
[41] UNI 10349-1: Heating and cooling of buildings - Climatic data - Part 1: Monthly means for evaluation of energy need for space heating and cooling and methods for splitting global solar irradiance into the direct and diffuse parts and for calculate the solar irradiance on tilted planes. 2016.
[42] UNI. Technical specification. Energy performance of buildings. Part 2. Evaluation of primary energy need and of system efficiencies for space heating and domestic hot water production, UNITS 11300-2; 2014.
[43] TerMus BIM, 2018 Acca Software. Available online: https://www.acca.it/software-certificazione-energetica. Accessed in November 2021
[44] Italian Presidential Decree n 74/2013. D.P.R. 16 April 2013, n. 74. Available online: https://www.gazzettaufficiale.it/eli/id/2013/06/27/13G00114/sg. Accessed in November 2021
[45] U.S. department of Energy Federal Management Program. M&G Guidelines: Measurement and verification of Performance-Based Contracts Version 4.0, 2015.
[46] Ascione, F., Bianco, N., De Masi, R. F., Mastellone, M., Mauro, G. M., & Vanoli, G. P. (2020). The role of the occupant behavior in affecting the feasibility of energy refurbishment of residential buildings: Typical effective retrofits compromised by typical wrong habits. Energy and Buildings, 223, 110217.
[47] ARERA Italian Regulatory Authority for Energy, Networks and Environment.
[48] Hong, T., Yan, D., D'Oca, S., & Chen, C. F. (2017). Ten questions concerning occupant behavior in buildings: The big picture. Building and Environment, 114, 518-530.
[49] Ajzen, I., & Madden, T. J. (1986). Prediction of goal-directed behavior: Attitudes, intentions, and perceived behavioral control. Journal of experimental social psychology, 22(5), 453-474.
[50] Strengers, Y., & Maller, C. (2011). Integrating health, housing and energy policies: social practices of cooling. Building Research & Information, 39(2), 154-168.

[51] Samaratunga, M., Ding, L., Bishop, K., Prasad, D., & Yee, K. W. (2017). Modelling and analysis of post-occupancy behaviour in residential buildings to inform BASIX sustainability assessments in NSW. Procedia Engineering, 180, 343-355.

[52] Gucyeter, B. (2018). Evaluating diverse patterns of occupant behavior regarding control-based activities in energy performance simulation. Frontiers of architectural research, 7(2), 167-179.

[53] Azar, E., & Menassa, C. C. (2015). Evaluating the impact of extreme energy use behavior on occupancy interventions in commercial buildings. Energy and Buildings, 97, 205-218.

[54] Azar, E., & Menassa, C. C. (2014). A comprehensive framework to quantify energy savings potential from improved operations of commercial building stocks. Energy Policy, 67, 459-472.

[55] Pisello, A. L., & Asdrubali, F. (2014). Human-based energy retrofits in residential buildings: A cost-effective alternative to traditional physical strategies. Applied Energy, 133, 224-235.

[56] Ascione, F., Bianco, N., De Masi, R. F., Mastellone, M., Mauro, G. M., & Vanoli, G. P. (2020). The role of the occupant behavior in affecting the feasibility of energy refurbishment of residential buildings: Typical effective retrofits compromised by typical wrong habits.*Energy and Buildings*,*223*, 110217.

[57] Tam, V., Almeida, L., & Le, K. (2018). Energy-Related Occupant Behaviour and Its Implications in Energy Use: A Chronological Review. Sustainability, 10(8), 2635.

[58] Stazi, F., & Naspi, F. (2018). Impact of Occupants' Behaviour on Zero-Energy Buildings. Cham, Switzerland: Springer.

CHAPTER 6.

A user-friendly tool for accurate energy simulation of residential buildings via few numerical inputs: conceptualization, development, and validation of EMAR

The accurate simulation of energy performance is fundamental to design low-energy buildings – newly-built or after refurbishment – and thus to promote sustainability. However, this is an involved task requiring high complexity in modeling and simulation. Most accurate building energy simulation tools are not user-friendly for building professionals, thereby hindering widespread use of effective methodologies – developed by researchers – for the transition to nearly- or net- zero energy buildings. The investigation reported in this chapter tries to solve such an issue by proposing a novel, accurate but user-friendly tool for building modeling and energy simulation. The tool is denoted as EMAR because it is based on the advanced coupling between ENergyplus and MAtlab® addressing Residential buildings, which are a major part of the existing stocks. EMAR completely works under MATLAB® environment and only needs around 60 numerical inputs to generate simplified building models and perform accurate energy simulations. The available outputs are numerous referring to energy and economic performance as well as thermal comfort. No drawings, no schemes of energy systems, no deep modeling expertise are required but only a few numbers. EMAR is validated against detailed EnergyPlus models of an ASHRAE test building and of two typical European buildings. The discrepancies are lower than 10% as concerns thermal and primary energy needs, and in most cases are lower than 5%, but the modeling complexity and computational burden are drastically reduced. Thus, EMAR can be a precious tool to perform user-friendly but accurate building energy modeling and simulations. Figure 6.1 represents the steps described in the following subsections, necessary for the development of EMAR tool.

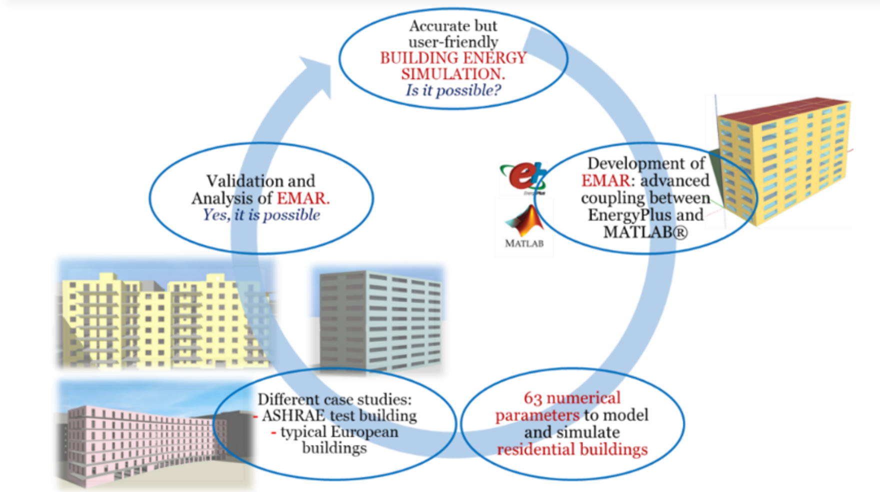

Figure 6.1 – Graphical representation of the steps for EMAR tool development

6.1. Introduction

Everyone knows by now that optimizing building energy performance is fundamental to promote energy transition and sustainable development. The diffusion of nZEB and NZEB is sought worldwide to minimize energy consumption and CO_2 emissions of the building sector, whose share is over 30% in most countries [1]. In this frame, how to perform building energy optimization (BEO)? It is a complex task involving multi-variable, multi-objective and multi-criteria problems [2]. Numerous and comprehensive methodologies have been proposed in this regard, as shown by the valuable reviews of Nguyen *et al.* [3] and, more recently, Longo *et al.* [4]. Definitely, a major issue of such methodologies is BES because the reliable prediction of energy performance is crucial for a robust and successful design of low energy buildings, newly-built or after refurbishment. However, most accurate BES tools are not user-friendly, thereby hindering a widespread use of the mentioned optimization methodologies for designing nZEBs because of complex modeling and simulation issues. It follows that simpler semi-steady-state BES tools are often used compromising the outcomes' accuracy and reliability. It can be said that the selection of the tool to be used involves a two-objective problem between complexity and reliability. This study tries to solve such a common problem for building professionals.

6.1.1. Building energy simulation: Background

Different software and engines are available, and the best choice depends on many factors such as the aim (*e.g.,* accurate prediction or energy labeling), the clients' needs, the designer skills. For instance, Poel *et al.* [5] proposed a comprehensive overview of the most used tools to assess the energy performance of residential buildings. Globally, the approaches can be classified in white-box, gray-box and black-box models [6], [7]. The white-box models are totally based on a theoretical structure developed through physical laws [8],[9]. The grey-box models couple a theoretical structure with measured or simulated data, ensuring higher adherence to reality [10], [11]. The black-box models provide hidden functions that correlate the outputs to the inputs (building characteristics), and are generally totally data-driven, based on the processing of historical data without the detailed knowledge of on-site physical information [6]. They usually apply meta-modeling, developing surrogate models through statistical regression, support vector machine (SVM), artificial neural networks (ANNs) or further machine learning techniques [12]. Definitely, the most consistent choice is using suitable BES tools that perform reliable dynamic simulations [13], *e.g.,* EnergyPlus, TRNSYS, ESP-r, IDA ICE, which provide accurate predictions of energy needs for the investigated scenarios after the proper development of calibrated building models. These tools are widely employed by the scientific community given their high capability and reliability [2]. They are white-box models based on robust and complex theoretical structures of physical laws, but they are often used as a sort of black-box models since the user is rarely able to handle such theoretical structures. Nevertheless, as outlined in [6], their high accuracy derives from high complexity in their use and low running speed, which do not allow their wide diffusion in the professionals' community. This issue is amplified when BEO is applied because optimization algorithms need to be applied to explore large solutions domains, thereby increasing the computational burden. That is why building professionals usually prefer other tools based on white box models, which apply simplified assumptions, such as semi-steady-state conditions, resistance-capacitance (RC) equivalent networks, degree day method, temperature frequency method, residential load factor method [6]. These latter ensure user-friendliness and high running speed at the cost of lower accuracy [6]. Therefore, as mentioned, they are often unreliable because they cannot properly simulate the dynamics in weather conditions and building performance as concerns envelope, energy systems, use and operation, such as schedules of occupation or HVAC setpoints.

Finally, there is an open issue that should be faced:

- the community of building professionals has few user-friendly but reliable options for the prediction of building energy performance.

As highlighted in [6], this is a critical issue because building energy simulation is fundamental for different crucial aims and functions, such as: *i)* optimization of building energy design/retrofit, *ii)* demand side management, *iii)* energy labeling, *iv)* energy mapping of geographical areas, *v)* establishing benchmarks for multi-scale building communities. Accordingly, the attention of building scientists, policymakers and all involved stakeholders is increasingly focused on such an issue, struggling for the development of new BES tools that can have a wide diffusion among practitioners [14]. In this vein, Ascione *et al.* [15] proposed a user-friendly tool denoted as EMA by coupling EnergyPlus and MATLAB® to predict different indicators related to building energy, environmental and economic performance. However, such tool was usable only for simplified office buildings, and was not subjected to a robust validation. The same authors addressed a further aspect of building models' simplification in [16], investigating whether considering the inter-building effect (IBE) is fundamental for reliable simulations. The outcomes showed that the IBE can be neglected with good reliability in some cases, *e.g.,* when there is an intensive use of shading systems, but the study did not answer the approached issue because a complex BPS tool – *i.e.,* EnergyPlus – was used. Thus, the IBE can be often neglected with acceptable approximation in building modeling, but which BES tool can be user-friendly and reliable? Cucca and Ianakiev [17] combined DesignBuilder® (and thus EnergyPlus) with Modelica-Dymola to achieve a simpler and clearer representation of energy systems and associated control schemes, but building modeling still featured high complexity considering the computational burden for co-simulation too. In this regard, building information modeling (BIM) software can help the users in combining different tools for a comprehensive and interactive design process, including BES tools to predict building energy performance at different design stages [18], [19]. However, the issue is still open because a smart and flexible tool is required, able to perform accurate energy simulations extrapolating the required inputs data from the building model under development.

6.1.2. Contribution of this study

Further similar studies may be cited but the scientific literature shows a crucial knowledge gap, *i.e.,* to the authors' knowledge, there are no validated user-friendly BES tools that ensure accurate predictions of dynamic building energy performance requiring only few numerical inputs. Such a tool would provide worthy contributions to the body of knowledge to promote the transition to a low energy and low carbon building stock, fundamental in the path of sustainable development. Indeed, it would ensure:

- user-friendly, fast but reliable predictions of building energy performance and energy labeling;
- easy/flexible integration in optimization and BIM frameworks to address building energy design/retrofit, thereby supporting the diffusion of robust building energy optimization in the community of professionals;
- easy/flexible integration in frameworks for the large-scale analysis of building energy performance, thereby supporting the energy transition of whole neighborhoods, districts and stocks, as well as the optimization of public energy policies for the building sector.

In this regard, this investigation aims at filling such a knowledge gap by proposing a reliable but user-friendly and flexible tool for building energy modeling and simulation, which can provide the mentioned novel contributions. The tool is denoted as EMAR because it is based on the advanced coupling between EnergyPlus [20] and MAtlab® [21] addressing Residential building. It requires only (a maximum of) 63 numerical inputs, and offers several possible outputs concerning energy (environmental) and economic performance. It derives from a deep enhancement of EMA [15] by increasing the level of detail in building modeling, addressing also residential buildings, and performing a robust validation against detailed EnergyPlus models of an ASHRAE test building and of two typical European buildings. As discussed, EMAR can be a precious tool for building stakeholders to perform user-friendly but accurate energy simulations, thereby supporting computer-aided design and optimization with a view to urban sustainable growth.

6.2. Materials and methods: EMAR

This study proposes EMAR, which is a novel, user-friendly building energy simulation (BES) tool, based on the advanced coupling between EnergyPlus [20] and MAtlab® [21] addressing (some) Residential buildings, which are a major part of existing stocks, worldwide.

6.2.1. Framework

As shown in the framework of Figure 6.2, EMAR works under MATLAB® environment and needs only numerical inputs to generate simplified building models and perform accurate energy simulations. No drawings, no schemes of energy systems, no deep modeling expertise are required, but only few numbers. The available outputs are numerous referring to energy, environmental, economic performance as well as thermal comfort.

EnergyPlus is used as simulation engine because of its high capability and reliability that make it the most used BES engine for building energy optimization [3]. Notably, EnergyPlus needs text-based inputs, the so-called *.idf* files, and provides *.csv* (comma separated variables) outputs. However, when it is used stand-alone, EnergyPlus features high modeling complexity and needs deep simulation expertise, especially as concerns building geometry and energy systems. Therefore, EMAR uses MATLAB® to simplify building modeling and simulation as well as for post-processing, offering a simple user-interface that requires only 63 numerical inputs.

The framework is based on an EnergyPlus parametrized mother-file *.idf* (text-based, see Figure 6.2a), where the building characteristics related to geometry, envelope and systems are parametrized. This means that parameters are present instead of typical EnergyPlus input data. Each parameter is enclosed between the symbols “<” and “>”, as shown for example in Figure 6.2a.

An EMAR simulation related to a specific building comprises the following steps, performed under MATLAB® environment:

- **step 1)** the user sets: *i)* the 63 EMAR inputs (Figure 6.2b); *ii)* the weather data file to be employed, which can be downloaded from EnergyPlus website [22]; *iii)* the required outputs, *i.e.,* performance indicators, to be assessed;
- **step 2)** MATLAB® runs an EnergyPlus simulation via a coupling function denoted as EMAR (Figure 6.2c) and collects the simulation output data (*.csv*), which refer to a typical climatic year;
- **step 3)** a post-process MATLAB® code simulates the performance of the energy systems and provides the required outputs.

In particular, when the user sets the inputs (**step 1**), EMAR generates a specific *.idf* file for the investigated building from the mother-file, properly replacing the mentioned parameters (“<>”). The model presents a simplified geometry (Figure 6.3a), as in [15], [23], because a regular rectangular plan is assumed with equal-height floors, setting a thermal zoning (Figure 6.3b) typical of the investigated use destination. Two dwellings per floor are considered, each dwelling subdivided in two night-zones and two day-zones, according to standard architectural designs. The two dwellings of each floor are separated by a landing, *i.e.,* a circulation zone. In addition, the windows' positions are fixed, but the "window to wall ratio" (%) can vary for each exposure. Six windows are assumed for each dwelling and one for each landing, having half area compared to the other windows of the same façade, with a symmetrical layout (Figure 6.3a). The vertical centre of the windows is at half height of the floor. The windows' height is equal to 1.5 m, if sufficient to ensure the window to wall ratio set by the user, or 2.4 m otherwise, while the width is computed from height and window to wall ratio [15], [23]. The mentioned simplifications about the building geometry facilitate the parameterization process, and these are suitable for most buildings, given the high percentage of rectangular shapes [23].

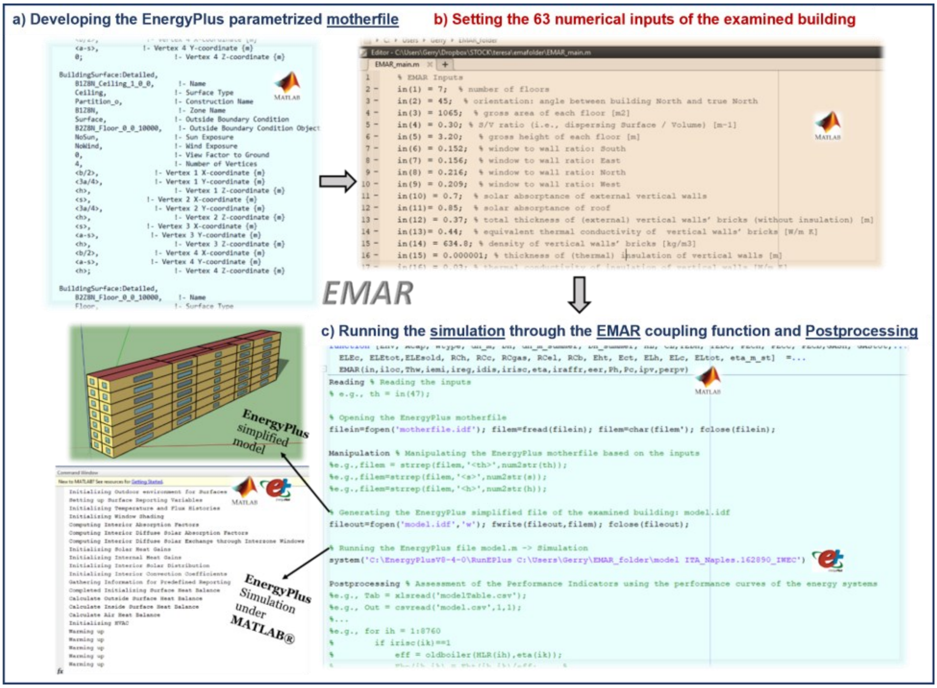

Figure 6.2 – EMAR framework

Then, **step 2** is performed. EnergyPlus simulation's output data consist of the hourly values for each dwelling of:

- thermal energy demands for space heating and space cooling;

- electricity demands for direct electric uses, *i.e.,* electrical equipment and artificial lighting;
- thermal comfort indicators;
- produced energy by photovoltaics, if present.

Finally, in **step 3**, the post-process MATLAB® code handles such data and applies the performance curves of the energy systems, which can be also set by the user. These curves provide the efficiency of each system as a function of nominal value at rated conditions, hourly part load ratio, temperatures of heat transfer fluid and outdoor environment (only for some systems such as air-source chillers and heat pumps). A database developed in MATLAB® enables to associate each technology chosen by the user with a proper performance curve. Using such curves, primary energy conversion factors and specific energy costs, the hourly values of thermal energy demand are converted into primary energy consumption and related costs. The on-site electricity conversion by possible photovoltaic systems is considered through hourly energy balances. Surplus energy can be stored and then used, sold to the grid or wasted. Finally, the required outputs are assessed both at dwelling and building levels, concerning energy, environmental, economic performance, thermal comfort as well as the geometry and thermal characteristics of the building envelope.

Sections 6.2.2 and 6.2.3 detail EMAR inputs and outputs, respectively.

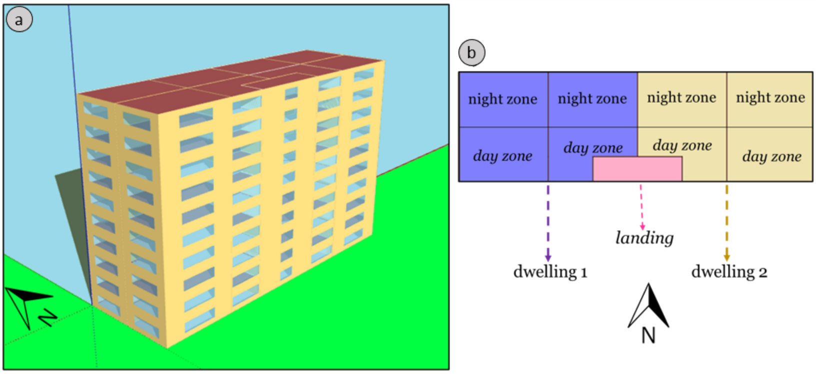

Figure 6.3 - a) 3D view of a building model developed through EMAR; b) plan view and thermal zones

6.2.2. Inputs

The 63 EMAR numerical inputs (denoted with “i”) are shown in Table 6.1, where they are classified in four groups, related to geometry, envelope, HVAC and photovoltaics, respectively.

Notably, no inputs related to building operation are present because only residential cases are addressed. Therefore, the values and schedules of building-plants use, occupation, operation of electric equipment and artificial lighting are set according to typical residential buildings from previous studies [16], [24] - [26] and can be modified depending on the examined case study. DHW consumption is considered fixed, equal to 25 kWh_p/m^2y, as typical of Italian dwellings [27], since it is not affected by the complex dynamics of the building envelope/systems. Also, this value can be modified according to the case study. It is noticed that the framework can be easily enhanced to consider different use destinations.

Table 6.1 – EMAR inputs

EMAR inputs	
<u>Geometry</u> i_1) number of floors i_2) orientation: angle between building north and true north i_3) gross area of each floor [m^2] i_4) S/V ratio (*i.e.,* dispersing surface / volume) [m^{-1}] i_5) gross height of each floor [m] i_6) window to wall ratio: south i_7) window to wall ratio: east i_8) window to wall ratio: north i_9) window to wall ratio: west <u>Envelope</u> i_{10}) solar absorptance of walls i_{11}) solar absorptance of roof i_{12}) thickness of walls' bricks (without insulation) [m] i_{13}) equivalent thermal conductivity of walls' bricks [W/m K] i_{14}) equivalent density of walls' bricks [kg/m^3] i_{15}) thickness of (thermal) insulation of walls [m] i_{16}) thermal conductivity of insulation of walls [W/m K] i_{17}) equivalent density of insulation of walls [kg/m^3] i_{18}) position of insulation of walls i_{19}) thickness of roof block (without insulation) [m] i_{20}) equivalent thermal conductivity of roof block [W/m K] i_{21}) equivalent density of roof block [kg/m^3] i_{22}) thickness of (thermal) insulation of roof [m] i_{23}) thermal conductivity of insulation of roof [W/m K] i_{24}) equivalent density of insulation of roof [kg/m^3] i_{25}) position of insulation of roof i_{26}) thickness of ground-floor block (without insulation) [m] i_{27}) equivalent thermal conductivity of ground-floor block [W/m K] i_{28}) equivalent density of ground-floor block [kg/m^3] i_{29}) thickness of (thermal) insulation of ground-floor [m] i_{30}) thermal conductivity of insulation of ground-floor [W/m K] i_{31}) equivalent density of insulation of ground-floor [kg/m^3] i_{32}) position of insulation of ground-floor i_{33}) fraction of dwellings with single-glazed, aluminum framed windows i_{34}) fraction of dwellings with single-glazed, wood framed windows	i_{35}) fraction of dwellings with double-glazed, aluminum framed windows i_{36}) fraction of dwellings with double-glazed, wood framed windows i_{37}) shading systems' type: south i_{38}) shading systems' type: east i_{39}) shading systems' type: north i_{40}) shading systems' type: west i_{41}) shading systems' position: south i_{42}) shading systems' position: east i_{43}) shading systems' position: north i_{44}) shading systems' position: west i_{45}) shading systems' radiation setpoint: south [W/m^2] i_{46}) shading systems' radiation setpoint: east [W/m^2] i_{47}) shading systems' radiation setpoint: north [W/m^2] i_{48}) shading systems' radiation setpoint: west [W/m^2] i_{49}) equivalent thickness of horizontal partitions [m] <u>Heating, Ventilating and Air Conditioning (per dwelling)</u> i_{50}) heating setpoint temperature [°C] [vector]* i_{51}) cooling setpoint temperature [°C] [vector]* i_{52}) efficiency of heating distribution-emission-regulation system [vector]* i_{53}) supply water temperature of heating terminals [vector]* i_{54}) type of heating generation system [vector]* i_{55}) efficiency of heating generation system [vector]* i_{56}) type of cooling generation system [vector]* i_{57}) energy efficiency ratio of cooling generation system [vector]* i_{58}) natural ventilation setpoint temperature [vector]* i_{59}) natural ventilation ACH [h^{-1}] [vector]* <u>PhotoVoltaics</u> i_{60}) type of PV panels i_{61}) percentage of roof covered by PV panels i_{62}) azimuth of PV panels i_{63}) tilt of PV panels

*the vectors include one value per dwelling

Most inputs have simple explanation and thus the attention is focused on the inputs that need further clarifications:

- the opaque components of the external building envelope (usually multi-layer) are modeled with equivalent mono-layer ones – with the same thickness t [m] (i_{12}, i_{19}, i_{26}) – that ensure the same values of thermal conductance K [W/m^{2}K] (and thus of thermal transmittance U_{value} [W/m^{2}K]) and areal heat capacity C_a [J/m^{2}K], because such physical quantities define the thermal performance of the building envelope, as concerns the resistance to heat transfer and the thermal inertia, respectively. In this regard, in order to reduce EMAR inputs simplifying its implementation, the specific heat c_p [J/kgK] of each opaque material is set equal to 1000 J/kgK – noting that most materials used in building applications have c_p around such a value –, while an equivalent density ρ_{eq} [kg/m^3] must be properly set to ensure the same C_a of the actual components;
- the equivalent thermal conductivity λ_{equiv} [W/m K] of external walls, roof and ground-floor (i_{13}, i_{20}, i_{27}) must be set to ensure the same K [W/m^{2}K] of the actual multi-layer components, not including the possible thermal insulation layers, *i.e.,* $\lambda_{eq} = K \cdot t$. The insulation layers are excluded from λ_{equiv} assessment because they are considered separately to appreciate the different performance due to the insulation position (i_{18}, i_{25}, i_{32}), which can be internal, external, or in-cavity. Indeed, this position affects the thermal inertia of the building envelope (the profiles of walls' temperature change), and thus it highly impacts envelope energy performance in transient conditions;
- the equivalent density ρ_{equiv} [kg/m^3] of external walls, roof and ground-floor (i_{14}, i_{21}, i_{28}) and related insulation layers (i_{17}, i_{24}, i_{31}) must be set to ensure the same C_a of the actual components, *i.e.,* $\rho_{equiv} = \frac{C_a}{t \cdot c}$ where c_p = 1000 J/kg K;
- the equivalent thickness of horizontal partitions t_{ho} [m] (i_{49}) is used to model the internal thermal inertia, since such partitions usually

provide a predominant share of building internal mass. Also in this case, an equivalent mono layer is assumed, with density ρ_{ho} = 1000 kg/m^3 and specific heat c_{ho} = 1000 J/kg K. t_{ho} must be set to ensure the same C_a of the actual components, *i.e.,* $t_{ho} = \frac{C_a}{\rho_{ho} \cdot c_{ho}}$;

- as concerns the transparent envelope, the dwellings can be provided with different windows' types. Thus, different windows' options can be defined as shown in Table 6.1, and the user sets the fractions (*i.e.,* probabilities) of dwellings associated with each option. Clearly, also other options – not reported in Table 6.1 that refers to the examined case studies (see Section 6.3) – can be considered. Infiltration is modeled as a function of the windows' type. Accordingly, the ACH (air changes per hour) value due to infiltration is set equal to 0.7 h^{-1} for old windows with low airtightness, and to 0.3 h^{-1} for new windows with high airtightness. Such values can be modified and customized for each dwelling according to windows' type and opening, linked to the occupant behavior.
- the shading systems are differentiated as a function of the exposure, which clearly affects their use. They are characterized by type, position and radiation setpoint. Different types can be selected, such as: *1)* no shading systems; *2)* low reflective – low transparent blinds (solar reflectance SR = 0.2, solar transmittance ST = 0.1); *3)* low reflective – medium transparent blinds (SR = 0.2, ST = 0.4); *4)* low reflective – high transparent blinds (SR = 0.2, ST = 0.7); *e)* medium reflective – low transparent blinds (SR = 0.5, ST = 0.1); *5)* medium reflective – medium transparent blinds (SR = 0.5, ST = 0.4); *6)* high reflective – low transparent blinds (SR = 0.8, ST = 0.1); *7)* blinds with inclined slats, *e.g.,* (see Figure 6.4 and some case studies in Section 6.3) with an inclination of 45°, thermal conductivity of 0.9 W/m K, solar reflectance for both front and back side equal to 0.5, solar transmittance equal to 0; etc.. The position can be internal or external, while the activation setpoint is intended as the value of incident solar radiation on the windows that triggers the shading use.

It is generally included between 150 to 450 W/m² [16] depending on the occupants' behavior;

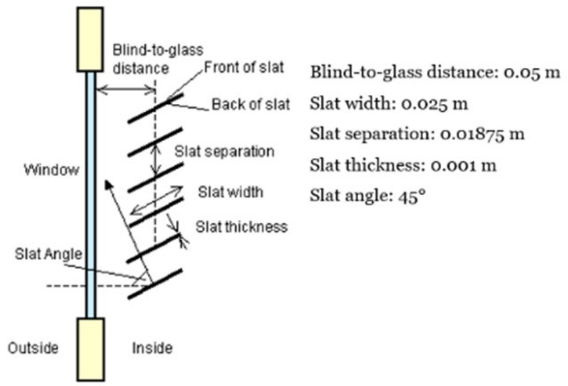

Figure 6.4 - Shading system 7: blinds with inclined (45°) slats

- the HVAC systems and operation can be differentiated for each dwelling. Therefore, each HVAC input is defined through a vector that collects the value for each dwelling. The EMAR database of performance curves enables to select different heating systems, *e.g.,* old (inefficient) gas boilers, condensing gas boiler, air-source heat pumps, ground-source heat pumps, and cooling systems, *e.g.,* old (inefficient) and new (efficient) electric air-source chillers, electric water-source chillers. Also, reversible heat pumps and centralized HVAC plants can be simulated. In addition, the user can provide itself the performance curves of the considered energy systems;
- natural ventilation can be considered. It is modeled by setting the natural ventilation setpoint temperature and ACH for each dwelling by means of two vectors of inputs, *i.e.,* i_{58} and i_{59}, respectively. The setpoint provides the temperature above which ventilation is activated. The ACH represents the air changes per hour due to ventilation, which should be carefully set by the user according to windows' size and opening, linked to the occupant behavior, deeply affecting the ventilation pattern;

- only photovoltaic panels are considered as renewable energy source systems because they are by far the most used and cost-effective one at the building level [23]. They are considered installed on the building roof to comply with architectural integration, and they can be defined in typology, size and panels' layout.

6.2.3. Outputs

EMAR can provide numerous outputs as concerns energy and economic performance, as well as thermal comfort, such as:

- discomfort hours and percentage of discomfort hours on occupied hours as concerns both the whole year and the cooling season to enable the investigation of summer overheating. Discomfort hours can be assessed according to the zone thermal comfort ASHRAE 55-2010 adaptive model [28] – 80% acceptability status or 90% acceptability status – or to the zone thermal comfort CEN 15251-2007 adaptive model [29] – category I (90% acceptability status), category II (80% acceptability status) or category III (65% acceptability status);
- heating and cooling loads, which can support the design of the HVAC systems;
- thermal energy demand and primary energy consumption for space heating and cooling;
- total primary energy consumption for all energy uses;
- fuel consumption;
- electricity consumed, self-used and supplied to the urban grid in presence of photovoltaics;
- running costs for space heating, cooling as well as for all uses.

These outputs are assessed for each dwelling – differentiated for exposure and floor number – and the arithmetic means provide the values related to the whole building, since the dwellings have the same extension, *i.e.,* useful and net area, which corresponds to the conditioned area (A_c).

In addition, EMAR provides precious indications about geometry and thermal characteristics of the building envelope, *i.e.*,:

- the area of all opaque and transparent components;
- the gross, net and conditioned volumes;
- the global heat transfer coefficient of the envelope;
- the thermal capacity of the envelope and of the whole building (considering internal partitions too).

Finally, also a 3d CAD model of the building is generated (see previous Figure 6.3).

6.2.4. Novelties compared to EMA [15]

As aforementioned, EMAR derives from a deep enhancement of EMA [15], and provides the following main novelties:

- the tool is enhanced to be applied to residential buildings, using a more complex and realistic internal subdivision into thermal zones;
- the level of detail in building modeling is increased, especially as concerns:
  - the geometry, since the input variable aspect ratio is replaced with the S/V ratio providing a simplified building model more consistent with the actual building;
  - the multi-layer components of the building envelope, which are modeled through the use of equivalent mono-layer ones;
  - the windows, since different dwellings can be modeled with different windows, as often occurs in the reality;
  - the HVAC systems, which are differentiated for each dwelling (each input is a vector), as often occurs in reality. In addition, further inputs are used to enhance the modeling reliability, *i.e.,* the efficiency of heating distribution-emission-regulation systems, the supply water temperature of heating terminals and the ventilation patterns;
- the possible outputs, which are provided both at dwelling and building levels, and increased in number including, *e.g.,* different thermal comfort models [28],[29];

- a robust validation is performed against detailed EnergyPlus models of an ASHRAE test building and of two typical European buildings, as shown in the following lines.

6.3. Case studies for EMAR validation

Three buildings are investigated in order to test, validate and analyze EMAR:

- an ASHRAE test building [24], [25];
- two typical buildings of the European building stock, which have been already investigated by the authors in previous studies for different aims [16], [26].

The outputs of EMAR are compared against the outcomes of detailed building models developed under EnergyPlus environment, which have been calibrated and validated against real data in the mentioned previous studies.

6.3.1. ASHRAE test building

The ASHRAE test building belongs to the 90.1 prototype building models developed by Pacific Northwest National Laboratory (PNNL) for the U.S. Department of Energy (DOE) [24], [25]. The prototypes models have been developed to quantify energy savings from newly published editions of ASHRAE Standard 90.1. The detailed building descriptions and EnergyPlus models can be found in [24],[25].The examined building hosts only dwellings, it is located in Denver (U.S.A, "BSk" semi-arid climate according to the Köppen–Geiger classification [30]) and characterized by ten floors. The inter-floor height is 3.05 m, each floor has a gross area of 783.6 m^2 with eight dwellings of 88.2 m^2 each, and a connection corridor of 77.7 m^2. The building has a regular shape and a rectangular plant, the total area is 7836.5 m^2 and the conditioned one is 7059.89 m^2. The overall height of the building is 30.5 m, the length 46.3 m and the width 16.9 m, so that a gross volume of 23884 m^3 is calculated. The longest façades have north and south exposures. The building is shown in Figure 6.5 and characterized in Table 6.2.

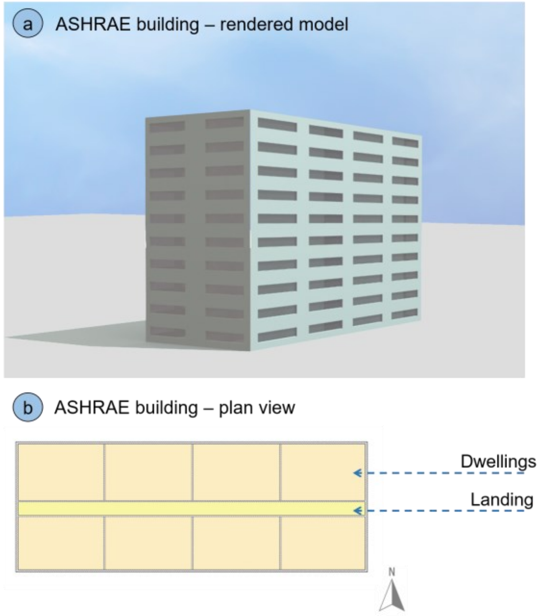

Figure 6.5 - ASHRAE test building: ***a)*** *3D view;* ***b)*** *plan view and thermal zones*

The main characteristics of the building thermal envelope are listed below:

- the walls have thermal transmittance (U_{value}) of 0.312 W/m^{2}K, and consist of an external layer of 2.5 cm of stucco, 1.6 cm of gypsum board, a block with thermal resistance of 2.8 m^{2}K/W, an inside layer of 1.6 cm of gypsum board;
- the roof slab has U_{value} of 0.182 W/m^{2}K and is characterized by a block with thermal resistance of 5.3 m^{2}K/W and very thin external and internal coatings;
- the ground-floor has U_{value} of 2.144 W/m^{2}K and has a concrete slab of 20 cm and a carpet coating on the inner side;
- the inner floors have two different lavers, *i.e.,* a concrete floor of 10 cm and a carpet coating;
- the windows are double glazed with U_{value} of 2.245 W/m^{2}K;
- there are no shading systems.

The heating and cooling services are provided by air circuits, with dedicated heating and cooling water, fueled by DX (direct expansion) heating and cooling coils, with COP – coefficient of performance, winter operation – and EER – energy efficiency ratio, summer operation – at rated conditions equal to 4.3 and 4.2, respectively. Thus, there is central air system terminal and a regulation thermostat for each dwelling.

Table 6.2 - Characterization of the ASHRAE test building

ENVELOPE - WINDOW TO WALL RATIO					
	Total	South	East	North	West
Gross wall area [m^2]	3855	1412	516	1412	516
Window opening area [m^2]	1150	424	153	424	153
Gross window-wall ratio	29.8%	30.0%	29.7%	30.0%	29.7%
INTERNAL GAINS					
Lighting system [W/m^2]	9.36	Light control is based on scheduled periods			
Electric equipment [W/m^2]	6.67	Occupancy [m^2/person]			35.3
BOUNDARY CONDITIONS					
Weather data	DENVER INTL AP CO USA TMY3 WMO#=725650				
Number of conditioned zones	80	Heating setpoint [°C]			21.7
Number of unconditioned zones	90	Cooling setpoint [°C]			24.4
Natural ventilation is calculated based on the window opening area of 0.1181 m^2. It is activated from 6:00 a.m. to 10:00 p.m. and when these conditions occur:		a) the indoor temperature is higher than 18.89 °C b) the indoor temperature is lower than 25.56°C c) the outdoor temperature is higher than 15.56 °C d) the outdoor temperature is lower than 26.67 °C e) the wind speed is lower than 40 m/s f) the difference between indoor and outdoor temperature is higher than -100 °C			
HEATING AND COOLING SYSTEMS					
Water to air heat pump COP [-] (heating mode)	4.30	Water to air heat pump EER [-] (cooling mode)			4.20

6.3.2. Typical European building 1

The typical European building 1 has been already investigated by the authors in [26] for what concerns the effects of the occupant behavior on energy performance. The building hosts only dwellings, it is located in Naples (Italy, Mediterranean “Csa” climate according to the Köppen–Geiger classification [30]) and it consists of two adjacent construction blocks, with an overall surface of 4985 m^2, a total height of 25.6 m. Length and width are 62.0 m and 10.5 m, respectively. The building, provided with two staircases, has six dwellings for each floor, with globally eight stories, including the ground-floor. Thus, the number of dwellings is 48. The conditioned floor area, excluding the staircases and the two entries, is 3877 m^2. The building is typical – for what concerns construction technology (reinforced concrete with a structural frame of pillars and beams) and heating systems – of the European building stock built in during 60ies-70ies, when most existing European buildings were constructed, due to the urban growth and development.

The building is shown in Figure 6.6 and characterized in Table 6.3.

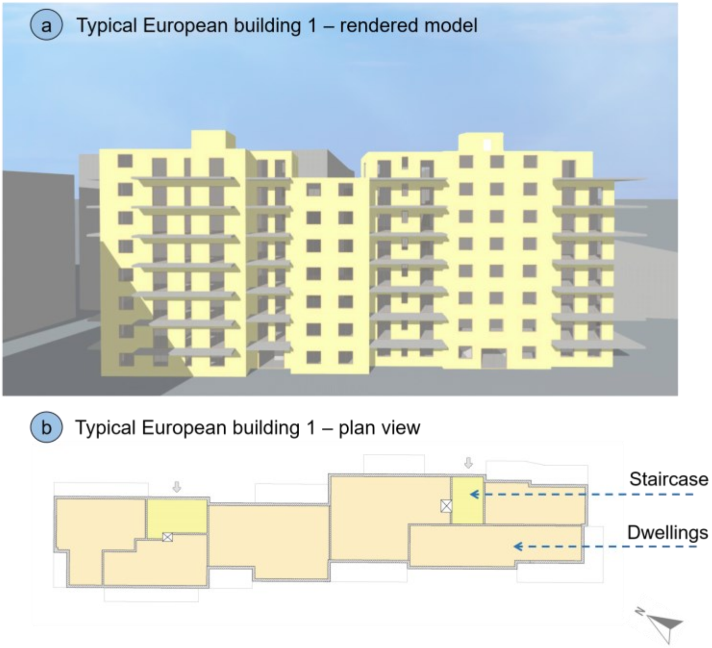

Figure 6.6 - Typical European building 1: a) 3D view; b) plan view and thermal zones

The main characteristics of the envelope are listed below:

- the walls have U_{value} of 1.01 W/m^{2}K, and consists of two layers of blocks – 12 cm the outer one, made of hollow blocks, 8 cm the inner layer, made of lapillus bricks – separated by an air cavity (12 cm), with cement plaster outside (3 cm) and lime plaster inside (2 cm);

- the roof slab has a U_{value} of 1.01 W/m^{2}K, with structural layer in reinforced concrete (beams, joists of 20 cm with interposed clay brick, and superior slab of 6 cm). At the bottom, the structure is plastered, at the top there is a further layer of lightweight concrete of 15 cm to give the right slope for the rainwater canalization, and waterproof layer;
- the ground floor has U_{value} of 1.35 W/m^{2}K, and the structure is similar to the roof with the exception of the slope layer. There is a thin light concrete slab as base of the ceramic pavement;
- the inner floors have mixed joists and hollow blocks structure, plastered at the bottom, with reinforced concrete slab, lightweight concrete slab and pavement at the top;
- the inner walls are made with lapillus blocks, typical of the region, plastered on both sides;
- the windows are single-glazed and wooden framed, with U_{value} of 4.9 W/m^{2}K. Averagely, one dwelling per floor has more recent windows (after refurbishment), double-glazed, wooden framed with U_{value} of 2.8 W/m^{2}K;
- the shading systems are external blinds with inclined slats (see previous Figure 6.4). The shading is activated when the direct solar radiation on the window is higher than 150 W/m^2. Each slat has an inclination of 45° and a conductivity of 0.9 W/m K. The slat solar reflectance, both for the front and back side is 0.5.

As concerns the heating system, there is a centralized natural gas boiler, not-condensing, with a thermal efficiency of 0.80 and thermal capacity of about 460 kW (slightly oversized, as typical for old buildings). The hot water is supplied to all dwellings through not-insulated vertical pipes, crossing the perimeter walls, and the in-room heat terminals are hot water radiators with thermostatic valves. The efficiency of heating distribution-emission-regulation system is 0.86, therefore the overall heating system efficiency is 0.69. Dwellings are equipped with DX cooling systems with EER equal to 3.0.

Table 6.3 - Characterization of the typical European building 1

ENVELOPE - WINDOW TO WALL RATIO					
	Total	South	East	North	West
Gross wall area [m^2]	4514	480	1756	509	1769
Above ground wall area [m^2]	3920	419	1527	438	1537
Window opening area [m^2]	743	51	323	40	330
Gross window-wall ratio	19.0%	12.2%	21.1%	9.1%	21.5%

INTERNAL GAINS			
Lighting system [W/m^2 - 100 lux]	2	Light control according to the daylight illuminance (dimming)	
Electric equipment [W/m^2]	4	Occupancy [person/m^2]	0.04

BOUNDARY CONDITIONS			
Weather data	NAPLES - ITA IWEC Data WMO#=162890		
Number of conditioned zones	48	Heating setpoint [°C]	20
Number of unconditioned zones	20	Cooling setpoint [°C]	26
Natural ventilation (time-dependent, till a maximum of 4 h^{-1}) is activated when both summer conditions occur:	a) the zone air temperature is higher than 27 °C b) the outdoor temperature is at least 2°C lower than indoor one		

HEATING AND COOLING SYSTEMS			
Efficiency of heating distribution-emission-regulation system [-]	0.86	Nominal heating capacity	463 kW$_t$
Efficiency of heating generation system [-]	0.80		
Packaged terminal air conditioner EER [-]	3.00	Nominal cooling capacity (assumed)	180 kW$_t$

6.3.3. Typical European building 2

The typical European building 2 has been already investigated by the authors in [16] as concerns the impact of inter-building effect and shading systems on energy needs. The building is located in Naples, in the same neighborhood of the previous case study, and hosts different use destinations. Length and width are 80 m and 14 m, respectively. The longest facades are oriented to north-west and south-east, respectively. The total building area is 7456 m² and the conditioned area is 6707.5 m². The building is made up of seven floors and the inter-floor height is 3.2 m. The first one hosts retails, the second one hosts offices and the other floors have a residential use. Dwellings have different net area and can accommodate from two to six people. The access to the dwellings is guaranteed by three stairwells. This case study is investigated to test EMAR on buildings that are partially (in this case for most part) residential hosting also other use destinations. Since EMAR is conceived for residential buildings, only the outcomes related to the dwellings – *i.e.,* floors 3-7 – are examined. The building has the same building envelope and energy systems of the typical European building 1, being representative the European building stock built in during 60ies-70ies. The building is shown in Figure 6.7 and characterized in Table 6.4.

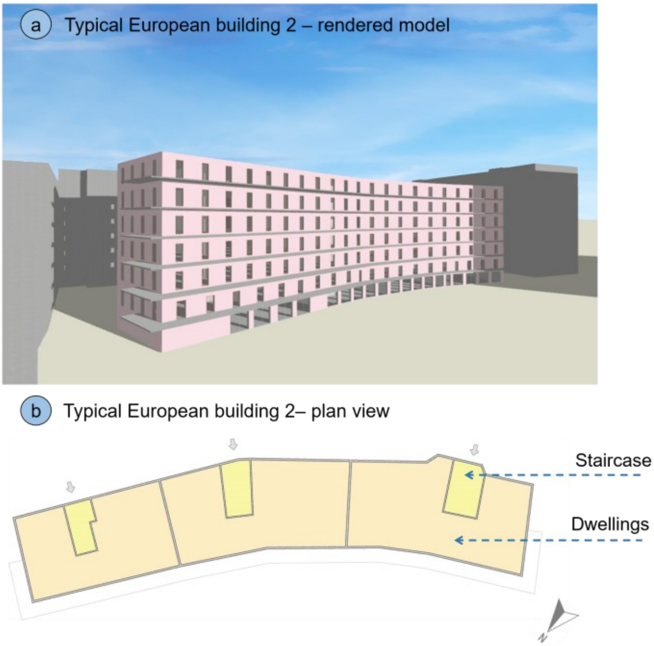

Figure 6.7 - Typical European building 2: a) 3D view; b) plan view and thermal zones

Table 6.4 - Characterization of the typical European building 2

ENVELOPE - WINDOW TO WALL RATIO					
	Total	South	East	North	West
Gross wall area [m^2]	4186	844	1025	782	1534
Window opening area [m^2]	778	128	160	169	321
Gross window-wall ratio	18.6%	15.2%	15.6%	21.6%	20.9%
INTERNAL GAINS					
Lighting system dwellings [W/m^2 - 100 lux]	5	Light control according to the daylight illuminance (dimming)			
Lighting system retail zones [W/m^2 - 100 lux]	6	Light control according to the daylight illuminance (dimming)			
Lighting system office zones [W/m^2 - 100 lux]	6	Light control according to the daylight illuminance (dimming)			
Electric equipment residential zones [W/m^2]	4				
Electric equipment retail zones [W/m^2]	7.5				
Electric equipment office zones [W/m^2]	2.5				
BOUNDARY CONDITIONS					
Weather data	NAPLES - ITA IWEC Data WMO#=162890				
Number of conditioned zones	28	Heating setpoint [°C]	20		
Number of unconditioned zones	20	Cooling setpoint [°C]	26		
Natural ventilation (time-dependent, till a maximum of 4 h^{-1}) is activated when both summer conditions occur:	a) the zone air temperature is higher than 27 °C b) the outdoor temperature is at least 2°C lower than indoor one				
HEATING AND COOLING SYSTEMS					
Efficiency of heating distribution-emission-regulation system [-]	0.86	Nominal heating capacity	300 kW$_t$		
Efficiency of heating generation system [-]	0.80				
Packaged terminal air conditioner EER	3.00				

6.4. Results: Validation and analysis of EMAR

This section shows the validation of EMAR as well as a detailed analysis of performance and outcomes of such a tool, addressing the aforementioned three case studies. The detailed EnergyPlus models of the three buildings have been developed, calibrated and validated in previous works [16], [24] - [26]. On the other hand, as concerns EMAR simulations, the used numerical inputs are reported in Table 6.5.

Table 6.5 - EMAR inputs for the case studies (no photovoltaics → the inputs i60, i61, i62 and i63 are not used)

EMAR inputs	ASHRAE test building	typical European building 1	typical European building 2
i_1) number of floors	10	8	7
i_2) orientation: angle building north - true north	90°	0°	45°
i_3) gross area of each floor	784 m^2	600 m^2	1065 m^2
i_4) S/V ratio	0.23 m^{-1}	0.32 m^{-1}	0.30 m^{-1}
i_5) gross height of each floor	3.05 m	3.2 m	3.2 m
i_6) window to wall ratio: south	30.0%	12.2%	15.2%
i_7) window to wall ratio: east	29.7%	21.1%	15.6%
i_8) window to wall ratio: north	30.0%	9.1%	21.6%
i_9) window to wall ratio: west	29.7%	21.5%	20.9%
i_{10}) solar absorptance of walls	0.70	0.70	0.70
i_{11}) solar absorptance of roof	0.70	0.85	0.85
i_{12}) thickness of walls' bricks	0.072 m	0.37 m	0.37 m
i_{13}) equivalent thermal conductivity of walls' bricks	0.024 W/m K	0.44 W/m K	0.44 W/m K
i_{14}) equivalent density of walls' bricks	1388 kg/m^3	634.8 kg/m^3	634.8 kg/m^3
i_{15}) thickness of insulation of walls	absent	absent	absent
i_{16}) thermal conductivity of insulation of walls	-	-	-
i_{17}) equivalent density of insulation of walls	-	-	-
i_{18}) position of insulation of walls	-	-	-
i_{19}) thickness of roof block	0.026 m	0.44 m	0.44 m
i_{20}) equivalent thermal conductivity of roof block	0.005 W/m K	0.514 W/m K	0.514 W/m K
i_{21}) equivalent density of roof block	1328 kg/m^3	1212 kg/m^3	1212 kg/m^3
i_{22}) thickness of insulation of roof	absent	absent	absent
i_{23}) thermal conductivity of insulation of roof	-	-	-
i_{24}) equivalent density of insulation of roof	-	-	-
i_{25}) position of insulation of roof	-	-	-
i_{26}) thickness of ground-floor	0.20 m	0.35 m	0.35 m
i_{27}) equivalent thermal conductivity of ground-floor	0.67 W/m K	0.603 W/m K	0.603 W/m K
i_{28}) equivalent density of ground-floor	2322 kg/m^3	1112 kg/m^3	1112 kg/m^3

i_{29}) thickness of insulation of ground-floor	absent	absent	absent
i_{30}) thermal conductivity of insulation of ground-floor	-	-	-
i_{31}) equivalent density of insulation of ground-floor	-	-	-
i_{32}) position of insulation of ground-floor	-	-	-
i_{33}) dwellings with single-glazed, aluminum windows	0%	0%	0%
i_{34}) dwellings with single-glazed, wood windows	0%	83 %	50 %
i_{35}) dwellings with double-glazed, aluminum windows	100%	0%	0%
i_{36}) dwellings with double-glazed, wood windows	0%	17 %	50 %
i_{37}) shading systems' type: south	absent	7: inclined (45°) slats	7: inclined (45°) slats
i_{38}) shading systems' type: east	absent	7: inclined (45°) slats	7: inclined (45°) slats
i_{39}) shading systems' type: north	absent	7: inclined (45°) slats	7: inclined (45°) slats
i_{40}) shading systems' type: west	absent	7: inclined (45°) slats	7: inclined (45°) slats
i_{41}) shading systems' position: south	-	exterior	exterior
i_{42}) shading systems' position: east	-	exterior	exterior
i_{43}) shading systems' position: north	-	exterior	exterior
i_{44}) shading systems' position: west	-	exterior	exterior
i_{45}) shading systems' radiation setpoint: south	-	150 W/m^2	150 W/m^2
i_{46}) shading systems' radiation setpoint: east	-	150 W/m^2	150 W/m^2
i_{47}) shading systems' radiation setpoint: north	-	150 W/m^2	150 W/m^2
i_{48}) shading systems' radiation setpoint: west	-	150 W/m^2	150 W/m^2
i_{49}) equivalent thickness of horizontal partitions	0.10 m	0.35 m	0.35 m
i_{50}) heating setpoint temperature*	21.7 °C	20 °C	20 °C
i_{51}) cooling setpoint temperature*	24.4 °C	26 °C	26 °C
i_{52}) efficiency of distribution-emission-regulation*	-	0.86	0.86
i_{53}) supply water temperature of heating terminals*	50 °C	70 °C	70 °C
i_{54}) type of heating generation system*	water to air heat pump	gas boiler	gas boiler
i_{55}) efficiency of heating generation system*	COP = 4.30	η = 0.80	η = 0.80
i_{56}) type of cooling generation system (chiller)*	water to air heat pump	electric air-source	electric air-source
i_{57}) energy efficiency ratio of cooling system*	4.20	3.00	3.00
i_{58}) ventilation setpoint temperature*	27 °C	27 °C	27 °C
i_{59}) ventilation ACH*	4 h^{-1}	4 h^{-1}	4 h^{-1}

*all dwellings have the same input, therefore a unique value is reported instead of a vector

6.4.1. Validation

The comparison between the outputs of the detailed EnergyPlus models and EMAR simulations is shown in Table 6.6 for validation purposes. The considered performance indicators refer to space conditioning demands, since these represent the most complex outputs to be assessed through building performance simulations tools, being highly affected by the dynamic behavior of building envelope and energy systems, as well as by the variable (during the year) boundary conditions linked to climatic conditions, building use and occupant behavior. Thus, Table 6.6 reports:

- TED_h: thermal energy demand for space heating [kWh_t/m^2y];
- TED_c: thermal energy demand for space cooling [kWh_t/m^2y];
- TED_{sc}: thermal energy demand for space conditioning = TED_h + TED_c [kWh_t/m^2y];
- PEC_h: primary energy consumption for space heating [kWh_p/m^2y];
- PEC_c: primary energy consumption for space cooling [kWh_p/m^2y];
- PEC_{sc}: primary energy consumption for space conditioning = PEC_h + PEC_c [kWh_p/m^2y];

As concerns PEC, the primary energy conversion factor is set equal to 1.05 for natural gas and 1.95 for electricity [31]. Also, the building conditioned area (A_c) is shown given that, clearly, EMAR provides different values because it automatically generates simplified building geometries. As aforementioned, for the typical European building 2 the outputs refer to the dwellings, *i.e.,* floors 3-7.

The validation results are very satisfactory. Concerning the energy performance indicators, as regards the ASHRAE building, the discrepancy between EMAR and EnergyPlus is always very low, under 2%. For the typical European buildings, discrepancies are slightly higher – around 5% as mean values – and the highest value of 9.2% (PEC_c for typical European building 2) is widely acceptable given the drastic simplification introduced by EMAR as concerns building modeling and simulation.

Table 6.6 - Validation results: Detailed EnergyPlus models vs EMAR simulations

		A_c	TED_h	TED_c	TED_{sc}	PEC_h	PEC_c	PEC_{sc}
		[m^2]	[kWh_t/m^2y]			[kWh_p/m^2y]		
ASHRAE test building	detailed EnergyPlus	7060	12.8	34.5	47.3	21.9	20.6	42.5
	EMAR	7266	12.6	34.6	47.2	21.9	20.9	42.9
	Discrepancy	*2.8%*	*-1.6%*	*0.3%*	*-0.2%*	*0%*	*1.4%*	*0.9%*
typical European Building 1	detailed EnergyPlus	3877	35.3	18.3	53.6	63.1	11.6	74.7
	EMAR	4119	35.4	17.2	52.6	63.6	10.9	74.5
	Discrepancy	*5.9%*	*0.3%*	*-6.4%*	*-1.9%*	*0.8%*	*-6.4%*	*-0.3%*
typical European Building 2	detailed EnergyPlus	4873	24.4	17.1	41.5	40.8	10.8	51.6
	EMAR	4661	23.2	18.0	41.2	39.0	11.9	50.9
	Discrepancy	*-4.6%*	*-5.2%*	*5.0%*	*-0.7%*	*-4.6%*	*9.2%*	*-1.4%*

In addition, the results can be partly justified by the geometrical differences between the buildings under investigation. The ASHRAE building has a regular shape and the same plan subdivision for each floor, thus the simplified building model generated by EMAR has a major geometry correspondence with the original building, with a discrepancy in A_c lower than 3%. The typical European building 1 has a rectangular shape but the last floor has a different area than the other ones. The EMAR building has all floors with the same area and geometry, causing a discrepancy in A_c around 6%. The typical European building 2 has an irregular plan with a curved front. In this case, the EMAR building has an equivalent rectangular plant, resulting in A_c discrepancy around -5%. Thus, for the last two case studies, the higher discrepancies in TED and PEC are motivated by the higher level of geometry simplification. Finally, EMAR shows good reliability and accuracy ensuring at the same time a user-friendly implementation. Notably, since the discrepancies are always lower than 10%, EMAR can be considered validated because the threshold of ±10% – assessed on yearly basis – is typically used at international level to assess the calibration/validation of building energy models [16], [32], [33]

6.4.2. Analysis of EMAR outputs

With the aim of conducting a comprehensive analysis of EMAR, the outputs achieved at dwellings' level are reported in Table 6.7, Table 6.8, and Table 6.9 for the three investigated buildings, respectively. As concerns the typical European building 2, the results related to the first two floors are not shown because there are not dwellings but retails and offices, while EMAR focuses on residential case studies. The analysis is not limited to TED and PEC, but – in order to show EMAR potentials – it addresses also the assessment of:

- heating (HL) and cooling loads (CL), which can support the design of the HVAC systems;
- discomfort hours (DH) for both the whole year and the cooling season (linked to summer overheating), which are assessed based on the ASHRAE 55-2010 adaptive model [28] with 80% acceptability, which is the most used worldwide for residential buildings. Also the DH percentages with respect to the occupied hours are reported to provide a clearer snapshot of thermal discomfort/comfort.

The outcomes allow to assess the differences among dwellings as a function of floor, exposure, and windows' type. For instance, dwellings at the ground floor have the lowest values of cooling demands because they can exploit the inertia of the whole building envelope and are subjected to a lower solar load, while dwellings at the top floor have the highest values given the major solar load. In addition, these latter – even if they feature double glazed windows for the typical European building 2 (Table 6.9) – have higher values of space heating demands because they are characterized by larger dispersing surfaces (roof surface). Clearly, as concerns the two typical European buildings, dwellings with double-glazed windows have lower values of heating demands, because such windows increase the envelope thermal resistance even if they imply a slight reduction of the solar heat gain coefficient. On the other hand, they increase the overheating risk, thereby exerting a lower influence on cooling demands, since there are contrasting effects. Fixing the windows type (see Floors 4, 6 and 7 of Table 6.9) dwellings with south exposure – compared to the north one – tend to have (slightly) lower heating demands and higher cooling demands because of the different solar gains/loads.

Definitely, EMAR can provide precious information to investigate energy demand and thermal comfort as well as to design the HVAC systems – thanks to the assessment of heating and cooling loads – for each dwelling.

Finally, EMAR provides outputs about the thermal characteristics of the building envelope, such as the global heat transfer coefficient (H) and the thermal capacity (C) of the external envelope and of the whole building (considering internal partitions too), as reported in Table 6.10. Clearly, these outputs refer to the simplified building models developed by EMAR. Therefore, there is not a perfect matching with the actual building data, but they provide a reliable snapshot of envelope thermal performance.

Table 6.7 - EMAR outputs at dwellings' level for the ASHRAE test building

	Thermal Comfort: Discomfort Hours (DH) and their percentage with respect to the occupied hours [%]**		Heating (HL) and Cooling (CL) Loads [W/m^2]		Thermal Energy Demand (TED) [kWh$_t$/m^{2}y]		Primary Energy Consumption (PEC) [kWh$_p$/m^{2}y]		
	year DH [h]	%	HL	CL	TED$_h$*	TED$_c$*	PEC$_h$*	PEC$_c$*	PEC$_{tot}$*
Dwelling North Floor 1	11.5	0.3%	17.4	15.1	16.6	18.4	27.4	11.6	131.1
Dwelling South Floor 1	10.5	0.3%	15.9	18.2	14.2	18.5	23.8	11.8	127.6
Dwelling North Floor 2	148.8	3.5%	16.3	19.8	11.8	32.3	20.7	19.4	132.1
Dwelling South Floor 2	129.5	3.0%	16.2	24.6	11.8	31.0	20.7	19.2	131.9
Dwelling North Floor 3	209.8	4.9%	16.4	21.1	10.9	36.9	19.5	21.8	133.3
Dwelling South Floor 3	193.0	4.5%	16.3	26.0	10.9	35.4	19.4	21.6	133.1
Dwelling North Floor 4	229.5	5.4%	16.5	21.4	10.6	38.1	19.1	22.5	133.6
Dwelling South Floor 4	212.8	5.0%	16.4	26.2	10.7	36.6	19.0	22.3	133.3
Dwelling North Floor 5	233.3	5.5%	16.6	21.4	10.6	38.4	19.0	22.6	133.6
Dwelling South Floor 5	217.0	5.1%	16.4	26.3	10.6	36.9	19.0	22.4	133.4
Dwelling North Floor 6	233.3	5.5%	16.6	21.4	10.7	38.3	19.2	22.6	133.7
Dwelling South Floor 6	217.5	5.1%	16.5	26.2	10.8	36.8	19.2	22.3	133.5
Dwelling North Floor 7	230.5	5.4%	16.7	21.4	10.9	38.1	19.6	22.4	134.0
Dwelling South Floor 7	213.0	5.0%	16.6	26.2	11.0	36.5	19.6	22.2	133.7
Dwelling North Floor 8	207.5	4.9%	17.2	21.5	12.2	37.7	20.9	22.3	135.2
Dwelling South Floor 8	225.8	5.3%	16.9	26.8	11.5	35.3	20.4	21.3	133.7
Dwelling North Floor 9	222.0	5.2%	17.9	21.8	13.1	37.3	22.9	22.1	137.0
Dwelling South Floor 9	205.5	4.8%	17.7	26.8	13.3	35.9	23.0	21.8	136.9
Dwelling North Floor 10	223.0	5.3%	21.9	24.6	19.3	37.4	32.4	22.5	146.9
Dwelling South Floor 10	207.0	4.9%	21.9	30.0	19.5	36.3	32.6	22.6	147.2

* subscripts: h = heating; c = cooling; tot = all uses
** summer overheating never occurs

Table 6.8 - EMAR outputs at dwellings' level for the typical European building 1

	Thermal Comfort: Discomfort Hours (DH) and their percentage with respect to the occupied hours [%]				Heating (HL) and Cooling (CL) Loads [W/m^2]		Thermal Energy Demand (TED) [kWh$_t$/m^{2}y]		Primary Energy Consumption (PEC) [kWh$_p$/m^{2}y]		
	year DH [h]	%	summer DH [h]	%	HL	CL	TED$_h$*	TED$_c$*	PEC$_h$*	PEC$_c$*	PEC$_{tot}$*
Dwelling North Floor 1	988.8	24.1%	404.8	12.0%	88.2	19.5	45.6	3.1	79.4	2.3	173.7
Dwelling South Floor 1	991.0	24.2%	415.0	12.3%	81.3	18.8	41.3	3.1	73.2	2.2	167.5
Dwelling North Floor 2	879.0	21.4%	424.8	12.6%	76.8	32.5	34.1	14.3	61.9	9.2	163.2
Dwelling South Floor 2	908.5	22.2%	450.3	13.3%	77.6	33.2	34.5	14.6	62.6	9.3	163.9
Dwelling North Floor 3**	689.3	16.8%	356.5	10.6%	52.8	35.4	20.3	17.0	39.3	10.9	142.2
Dwelling South Floor 3	867.0	21.1%	431.0	12.8%	76.8	36.1	33.3	18.6	60.6	11.8	164.4
Dwelling North Floor 4**	709.5	17.3%	379.3	11.2%	53.1	36.4	20.5	17.9	39.5	11.3	142.9
Dwelling South Floor 4	867.0	21.1%	437.5	13.0%	76.9	36.5	33.3	19.4	60.5	12.2	164.8
Dwelling North Floor 5	881.3	21.5%	444.3	13.2%	77.4	36.4	33.6	19.4	61.1	12.2	165.3
Dwelling South Floor 5	865.5	21.1%	436.8	12.9%	76.8	36.7	33.3	19.4	60.6	12.2	164.9
Dwelling North Floor 6	909.3	22.2%	456.0	13.5%	78.8	36.0	34.9	19.1	63.1	12.0	167.1
Dwelling South Floor 6	899.3	21.9%	454.8	13.5%	78.1	36.5	34.3	19.4	62.1	12.2	166.4
Dwelling North Floor 7	987.5	24.1%	499.5	14.8%	81.2	37.3	37.2	19.8	66.6	12.4	171.1
Dwelling South Floor 7	964.5	23.5%	492.8	14.6%	80.6	37.6	36.4	20.1	65.4	12.6	170.1
Dwelling North Floor 8	1301.8	31.8%	686.3	20.3%	93.0	49.6	47.5	24.7	81.8	15.8	189.6
Dwelling South Floor 8	1282.8	31.3%	674.5	20.0%	92.4	49.9	46.8	25.0	80.7	15.9	188.7

* subscripts: h = heating; c = cooling; tot = all uses
** dwellings with double glazed windows; the other ones have single-glazed windows

Table 6.9 - EMAR outputs at dwellings' level for the typical European building 2

	Thermal Comfort: Discomfort Hours (DH) and their percentage with respect to the occupied hours [%]				Heating (HL) and Cooling (CL) Loads [W/m^2]		Thermal Energy Demand (TED) [kWh$_t$/m^{2}y]		Primary Energy Consumption (PEC) [kWh$_p$/m^{2}y]		
	year DH [h]	%	summer DH [h]	%	HL	CL	TED$_h$*	TED$_c$*	PEC$_h$*	PEC$_c$*	PEC$_{tot}$*
Dwelling North Floor 3	735.5	17.9%	348.3	10.3%	69.7	37.3	28.4	15.8	47.6	10.5	150.2
Dwelling South Floor 3**	567.3	13.8%	278.5	8.3%	46.9	38.6	16.3	14.8	27.7	10.1	129.8
Dwelling North Floor 4	703.3	17.2%	339.5	10.1%	68.2	39.1	27.3	17.2	45.9	11.3	149.2
Dwelling South Floor 4	698	17.0%	338.5	10.0%	67.8	38.9	27.2	17.3	45.7	11.3	149.0
Dwelling North Floor 5**	646.3	15.8%	382.8	11.4%	46.2	42.8	15.6	16.9	26.6	11.3	129.9
Dwelling South Floor 5	711.8	17.4%	350.3	10.4%	67.9	39.1	27.3	17.7	45.9	11.5	149.4
Dwelling North Floor 6**	708.3	17.3%	401.5	11.9%	49.0	42.2	17.6	17.6	29.8	11.6	133.5
Dwelling South Floor 6**	706.	17.2%	414.3	12.3%	48.3	42.3	17.0	17.8	28.8	11.7	132.5
Dwelling North Floor 7**	1153	28.1%	662.8	19.7%	66.3	55.9	27.8	22.4	46.2	15.0	153.3
Dwelling South Floor 7**	1149.3	28.0%	659.8	19.6%	65.9	55.9	27.7	22.4	46.1	15.0	153.1

* subscripts: h = heating; c = cooling; tot = all uses

** dwellings with double glazed windows; the other ones have single-glazed windows

Table 6.10 - EMAR outputs related to the thermal characteristics of the building envelope

	ASHRAE test building	typical European building 1	typical European building 2
H [kW/K]	5.43	8.23	10.26
$C_{external}$ [MJ/K]	670	1180	1740
C_{total} [MJ/K]	1370	2520	3820

6.4.3. Example of photovoltaics' simulation

The case studies do not feature the presence of PV. Thus, in order to show how PV systems can be simulated through EMAR, an example is provided referring to the typical European building 2, since this latter is the most complex building investigated.

The implementation of PV systems is simulated performing both energy and cost-optimal analyses to outline the capabilities of EMAR. Systems of different type and size are investigated:

- cells in poly- and mono-crystalline silicon, with investment costs equal to 1500 €/kW_{peak} and 1700 €/kW_{peak}, respectively, taken from a market research;
- PV panels are installed on the building roof to ensure architectural integration. The roof area covered by panels varies in the range 0 – 100% with a step of 10%.

Thus, 21 possible PV configurations are examined. In all cases, the panels' location is optimized setting the tilt angle equal to 30° and the azimuth angle to 0° (orientation to south) to maximize the annual electric conversion for the considered location – Naples, latitude 40° 51' 22 N, longitude 14° 14' 47 E. For each combination, EMAR enables to predict total primary energy consumption and global cost of the building facility as shown in Figure 6.8 and Figure 6.9. The discounted payback period is even provided – Figure 6.10 – for a more comprehensive economic analysis. Primary energy consumption includes all energy uses taken from EnergyPlus simulations. Global costs are assessed over a calculation period (τ) of 20 years to match a conservative PV lifespan. They include the investment cost for PV and the running cots over τ, which are actualized considering a discount factor of 3%

[34]. In order to simulate the PV implementation, EMAR performs hourly balances between produced and required electrical energy. The PV hourly electrical conversion is achieved from EnergyPlus simulations. Surplus electricity is sold to the grid. According to the Italian context, the specific cost of electricity is set equal to 0.22 €/kWh_{el}, the remuneration for the electricity sold to the grid to 0.07 €/kWh_{el} (around 1/3 of the purchase cost [35]), the natural gas cost (for running cost assessment) to 0.90 €/m^3.

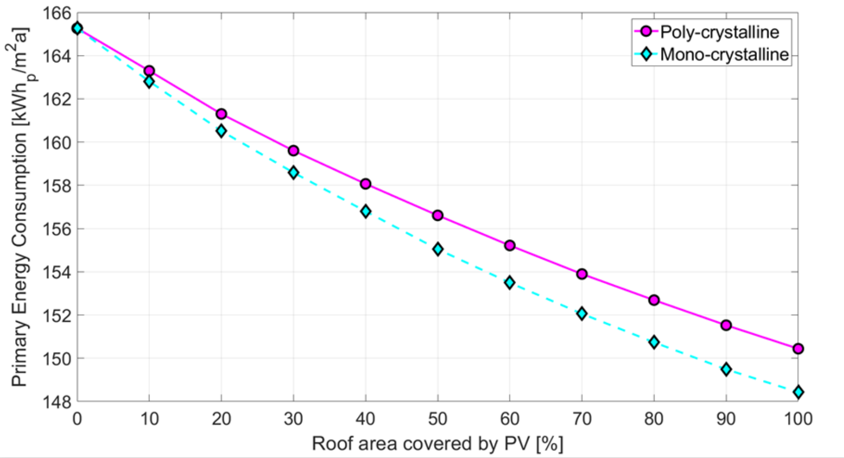

Figure 6.8 - Energy analysis of PhotoVoltaics: total primary energy consumption vs PV size

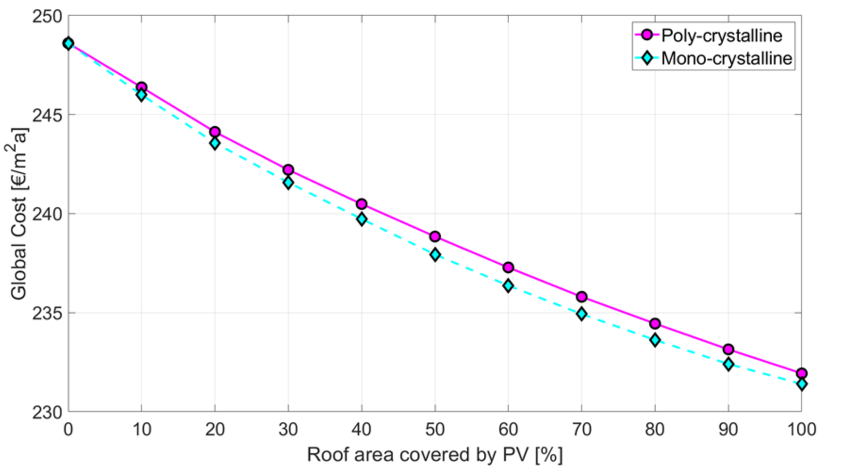

Figure 6.9 - Cost analysis of PhotoVoltaics: global cost vs PV size

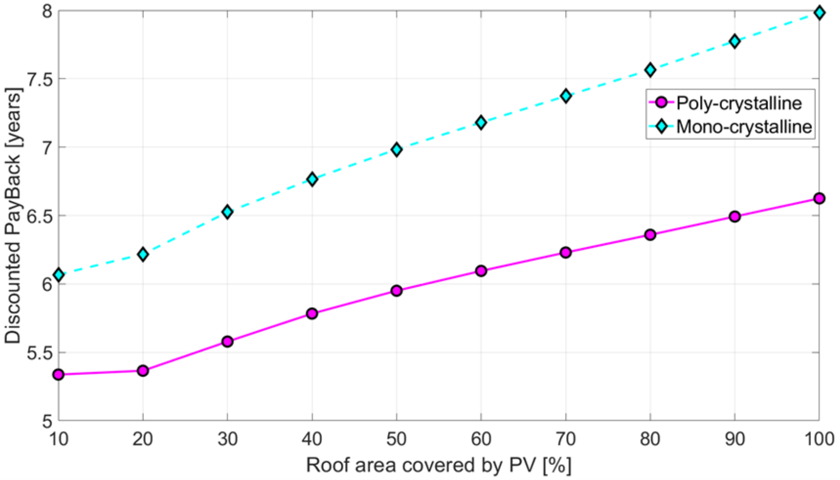

Figure 6.10 - Cost analysis of PhotoVoltaics: DPB vs PV size

The outcomes show that the maximum size of photovoltaic – *i.e.,* a full-roof PV system – is the optimal solution from both energy and economic perspectives, even if the payback time is the highest one, given the higher investment cost, but acceptable (lower than 10 years). In this regard, such systems usually receive public financial grants that increase their cost-effectiveness. Clearly, EMAR can consider such grants in the cost analysis. This result is motivated by the cost reduction – due to technology development and macro-scale economic – that PV systems have experienced in the last years. That is why they are by far the most effective renewable energy system at the building level.

The investigation shows a simple example of how EMAR can be used to optimize building energy performance performing a cost-optimal analysis as well. Therefore, it can be a precious tool for building professionals and public stakeholders to promote a more energy-efficient and cost-effective, *i.e.*, sustainable, building stock.

6.5. Conclusive remarks

Are few numerical inputs sufficient for accurate energy simulations of residential buildings?

This study answers "*Yes*" by proposing EMAR, an accurate but user-friendly tool for energy modeling and simulations of residential buildings. EMAR is based on the coupling between EnergyPlus and MATLAB® and it is a deep upgrade of a previous version – EMA – conceived for office buildings. It works under MATLAB® environment and needs only 63 numerical inputs to carry out modeling and simulations. No drawings, no schemes of energy systems, no deep modeling expertise are required but only few numbers. EMAR is validated against detailed EnergyPlus models of an ASHRAE test building and of two typical European buildings. The discrepancies are lower than 10% as concerns thermal energy demand and primary energy consumption for space conditioning, and in most cases are lower than 5%. The lowest discrepancies – always lower than 3% – are achieved for the ASHRAE test building because this latter is isolated (no external shading elements, such as other constructions) and has a regular rectangular shape. Thus, the simplified building model generated by EMAR has a higher geometry correspondence with the original building. Nonetheless, EMAR shows good reliability for irregular buildings too, as the other two case studies, whose original models take into account the external environment and shading elements (urban context) too. On the other hand, EMAR introduces a drastic reduction of modeling and computational burden, so that it can be easily used by building professionals. In addition, EMAR can provide outputs at dwellings' level, thereby enabling deep investigations of energy demands, thermal comfort and heating/cooling loads for different stakeholders. Accordingly, the public actors can achieve precious guidelines to drive energy audit, design and retrofit of entire building stocks, while the private actors, *i.e.,* the building tenants, can obtain detailed information about energy performance and labeling of their houses, as well as for HVAC systems' design. Moreover, indicators related to the building thermal envelope – *e.g.,* global heat transfer coefficient and capacity – are assessed providing a comprehensive outline of the building system's energy performance.

Therefore, EMAR can be a precious tool to perform user-friendly but accurate building energy modeling and simulations, which are fundamental for a wide diffusion of methodologies and procedures addressing the energy transition of the building stock towards nearly-zero energy buildings. For instance, EMAR can be integrated in tools and frameworks for:

- building energy audit and labeling;
- design of HVAC systems;
- building information modeling (BIM);
- building energy optimization for the design of new buildings or the retrofit of existing ones;
- large-scale analysis of buildings stock to address public energy policies.

Future studies will aim at the development of free graphical interfaces (without the use of MATLAB®) as well as to the integration of EMAR in some of the aforementioned frameworks.

CHAPTER 6 – References

[1] IEA (International Energy Agency) Report. Available online at: https://www.iea.org/topics/buildings. Last accessed on: 07/10/2020.

[2] Hamdy, M., & Sirén, K. (2016). A multi-aid optimization scheme for large-scale investigation of cost-optimality and energy performance of buildings. Journal of Building Performance Simulation, 9(4), 411-430.

[3] Nguyen, A. T., Reiter, S., & Rigo, P. (2014). A review on simulation-based optimization methods applied to building performance analysis. Applied Energy, 113, 1043-1058.

[4] Longo, S., Montana, F., & Sanseverino, E. R. (2019). A review on optimization and cost-optimal methodologies in low-energy buildings design and environmental considerations. Sustainable cities and society, 45, 87-104.

[5] Poel, B., van Cruchten, G., & Balaras, C. A. (2007). Energy performance assessment of existing dwellings. Energy and Buildings, 39(4), 393-403.

[6] Wei, Y., Zhang, X., Shi, Y., Xia, L., Pan, S., Wu, J., ... & Zhao, X. (2018). A review of data-driven approaches for prediction and classification of building energy consumption. Renewable and Sustainable Energy Reviews, 82, 1027-1047.

[7] Langevin, J., Reyna, J. L., Ebrahimigharehbaghi, S., Sandberg, N., Fennell, P., Nägeli, C., ... & Webster, J. (2020). Developing a common approach for classifying building stock energy models. Renewable and Sustainable Energy Reviews, 133, 110276.

[8] Martínez, S., Eguía, P., Granada, E., Moazami, A., & Hamdy, M. (2020). A performance comparison of Multi-Objective Optimization-based approaches for calibrating white-box Building Energy Models. Energy and Buildings, 216, 109942.

[9] Drgoňa, J., Picard, D., & Helsen, L. (2020). Cloud-based implementation of white-box model predictive control for a GEOTABS office building: A field test demonstration. Journal of Process Control, 88, 63-77.

[10] De Coninck, R., Magnusson, F., Åkesson, J., & Helsen, L. (2016). Toolbox for development and validation of grey-box building models for forecasting and control. Journal of Building Performance Simulation, 9(3), 288-303.

[11] Arroyo, J., Spiessens, F., & Helsen, L. (2020). Identification of multi-zone grey-box building models for use in model predictive control. Journal of Building Performance Simulation, 13(4), 472-486.

[12] Bracht, M. K., Melo, A. P., & Lamberts, R. (2021). A metamodel for building information modeling-building energy modeling integration in early design stage. Automation in Construction, 121, 103422.

[13] Lee, S. H., Hong, T., Piette, M. A., & Taylor-Lange, S. C. (2015). Energy retrofit analysis toolkits for commercial buildings: A review. Energy, 89, 1087-1100.

[14] Mathew, P. A., Dunn, L. N., Sohn, M. D., Mercado, A., Custudio, C., & Walter, T. (2015). Big-data for building energy performance: Lessons from assembling a very large national database of building energy use. Applied Energy, 140, 85-93.

[15] Ascione, F., Bianco, N., De Stasio, C., Mauro, G. M., & Vanoli, G. P. (2017). EMA: A user-friendly tool for reliable simulations of building energy performance in dynamic conditions by coupling EnergyPlus and MATLAB®. In ECOS 2017–The 30th International Conference on Efficiency, Cost, Optimization, Simulation and Environmental Impact of Energy Systems, San Diego (California, USA) 2-6 July 2017.

[16] Ascione, F., Bianco, N., Iovane, T., Mastellone, M., & Mauro, G. M. (2020). Is it fundamental to model the inter-building effect for reliable building energy simulations? Interaction with shading systems. Building and Environment, 107161.

[17] Cucca, G., & Ianakiev, A. (2020). Assessment and optimisation of energy consumption in building communities using an innovative co-simulation tool. Journal of Building Engineering, 32, 101681.

[18] Andriamamonjy, A., Saelens, D., & Klein, R. (2019). A combined scientometric and conventional literature review to grasp the entire BIM knowledge and its integration with energy simulation. Journal of Building Engineering, 22, 513-527.

[19] Pezeshki, Z., Soleimani, A., & Darabi, A. (2019). Application of BEM and using BIM database for BEM: A review. Journal of Building Engineering, 23, 1-17.

[20] US Department of Energy. Energy Efficiency and Renewable Energy Office, Building Technology Program, EnergyPlus (version 8.4). Available online at: https://energyplus.net/. Accessed in November 2021

[21] MathWorks, MATLAB – MATrixLABoratory (version 2015). https://it.mathworks.com/products/matlab.html. Accessed in November 2021

[22] Available online at: https://energyplus.net/weather. Accessed in November 2021

[23] Mauro, G. M., Hamdy, M., Vanoli, G. P., Bianco, N., & Hensen, J. L. (2015). A new methodology for investigating the cost-optimality of energy retrofitting a building category. Energy and Buildings, 107, 456-478.

[24] Goel, S., Athalye, R. A., Wang, W., Zhang, J., Rosenberg, M. I., Xie, Y., ... & Mendon, V. V. (2014). Enhancements to ASHRAE standard 90.1 prototype building models (No. PNNL-23269). Pacific Northwest National Lab.(PNNL), Richland, WA (United States).

[25] Goel, S., Rosenberg, M. I., & Eley, C. (2017). ANSI/ASHRAE/IES Standard 90.1-2016 Performance Rating Method Reference Manual (No. PNNL-26917). Pacific Northwest National Lab.(PNNL), Richland, WA (United States).

[26] Ascione, F., Bianco, N., De Masi, R. F., Mastellone, M., Mauro, G. M., & Vanoli, G. P. (2020). The role of the occupant behavior in affecting the feasibility of energy refurbishment of residential buildings: typical effective retrofits compromised by typical wrong habits. Energy and Buildings, 110217.

[27] Oberegger, U. F., Pernetti, R., & Lollini, R. (2020). Bottom-up building stock retrofit based on levelized cost of ved energy. Energy and Buildings, 210, 109757.

[28] Standard, A. S. H. R. A. E. (2010). Standard 55-2010, Thermal environmental conditions for human occupancy. American Society of Heating, Refrigerating and Air Conditioning Engineers.

[29] CEN, (2007). 15251-2007. Criteria for the indoor environment including thermal indoor air quality, light and noise. Brussels: European Committee for Standardization.

[30] Kottek, M., Grieser, J., Beck, C., Rudolf, B., & Rubel, F. (2006). World map of the Köppen-Geiger climate classification updated. Meteorologische Zeitschrift, 15(3), 259-263.

[31] D.M. (Interministerial Decree) 26 giugno 2015. Available online: http://www.sviluppoeconomico.gov.it/index.php/it/normativa/decreti-interministeriali/2032966-decreto-interministeriale-26-giugno-2015-applicazione-delle-metodologie-di-calcolo-delle-prestazioni-energetiche-e-

definizione-delle-prescrizioni-e-dei-requisiti-minimi-degli-edifici#page_top. Accessed in November 2021 (in Italian)

[32] Webster, L., Bradford, J., Sartor, D., Shonder, J., Atkin, E., Dunnivant, S., ... & Schiller, S. (2015). M&V Guidelines: Measurement and Verification for Performance-Based Contracts. Version 4.0, Technical Report.

[33] Ascione, F., Bianco, N., De Masi, R. F., de' Rossi, F., & Vanoli, G. P. (2015). Energy retrofit of an educational building in the ancient center of Benevento. Feasibility study of energy savings and respect of the historical value. Energy and Buildings, 95, 172-183.

[34] European Parliament and the Council Directive 2018/844/EU of 30 May 2018 amending Directive 2010/31/EU on the energy performance of buildings and Directive 2012/27/EU on energy efficiency. Available online: https://eur-lex.europa.eu/legal-content/EN/TXT/PDF/?uri=CELEX:32018L0844&from=EN. Accessed in November 2021

[35] Ascione, F., Bianco, N., Mauro, G. M., & Napolitano, D. F. (2019). Retrofit of villas on Mediterranean coastlines: Pareto optimization with a view to energy-efficiency and cost-effectiveness. Applied Energy, 254, 113705.

Conclusions

The research activities. conducted during the three years of PhD, concluded in this Thesis work, entitled: "*Towards a decarbonized built environment: energy ratings and technologies for refurbishing the existing building stock*".

Global warming, urban overheating and heat islands, extreme weather phenomena are the most serious issue of this century and the main cause of it is probably anthropogenic activity. Reducing the disproportionate use of fossil sources and the high energy consumption is the only way to combat climate change. The current and future direction must point to energy saving, the use of energy from renewable sources, and the efficient use of energy resources. In this context, the construction sector plays an important role by contributing significantly to global energy consumption and emissions. During the last decades, many national and international Directives and guidelines have been adopted to regulate the construction of new buildings and the renovation of existing ones, to decarbonize the built environment. Chapter 1 of this work, indeed, is entirely focused on these topics. This was precisely the starting point of the entire PhD program and therefore of the work developed in the last years.

The Thesis is centered on building energy efficiency, and specifically, on technologies and design strategies for the optimization of the energy performances of existing buildings. All three levers of energy efficiency were considered for the energy retrofit of buildings: the thermophysics of the transparent and opaque building envelope, the systems for the active microclimate control, and the conversion systems from renewables at the building scale. Passive and active strategies were adopted singularly or together aiming at reducing the energy demand of buildings and improve their performances. The energy refurbishments concern private or public buildings with different uses, such as residential or educational.

After the presentation of adopted investigation methods (Chapter 2), Chapter 3 presents refurbishments of buildings through exclusively passive strategies for the envelope of an educational edifice of the University of Molise (Italy), with the main scope that is the reduction of the cooling energy demand. Furthermore, CHAPTER 4 4 regards the energy refurbishment through active strategies of another educational building in Campobasso (Italy). The aim was to improve and adapt educational spaces for in presence activities during and after the Covid-19 pandemic. Energy building refurbishments, intervening on all three levers of energy efficiency, were reported in CHAPTER 5 which account for two different investigations regarding the energy retrofit of the whole HVAC/building systems. The first one regards the energy retrofit and seismic enhancement of a student dormitory in Athens, the second one is an energy refurbishment of three residential buildings located in different Italian climatic zones.

Concerning the methodological approach to evaluate the energy efficiency measure proposed for the energy refurbishments of different case studies (as aforementioned, deepened in CHAPTER 2), several types of analysis were performed, in a cost-optimal perspective as suggested by Directive 844/2018:

- numerical and experimental analysis,
- energetic analysis through transient (BES) and, or steady-state evaluations employing consolidated commonly used software (i.e., EnergyPlus, DesignBuilder),
- computational fluid dynamic analysis (CFD) for the prediction of the parameters that define indoor air quality,
- economic and emissions analysis to perform cost-optimal evaluations,
- visual and thermal comfort analysis.

These investigations were conducted on different real building case studies, pointing out interesting and innovative outcomes, that the following lines report.

Passive strategies for the building envelope

The investigation of CHAPTER 1 has evidenced the main potentialities and criticalities in the use of passive strategies for the improvement of the building energy performances.

Specifically, green walls have a great potential for improving local air quality and indoor microclimatic comfort, as well as, several positive effects are achieved at the urban scale, with positive environmental changes in dense urban areas. It was also showed that, even if the benefits of this technology are evident, its use in the building sector is not yet adequately diffused in consideration of the large potentialities. This is probably due to some weaknesses like the water requirement, the maintenance costs, the inexperience of designers, the lack of technical data. The study also underlines the incomparability of experimental and numerical results in terms of energy-saving and thermal comfort.

By considering other passive strategies for the building envelope, like cool roof and green roof for the horizontal building envelope, thermal insulation, phase change materials, and vented façades for the vertical envelope, a deep investigation for an educational building in Molise was presented. After an economic, environmental, and energy analysis, advantages in using PCM as a cooling strategy were pointed out. Different PCMs were compared, varying their melting temperature from 18 °C to 29 °C to bring out the best solution in terms of microclimatic indoor comfort and reduction of energy consumption. The innovative solution of phase change wallboard with a melting temperature of 23 °C resulted as the best, causing a reduction in primary energy demand during summertime (11.7%), and a consequent decrement of CO_2 emissions. A comfort analysis was also conducted, and the increase in the summer indoor comfort was demonstrated both according to the Fanger and ASHRAE 55-2004 comfort analyses. The economic evaluations revealed a criticality in the adoption of this passive strategy. Indeed, the PCM intervention is not actually economically convenient but considering the future climate evolution and the increase of energy prices, PCM wallboard could become a convenient measure for the improvement of the building energy efficiency.

What emerges of the utmost importance is that only an innovative solution as a PCM could effectively improve the thermal comfort and the energy saving of the building. So that, traditional passive strategies are not energetically effective for a building like the one analyzed, renovated in 2005, and with an envelope of low thermal transmittances. Only an innovative solution, like PCM, that influences the apparent thermal capacity (employing the latent heat-storing) of the opaque envelope acting from the inner side, can be considered as a valid solution.

Active strategies for an energy refurbishment

This Thesis work has also investigated the renovation of classrooms of an Italian Educational building, with a view to the necessities of safety and healthiness during the COVID-19 pandemic (CHAPTER 4). Specifically, with reference to an already planned architectural renovation of the Department of the University of Molise (Italy), in which new classrooms were built, a novel investigation was proposed to evaluate several HVAC configurations. Two different numerical approaches were coupled: a building energy performance (BES) simulation, 0-D and in the domain of the time and with sub-hourly calculations extended to the whole year, and a computational fluid dynamic (CFD) analysis, 3-D and referred to specific hours.

The necessity of such investigation is relevant because university and educational buildings, given the high occupancy rates, must be safe and secure even during emergency periods. Architectural novel designs are necessary in order to contrast and avoid contagions of COVID-19 and other severe syndromes. At the same time, strong ventilation is required to reduce the transmission of nuclei droplets and small aerosols.

The investigation which begins with an accurate audit of the present building (including monitoring of the indoor conditions) proposes a suitable energy model, necessary to evaluate and simulate different HVAC alternatives.

With reference to the building energy analysis, different configurations were examined: an all-air system with and without the sensible heat recovery from the exhaust air, with variable amount of outdoor air (from 33% to 100%, with a minimum of 7 l/s pers of OA) and air change rates varying from 6.5-7.9 h^{-1} (configurations with total supply air of 14 l/s person) to 9.7-11.9 h^{-1} (configurations with total supply air of 21 l/s person). The main outcomes reveal that, for the new classrooms, the annual primary energy demand for the space heating (EP_H) can vary from 64.4 kWh_p/m^2 (OA 7 l/s pers, activation of sensible heat recovery and recirculation air) to 203.6 kWh_p/m^2 (21 l/s pers, 100% outdoor air, bypass of the heat recovery). In addition, it was pointed out a significant energy saving by using sensible heat recovery, but AHUs must be equipped with flat plate heat exchangers, avoiding contamination of the outdoor air with the exhaust air.

Two other significant outcomes can be evidenced:

- Increasing the amount of outdoor air causes higher energy demands but this improves indoor air quality and reduce the concentration of CO_2 and allow a lower age of air. Obviously, this will have a positive impact on space livability.
- The role of the heat recovery for the examined case study and the considered climatic conditions is marginal in the cooling period. Indeed, the simulated configurations results in similar energy demands for cooling, with EP_C from 8 kWh/m^2 to 12.9 kWh/m^2.

The CFD analysis added some other new outcomes and was operated by investigating the air diffusion performances of four configurations (allowing 7.5 h^{-1} air changes per hour): 6 ceiling square diffusers, 4 wall-mounted grilles, 10 wall-mounted nozzles (high turbulence), 6 parallel strips of ceiling linear slot diffusers. Each one of the alternatives gave satisfactory result in terms of thermal comfort, but the configuration which guaranteed better results regarding uniformity of the air distribution and its purity, as well as optimal comfort conditions, was the one with linear slot diffusers. Indeed, this alternative (linear slot diffusers, in six strips, parallel to the students' row and extraction grilles on the floor) involves uniformity of air temperature, age of air, and flow and thermal fields. The position of diffusers and extraction grilles causes an almost vertical air movement so that the air breathed and exhaled by persons is then directed towards the grilles, positioned on the floor and at the lower part.

The investigation has provided a valuable example of correct HVAC system design, not limited to evaluations of different HVAC configurations in terms of energy, economy, and emissions, but also in terms of comfort and IAQ. The presence of stagnancy zones, uniformity of thermal comfort in indoor spaces according to the typology of air diffusers, is an aspect often neglected but that was widely discussed in this Thesis work.

It must be underlined not so much the specific results, merely related to the case study and the climatic conditions, but the methodology adopted. Experimental and numerical evaluations, BES and CFD simulations, as well as comfort analysis, can support a conscious and effective design.

CHAPTER 5 is entirely dedicated to energy redevelopment of the building/HAVC system, by intervening on all three levels of energy efficiency. Specifically, the benefits in terms of energy saving, reduction of CO_2 emissions, and visual and thermal comfort are evidenced for a seismic and energy redevelopment of a student dormitory in Athens (Greece). In this case, the building renovation has also interested the building geometry and shape, indeed, new spaces (ER and SS) and balconies (BAL) were added according to the European project “Proactive synergy of inteGrated Efficient Technologies on buildings’ Envelopes”.

The main interventions were:

- Geometry and spaces reorganization.
- Thermal insulation of the building envelope and replacement of windows.
- Replacement of the DHW and microclimatic control systems.
- Addition of photovoltaic and solar collector systems.

Very promising results were pointed out, from an energy and environmental point of view. It was found total primary energy saving of 51%

and the CO_2 emissions reduction of approximately 49%. The retrofit intervention included also the addition of two new energy services (i.e., the ventilation and the cooling systems) which determines an increase in energy demand only for that end-use, but heavily contributing to the occupant's well-being. An extensive thermal comfort analysis has demonstrated the improvement of indoor comfort conditions. On the other hand, the daylight analysis has shown that geometry modifications (i.e., the addition of balconies and sunspaces) could lead to a decrease in the average DF in the post-retrofit configuration. However, it should be noticed that the building will be equipped with lighting and control systems which will allow an adequate level of illumination to all users.

In the same chapter, another investigation concerning the energy refurbishment of residential buildings was reported. Energy, environmental and economic analysis were performed. The energy efficiency measures were evaluated according to new funding incentives of the Italian Government (Superbonus 110%), established by the so-called "relaunch Decree and into force in the period 2020-2023 (thus, we are just in this time), in comparison with the previous funding measures for energy retrofit.

Three typologies of residential buildings, representing the Italian residential building stock, were considered as case studies, and each of them was located in three Italian cities, i.e., three climatic zones. Two different approaches for the energy simulation were employed (transient and steady-state). In compliance with legislative requirements, the energy efficiency measures regarded the insulation of the building envelope (D1), the replacement of the windows (W) and of the heating systems (D2), and the addition of a Solar Collector system (SC). These interventions were simulated singularly or coupled according to the following configurations: D1, D1+W, D2, D2+SC, D1+D2+W+SC. Finally, three different funding scenarios were considered:

- SC1: 110% tax saving, over 5 years based on the new "Super-bonus" incentive mechanism.

- SC2: tax saving of 50-65% in 10 years based on the previous “Eco-bonus” incentive, here simplified (50% for envelope EEMs and 65% for heating system EEMs).
- SC3: no incentives are considered.

The investigation revealed that with a benefit of 110% of the investment cost, the energy efficiency measures that would be chosen from an energy point of view (i.e., insulation of opaque building envelope, replacement of windows and heating system) is also the most economically profitable.

With the application of the previous incentive mechanism (tax deduction between 50 and 65%), or in case of absence of incentive, the most convenient choice is the cheaper one (that is also the less efficient) and thus the mere replacement of old gas boilers. In any case, the best energy and environmental performances are achieved if the retrofits involve the whole building-HVAC system. The Italian funding system leads to prefer EEMs characterized by the best energy performance and not by the best cost/benefit ratio.

The Building Energy Simulations (BES) reported in CHAPTER 1, CHAPTER 4, CHAPTER 5 on real case studies were all performed with numerical models calibrated according to the real energy consumption of the buildings, by considering a standard use of the occupants, according to the building use.

But what would happen if we considered (and modeled…) an incorrect behavior of the occupants? Of course, operational patterns and unsuitable use of buildings and facilities largely impact energy demand. These wrong habits are much more common than we think. Examples of energy-impacting actions of users are:

- the occasional opening/closing of the windows,
- the increment or decrement of the heating setpoint,
- the adjustment of the shading systems,
- the addition of electric equipment,
- the energy-intensive use of the lighting system.

By considering wrong habits in a residential building of eight floors, built during the 60s – 70s and located in Naples Italy), and by comparing its energy demand in case of the standard used and energy-intensive use, it can be seen a big energy demand variation due to the occupant wrong habits. Indeed, when all the wrong actions were taken into account in their more energy-intensive version (e.g., the heating setpoint was set at 23°C and the power of the lighting system was set at 10 W/m^2) the yearly energy demand of the building resulted equal to 202 kWh_p/m^2, which corresponds to a higher value compared to both the refurbished standard building (94 kWh_p/m^2) and the base building before the refurbishment (156 kWh_p/m^2). The energy demand of the energy-intensive building could be considered as the maximum primary energy demand of a refurbished residential building in Naples.

More in general, it was also evidenced that wrong occupant behaviors have a more significant impact on the cooling demand rather than the heating demand.

Regarding BES, by considering the complexity in the use of common commercial software, the last chapter (CHAPTER 6) proposes a user-friendly but accurate tool to perform building energy modeling and simulations of residential buildings (EMAR). No modeling expertise and no detailed definition of the envelope and technical systems are necessary, but only a few inputs. EMAR is based on the coupling of EnergyPlus and MATLAB® and can carry out accurate simulations through the input of 63 parameters. The tool was validated through detailed EnergyPlus models of an ASHRAE test building and of two typical European buildings. The results showed discrepancies lower than 10% as concerns thermal energy demand and primary energy consumption for space conditioning, and in most cases lower than 5%.

In any case, EMAR introduces a drastic reduction of modeling and computational burden, so that it can be easily used by building professionals. In addition, this tool can provide outputs at the dwellings' level, thereby enabling deep investigations of energy demands, thermal comfort, and heating/cooling loads for different stakeholders. Future studies will aim at the development of free graphical interfaces (without the use of MATLAB®) as well as to the integration of EMAR in building energy audit and labeling, design of HVAC systems, building information modeling (BIM), building energy optimization for the design of new buildings or the retrofit of existing ones or large-scale analysis of buildings stock to address public energy policies.

A still open line of research is aimed at developing simplified graphical interfaces for complex codes aimed at accurately simulating the energy performance of buildings. This paves the way for future digital twin developments also with respect to predictive control.

In conclusion, this Thesis work has led us through a journey in building energy efficiency, by considering several intervention technologies, innovative and traditional, several methodological approaches, and several building cases studies. Experimental and numerical evaluations, BES and CFD simulations, transient and steady-state analysis, environmental and economic analysis were performed according to different case studies.

The evaluation of an energy refurbishment can be carried out according to different methodological approaches, identifying different types of proper analysis to choose optimal solutions for energy retrofit. This work is an example of the effective use of the instruments at our disposal to understand and evaluate the best choices in the building energy field.

This is a reference work for professionals, researchers, and institutions which give a high contribution in the field of energy efficiency.

Nomenclature

Acronyms		
BAL	Balconies	
BAU	Business and Usual	
BEO	Building Energy Optimization	
BES	Building Energy Simulation	
C	Cost	€
CAV	Constant Air Volume	
CBR	cost to benefit ratio	[-] or seJ/seJ
CL	Cooling Loads	
CO_2	Carbon Dioxide	
COD	chemical oxygen demand	mg/l
CFD	Computational Fluid Dynamic	
CNR	Italian national research council	
Con-FD	Conduction finite difference algorithm	
CTF	Conduction Transfer Function	
CV(RMSE)	Coeff of variation of Root Mean Square Error	%
DH	Discomfort Hours	
DHW	Domestic Hot Water	
DOAS	Dedicated Outdoor Air System	
DPB	Discounted Pay Back	Years
DX	Direct Expansion	
E. coli	escherichia coli	MPN/100 ml
Exp	experimental study	
EED	Energy Efficiency Directive	
EEM	Energy Efficiency Measures	
EM	Emissions	
EMAR	EnergyPlus + MAtlab® for Residential	
EP	Primary Energy Performance	
EPBD	Energy Performance of Building Directive	
EPS	Expanded Polystyrene insulation	
ER	Extra Room	
EU	European Union	
FGN	Functionalized Graphene	
GET	inteGrated Efficient Technology	
GF	Green Façade	

GSE	Energy Service Manager	
GST	Green Vertical System	
GW	Green Wall	
HI	Heat Index	°C
HL	Heating Loads	
HVAC	Heating, Ventilation and Air Conditioning	
IPCC	Intergovernmental Panel on Climate Change	
ISAC	Institute of Atmospheric Sciences and Climate	
LAI	Leaf Area Index	[-] or m^2/m^2
LW	Living Wall	
MBE	Mean Bias Error	
MeP	Methyl Palmitate	
MeS	Methyl Stearate	
MS	Member State	
MW	Mineral Wool	
NPV	Net Present Value	€
Num	numerical study	
nZEB	nearly Zero Energy Building	
NZEB	Net Zero Energy Building	
OA, RA, TA	Outdoor, Recirculation, Total Air	
PCM	Phase Change Material	
PEF	Primary Energy Factor	kWh/kWh
PES	Primary Energy Saving	kWh_t/m^2y
PMV	Predicted Mean Value	%
PPD	Predicted Percentage of Dissatisfied	%
PV	Photovoltaic	
SLA	Specific Leaf Area	m^2/kg
SS	Sun Space	
SWOT	Strengths Weaknesses Opportunities Threats	
TAC	task/ambient air conditioning system	
TN	Total Nitrogen	mg/l-N
TP	Total Phosphorus	mg/l-P
TSS	Total Suspended Solids	mg/l
UHI	Urban Heat Islands	
UV	Ultraviolet	
WTP	Willingness To Pay	
XPS	Extruded polystyrene insulation	

<u>Symbols</u>

A_c	conditioned area	m^2
ACH	air changes per hour	h^{-1}
C	Thermal capacity	
C_a	Areal heat capacity	J/m^2K
c_p	specific heat	J/kg K
COP	Coefficient of Performance	Wh_t/Wh_e
DF	Average daylight factor	
EER	Energy Efficiency Ratio	Wh_t/Wh_e
g	Solar factor	
Gc	Global cost	€
H	Global heat transfer coefficient	
i	EMAR input	
I	Illuminance level	lux
Y_{IE}	Periodic thermal transmittance	W/m^2 K
K	thermal conductance	W/m^2 K
k	radiation attenuation coefficient	
PEC	Primary Energy Consumption	kWh_p/m^2y
r_l	stomatal resistance	s/m
SR	Solar Reflectance	
ST	Solar transmittance	
S/V	Surface to Volume Ratio	m^{-1}
t	thickness	m
$T_{set-poit}$:	set-point temperature	°C
TED	thermal energy demand	kWh_t/m^2 y
U_{value}	Thermal transmittance	W/m^2K
U_f	Thermal transmittance of window’s frame	W/m^2K
U_g	Thermal transmittance of window’s glass	W/m^2K

<u>Greek symbols</u>

α_l	absorption coefficient of the leaf	
α_s	absorption coefficient of the soil	
ε_l	emissivity of the leaf	
ε_s	emissivity of the soil	
Δ	difference	-

ρ	density	kg/m^3
λ	thermal conductivity	W/mK
Subscripts	(Referred to)	
a	area	
C	space cooling	
e	electricity	
equiv	equivalent	
g	natural gas	
H	space heating	
ho	horizontal	
mean	mean value	
max	maximum value	
min	minimum value	
p	primary	
t	thermal	
tot	all energy uses	
SC	space conditioning (heating + cooling)	

List of publications

In the following section, the list of the scientific papers written within my research group, during the three-years PhD School.

<u>*International journals*</u>

1) Ascione, F., Bianco, N., De Masi, R. F., Mastellone, M., & Vanoli, G. P. (2019). Phase change materials for reducing cooling energy demand and improving indoor comfort: A step-by-step retrofit of a Mediterranean educational building. Energies, 12(19), 3661.
2) Ascione, F., De Masi, R. F., Mastellone, M., Ruggiero, S., & Vanoli, G. P. (2020). Green walls, a critical review: knowledge gaps, design parameters, thermal performances and multi-criteria design approaches. Energies, 13(9), 2296.
3) Ascione, F., Bianco, N., De Masi, R. F., Mastellone, M., Mauro, G. M., & Vanoli, G. P. (2020). The role of the occupant behavior in affecting the feasibility of energy refurbishment of residential buildings: Typical effective retrofits compromised by typical wrong habits. Energy and Buildings, 223, 110217.
4) Ascione, F., Bianco, N., Iovane, T., Mastellone, M., & Mauro, G. M. (2020). Is it fundamental to model the inter-building effect for reliable building energy simulations? Interaction with shading systems. Building and Environment, 183, 107161.
5) Ascione, F., De Masi, R. F., Mastellone, M., & Vanoli, G. P. (2021). The design of safe classrooms of educational buildings for facing contagions and transmission of diseases: A novel approach combining audits, calibrated energy models, building performance (BPS) and computational fluid dynamic (CFD) simulations. Energy and Buildings, 230, 110533.
6) Ascione, F., Bianco, N., Iovane, T., Mastellone, M., & Mauro, G. M. (2021). The evolution of building energy retrofit via double-skin and responsive façades: A review. Solar Energy, 224, 703-717.
7) De Masi, R. F., Festa, V., Gigante, A., Mastellone, M., Ruggiero, S., & Vanoli, G. P. (2021). Effect of Climate Changes on Renewable Production in the Mediterranean Climate: Case Study of the Energy Retrofit for a Detached House. Sustainability, 13(16), 8793.

8) Ascione, F., Bianco, N., Iovane, T., Mastellone, M., & Mauro, G. M. (2021). Conceptualization, development and validation of EMAR: A user-friendly tool for accurate energy simulations of residential buildings via few numerical inputs. Journal of Building Engineering, 44, 102647
9) De Masi, P. D. R. F., Mastellone, P. D. C. M., & Vanoli, F. P. G. P. (2021). Building rating systems: A novel review about capabilities, current limits and open issues. Sustainable Cities and Society, 103498.

Conference proceedings

1) Ascione, F., De Masi, R. F., Mastellone, M., Mauro, G. M., & Ruggiero, S (2020). “Energy efficiency measures for an existing residential building in Italy. Improvement of energy certification and fulfilling of the nZEB standard”. Volume 11: Proceedings of 12th International Conference on Applied Energy, Part 3, Thailand/Virtual, 2020. ISBN 978-91-986738-2-1.
2) Ascione, F., Bianco, N., A. Di Lorenzo, Mastellone M., Mauro G. M., D.F. Napolitano (2021) “A social housing district upgraded to an nZEB settlement: a real case study in the southern Italy coastline” Proceedings of 9th Global Conference on Global Warming (GCGW-2021) ISBN 978-605-64806-1-4
3) Ascione, F., De Masi, R. F., Mastellone M., Ruggiero, S., Tariello F., & Vanoli G.P. (2021) “Energy Performance of Buildings: improvements, limits and future perspectives during the last twenty years of energy and sustainability policies” Proceedings of 6th International Conference on Smart and Sustainable Technologies (SPLITECH 2021).

Contributions in volumes

1) “Oltre il risparmio energetico ed il comfort: la progettazione termotecnica per la sicurezza. analisi energetiche e termofluidodinamiche presso l’Università degli Studi del Molise” (2020). Volume II: OLTRE LA PANDEMIA - Società, salute, economia e regole nell’era post Covid-19 a cura di Giovanni Palmieri - EDITORIALE SCIENTIFICA NAPOLI, ISBN 978-88-9391-846-6.
2) TIPOLOGIE EDILIZIO PREZZARIO aggiornamento 2020- “Il prezzario per tipologie edilizie di Napoli e provincia” (2021) promosso da ACEN - Associazione Costruttori Edili di Napoli. Edizioni Graffiti, ISBN 978-88-86983-945.

Index of Figures

Chapter 1

Chapter 2

Chapter 3

Chapter 4

Chapter 5

Chapter 6

Index of Tables

Chapter 3

Chapter 4

Chapter 5

Chapter 6

Acknowledgements – *Ringraziamenti*

Per quanto complicato, il percorso che mi ha portato a scrivere questa Tesi, è stato pieno di soddisfazioni e non sarebbe stato lo stesso senza il sostegno di diverse guide a compagni di viaggio.

Ringrazio il mio tutor, il Prof. Fabrizio Ascione, che mi ha appoggiata e guidata come nessuno avrebbe potuto fare. I consigli, il metodo e le conoscenze tramesse, sono state indispensabili per portare avanti l'attività di ricerca. È stato un piacere ed un onore avere la possibilità di lavorare con lui.

Ringrazio il Direttore del Dipartimento di Ingegneria Industriale, il Prof. Nicola Bianco, per gli incoraggiamenti e il supporto mai mancato. L'ambiente e il clima che ha creato sono stati ottimali per la mia crescita culturale e per quella dell'intero gruppo di ricerca.

Ringrazio il Prof. Gerardo Mauro e la Prof.ssa Rosa Francesca De Masi per aver contribuito il modo significativo ad arricchire le mie conoscenze.

Ringrazio il gruppo di ricerca de la "National and Kapodistrian University of Athens" ed i professionisti dell'Associazione Costruttori Edili di Napoli per aver avvalorato il fondamento scientifico e culturale del mio lavoro di ricerca.

Ringrazio tutti i docenti e ricercatori incontrati durante questi anni, per i consigli e le opinioni scambiate. In particolare, ringrazio Davide, Diana, Teresa e Silvia per i momenti di lavoro condivisi ma soprattutto per i momenti di spensieratezza.

Ringrazio i miei genitori per avermi spronata a fare meglio, per aver appoggiato le mie scelte più difficili e per avermi supportata sempre; senza di loro tutto questo non sarebbe stato possibile.

Ringrazio mia sorella perché con la sua dolcezza e la sua bontà mi ha aiutata nei momenti più complicati e di incertezza.

Ringrazio mio fratello perché mi fa ridere con le battute più improbabili.

Ringrazio i miei nonni per avermi fatto capire che con l'umiltà si può arrivare dappertutto.

Ringrazio infine Alberto che ha creduto in me molto più di quanto abbia fatto io stessa.

Meta, 08/11/2021 *Margherita Mastellone*